Molecular mechanisms underlying the regulation of interleukin-10 production in macrophages

Christina Maria Taubert

The Francis Crick Institute
and
University College London
PhD Supervisor: Anne O'Garra

A thesis submitted for the degree of
Doctor of Philosophy
University College London
August 2017

Declaration

I Christina Maria Taubert confirm that the work presented in this thesis is my own. Data presented within this thesis (parts of Chapter 3 and Chapter 4) were published in the Journal of Immunology in co-authorship with Ashleigh Howes (Howes A, Taubert C, Blankley S, Spink N, Wu X, Graham CM, Zhao J, Saraiva M, Ricciardi-Castagnoli P, Bancroft GJ, O'Garra A. 2016. Differential Production of Type I IFN Determines the Reciprocal Levels of IL-10 and Proinflammatory Cytokines Produced by C57BL/6 and BALB/c Macrophages. *J Immunol* 197: 2838-53). Where information has been derived from other sources, I confirm that this has been indicated in the thesis.

Abstract

Interleukin (IL)-10 is an immunosuppressive cytokine that plays a crucial role in preventing inflammatory and autoimmune pathology. The dysregulation of IL-10 during infection can lead to either an over-exuberant response damaging the host, or conversely ineffective pathogen clearance. Macrophages are important players in inflammatory responses and produce IL-10 in response to Toll-like receptor (TLR) ligation along with protective pro-inflammatory cytokines. The collective regulation of these cytokines is central to the generation of an effective but balanced immune response. We observed that type I IFN is one factor that leads to differential production of IL-10 and pro-inflammatory cytokines in TLR4 stimulated C57BL/6 and BALB/c macrophages. The effects of type I IFN on pro-inflammatory cytokine production were IL-10 dependent and independent. Hence, we further investigated how type I IFN regulates IL-10 production and showed that type I IFN acts as a transcriptional regulator of *Il10* mRNA via activation of ERK1/2, and additionally stabilises *Il10* mRNA transcripts in TLR4 stimulated macrophages. Using an assay for transposase-accessible chromatin with high throughput sequencing we further unravelled how type I IFN regulates *Il10* transcription. We were able to demonstrate that type I IFN increases chromatin accessibility and augments the recruitment of the transcription factors ATF3 and JUNB to the *Il10* locus in macrophages upon LPS stimulation. These findings highlight key pathways responsible for the type I IFN-dependent regulation of IL-10, and may provide valuable information for the development of immunomodulatory treatments of inflammatory diseases.

Acknowledgement

This thesis would not have been possible without the guidance and the help of several individuals who in one way or another contributed and extended their valuable assistance in the preparation and completion of this thesis. First, I would like to begin by thanking my principal supervisor, Dr Anne O'Garra, for the continuous support and for giving me the chance to explore different scientific areas. I am also thankful to the members of my thesis committee Dr Gregory Bancroft, Dr Steve Ley and Dr Jean Langhorne, for their support and helpful suggestions throughout my PhD. I would like to thank Dr Ashleigh Howes who paved the way for me at the beginning of my PhD, who trained me in the lab, gave her continued advice and also proofread parts of this thesis. I would also like to thank all my colleagues, past and present, from the O'Garra lab for their support, motivation as well as for all the laughter and joy we had together. A special thank you to Dr Lúcia Moreira-Teixeira for all her guidance, helpful suggestions and moral support. I wish also to thank her for proofreading the chapters of this thesis. I thank Evangelos Stavropoulos, Dr Christine Graham, Dr Xuemei Wu and Dr Damian Carragher for their support throughout the years. I want to also thank the HTS facility specifically Leena Bhaw and Dr Abdul Sesay for all their help with setting up the ATAC-sequencing as well as Dr Vicki Metzis and Dr George Young without their help I would not have been able to tackle the analysis of the ATAC-seq data. Moreover, a lot of the work would have been much harder without the help of Olga O'Neill from the equipment park, the Flow facility and the BRF staff. I wish also to thank Rosa Gomes Faria and Dr Bathilde Ambroise for giving me a quiet place to write this thesis. On a personal note, I would like to thank my "crazy chickens" for being a great company and providing

encouragement when needed even from far away. I also want to thank Ricardo for his support, particularly during the phase of writing this thesis. Last but not the least, I would like to say a big thank you to my mum who has always had confidence in me and has given me her greatest support throughout all of the years.

Table of Contents

Table of figures

Chapter 1

Chapter 3

Chapter 4

Chapter 5

Chapter 6

Chapter 7

List of tables

Chapter 1

Chapter 2

Chapter 7

Abbreviations

ABTS	2,2'-azino-bis(3-ethylbenzothiazoline-6-sulphonic acid)
ALR	AIM2-like receptor
ANOVA	analysis of variance
AP	activator protein
APC	antigen presenting cell
ATAC	assay for transposase accessible chromatin
ATF3	activating transcription factor 3
BH-FDR	Benjamini-Hochberg False Detection Rate
BMDM	bone marrow-derived macrophages
Bps	*Burkholderia pseudomallei*
CD	cluster of differentiation
cDNA	complementary deoxyribonucleic acid
C/EBP	CCATT enhancer/binding protein
cGAS	cyclic GMP-AMP synthase
ChIP	chromosome immune precipitation
cMaf	c-musculoaponeurotic fibrosarcoma factor
CREB	cAMP response element binding protein
CTL	C-type lectin
DAMP	danger-associated molecular pattern
DC	dendritic cell
DMSO	dimethyl sulfoxide
DNA	deoxyribonucleic acid

EAE	experimental autoimmune encephalitis
EDTA	ethylenediaminetetraacetic acid
ELISA	enzyme-linked immunosorbent assay
ERK	extracellular signal–regulated kinases
FCS	fetal calf serum
GSK-3	glycogen-synthase-kinase 3
HAT	histone acetyltransferases
HDAC	histone deacetylase
HkBps	heat-killed *B.pseudomallei*
HRP	horseradish peroxidase
IFN	interferon
IKK	IκB kinase
IL-	interleukin
IPA	Ingenuity Pathway Analysis
IRAK	interleukin-1 receptor-associated kinase
IRF	interferon regulatory factor
ISG	interferon-stimulated gene
JAK	janus kinase
LBP	LPS-binding protein
LPS	lipopolysaccharide
MAPK	mitogen-activated protein kinase
MAVS	mitochondrial antiviral signalling protein
M-CSF	macrophage colony-stimulating factor
MHC	major histocompatibility complex
mRNA	messenger ribonucleic acid

mTOR	mechanistic target of rapamycin
MyD88	myeloid differentiation primary response gene 88
NFIL3	nuclear factor, interleukin 3 regulated
NF κ-B	nuclear factor kappa-light-chain-enhancer of activated B cells
NK	natural killer
NLR	NOD-like receptor
ns	not significant
OLR	OAS-like receptor
PAMP	pathogen associated molecular pattern
PBS	phosphate buffered saline
PCA	principle component analysis
PCR	polymerase chain reaction
pDC	plasmacytoid DC
PI3K	phosphoinositid-3-Kinasen
PRR	pattern recognition receptor
qPCR	quantitative polymerase chain reaction
RLR	RIG-I-like receptor
RNA	ribonucleic acid
RT	room temperature
RU	relative units
SD	standard deviation
SDS	sodium dodecyl sulfate
SLE	systemic lupus erythematosus
Sp	specificity protein
ssRNA	single stranded ribonucleic acid

STAT	signal transducer and activator of transcription
TAB	TAK1 binding protein
TAD	topologically associating domain
TAK1	transforming growth factor β activating kinase 1
TBK1	TANK Binding Kinase 1
TF	transcription factor
T_H	T helper
TIR	Toll/Interleukin-1 receptor
TLR	toll-like receptor
TMB	tetramethylbenzidine
TNF-α	tumour necrosis factor α
TPL-2	tumour progression locus-2
TRAF	TNF receptor-associated factor
TRIF	TIR domain–containing adapter-inducing IFN-β
TSS	transcription start site
TTP	tristetraprolin
TYK	tyrosine kinase
WT	wild type
-/-	knock-out

Chapter 1.
General introduction

1.1 The innate immune response and its interaction with the adaptive immune system

The immune response is composed of an innate and an adaptive component. While the innate immune system is invoked by the activation of germ-line encoded receptors for microbial moieties, the adaptive immune system is activated by antigen presenting cells of the innate immune system.

The effector mechanisms of innate immunity, which include antimicrobial peptides, phagocytes, and the alternative complement pathway, are activated immediately after a pathogen penetrates the physical barriers and provides a rapid, non-specific response that acts against a broad range of different pathogens (1). The function of the innate immune system is to recognise and actively remove invading pathogens, as well as to activate the adaptive immune system. Phagocytic cells such as macrophages and DCs are particularly important in the recognition of infection as they express pattern recognition receptors (PRRs). PRRs are germ-line encoded and recognise highly conserved structures that are present in large groups of microorganisms but not in vertebrates (2), so called pathogen-associated molecular patterns (PAMPs). Hence, innate immunity can very effectively recognise pathogens as ‘non-self’. After macrophages and neutrophils recognised an infection, they directly kill the microorganism and initiate an inflammatory response leading to the recruitment of new phagocytic cells and circulating effector cells to the site of infection. The stimulation of macrophages and DCs by some of these receptors leads to their maturation resulting in the production of co-stimulatory molecules, cytokines

and chemokines which recruit and activate other immune cells to the site of infection, and also initiate the adaptive immune response (2).

Upon activation, antigen presenting cells (APCs, which include DCs and macrophages) express co-stimulatory molecules such as CD80 and CD86 together with major histocompatibility complex (MHC) class II proteins. MHC class II proteins then present microbial peptides leading to the activation of CD4+ T cells (3, 4). However, the recognition of an antigen in the absence of CD80 or CD86 leads to permanent inactivation or apoptosis of the T cell. In the presence of different innate cytokines and of co-stimulation, CD4+ T cells expand and differentiate into distinct T helper (T_H) subsets, each with specialised effector functions (5). T_H1 cells express the master transcription factor (TF) TBET and produce IFN-γ as a hallmark cytokine. T_H1 cells play an important role in the immune defence against intracellular pathogens (6-9), while T_H2 cells are central in immune responses against parasitic helminths. Their master TF is GATA3 and they produce cytokines such as interleukin- (IL-) 4, IL-5 and IL-13 (7, 10, 11). T_H17 cells express the master TF RORγT and produce IL-17A and IL-17F. T_H17 cells play a role in the immune response against fungal infections and extracellular bacteria (12, 13). Regulatory T (T_{reg}) cells express FOXP3 and have an important role in regulating immune responses to maintain immunological tolerance and homeostasis (14, 15). In the context of antigen presentation by MHC class I, CD8+ T cells are activated and can mediate the killing of infected cells through their cytotoxic functions, but also produce cytokines such as IFN-γ that further activates innate immune cells to control the infection (16). Additionally, B cells form a critical part of the adaptive immune system through the production of antibodies and the formation of memory cells (17).

Thus, the immune response is a complex network of many different cells, whose activity has to be carefully coordinated to ensure effective pathogen clearance but minimal damage to the host. Cytokines, such as IL-12, IL-10 and type I interferons, contribute to the orchestration of many of these processes and are regulated on various different levels.

1.2 Macrophages and their role within the immune system

Macrophages are a heterogeneous group of hematopoietic cells that are part of the innate immune system and therefore crucial in the early phase of immune responses (2). The majority of tissue-resident macrophages in healthy tissue arise from embryonic precursors and are seeded prenatally. Tissue-resident macrophages self-maintain locally and are self-sufficient and independent from further hematopoietic input (18-22). Depending on the anatomical location, different tissue resident macrophages are known including lung alveolar macrophages, liver Kupffer cells, spleen red pulp macrophages, skin Langerhans cells, central nervous system microglial cells and intestine, heart, kidney and peritoneal macrophages (22). Tissue-resident macrophages exhibit substantial heterogeneity, which evolves through the different tissue microenvironments (23, 24). Moreover, in pathological, but also homeostatic and inflammatory settings circulating monocytes derived from the bone marrow can give rise to inflammatory macrophages that infiltrate the tissues. In general, these monocyte-derived macrophages display a limited life span (18-22). In addition to the tissue specific classifications, functional classifications such as that of M1 and M2, have also been suggested. M1 macrophages are considered to be ‘classically’ activated by toll-like receptor (TLR) ligands (such as LPS) and IFN-γ (25).

They produce high levels of pro-inflammatory cytokines, including IL-12, and are important in immune defence, although they may have pathogenic roles in autoimmune conditions (25). The production of nitric oxide is another hallmark of M1 macrophages that is very important in microbial killing (26). M1 macrophages metabolise arginine to nitric oxide and citrulline via the enzyme nitric oxide synthase, whereas M2 macrophages metabolise arginine to ornithine and urea, having an importance for cellular proliferation and tissue repair (26). M2 macrophages, or so called alternatively activated macrophages, result from macrophage activation by T_H2 associated cytokines such as IL-4 or IL-13 (27). The expression of Arginase-1 is a key feature of M2 macrophages and they play important roles in tissue repair (27) and immune defence against helminths (28).

Macrophages contribute to host defence by phagocytosis and neutralisation of cellular debris and potentially hazardous agents, including pathogens. They form the first line of defence during infection and assist in promoting immune tolerance in steady state (20, 23, 29). However, they are also involved in tissue remodelling, metabolism, homeostasis and sense tissue damage and orchestrate tissue-repair responses and have tissue specific functions (30). Macrophages exert their function mostly by secreting pro-inflammatory cytokines such as TNF-α, IL-1β and IL-6 as well as antimicrobial molecules such as nitric oxide (20, 23, 29). This cytokine secretion leads to an increased endothelium permeability leading to recruitment of other innate immune cells such as neutrophils and monocytes (20). They also produce IL-12 and IL-23 that lead to the differentiation and expansion of T_H1 and T_H17 cells respectively that help to drive inflammatory responses (29). Additionally, these cytokines stimulate resident DCs to leave the tissue, move to the draining

lymph node and activate the adaptive immune response. Macrophages also load extracellular antigens on MHC class II molecules and therefore contribute to the differentiation of regulatory and effector CD4+ T cells (20). Presentation of antigens on MHC class I by macrophages can also lead to activation of CD8+ T cells. A crucial role of macrophages is also the clearance of apoptotic cells and pathogens by phagocytosis, which is facilitated by opsonins, host products of the acute-phase response and the complement system (2).

Macrophages recognise a wide range of PAMPs and danger-associated molecular patterns (DAMPs) via a variety of PRRs such as TLR, NOD-like receptors (NLRs), retinoic acid inducible gene-1 (RIG-I) family, lectins and scavenger receptors, AIM2-like receptors (ALRs) and intracellular DNA sensors such as cyclic GMP-AMP synthase (cGAS), which trigger the early immune response (discussed in depth in chapter 1.3) (31-33). They are also activated by IFN-γ which is produced by some innate cells as well as CD4+ T_H1 cells and CD8+ T cells (2). Through the expression of these sensors macrophages are responsive to changes in their environment. However, if the inflammatory response of macrophages is not controlled, it can lead to chronic inflammation or autoimmune diseases (29). Therefore, macrophages undergo apoptosis or switch into an anti-inflammatory or suppressive phenotype (34), characterised by the production of the anti-inflammatory cytokine IL-10, to prevent excessive inflammation (35). These silencing programs most likely set tissue-specific thresholds for their activation and allow the cells to gradually respond and assess the quality and intensity of the stimulus (19).

Accordingly, with such a broad array of essential functions, macrophages are also reported to be important contributors to various pathological conditions that reflect the dysregulation of their functions. In this context, macrophages have been described to play a critical role in atherosclerosis, osteoporosis, obesity and type 2 diabetes, fibrosis and cancer (29, 30).

1.3 Detection of infectious agents and signalling by pattern recognition receptors

1.3.1 Non-TLR PRRs

Invading microorganisms or cellular damage in tissues are initially recognised by the innate immune system through PRRs that are germline encoded and show a broad specificity for conserved and invariant features of microorganisms, PAMPs and DAMPs. According to protein structure and domain function, six families of PRRs can be distinguished:

(i) TLRs are a family of membrane-bound proteins that will be discussed in more detail in chapter 1.3.2.

(ii) C-type lectins (CTLs) are membrane-bound carbohydrate receptors that consist of two types: type I CTLs (such as DEC-205 and MMR), and type II CTLs (including dectin 1, dectin 2, Mincle, DC- SIGN, DNGR-1) (36, 37). An additional member of the CTL family is the soluble carbohydrate receptor mannose-binding lectin. Dectin-1 for example recognises mycobacterial motifs (38), fungal β-glucans (39)

and the pure β-glucan, Curdlan (40). Intracellularly, CTLs trigger a pathway that is dependent on the kinase SYK and phospholipase C.

(iii) NLRs are expressed in the cytoplasm and recognise various microbial and non-microbial stimuli including the muramyl dipeptide motif of peptidoglycan present within most types of bacteria, and bacterial and viral RNA. The NLR family includes NOD1, NOD2 and NLRP1-10 (41). Upon stimulation NOD1 and NOD2 lead to the activation of NF-κB and MAP kinase signalling (42). It has also been shown that NOD2 can activate interferon regulatory factor (IRF) 5 (43) as well as IRF3 (44). Other members of this family initiate the formation of the inflammasome complex, the best characterised of which is the NLPR3 inflammasome (45). The inflammasome recruits and activates the enzyme caspase 1, which mediates the proteolytic cleavage and maturation of IL-1 family cytokines (e.g. IL-1β, IL-18) into their biologically active forms (46).

(iv) RIG-I-like receptors (RLRs), including RIG-I, melanoma differentiation-associated gene 5 (MDA-5) and laboratory of genetics and physiology 2 (LGP2) (47), are cytoplasmic sensors of RNA. Upon activation, these receptors signal to the mitochondrial anti-viral signalling protein (MAVS) to induce an IRF3- and IRF7-mediated type I IFN response (48).

(v) ALRs are cytoplasmic DNA sensors. Some of these sensors, including IFI-16 and DAI, signal through the endoplasmic reticulum-associated adapter STING to initiate downstream signal transduction. Others, such as AIM2, are capable of forming an inflammasome (49).

(vi) OAS-like receptors (OLRs) are a recently identified group of cytoplasmic innate sensors of nucleic acids. Members of this family are the oligoadenylate synthase (OAS) proteins and cGAS. These PRRs are unique in their signal transduction mechanisms because they produce 20–50-linked second messenger molecules that initiate downstream antiviral immune responses (50).

Upon exposure of immune cells to ligands of these receptors, intracellular signalling pathways are triggered and lead to the induction of innate immune responses by producing inflammatory cytokines, type I IFNs and other mediators (2, 32, 33). Some receptors can be activated by similar ligands, and initiate the same signalling and effector modules, thereby inducing a complex and multi- faceted immune response (51).

1.3.2 TLR signalling

One of the PRRs are TLRs, which are evolutionarily conserved trans-membrane receptors, where the extracellular part consists of a leucin-rich repeat motif. The intracellular part is comprised of a conserved region of around 200 amino acids and is known as the Toll/Interleukin-1 receptor (TIR) domain as it shows high similarity to

that of the IL-1 receptor family (31, 32, 52). However, the extracellular portions of TLRs and the IL-1R are structurally unrelated (31). Ten different TLRs (TLR1-10) were characterised in human and twelve (TLR1-9, TLR11-13) in mouse with each TLR recognising specific patterns of microbial components (Table 1.1).

Some TLRs are localised on the cell surface (TLR1, 2, 4, 5, 6, 10, 11, 12) recognising bacterial motifs such as lipopolysaccharide (LPS) (TLR4) or peptidoglycan (TLR2), while others are expressed in the endosomal membrane (TLR3, 7, 8, 9, 13) and detect mainly nucleic acids from viruses or internalised bacteria (Table 1.1). For instance, TLR3 recognises viral double-stranded RNA, small interfering RNAs and self-RNAs from damaged cells, while TLR9 recognises bacterial and viral DNA that is rich in un-methylated CpG-DNA motifs (31, 33, 53).

TLRs are synthesised in the endoplasmic reticulum, traffic to the Golgi and from there are recruited to the cell surface or intracellular compartments. TLRs are expressed on many different immune cells such as macrophages, neutrophils, DCs, NK cells, mast cells, B cells, subtypes of T cells and even on non-immune cells such as fibroblasts and epithelial cells. The expression of TLRs is dynamic and is modulated rapidly in response to pathogens, a variety of cytokines and environmental stress (33). TLR signalling in macrophages leads to recruitment of the same molecules as used for IL-1R signalling and initiates the production of pro-inflammatory cytokines and type I IFNs, but also to the secretion of the anti-inflammatory cytokine IL-10.

Table 1.1 The TLRs and their ligands

Adapted from Takeda, Akira *et al.* (52) and Kumar *et al.* (53). * only expressed in human, # only expressed in mouse.

TLR	Location of expression	PAMPs recognised	Signalling adapter
TLR1:2	Plasma membrane	Triacyl lipopeptides, Pam3CSK4 (synthetic)	TIRAP, MyD88
TLR2:6 (CD36)	Plasma membrane	Diacyl lipopeptides, zymosan	TIRAP, MyD88
TLR3	Endosome	ssRNA, dsRNA, Poly I:C (synthetic)	TRIF
TLR4 (LBP/CD14/MD-2)	Plasma membrane	LPS, Mannan, envelope proteins	TIRAP, MyD88, TRAM, TRIF
TLR5	Plasma membrane	Flagellin	MyD88
TLR7	Endosome	ssRNA, R848 (synthetic)	MyD88
TLR8*	Endosome	ssRNA, R848 (synthetic)	MyD88
TLR9	Endosome	CpG DNA motif, dsDNA	MyD88
TLR10*	Plasma membrane	Unknown	MyD88
TLR11#	Plasma membrane	Profilin, Flagellin	MyD88
TLR12#	Plasma membrane	Profilin	unknown
TLR13#	Endosome	Bacterial 23S ribosomal RNA	unknown

Upon microbial recognition TLRs homo-dimerise, except for TLR2, which is shown to hetero-dimerise with TLR1 (54) or TLR6 (55). Dimerisation of TLRs triggers the activation of signalling pathways, which originate from the TIR domain. In the

signalling pathways, downstream of the TIR domain, a TIR domain–containing adaptor, myeloid differentiation primary-response protein 88 (MyD88) (56-58), was first shown to be essential for induction of inflammatory cytokines such as TNF-α and IL-12 through all TLRs except for TLR3. However, subsequent studies have demonstrated that individual TLR signalling pathways are divergent, and there are MyD88-dependent and TIR domain-containing adaptor-inducing IFN-β (TRIF)-dependent pathways (52, 59) (Figure 1.1).

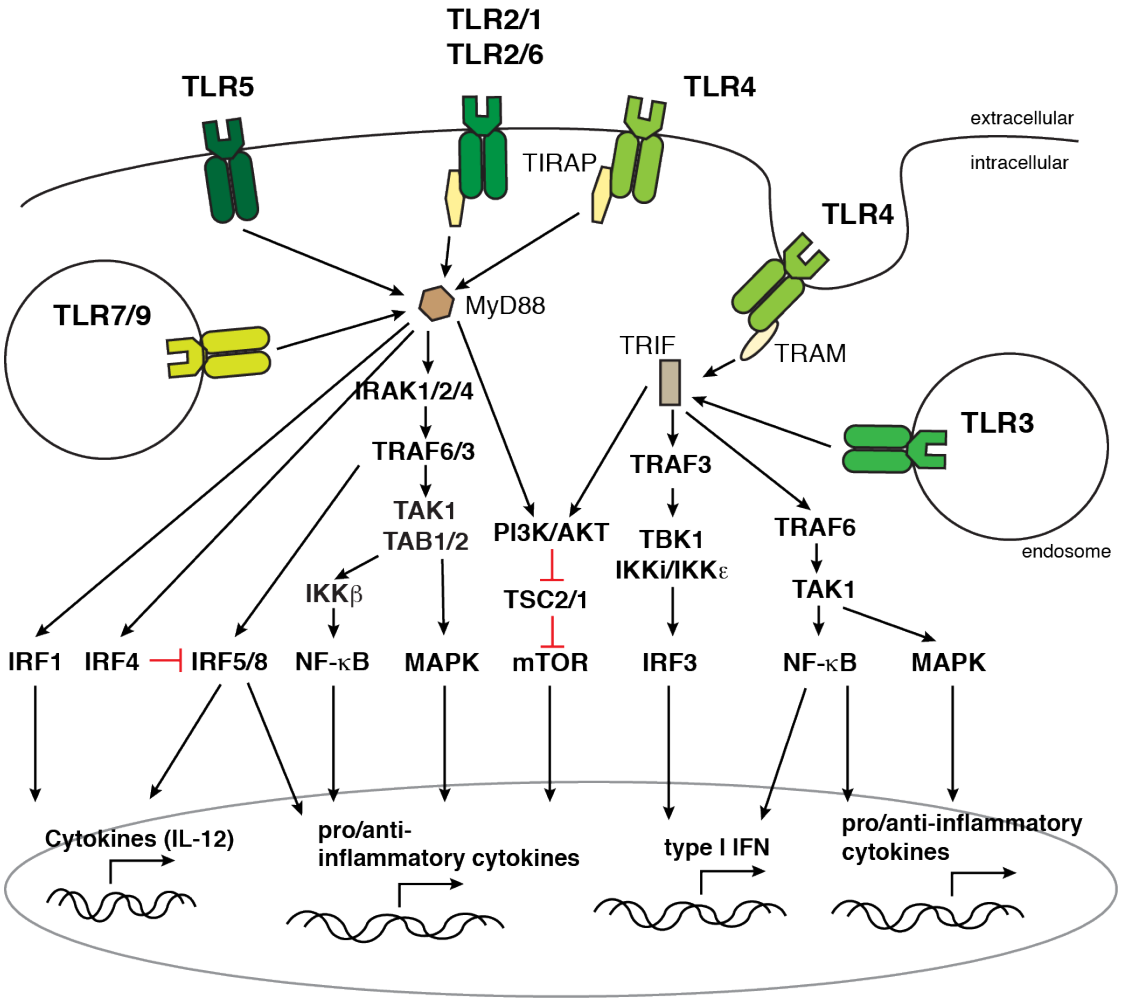

Figure 1.1 Summary of TLR signalling in macrophages.

TLR2, 4 and 5 are localised on the cell surface recognising bacterial motifs such as lipopolysaccharide (TLR4) or peptidoglycan (TLR2), while TLR3, 7 and 9 are expressed in the endosomal membrane and detect mainly nucleic acids from viruses or internalised bacteria. Upon stimulation TLR5, 7 and 9 recruit MyD88, TLR2

recruits MyD88 and TIRAP, TLR3 signals through the adaptor protein TRIF and TLR4 as an exception signals via MyD88, TIRAP, TRAM and TRIF, leading to distinct and overlapping signalling downstream of these adaptors. Adapted from Kawai *et al.* (60), Takeda *et al.* (52) and Ikushima *et al.* (61).

1.3.2.1 MyD88-dependent TLR signalling

MyD88 possesses a C-terminal TIR domain and a N-terminal death domain, and associates with the TIR domain of TLRs with exception of TLR3 (Figure 1.1). Upon stimulation of the TLR, the death domain of MyD88 recruits IL-1 receptor-associated kinase (IRAK) proteins (Figure 1.1 and Figure 1.2). IRAK1 is recruited to the complex and phosphorylated by IRAK4 (62, 63). The IRAK family members are differentially involved between the human and mouse TLR pathways. In mouse, TLR signalling is dependent primarily on IRAK4 and IRAK2, while IRAK1 only plays a little or no role. However, in human macrophages TLR signalling and pro-inflammatory cytokine production is depended on IRAK1 (64). The E3 ligase TNF receptor-associated factor 6 (TRAF6) is then recruited to the receptor complex (Figure 1.1 and Figure 1.2) where it associates with phosphorylated IRAK1 or IRAK2 (60). Phosphorylated IRAK1 and TRAF6 then form a complex with transforming growth factor β activating kinase (TAK) 1, TAK1 binding protein (TAB) 1 and TAB2 at the plasma membrane, which induces the phosphorylation of TAB2 and TAK1. IRAK1 is degraded at the plasma membrane, and the remaining TRAF6/TAK1/TAB1/TAB2 complex translocates to the cytosol leading to the ubiquitination of TRAF6, and activation of TAK1 (63). This is leading to the activation of distinct signalling pathways.

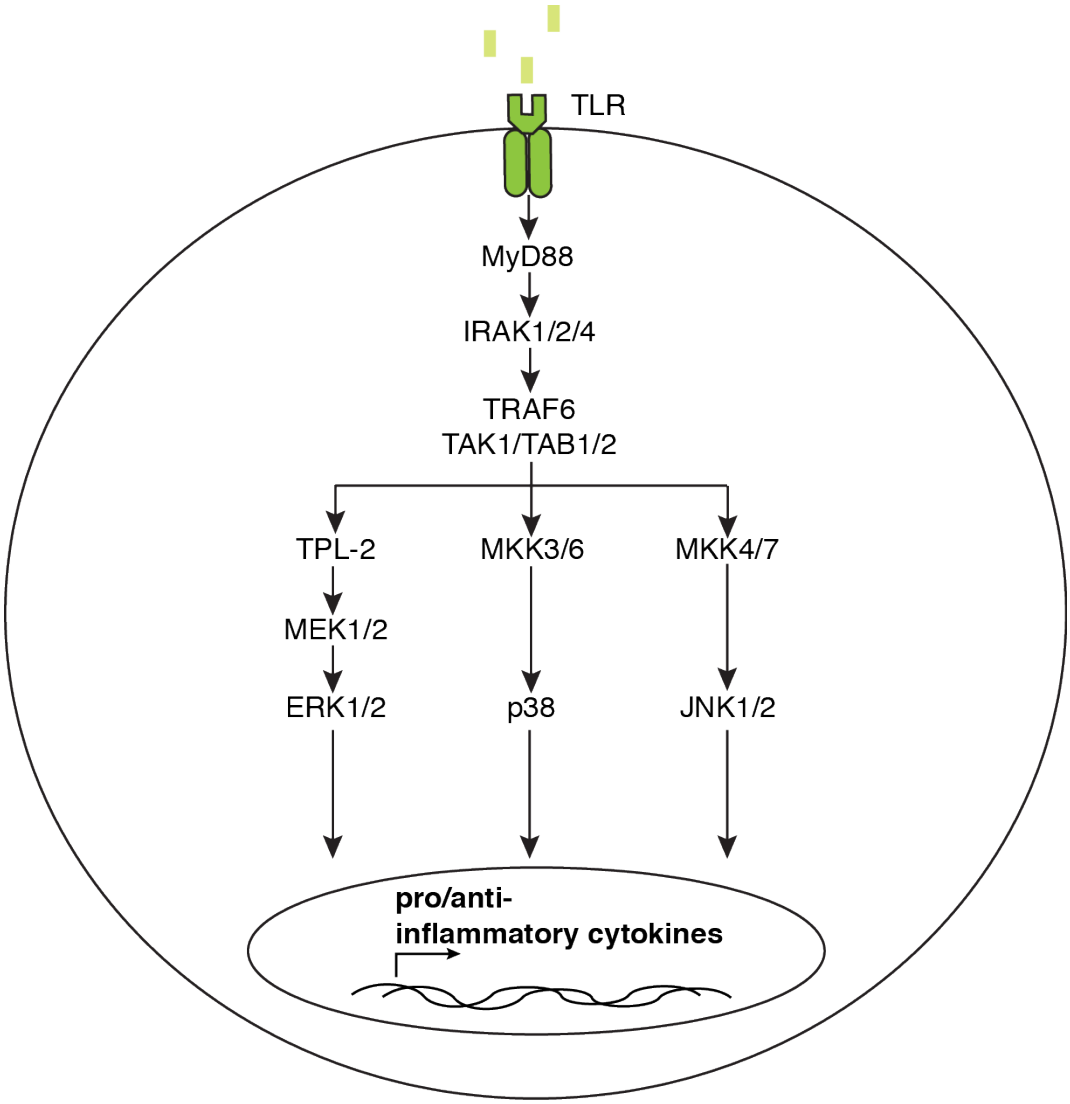

Figure 1.2 Activation of MAPK pathways following TLR stimulation.

Upon TLR ligation MyD88 is activated and interacts with IRAK4, leading to the formation of a complex with IRAK1/2 and TRAF6. TAB1 and 2 then recruit TAK1 to TRAF6, triggering the activation of the ERK1/2, p38 and JNK1/2 pathways. Adapted from Arthur *et al.* (65).

Activated TAK1 triggers the NF-κB pathway through the activation of the IκB kinase (IKK) complex (66) (Figure 1.1). Activated TAK1 modulates IKKβ of the IKK complex which induces phosphorylation and subsequent degradation of IκB, leading to translocation of the TF NF-κB to the nucleus (31, 66, 67). The IKK complex also mediates the activation of tumour progression locus-2 (TPL-2), a MAP 3-kinase,

through proteolysis of the inhibitory NF-κB precursor protein p105 (68). Once activated, TPL-2 phosphorylates the MAP 2-kinases, MEK 1 and 2, which in turn activate the MAP kinases extracellular-signal-regulated kinase (ERK) 1 and 2 (Figure 1.2) (69). This TPL-2/ERK1/2 dependent pathway is important in the regulation of several cytokines including TNF-α and IL-10 but also negatively regulates IL-12 and IFN-β (69-72). Bouhamdan *et al.* showed that ERK1/2 can also be activated independently of MEK1 in the presence of IL-10 and retinoic acid leading to a negative regulation of IL-12, but positively regulates IL-10 production (73).

TAK1 also activates the MAP kinase kinase MKK3/6-p38α/β/γ/δ signalling cascade (Figure 1.2), leading to cAMP response element binding (CREB) nuclear transcription factor activation. Furthermore, it triggers the MKK4/7-Jun N-terminal kinase (JNK) (Figure 1.2) mediated activation of the TF activator protein-1 (AP-1) composed of dimers from the Fos, Jun, activating transcription factor (ATF) and Jun dimerising partner (JDP) protein families (63, 74).

In addition, multiple IRFs are also recruited to the MyD88 and/or TRAF6 complex (Figure 1.1). Members of the IRF protein family, initially identified as transcriptional regulators of the type I IFN system, have been shown to play an important role in the signalling of PRRs. The IRF family consists of nine members, IRF1–9 (61). IRF5 is an important TF for pro-inflammatory gene induction downstream of the MyD88-dependent signalling pathway (75). It interacts with MyD88 and TRAF6 and translocates to the nucleus and binds to ISREs within promoters of target genes such as *Il12b*. Indeed, the induction of pro-inflammatory cytokines, such as IL-12, TNF-α, and IL-6, is impaired in *Irf5*$^{-/-}$ macrophages after stimulation with Poly I:C, LPS,

flagellin, ssRNA, and CpG (75). However, IRF5 interacts with the central region of MyD88, causing the competition with IRF4, which also forms a complex with MyD88 (76). As IRF4 binds to the same region of MyD88 as IRF5, TLR-induced IRF4 competes with and inhibits the sustained activity of IRF5. Hence, IRF4 negatively regulates TLR signalling, as TLR-induced pro-inflammatory cytokines are enhanced in *Irf4*$^{-/-}$ cells (76, 77). IRF4 is also suggested as a negative regulator of TLR-mediated NF-κB activation (77). Another IRF family member, IRF1, directly interacts with MyD88 (78) and induces IL-12 downstream of TLR4 in macrophages (79). IFN-γ strongly induces IRF1. However, IFN-γ signalling itself is not sufficient to fully activate IRF1. Rather, the stimulation of TLR9 leads to post-translational modifications of MyD88-associated IRF1 and its migration into the nucleus (78). IRF8, another IRF family member, modulates inflammatory cytokine production in response to LPS (80). Although IRF8 does not bind to MyD88, it does interact with TRAF6 (80), suggesting that IRF8 functions in the cytosol. The role of IRFs in the TRIF-dependent pathway, will be discussed below.

In TLR2 and 4 stimulated macrophages the TIR domain-containing adaptor protein (TIRAP)/MyD88-adaptor-like (Mal), has been shown to be essential for the MyD88-dependent signalling pathway (81) (Figure 1.1). Furthermore, the MyD88-dependent pathway is also activated downstream of the IL-1 receptor (57).

1.3.2.2 TRIF-dependent TLR signalling

Kawai *et al.* (59) identified a MyD88-independent pathway leading to NF-κB activation in TLR4 stimulated *Myd88*$^{-/-}$ macrophages – the TRIF-dependent pathway.

This pathway is unique to TLR3 and 4 signalling and promotes an alternative pathway that leads to the activation of IRF3, NF-κB, and MAPKs for induction of type I IFN and inflammatory cytokine genes downstream of these receptors (31, 33, 82) (Figure 1.1). TRIF recruits TRAF3, which forms a signalling complex with the IKK proteins TANK-binding kinase 1 (TBK1) and IKKi/IKKε (83-85). TBK1 and IKKi/IKKε are members of the non-canonical IκB kinases that directly activate IRF3 (86), which subsequently forms a dimer and translocates into the nucleus and induces the production of type I IFN in TLR3 and 4 stimulated APCs (87) (Figure 1.1). TRIF is essential for TLR3- and TLR4-mediated IRF3 activation, whereas TRIF-related adaptor molecule (TRAM) is additionally needed as a linker between TRIF and TLR4 to lead to activation of IRF3 via TLR4 (82, 83, 88) (Figure 1.1). In the case of TLR4, TRAF3 is also recruited to MyD88 and the subsequent degradation of TRAF3 is important for MAP kinase activation and pro-inflammatory cytokine production (89). TRIF also binds TRAF6 (90), and together with TNFR-associated death domain protein, receptor interacting protein-1 and the E3 ubiquitin ligase Pellino-1, forms a multiprotein signalling complex that activates TAK-1 (60). Subsequently, the late production of cytokines through NF-κB and MAP kinase pathways is activated (60) (Figure 1.1).

TLR ligation additionally to NF-κB, MAPK and IRF activation also triggers the mammalian target of rapamycin (mTOR) pathway downstream of MyD88 and TRIF (91) (Figure 1.1). This occurs via activation of the Phosphatidylinositol 3-kinase (PI3K)/AKT pathway, in which PI3K becomes activated and recruits the kinase AKT. AKT is then activated by phosphorylation which leads to the downstream inhibition of tuberous sclerosis complex protein 1/2 (TSC2-TSC1), an inhibitor of mTOR

complex 1 (mTORC1) (92). In macrophages, monocytes and mDCs, inhibition of mTORC1 modulates the production of pro- and anti-inflammatory cytokines, confirming its role in innate immune responses (91, 93, 94). Recently Rab8a, a small GTPase, has been shown as a novel regulator of the AKT/mTOR pathway downstream of endosomal TLRs (95).

1.3.2.3 Specificities of TLR4 signalling

TLR4 was the first member of the TLR family to be characterized functionally (96) and it is the only TLR that uses all four adaptor proteins leading to the activation of two distinct signalling pathways — one pathway is activated by the adaptors TIRAP and MyD88, and the second pathway is activated by the adaptors TRIF and TRAM (Figure 1.1) (52). Recently, SLP adaptor and C-terminal Src kinase (CSK)-interacting membrane protein (SCIMP), a non-TIR-containing adaptor, has been described to promote selective pro-inflammatory cytokine responses by direct modulation of TLR4 (97). TLR4 is essential for LPS signalling (98, 99). However, in order to sense LPS from bacteria and promote TLR4 signalling, TLR4 requires a multi-receptor complex comprised of LPS-binding protein (LBP), CD14, and MD-2. LPS binds to LBP which then forms a complex with a glycosylphosphatidylinositol–anchored molecule, CD14. CD14 then transfers LPS to TLR4-bound MD-2, a secreted protein that associates with the extracellular portion of TLR4 (100) leading to dimerisation of TLR4 and subsequent signalling (101, 102). Firstly, ligand engagement of TLR4 at the plasma membrane induces the TIRAP–MyD88 pathway which is followed by endocytosis of the TLR4 into the endosomes where it engages the TRAM–TRIF pathway (103) (Figure 1.1).

CD14 is important for this pathway as it was shown to control endocytosis and the internalisation of TLR4 from the plasma membrane into endosomes (104-106) and therefore TLR4-mediated type I IFN production. CD14-dependent internalisation of TLR4 is dependent on immunoreceptor tyrosine-based activation motif (ITAM) adaptors, the tyrosine kinase Syk, PLCγ2, and the IP3 receptor (104-107). In conjunction with or independently of CD14, factors such as Rab11a and Arf6 have been shown to regulate TLR4 trafficking (108, 109). TLR4 signalling and adaptor engagement are sequential. The movement of LPS to the TLR4 is dependent on CD14 and subsequently leads to the initiation of TIRAP/MyD88 signalling. Consequently, the receptor becomes internalised in a CD14-dependent manner and TRAM/TRIF signalling from endosomes is activated (104). However, MyD88-dependent signalling is only CD14-dependent at low LPS concentrations, whereas activation of the TRIF pathway requires CD14 at all LPS concentrations (110).

Another factor, CD300b has recently been identified as a LPS-binding receptor (111). CD300b together with its adaptor DAP12 associated with TLR4 upon LPS binding leading to the recruitment of Syk and PI3K. Subsequently, ERK1/2 and NF-κB signalling pathways are inhibited, resulting in reduced IL-10 production in CD300b+ macrophages (111).

1.4 The role of IL-12 in the immune response

IL-12, a heterodimeric protein of two subunits (p35 – *Il12a*, p40 – *Il12b*), was first described as natural killer cell stimulating factor (NKSF) by Kobayashi *et al.* in 1989 (112) due to its ability to induce cytotoxic activity, IFN-γ production, and to enhance phytohaemagglutinin (PHA)-induced proliferation of human peripheral blood lymphocytes (112). Independently, Stern and colleagues reported the finding of cytotoxic lymphocyte maturation factor (CLMF) (113), which was later proposed to be called IL-12 and found to be identical with NKSF (114). IL-12 is secreted predominantly by macrophages, monocytes, DCs and granulocytes in response to microbial products (115-117).

The subunit *Il12a* is constitutively transcribed at low levels. However, translation is blocked until cells get stimulated with microbial products like LPS (118). Furthermore, interferon regulatory factors (IRFs) such as IRF1 and IRF8 can increase *Il12a* mRNA expression through binding to appropriate response elements in the p35 DNA sequence (79, 119, 120). The common subunit IL-12p40 (*Il12b*) is highly induced by microbial stimuli such as LPS (121). Regulation of IL-12p40 production mainly occurs on the transcription level. The p40 promotors contain a number of binding sites for several TFs such as NF-kB and ETS (122-124). Kobayashi *et al.* (125) also demonstrated a role for nuclear factor, interleukin 3 regulated (NFIL3) as a negative regulatory TF in macrophages, controlling IL-12p40 production induced by bacterial products and the enteric microbiota (125). The activation of most TLRs leads to the induction of IL-12p40, while IL-12p35 expression is mainly induced upon TLRs 3, 4 and 8 ligation (119, 126, 127). Moreover, IFN-γ can maintain high levels of IL-12p70 by both DCs and macrophages in the course of an immune response (128).

Furthermore, IL-12 production of DCs can be augmented by interaction of T cells with APCs via CD40/CD40L (129, 130). The co-expression of both subunits, p35 and p40, yields to the formation of the biologically active p70 compound (112). This differential regulation also contributes to balancing the secretion of the different members of the IL-12 family (131) which additionally to IL-12 also includes IL-23, IL-27 and IL-35 (132). All cytokines in this family are heterodimeric, and subunits are shared between family members. For example, p40 is also a component of IL-23 when bound to p19 (133), and p35 is a component of IL-35 when bound to Ebi3 (134, 135). Ebi3 additionally dimerises with p28 to form IL-27 (136).

Activated T and NK cells are the main cell types that express the IL-12 receptor and therefore respond to this cytokine (137). The IL-12 receptor is composed of two subunits, IL-12Rβ1 and IL-12Rβ2 (138). Signalling via the IL-12R depends on janus kinase (JAK) 2 and tyrosine kinase (TYK) 2 (139) and leads to the activation of STAT family members STAT1, STAT3, STAT5 and, in particular, STAT4 (140, 141). STATs are phosphorylated by JAK2 and are then able to form homo- or heterodimers and translocate to the nucleus where they can regulate gene expression (139, 141) mainly of IFN-γ in T and NK cells (142). STAT4 plays a very central and non-redundant role in the IL-12 signalling cascade as has been demonstrated in different animal models. For instance, STAT4 deficient mice lack IL-12-mediated T_H1 differentiation, IFN-γ induction or NK cytolytic function (143, 144).

The action of IL-12 on T cells and NK cells has several effects. IL-12 promotes differentiation of naive CD4 T cells into IFN-γ–producing T_H1 cells. (116, 145, 146). Importantly, the synergy of IL-12 with other activation signals such IL-2 and in the

case of T cells, T cell receptor/CD3 and CD28 signalling, ensures robust IFN-γ production from these cells (147). Additionally, IL-12 promotes NK cell and CD8+ cytotoxic T lymphocyte proliferation and cytotoxic potential by stimulating production of granzymes and perforins. IL-12 can also drive IFN-γ production from NK cells (112) (148). Moreover, B cells are prompted to particularly secrete antibody isotypes associated with T_H1 responses in response to IL-12 signalling (147). On the other hand, IFN-γ is a potent activator of macrophages (149), which possess many antimicrobial effector functions (23). This results in an enhancement of phagocytic function and local inflammation (150). Thus, this network forms a positive feedback loop where macrophage or DC derived IL-12 drives the differentiation of T_H1 cells to produce IFN-γ which further activates effector mechanisms of the innate immune system. Consistent with these implications in mainly cellular immune responses, mice where IL-12p35 or IL-12p40 genes have been deleted, display greater susceptibility to infections with intracellular pathogens such *as Toxoplasma gondii* (151, 152) and *Listeria monocytogenes* (153) or the acid-fast bacillus *Mycobacterium tuberculosis* (154) than wild-type (WT) mice. Interestingly, there is evidence that the immune defect in p40-deficient animals is more pronounced than in p35 deficient counterparts, which matches to the appearance of p40 as constituent of both IL-12 and IL-23 (150). Additionally, mutations in the IL-12/IFN-γ axis in humans have been shown to increase susceptibility to tuberculosis (155). However, in comparison to intracellular bacterial and parasitic infections, IL-12 may have less of an important role in generating protective immune responses against viral infections. In a murine model of flu, IL-12p40 blockade reduced IFN-γ production, but only at early time points (156). In a model of murine lymphocytic choriomeningitis virus (LCMV) infection, IL-12p35 deficient mice had no defect in the generation of anti-viral

responses (157). Furthermore, in experimental models of intestinal inflammation members of the IL-12 family play a central role (158). In this context, Ustekinumab, a therapeutic agent targeting p40 and hence, both IL12 and IL-23, was recently approved to treat psoriasis and psoriatic arthritis, and related agents are in clinical testing for a variety of inflammatory disorders. The difference in IL-12– and IL-23–dependent signalling is due in part to the preferential activation of STAT4 by IL-12 and of STAT3-dependent target genes by IL-23 (159).

Taken together, IL-12's hallmark is the induction of IFN-γ production, therefore enhancing immune system activation, bridging both innate and adaptive cell-mediated immune responses. However, pro-inflammatory immune responses, including those driven by IL-12, can be harmful to the host and give rise to infection induced immunopathology or autoimmunity if not appropriately regulated (160). It is therefore critical that these pathways are controlled in order to provide protection to the host.

1.5 The role of IL-10 in the immune response

1.5.1 Cellular sources of IL-10

IL-10 was first characterised by Fiorentino *et al.* as a 'cytokine synthesis inhibitory factor' (CSIF) which was secreted from a murine T_H2 clone and inhibited the synthesis of several T_H1 cytokines such as IFN-γ (161). IL-10 was then found to also inhibit pro-inflammatory cytokine production from macrophages (162) and to mediate its inhibitory effect through the dampening of APC activity (163, 164). IL-10 is now considered an anti-inflammatory cytokine with a crucial role in limiting the immune response to pathogens and preventing immune pathology (165). It is a homo-dimeric cytokine and the founding member of the IL-10 family of cytokines including IL-19, IL-20, IL-22, IL-24, IL-26, IL-28A, IL-28B and IL-29. IL-10 is the only member of the IL-10 family with a clearly established anti-inflammatory activity (166). IL-10 has been shown to be produced by many cells of the innate as well as the adaptive immune system such as macrophages, myeloid DCs (but not plasmacytoid DCs) (71, 167, 168) and natural killer cells, neutrophils, eosinophils, mast cells as well as $CD4^+$ T_H1, T_H2, T_H17, T_{reg} cells, $CD8^+$ T cells and B cells (160, 165, 169, 170). The recognition of PAMPs through TLRs on APCs results into the production of IL-10 and will be further discussed in chapter 1.6. The interaction of T_{reg} cells, B cells and neutrophils with DCs then promotes IL-10 production by these cells and thereby suppressing the immune response (171). IL-10 has a short half-life and short range of activity (170).

1.5.2 IL-10 signalling and gene targets of IL-10

IL-10 mediates its anti-inflammatory properties via the IL-10 receptor which is expressed on most haematopoietic cells. The highest level of expression is on macrophages and DCs (172), resulting in the highest effect on these cells. The IL-10 receptor consists of IL-10R1 (173) and IL-10R2 (174) subunits. IL-10R1 is specific for the binding of IL-10 and its expression is restricted mainly to immune cells and particularly highly on monocytes and macrophages (175), whereas IL-10R2 is widely expressed and binds IL-10 only after IL-10 binds to the IL-10R1 (176). However, IL-10R2 is critical for the signal transduction (174). IL-10R2 is also used in the signalling of IL-22, IL-26, IL-28A, IL-28B and IL-29 (166). Binding of IL-10 to IL-10R1 leads to conformational changes in IL-10 allowing its association with the IL-10R2 forming the IL-10/ IL-10R complexes (176).

IL-10 signalling leads to the activation of JAK1 and TYK2 receptor associated tyrosine kinases and subsequent activation of STAT3, which is known to be essential for all known functions of IL-10 (160). Other STATs can be activated downstream of the IL-10 receptor (160), such as STAT1 in human monocytes (177), however STAT3 is considered most important for the immunosuppressive activity of IL-10 (178, 179). Phosphorylated STATs translocate as homodimers or heterodimers into the nucleus and regulate the expression of a number of different genes. Additionally, IL-10 can also activate the PI3K-AKT-GSK-3 signalling pathway which leads to the suppression of inflammatory gene expression (180).

Importantly, in macrophages and DCs IL-10 regulates only subsets of genes induced by TLR ligation primarily at the level of transcription (172, 179, 181). For example, in

human monocytic cells, it was demonstrated that IL-10 can inhibit TNF-α production by binding either to the 5' promoter region (transcriptional mechanism) or the 3' UTR (post-transcriptional mechanism) (182). More recently, in human macrophages, Smallie *et al.* showed that IL-10 inhibits TNF-α production by inhibiting the elongation of the *Tnf* transcript (183). IL-10 also inhibits the transcription of *Il12b* (IL-12p40) via the TF NFIL3 (184, 185) and *Il12a* (IL-12p35) (185). Additionally, it was shown that histone deacetylation on the *Il12b* promoter by HDAC3 was IL-10 driven in macrophages (186). Other downstream targets of IL-10 that may be involved in mediating its anti-inflammatory effects are the transcriptional repressors Ets variant 3 (ETV3) and Strawberry notch homologue 2 (SBNO2) (187). Hutchins *et al.* proposed in a genome-wide study over 40 additional transcription factor targets of IL-10 signalling (188). Furthermore, there is also evidence that IL-10 regulates target genes post-transcriptionally as IL-10 mediated expression of microRNA-187 has been shown to directly negatively regulate TNF-α production in human monocytes (189). Recently, Ip *et al*. showed that mTORC1 inhibition by IL-10 is required for the autophagic clearance of dysfunctional, ROS-producing mitochondria. Therefore, IL-10 signalling prevents the accumulation of dysfunctional mitochondria in macrophages which would result in the activation of the NLRP3 inflammasome and production of IL-1β (190).

1.5.3 General role of IL-10

As a potent immunosuppressive cytokine, IL-10 exerts its inhibitory function at different levels by acting directly and indirectly on both the innate and adaptive arms of the immune response (170). IL-10 primarily leads to a down-regulation of activator

function of macrophages and DCs (160, 162-164). Indirectly, this mechanism inhibits the adaptive immune response including T cell responses. By acting on DCs and macrophages IL-10 inhibits the development of T_H1- and T_H2-type responses. IL-10 also leads to an increased differentiation of IL-10 producing T_{reg} cells forming a positive feedback loop for its production (165, 172, 181). It was also shown that IL-10 can act directly on different CD4+ T cell subsets. T_H17 cells were found to express the IL-10 receptor, and inhibition of IL-10 receptor activity specifically on these cells leads to an increase in pro-inflammatory IL-17A expressing effector T cells (191). It also has been shown that IL-10 acts on T_{reg} cells (192, 193) whose function is promoted by IL-10 through maintenance of their FOXP3 expression. However, positive effects of IL-10 such as the activation of mast cells, NK cells and CD8+ T cells have also been shown (160, 165). Furthermore, IL-10 can promote the humoral immune responses by enhancing class II expression on B cells in mouse and man and inducing immunoglobulin (Ig) production, particularly in the human system (160, 170).

1.5.4 The role of IL-10 in disease

IL-10 is expressed by many different cells types and also exerts various different effects. Consistent with this notion, IL-10 has many implications in disease. IL-10 can be beneficial to the host in the case of an exuberant pro-inflammatory immune response which might lead to damage of the host such as in septic shock, where inflammatory mediators can drive multi-organ failure and even death during severe bacterial infections (194). It was demonstrated that IL-10–deficient mice have an enhanced susceptibility to septic shock (195) while the treatment of mice with IL-10

protects them from LPS-induced shock (196). Additionally, IL-10 was shown to prevent immunopathology during infections with *Plasmodium chabaudi chabaudi* (197), and *T. gondii* (198, 199) with IL-10 from T_H1 cells being the source of protection (200, 201). Furthermore, a protective effect of IL-10 against immunopathology was also seen in *Trypanosoma cruzi* (202) and *Helicobacter hepaticus* infections (203). IL-10 also plays a role in the protection against inappropriate inflammatory responses to commensal microorganisms in the gut. In humans, polymorphisms in the *Il10* locus as well as mutations in genes encoding the IL-10 receptor chains (*Il10ra* and *Il10rb*) confer increased risk for inflammatory bowel disease, including ulcerative colitis and Crohn's disease (204, 205) (206). IL-10-deficient mice develop colitis (207) due to an increased T_H1 response (208). In line, it was shown that T cells are an important source of protective IL-10 in this context (209). Last but not least, IL-10 may also have a protective role in allergic asthma (210).

However, not every immune response has the potential to cause damage. Hence, the inappropriate production of IL-10 can inhibit an adequate clearance of an infection. In the mouse model of *L. monocytogenes* (211) and *M. tuberculosis* (212) infection, IL-10 deficiency enhanced protection to the infection. In line, Moreira-Teixeira *et al.* showed recently that IL-10, derived from T cells, renders mice more susceptible to *M. tuberculosis* infection (213). Additionally, *L. major* infected, IL-10-deficient mice were able to completely clear infection whereas WT mice developed a chronic infection (214, 215). In the context of vaccination, the generation of a strong immune response is also anticipated; hence, the production of IL-10 during vaccination may be disadvantageous (216). In support of this idea, Pitt *et al.* showed

that blockade of IL-10 signalling at the time of BCG vaccination could enhance vaccination efficacy, with a subsequent reduction in the bacterial load after *M. tuberculosis* challenge (217).

IL-10 has also been shown to play a role in autoimmune diseases. On the one hand IL-10 may be protective in rheumatoid arthritis (218), psoriasis (219) and multiple sclerosis (220, 221). On the other hand, IL-10 has been suggested to promote systemic lupus erythematosus (SLE) (222) and in humans, IL-10 polymorphisms have been associated with the development of SLE (223).

The role of IL-10 in anti-tumour immune responses is unclear and the heterogeneity of cancer as a disease may contribute to varying roles of IL-10 in anti-tumour immune responses (216).

1.6 Regulation of IL-10 production in macrophages

Cells within the innate immune system require activation of PRRs to produce IL-10 (165). IL-10 production by macrophages, amongst other cytokines, is induced by TLRs via the MyD88-dependent and TRIF-dependent pathways (Figure 1.3) (167). Stimulation of TLR4 leads to an activation of both signalling pathways and, importantly, optimal IL-10 production through TLR4 signalling requires the activation of both, the MyD88 and TRIF-dependent pathways (Figure 1.3) (167).

The *Il10* gene is located within the *Il10* gene family cluster on Chromosome 1 (224). It is flanked upstream by *Il19*, *Il20* and *Il24*, other members of the IL-10 family of cytokines. Downstream of the *Il10* gene is the *Mapkapk2* (Mitogen–activated protein (MAP) kinase-activated protein kinase 2) gene. The *Il10* gene itself spans around 5 kb in total and consist of 5 exons and 4 introns which are followed by a 3' untranslated region (UTR). Human and mouse *Il10* gene loci are highly homologous with a number of conserved non-coding sequences (224).

IL-10 production is regulated at different stages such as chromatin remodelling at the *Il10* locus, transcriptional regulation of *Il10* mRNA expression and post-transcriptional regulation of *Il10* mRNA. Some characteristics of *Il10* gene regulation are conserved between various immune cell types, while others are cell type- or stimulus-specific. Here, we outline, how, *Il10* expression is regulated at the level of signal transduction, chromatin remodelling, transcription factor binding and gene activation in macrophages (165).

1.6.1 The induction of IL-10 production by PRRs in macrophages

TLR signalling via MyD88 and/or TRIF leads to activation of MAPKs, PI3K/AKT and NF-κB as well as IRFs (Figure 1.3) (31, 60). It has been shown that the activation of ERK1/2 is critical for the production of IL-10 in TLR2, 4 and 9 activated macrophages and mDCs (70, 71, 225, 226), and in *M. tuberculosis* infected macrophages and monocytes (72). This is in line with studies showing that differences in IL-10 production in macrophages, mDCs and pDCs correlate with their level of ERK1/2 activation in response to a common TLR-ligand (71). This is supported as well by the fact that macrophages deficient in TPL-2 (71) or NF-κB (70), upstream activators of ERK1/2, show lower IL-10 expression compared to WT macrophages. However, NF-κB regulates IL-10 via ERK-dependent and independent mechanisms (70).

Saraiva *et al.* showed an NF-κB binding site at HSS −4.5 kb upstream of the *Il10* TSS and recruitment of the NF-κB subunit p65 in TLR4 stimulated macrophages (227), while Chakrabarti *et al.* reported an additional site in the *Il10* promoter in dsRNA stimulated macrophages (228). Additionally, p105 (70) as well as p50 (229) have also been shown to promote IL-10 production in macrophages.

The MAP kinase p38 has also been shown to positively regulate IL-10 production in LPS and CpG stimulated macrophages (Figure 1.3) which involves the activation of downstream kinases MSK1 and MSK2 (230). As both, ERK and p38, contribute to the activation of MSK1 and MSK2, which in turn promote IL-10 production in macrophages, ERK and p38 may also cooperate in their regulation of IL-10 production (Figure 1.3) (230). ERK1/2 and p38-dependent IL-10 production is furthermore negatively regulated by IFN-γ, as IFN-γ induces the release of glycogen

synthase kinase 3 (GSK-3) by blocking phosphoinositide 3-kinase (PI3K)-Akt activation. GSK-3 then antagonises the binding of activator protein1 (AP1) and CREB to the *Il10* promoter (231, 232). p38 activation also increases *Il10* mRNA transcript stability upon TLR4 ligation by protecting it from rapid degradation induced by the RNA binding protein tristetraprolin (233, 234).

Not much is known about the role of the third MAP kinase, JNK, but there are reports suggesting a positive effect on IL-10 production in TLR stimulated macrophages and monocytes (231) (228).

The PI3K-AKT pathway was additionally proposed to contribute to IL-10 production in macrophages, monocytes and mDCs (Figure 1.3) (93, 94, 235). PI3K activates ERK and therefore might promote IL-10 production (235). However, PI3K also inhibits GSK-3β in macrophages (94, 236), which inhibits the production of IL-10 by antagonising the DNA binding activity of CREB (232). Furthermore, the PI3K-AKT pathway also leads to the activation of mammalian target of rapamycin (mTOR) (93, 94) as well as the activation of mTOR by p38 (237), which also promotes IL-10 production. However, recently Hayashi *et al.* (238) showed a negative role of the subunit p85α of PI3K in the production of IL-10 in intestinal macrophages in the DSS-induced acute colitis model using BALB/c mice as well as in LPS stimulated BMDMs. Additionally, IL-10 itself feeds back to dual-specificity protein phosphatase 1 (DUSP1), which negatively regulates p38 phosphorylation and therefore modulates the activity of the TTP leading to a decrease in IL-10 production (239, 240). On the other hand, IL-10 positively feeds back to up-regulate *Tpl2* expression (179).

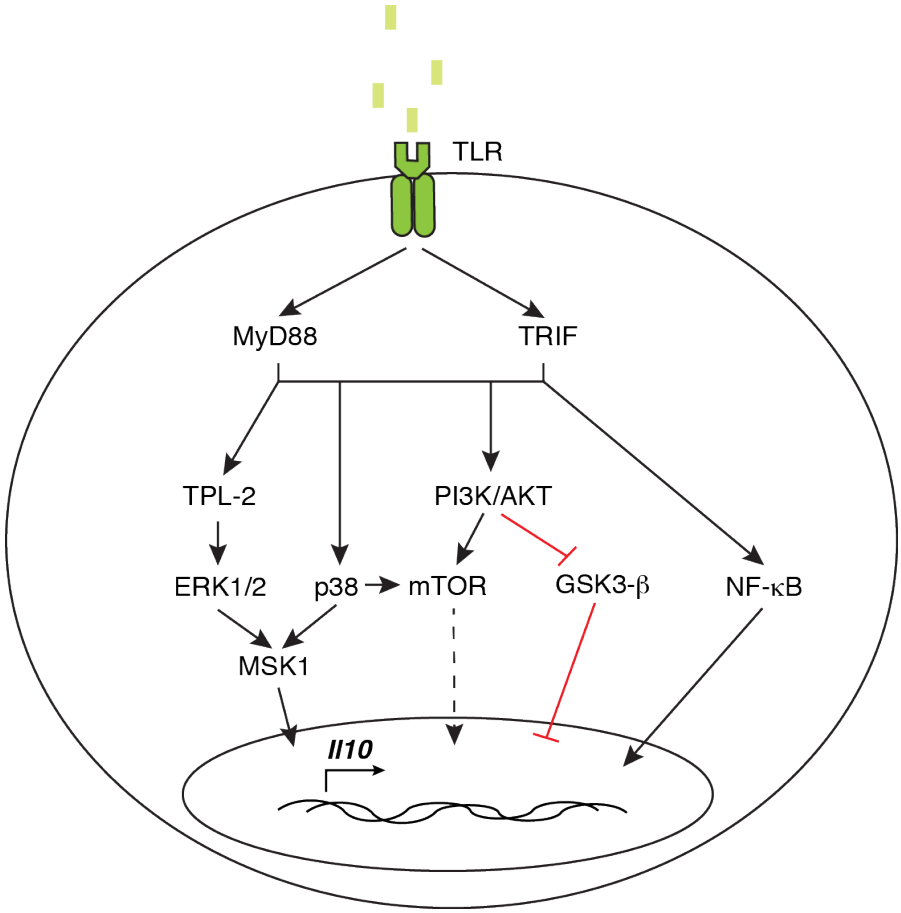

Figure 1.3 Signalling molecules involved in the regulation of IL-10 production in macrophages

Il10 mRNA expression is induced downstream of PRRs like TLRs and depends on MyD88 and TRIF adaptor proteins which collectively lead to the activation of the NF-κB pathway, MAP kinases (ERK1/2, p38), the PI3K/AKT/mTOR pathway and IRFs (not shown here). Importantly, several of these pathways also lead to the induction of pro-inflammatory cytokines. Adapted from Gabrysova *et al.* (241).

1.6.2 The involvement of chromatin modifications in the regulation of IL-10

Changes in chromatin structure at the *Il10* gene locus are fundamental to the regulation of its production (227, 242). The initial event leading to *Il10* transcription is chromatin remodelling. Remodelling of the *Il10* locus occurs following TLR ligation (227). Additional signals are then necessary to allow increased IL-10 production.

Factors that influence the accessibility of chromatin include DNA methylation, nucleosome remodelling and covalent histone modification such as acetylation or methylation mediated by histone acetyl transferases (HATs), histone deacetylases (HDACs) or histone methyl transferases (HMTs). These enzymes alter histone 'tails' to form repressive or active marks, remodelling the chromatin from high density transcriptionally inactive heterochromatin to low density transcriptionally active euchromatin and vice versa thus governing gene expression (243). Histone modifications have been reported to be associated with various functional elements such as promoters or distal regulatory elements (enhancers or insulators) (244). In IL-10 producing macrophages, an increased level of epigenetic imprinting, measured by histone acetylation, was demonstrated (227). It was observed that histones of macrophages producing high levels of IL-10 show highly acetylated H4 (active mark) (227). Along with that, it was shown that HDAC11 gets recruited to the *Il10* promoter to negatively regulate its expression (245). In contrast, HDAC6 is required for *Il10* transcriptional activation in APCs and physically interacts with HDAC11 leading to dynamic changes in the expression of *Il10* (246). Additionally, histones at the *Il10* locus were also reported to be hyper-phosphorylated (247, 248) and ERK dependent phosphorylation of serine 10 on histone H3 correlates with high IL-10 production (247). These histone modifications enhance the accessibility of the *Il10* promoter, providing a permissive chromatin structure for the binding of TFs such as SP1 (247, 248). In macrophages five DNaseI hypersensitivity sites were found at positions −4.5, −2, −0.12 kb upstream and +1.65 and +2.98 kb downstream of the *Il10* TSS, however just one regulatory element (HSS-4.5) was macrophage- and DC-specific (Figure 1.4) (227).

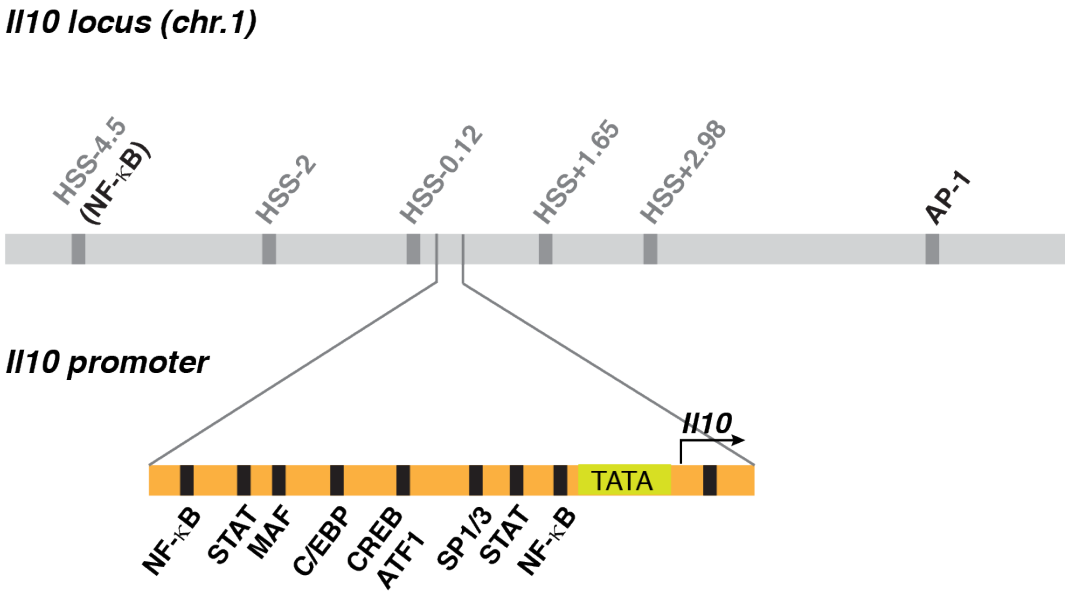

Figure 1.4 Regulation of *Il10* expression in macrophages on the molecular level: *Il10* locus and promoter.

Representation of the mouse *Il10* locus and promoter on chromosome 1 with DNase hypersensitivity sites (HSS) (grey bars) and transcription factor binding sites (black bars). HSS-4.5 contains an NF-κB binding site. Direct transcription factor binding has not yet been shown for all of the indicated motifs. Adapted from Saraiva *et al.* (165) and Gabrysova *et al.* (241).

1.6.3 Involvement of transcription factors in the regulation of IL-10

The enhancement or silencing of *Il10* transcription also depends on various TFs (165). TFs so far shown to be involved in the positive regulation of IL-10 in macrophages and DCs include SP1 (249), SP3 (250), CREB-1 and ATF-1 (230, 251), c-Fos (71), c-Maf (252), STAT1, STAT3 (253) and NF-κB (229) (as described before in 1.6.1) (Figure 1.4).

In TLR stimulated macrophages and mDCs, the TF c-FOS has been associated with the ERK-dependent positive regulation of IL-10 (71, 225, 231). C-FOS is a member of the activator protein 1 (AP-1) family which is composed of dimers of Fos, Jun, Jun

dimerising protein (JDP) and activating TF (ATF) members (74). In line with these findings, an AP-1 consensus binding site has been shown within a conserved non-coding sequence ~1 kb downstream of the *Il10* gene in T cells (Figure 1.4) (254).

In addition to the activation of AP-1 in macrophages, ERK-dependent phosphorylation of histone H3 at sites across the *Il10* promoter (247, 248) leads to increased accessibility of the *Il10* promoter, allowing the binding of TFs such as the constitutively expressed specific protein 1 (SP-1) (Figure 1.4) (247, 248). SP-1 was shown to be a central mediator in the IL-10 production in LPS stimulated macrophages (249). SP-3 has also been reported to bind at the *Il10* promoter and leading to a positive regulation of *Il10* mRNA transcription in the Drosophila SL2 cell line (250). However, in a TLR4 stimulated human monocytic cell line, p38 was shown to regulate LPS-induced activation of Sp1, but not ERK1/2, which was important to regulate the transcription of the hIL-10 gene in this system (255). Additionally, downstream of p38, the pre-B cell leukaemia homeobox 1 (PBX1) and PBX-regulating protein 1 (PREP1) are implicated in the expression of IL-10 production in response to apoptotic cells (256).

The TFs cyclic adenosine monophosphate (cAMP) response element-binding protein (CREB) and ATF1 have been shown to be activated by MSKs in LPS stimulated macrophages and were found to bind the *Il10* promoter (Figure 1.4) (230). This has been confirmed in a cAMP-treated human monocytic cell line, where CREB and ATF1 bound at the *Il10* gene locus and activated the *Il10* promoter (251). Furthermore, the complexing of NF-κB p50 homodimers with the coactivator CREB-

binding protein (CBP) further enhances *Il10* promoter activity (229). Other NF-κB subunits are involved in *Il10* gene regulation and have been discussed in 1.6.1.

Another kinase, mTOR, also increases the production of IL-10 via the activation of the TF STAT3 (93), which binds at a STAT consensus site within the proximal *Il10* promoter, important for activation of the *Il10* gene (Figure 1.4) (253). However, STAT3 activation also occurs downstream of the IL-10 receptor (172) and a direct role for STATs was suggested, as IL-10 induces its own expression in human monocyte-derived macrophages in an autocrine manner through the activation of STAT3 (257). Therefore, STAT3 might regulate IL-10 downstream of PRR stimulation in an mTOR-dependent manner, or/and downstream of autocrine IL-10 signalling.

Another TF that has been implicated in the positive regulation of *Il10* gene expression is c-MAF (Figure 1.4) (252). c-MAF is upregulated upon LPS and IL-4 stimulation in monocytes/macrophages and binds at the *Il10* promoter and enhances IL-10 production (252). Furthermore, the *Il10* promoter harbours several CCAAT/enhancer binding protein (C/EBP) sites (Figure 1.4) (258) to which C/EBPs can bind as homo- or heterodimers. Roles for C/EBPβ and C/EBPδ in cooperation with Sp1, have also been identified in the regulation of *Il10* mRNA in a murine macrophage cell line stimulated with TLR4 agonist (259). The ligand-activated TF aryl hydrocarbon receptor (AHR) was also reported to be required for maximal production of IL-10 in TLR4 but not TLR9 stimulated macrophages (260).

In contrast, MHC class II transactivator (CIITA) was shown to have a negative regulatory effect on expression on the *Il10* promoter in a mouse macrophage cell line (261). Furthermore, IRF5 has been shown to be recruited to the IL-10 promoter and directly negatively regulate IL-10 production in human monocytes (262).

1.6.4 Modulation of IL-10 by autocrine and paracrine factors

IL-10 is regulated by autocrine and paracrine regulatory loops. As already described in 1.6.1, IL-10 can inhibit its own production by inducing the production of the dual phosphatase DUSP1 (239), as well as the production of TTP which destabilises *Il10* mRNA (263, 264). However, IL-10 can also induce the production of *Tpl2*, which leads to an increase in *Il10* mRNA transcription (70, 71).

Recently, Lee *et al.* (265) identified a novel regulator of IL-10 production in macrophages, the selenoprotein MsrB1. *MsrB1*$^{-/-}$ macrophages show reduced *Il10* mRNA expression upon LPS stimulation. It was postulated that MsrB1 function is based on its reductase activity.

It has further been reported that IL-27 is important for the maximal induction of IL-10 in response to type I IFN in TLR4 stimulated murine macrophages (266). However, another study reported that resting murine macrophages are unresponsive to IL-27 (267). Furthermore, in our study (268) as well as in the study by McNab *et al.* (269), no effect of IL-27 on IL-10 production in macrophages was observed. Thus, the role of IL-27 in the regulation of IL-10 remains incompletely understood. In contrast, in TLR2 stimulated human macrophages, IFN-γ has been shown to inhibit the

production of IL-10 through the inhibition of the PI3K/AKT pathway (231). This led to the enhancement of GSK-3β activity and therefore to a suppression of the TFs AP-1 and CREB activity (231).

Furthermore, endogenous and exogenous type I IFNs can enhance IL-10 production from macrophages and DCs. This was first shown in LPS stimulated human monocytes where the addition of high concentrations of IFN-α enhanced IL-10 production (270). Subsequently, it was shown that type I IFN signalling is important for maximal IL-10 production in LPS stimulated macrophages (271) as well as in *M. tuberculosis* infected macrophages (269, 272) and as recently reported for TLR-activated microglia (273). Potential mechanisms of how type I IFN enhances IL-10 production in PRR stimulated cells have been described. Guarda *et al.* demonstrated that the activation of STAT1 downstream of the type I IFN receptor in LPS stimulated macrophages leads to an increase in IL-10 (274), while in human DCs Wang *et al.* showed the activation of the PI3K/AKT pathway leads to the inhibition of GSK-3β and subsequent increase in IL-10 (275). Furthermore, in human B cells binding of IRF1 and STAT3 to the *Il10* promoter was reported (276).

1.7 The role of type I IFN in the immune system

Type I IFNs consist of many different IFNs with structural homology such as IFN-α (13 different subtypes in human, 14 in mice), IFN-β and other type I IFNs that are less well characterised such as IFN-δ, IFN-ε, IFN-κ, IFN-τ, IFN-ζ and IFN-ω. IFN-δ and IFN-τ are only described in pigs and cattle and do not have a homologue in humans (277). Type II IFN (IFN-γ) and type III IFNs (IFN-λ1, IFN-λ2, IFN-λ3, IFN-λ4 (278)) also contribute to the broader family of IFNs (277).

1.7.1 Cellular sources and targets of type I IFN

A diverse range of cells produces type I IFNs, including most immune cells (279). All type I IFNs bind to a common heterodimeric transmembrane receptor, the type I IFN receptor that is composed of 2 distinct subunits: the IFNAR1 and IFNAR2. IFNAR1 is constitutively associated with TYK2, while IFNAR2 is associated with JAK1 (Figure 1.5). Upon ligation of the receptor these kinases get auto-phosphorylated. Activated JAK1 and TYK2 subsequently phosphorylate STAT molecules that are present in the cytosol. STATs that are activated in response to type I IFNs are STAT1, 2, 3 and 5 (280). After phosphorylation activated STAT1 and STAT2 form heterodimers and translocate to the nucleus where they initiate transcription of IFN-stimulated genes (ISGs) (280). The most important transcriptional complex that is induced is the STAT1-STAT2-IRF9 complex, known as IFN-stimulated gene factor 3 (ISGF3) (Figure 1.5). This complex then binds to IFN-stimulated response elements (ISREs) to initiate gene transcription. This leads to the expression of several hundred ISGs, a large number of which function to induce an antiviral state within the cell (280). Wang *et al.* (281) recently reported a novel phosphorylation site of STAT2 on T387

which leads to a negative regulation of this response and is constitutively phosphorylated in untreated cells. Upon type I IFN stimulation other additional STAT complexes, specifically STAT1 homodimers, can form (Figure 1.5), translocate to the nucleus and bind to γ-activated sequences within DNA to regulate gene expression (282). In addition to JAK/STAT signalling, MAPKs are activated downstream of the type I IFN receptor including ERK2 (283) and p38 (284), although the first has been less well documented (Figure 1.5). p38 can generate IFN-mediated signals independent of STATs (284). Type I IFNs also activate PI3K signalling downstream of JAKs in an IRS-dependent but STAT-independent manner leading to activation of mTOR (Figure 1.5) (280).

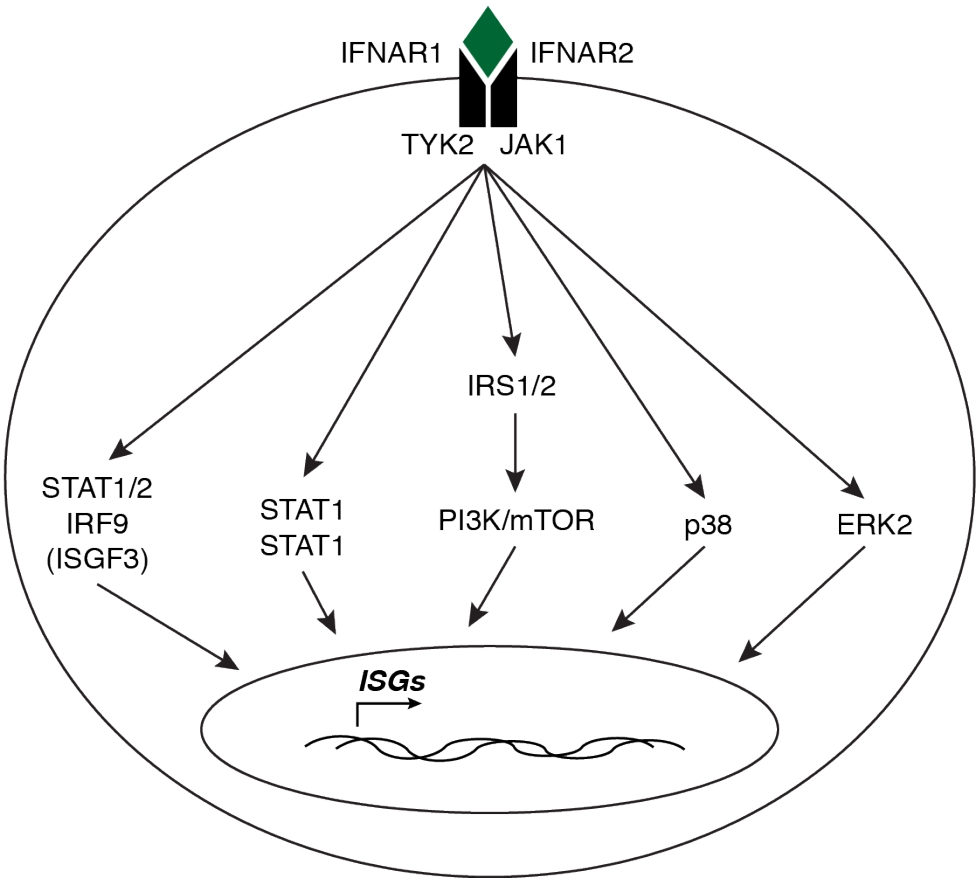

Figure 1.5 Type I IFN signalling.

Various downstream signalling pathways are induced upon the binding of type I IFN to its receptor leading to the transcription of interferon inducible genes (ISGs). The IFN-stimulated gene factor 3 (ISGF3) complex binds to IFN-stimulated response elements in gene promoters, leading to induction of a large number of ISGs. Additionally, type I IFNs can also signal through STAT1 or other STAT homodimers. Independent of the JAK/STAT activity, type I IFN signalling activates p38, ERK2 and PI3K pathways. Adapted from McNab *et al.* (285).

This diversity of signalling pathways leads to the transcription of a wide range of genes including genes that encode cytokines and chemokines, antibacterial effectors, pro-apoptotic and anti-apoptotic molecules, and molecules involved in metabolic processes (286). Hence, the type I IFN response has several intracellular ‘‘check-points’’ and the regulation of its pathway is achieved by targeting signalling pathways leading to its expression, the transcription of ISGs, and the function of IFN-regulated proteins that they encode (287). Mechanisms involved in these processes including the induction of the regulatory proteins suppressor of cytokine signalling (SOCS) (288) and ubiquitin specific peptidase (USP)18 (289, 290). SOCS proteins are known to target the JAK/STAT pathway, thereby inhibiting STAT receptor binding and subsequent block of downstream signalling (288). USP18 is involved in the process of deISGlyation (290) and was recently shown to bind to the intracellular domain of the IFNAR2, therefore inhibiting JAK1 binding and downstream IFN-α signalling (289).

1.7.2 The role of type I IFN in immune responses and in disease

Type I IFNs induce a program of gene transcription interfering with multiple stages of viral replication but also influence the innate and adaptive immune response to various pathogens (279, 285). The ability of type I IFNs to restrict viral replication is

largely due to ISGs which are either expressed constitutively in cells in response to low levels of type I IFN in the microenvironment or most importantly different ISGs are activated or repressed depending on the pathways triggered upon IFNAR activation. Several ISGs such as *Irf1*, *Ifitm3* and *Oasl*, have been shown to inhibit viral replication (291). It was reported that *Ifnar1*$^{-/-}$ mice are susceptible to vesicular stomatitis virus, Semliki forest virus, vaccinia virus and lymphocytic chorio-meningitis virus. However, susceptibility to influenza virus infection is dependent on type I IFN as well as type III IFN (292-295). However, a detrimental role for type I IFN in mouse models of intracellular bacterial infections including *L. monocytogenes* (72, 296) and *M. tuberculosis* (72, 297) has been shown. Type I IFN has been shown to promote lymphocyte apoptosis and subsequent dampening of the innate immune response which is in part due to the induction of IL-10 production by phagocytic cells in *L. monocytogenes* infection (298). Additionally, type I IFN mitigates responsiveness to IFN-γ in *L. monocytogenes* infected macrophages (299). In the context of *M. tuberculosis* infection, type I IFN mediated the inhibition of the protective cytokine IL-1 (272). Furthermore, type I IFN was shown to induce IL-10 as well as block the responsiveness to IFN-γ for IL-12 production and bacterial killing in *M. tuberculosis* infected macrophages (269). In humans, a type I and type II IFN related gene expression signature in the blood has been shown to correlate with the radiological extent of disease (300). Nevertheless, type I IFNs can also have protective effects in bacterial infections such as *Chlamydia trachomatis, Chlamydia pneumoniae, Legionella pneumophila, Shigella flexneri* and *Salmonella enterica* (285).

Type I IFN also plays a role in autoimmune diseases such as SLE through the over-production of ISGs in active disease (301), Sjögren's syndrome and rheumatoid arthritis (302). Conversely, type I IFN has been used as a therapy in the treatment of multiple sclerosis (303). Patients treated with IFN-β, demonstrate an increase in *Il10* mRNA levels (304) and IL-10 has been linked to the suppression of experimental autoimmune encephalitis (EAE), the mouse model for multiple sclerosis (220, 221). IFN-α therapy is used to treat some chronic viral infections and cancers (305).

1.7.3 The regulation of type I IFN production in macrophages

Innate immune cell types such as macrophages produce type I IFN in response to the stimulation of PRRs by microbial products (279). In macrophages, TLR3 and 4 induce *Ifnb1* mRNA expression via the TRIF-dependent pathway (82). However, in other cell types, mostly pDCs, the ligation of TLR7, 8 and 9 can activate pathways leading to type I IFN production (279). However, the induction of a positive feedback loop is necessary to induce the expression of *Ifna* genes (306). Therefore, IFN-β signals through the type I IFN receptor to activate IRF7 which subsequently promotes the expression of *Ifna* genes, with exception of IFN-α4 (306). Other PRRs such as the RLR RIG-I and melanoma differentiation-associated gene 5 (MDA5), are the main cytosolic receptors and induce robust type I IFN production in response to viral nucleic acids through the activation of IRF3, IRF7, NF-κB and MAPKs (47, 307). The cytosolic molecular sensors NLRs NOD1 and NOD2 have also been shown to induce type I IFN in response to *Helicobacter pylori* (308) and *M. tuberculosis* infection (309) as well as the receptor cytosolic GAMP synthase (cGAS) (310, 311). Furthermore, other DNA motifs in the cytosol can be recognised by the DNA-dependent activator

of IFN-regulatory factors (DAI) and the DEAD box and DEAH box (DEXD/H box) helicases, and lead to the induction of type I IFN production (307, 312). All these signalling pathways converge on a few signalling molecules, such as the IRF family of TFs, leading to the transcription of genes encoding type I IFNs. The *Ifnb1* gene contains consensus binding sites for IRFs, NF-κB TFs as well as AP-1 sites (313). In line, co-operation between these factors in the induction of *Ifnb1* mRNA expression was reported (314). ATF3, a member of the AP-1 family was found to regulate IFN-β via direct binding distal to the *Ifnb1* promoter and act as a transcriptional repressor in macrophages. Yet, ATF3 itself is induced by type I IFN (315). However, IRF3 and IRF7, in most cases the fundamental IRFs, are activated by upstream kinases such as IKKε and TBK1 (60). RIG-I and MDA5 use the adaptor MAVS to activate TBK1, whereas TLR3 and TLR4 use the adaptor molecule TRIF. TLR7 and TLR9 signals rather via MyD88 than TRIF (316, 317).

However, a negative regulatory mechanism also exists, which can attenuate the production of type I IFN. In TLR4 and TLR9 stimulated macrophages, the IFN-β production is negatively regulated by the TPL-2/ERK pathway (71, 318), which might depend on the TF c-FOS (71).

1.8 C57BL/6 and BALB/c as strains of different disease susceptibilities

Mouse models are often the organism of choice for immunologists due to the breadth of tools available. Two of the most commonly used inbred mice strains are C57BL/6 and BALB/c mice. As they differ significantly in their immune responses, they have been used as models to study susceptibility or resistance to various pathogens (Table 1.2). C57BL/6 mice are considered more resistant than BALB/c mice to *Burkholderia pseudomallei* (319) and *L. major* infection (320) as well as to infection with *Listeria spp.* (321) and *M. avium* (322) (Table 1.2). BALB/c mice have been shown to be more resistant than C57BL/6 mice to *T. gondii* (323) and *Helicobacter spp*. infections (324) (Table 1.2). Differences in resistance and susceptibility are also evident in *Il10*$^{-/-}$ mice in the C57BL/6 and BALB/c background. The deficiency in IL-10 leads to spontaneous onset of enterocolitis dependent on the presence of the gut flora (325). However, C57BL/6 mice were less susceptible to the onset of disease than BALB/c mice (208).

Thus, C57BL/6 and BALB/c mice show different immunological responses in various contexts and these differences have been studied in order to better understand the underlying mechanisms. C57BL/6 mice have been correlated to a dominant T_H1 response, while BALB/c mice are associated with a dominant T_H2 response but only in *L. major* infections (326). Other mechanisms leading to their distinct phenotypes have been raised such as differential production of nitric oxide due to increased IFN-β-depentent iNOS expression in C57BL/6 cells in comparison with BALB/c cells (327) or differences in abundance of respiratory chain complexes and lysosomal proteins

as well as differential regulation of components belonging to various antioxidant stress systems in C57BL/6 and BALB/c macrophages (328). Furthermore, we recently demonstrated that C57BL/6 macrophages stimulated with LPS, Pam3CSK4 or *B. pseudomallei* produce high levels of IL-10 and low levels of pro-inflammatory cytokines such as IL-12, TNF-α, and IL-1β while BALB/c macrophages showed a reciprocal pattern of cytokine production (268). In B cells the reduced surface expression of TLR4 in BALB/c cells accounts for the low response of these B cells to LPS (329). Although some immunological factors have been found to explain the differences in disease outcome between C57BL/6 and BALB/c macrophages, the mechanisms underlying these traits are complex and only partially understood.

Table 1.2 Differences in resistance and susceptibility in the context of infectious diseases in C57BL/6 and BALB/c mice strains

Pathogen	More resistant strain
Burkholderia pseudomallei	C57BL/6
Leishmania major	C57BL/6
Listeria spp.	C57BL/6
Mycobacterium avium	C57BL/6
Toxoplasma gondii	BALB/c
Helicobacter species	BALB/c

1.9 Overview

Data from the O'Garra laboratory showed that macrophages from C57BL/6 mice produce high levels of IL-10 and low levels of pro-inflammatory cytokines such as IL-12, IL-1β and TNF-α upon stimulation with different TLR ligands, whereas macrophages from BALB/c mice showed a reciprocal cytokine profile (data now published (268)). In addition, it was found that type I IFN production was higher in C57BL/6 macrophages compared to BALB/c macrophages. Hence, we hypothesised that type I IFN via various mechanisms regulates the production of IL-10 and pro-inflammatory cytokines in TLR stimulated C57BL/6 and BALB/c macrophages. Firstly, we aimed to use microarray analyses to investigate in an unbiased way pathways that are involved in the differential IL-10 and pro-inflammatory cytokine production in TLR stimulated C57BL/6 and BALB/c macrophages. Furthermore, we explored mechanisms leading to differences in type I IFN production between C57BL/6 and BALB/c stimulated macrophages. To evaluate the context specificity of the type I IFN mediated effect we stimulated macrophages with various TLR ligands and investigated mechanisms of how type I IFN mediates the regulation of IL-10 using kinase inhibitors. Using ATAC-sequencing, we explored in further detail the effects of type I IFN on chromosome accessibility and transcription factor recruitment to the *Il10* locus in LPS stimulated macrophages. Thus, this study described here in this thesis will shed light on the type I IFN-mediated regulation of IL-10 in LPS stimulated C57BL/6 macrophages and contribute to the understanding of how IL-10 expression is controlled which is critical in the design of immune intervention strategies.

Chapter 2.
Materials and Methods

2.1 Mice strains

C57BL/6 wild-type (WT), BALB/c WT, C57BL/6 *Ifnar1*$^{-/-}$, C57BL/6 *Tlr4*$^{-/-}$ and C57BL/6 *Nfil3*$^{-/-}$ mice were bred and maintained at The Francis Crick Institute, Mill Hill Laboratory and the Francis Crick Institute under specific pathogen-free conditions in accordance with the Home Office, U.K., Animal Scientific Procedures Act, 1986. C57BL/6 *Ifnar1*$^{-/-}$ breeders were provided by B&K Universal (Hull, U.K.). C57BL/6 *Tlr4*$^{-/-}$ breeding pairs were kindly given to us by Prof. S. Akira (Osaka University, Osaka, Japan). C57BL/6 *Nfil3*$^{-/-}$ mice were provided by Andreas Wack. C57BL/6N and BALB/cAnN *Myd88*$^{-/-}$ mice were purchased from Oriental BioService Inc. and appropriate WT controls were ordered from Taconic (Taconic Farms Inc.). All mice used were female, between 8-16 weeks of age.

2.2 Reagents

2.2.1 Cell culture medium

For all *in vitro* experiments the following culture medium was used (referred to as cRPMI): RPMI 1640; 5% heat-inactivated FCS (Gibco, Thermo Scientific); 0.05 mM 2-Mercaptoethanol (Sigma); 10 mM HEPES buffer; 100 U/ml penicillin; 100 µg/ml streptomycin; 2 mM L-glutamine; 1 mM sodium pyruvate. Unless otherwise stated, all components were purchased from BioWhittaker.

2.2.2 PRR ligands, heat-killed bacteria and recombinant cytokines

Cells were stimulated, unless otherwise stated, with either cRPMI culture medium (control), Salmonella Minnesota LPS (Alexis) at a final concentration of 10 ng/ml, Pam3CSK4 (InvivoGen) at a final concentration of 200 ng/ml, heat-killed *B. pseudomallei* 576 (from DSTL, Porton Down) at a final concentration of 500 HkBps : 1 BMDM, CpG1668 (TriLink Biotech) at a final concentration of 0.5 μM, Poly I:C (InvivoGen) at a final concentration of 50 μg/ml. When indicated, cells were additionally treated with recombinant murine IFN-β or IFN-α (PBL) at a final concentration of 2 or 20 ng/ml. Doses have been established in the laboratory beforehand. Duration of stimulations are indicated in figure legends.

2.2.3 Inhibitors

Kinase inhibitor stocks were diluted in DMSO (DMSO vehicle control was included in every experiment) and used at the following final concentrations: 0.1 μM BIRB0796 (p38 inhibitor), 0.5 μM SB203580 (p38 inhibitor), 0.1 μM PD0325901 (MEK1 inhibitor), 1 μM U0126 (MEK1/2 inhibitor), 1 μM Arry142886 (MEK1/2 inhibitor), 0.125 μM rapamycin (mTOR inhibitor, InVitrogen), 0.03 μM PI-103 (PI3K inhibitor) and 1 μM CT99021 (GSK-3 inhibitor). BIRB0796, SB203580, PD0325901, PI-103, U0126, Arry142886 and CT99021 were kind gifts of Philip Cohen (University of Dundee). Inhibitors were added to BMDM cultures 1 h prior or 2 h after stimulation with PRR ligands as indicated in the figure legends. The doses were based on recommendations by Cohen *et al.* for maximal efficiency with minimal off-target effects (330, 331) as well as by the Kinase Profiling Inhibitor Database

(http://www.kinase-screen.mrc.ac.uk/kinase-inhibitors). Data from this database have been generated by the International Centre for Kinase profiling within the MRC Protein Phosphorylation Unit at the University of Dundee. Concentrations were confirmed by titration experiments using BMDMs (Figure 4.9).

2.3 Differentiation of bone marrow-derived macrophages

Bone marrow was flushed from tibias and femurs and cultured (37°C, 5% CO_2) in 9 cm Petri dishes (Sterilin Ltd.) at $0.5x10^6$ cells/ml in 8 ml cRPMI supplemented with 10% FCS and 20% L929-cell conditioned medium, containing M-CSF. L929-cell conditioned medium was generated from the L929 cell line with the assistance of Jackie Wilson (Large Scale Laboratory Facility, National Institute for Medical Research). On day 4, 10 ml cRPMI supplemented with 10% FCS and 20% L929-cell conditioned medium was added to the culture. On day 6, non-adherent cells were removed and adherent cells were harvested by gentle flushing with cold PBS (Gibco, Invitrogen). Cells were seeded in either 48-well tissue culture plates (Corning Inc.) at $0.5x10^6$ cells/well or 6-well tissue culture plates (Corning Inc.) at $4x10^6$ cells/well in cRPMI and rested for 18 – 24 h prior to stimulation.

2.4 Enzyme-linked immunosorbent assay

2.4.1 Quantification of cytokine concentrations

Supernatants were collected from cell cultures and cytokine concentrations quantified by sandwich enzyme-linked immunosorbent assay (ELISA). Maxisorp 96-well plates (Nunc, Thermo Scientific) were used for the assay. IFN-β and IFN-α were

quantified using a commercially available ELISA kit (PBL) following the manufacturer's instructions. Matched-pair sandwich ELISAs were used to measure IL-10 and IL-12p40 concentrations. Details are summarised in Table 2.1. ELISA plates were read on a Safire^2 microplate reader (TECAN). Standard curve calculation and cytokine concentration were determined using Magellan software.

Table 2.1 IL-10 and IL-12p40 ELISA details

Cytokine	Standard	Coating antibody	Detection (biotinylated) antibody	HRP-streptavidin	Developing substrate	Detection limit
IL-10	Recombinant IL-10 (R&D)	JES5-2A5 5 μg/ml (eBio)	SXC-1 0.25 μg/ml (BD Biosciences)	1 μg/ml (Jackson Immuno Research)	TMB	50 pg/ml
IL-12p40	Recombinant IL-12p40 (R&D)	C15.6.7 5 μg/ml (DNAX)	C17.8 0.5 μg/ml (DNAX)	1 μg/ml (Jackson Immuno Research)	ABTS	50 pg/ml

2.4.2 Quantification of the activity of interferon regulatory factor 3

Nuclear extracts of 2 h heat-killed *B. pseudomallei* stimulated BMDMs (500:1 *B. pseudomallei*:BMDM) were prepared using the Nuclear Extract Kit and analysed with the TransAM IFN regulatory factor (IRF) 3 kit for mouse (both from Active Motif) according to the manufacturer's instructions. Plates were read on a Safire^2 microplate reader (TECAN). Specificity of the assay was tested using wild type consensus oligonucleotides or mutated oligonucleotides as provided by the kit (Figure 7.1).

2.5 Real-time polymerase chain reaction

Supernatants from the cell culture were discarded at the indicated time points and cells washed with pre-warmed PBS. Cells were then lysed with RLT buffer (Qiagen) containing 1% β-Mercaptoethanol (Sigma). Lysates were stored at -80°C. RNA was harvested and isolated according to the manufacturer's instructions using RNeasy Mini Kit (QIAGEN) with an on-column DNase digestion step to remove contaminating DNA (RNase-Free DNase kit, Qiagen). Purified RNA concentration was determined with a Nanodrop spectrophotometer (NanoDrop1000, Thermo Scientific).

cDNA was synthesised using High Capacity cDNA Reverse Transcription kit (Applied Biosystems), following the manufacturer's instructions. Subsequently, samples were treated for 30 min at 37°C with RNase H (Promega) to degrade leftover RNA.

Il10, Il12a, Ifnb1, Oas1g, Stat1, Stat3, Irf7 and *Irf9* gene expression were quantified by real-time PCR (7900HT, Applied Biosystems and QuantStudio3, ThermoFisher) using the TaqMan assay system and normalised to *Hprt1* mRNA. A no-cDNA template control and water only control was always included to ensure that reagents were not contaminated. The primer-probes used are summarised in Table 2.2.

For the quantification of un-spliced *Il10* mRNA transcripts, TaqMan primer/probe pairs were designed so that the forward (sense) primer and TaqMan probe annealed within an exon sequence (in this case exon 3 of the 5 *Il10* exons), and the reverse (antisense) primer annealed within an intron sequence (in this case intron 4). Primers were designed by Ashleigh Howes using Primer Express 2.0 software and were

custom made by Applied Biosystems. Primer sequences are summarised in Table 2.3.

Table 2.2 TaqMan primer probes for qRT-PCR

Target gene	Applied Biosystems code
Il10	Mm00439616_m1
Il12a	Mm00434165_m1
Ifnb1	Mm00439552_s1
Oas1g	Mm01730198_m1
Stat1	Mm_00439518_m1
Stat3	Mm_01219775_m1
Irf7	Mm_00516793_g1
Irf9	Mm_00492679_m1
Hprt1	Mm_00446968_m1

Table 2.3 Un-spliced *Il10* mRNA primer probe sequences

Forward primer	5'-AGCATGGCCCAGAAATCAAG-3'
TaqMan probe	5'-CTCAGGATGCGGCTGA-3'
Reverse primer	5'-AGAACGCATCTGCTACTCACACA-3'

The gene expression value, expressed in relative units (RU), for each sample was determined and normalised to the house-keeping gene *Hprt1* using the delta Ct (ΔCt) calculation: $\Delta Ctgene = 1.8^{(Ct\textit{Hprt1}\text{-}Ct\textit{gene})} \times 100{,}000$.

2.6 Determination of mRNA stability

BMDMs were stimulated with LPS or LPS and IFN-β. 1 h post stimulation Actinomycin D from *Streptomyces sp.* (Sigma-Aldrich, 10 µg/ml) was added to the cultures (t = 0) to inhibit RNA synthesis. 30, 60, and 90 min later mRNA was isolated, reverse transcribed into cDNA, and *Il10* mRNA quantified as described in 2.5.

2.7 Immunoblotting

In experiments where phosphorylation of proteins was evaluated, BMDMs were rested in 1% FCS for 20 h prior to stimulation in order to reduce the background signal caused by serum response. In all other cases BMDMs were rested as described before (2.3). Cells were stimulated as indicated, after which supernatant was removed and cells washed with PBS and lysed in RIPA buffer composed of 50 mM Tris HCl (Sigma), pH 8; 150 mM NaCl (Sigma); 2 mM EDTA (Sigma); 2 mM sodium pyrophosphate (Sigma); 50 mM sodium fluoride (Sigma); 0.1% SDS (BioRad); 1% NP-40 (Fluka); 0.5% deoxycholate acid (Sigma); 100 mM vanadate (Sigma); complete EDTA-free protease inhibitor cocktail (Roche) or in Triton X-100 lysis buffer (for IRF3 Western blots) composed of 50 mM Tris HCl (Sigma), 1mM EGTA (Sigma), 1mM EDTA (Sigma), 1 mM vanadate (Sigma); 50 mM sodium fluoride (Sigma); 5 mM sodium pyrophosphate (Sigma); 10 mM Sodium glycerophosphate (Sigma), 270 mM Sucrose (Sigma); 1% Triton X-100 (Sigma); 0.1% β-Mercaptoethanol (Sigma) and complete EDTA-free protease inhibitor cocktail (Roche). For the separation of cellular and nuclear extracts the Nuclear Extract Kit from Active Motif was used.

Protein concentration was measured using a reducing agent compatible Bicinchoninic Acid (BCA) Protein Assay Kit according to the manufacturer's instructions (Thermo Scientific).

Proteins were denatured in SDS sample buffer (5 min, 95 °C), and resolved on a 10 or 12.5% SDS-polyacrylamide gel and subsequently transferred to polyvinylidene difluoride membranes (Millipore). Membranes were probed with antibodies against phospho-p38 (T180/Y182), total p38 (both Cell Signaling), phospho-ERK1/2 (T185/Y187), total ERK1/2 (both Invitrogen), phospho-IRF3 (S396, 4D4G) (Cell Signaling), total IRF3 (Santa Cruz Biotechnology), phospho-STAT1 (Y701), total STAT1, phospho-TBK1 (S172), total TBK1 (both Cell signaling), phospho-GSK-3α/β (S21/9) , total GSK-3α/β (both from Cell signaling), JUNB (Cell signaling), ATF3 (Atlas antibodies), cJUN (Santa Cruz Biotechnology), BATF (Cell signaling) and GAPDH (FL-335), heat shock protein 90a/b (H-114) (Santa Cruz Biotechnology), actin (Calbiochem) or αTubulin (Abcam) followed by HRP-conjugated rabbit anti-goat IgG, goat anti-rabbit IgG (SouthernBiotech), or goat anti-mouse IgM (Calbiochem). For visualisation, the membrane was incubated with Pierce ECL Western blotting substrate (Thermo Scientific) and exposed to X-ray film (SLS).

2.8 Flow cytometry analysis

BMDMs were stimulated with LPS for 0, 10, 30 and 90 min, washed twice with PBS, and blocked with anti-CD16/CD32 Ab. Subsequently, BMDMs were stained with APC-labelled anti-mouse CD14 (SA14-2, BioLegend), PE-labelled anti-mouse TLR4 (SA15-21; BioLegend) or isotype control (Rat IgG2a, κ) for 30 min at 4℃ and

acquired using a BD LSR II (BD Biosciences). Data were analysed by FlowJo software.

2.9 Processing of microarray samples and analysis of microarray data set

2.9.1 Microarray processing

BMDMs were stimulated with LPS, heat-killed *B. pseudomallei* 576 or media (control) at $1x10^6$ cells/ml in a 48-well plate (500 ul cells/well) for 0.5, 1, 3, 4 and 6 h. RNA was isolated and purified as described in 2.5. These steps were carried out by Ashleigh Howes. I then confirmed RNA quality (RNA integrity number, range 9 – 10) using an Agilent 2100 Bioanalyzer (Agilent Technologies) and prepared RNA for microarray using the Illumina®TotalPrep-96 RNA Amplification kit. RNA concentration was determined using a Nanodrop1000 (Thermo Scientific) and quality checked again using an Agilent 2100 Bioanalyzer (Agilent Technologies). 1500 ng cRNA was loaded onto 6 sample Illumina BeadChip Arrays (MouseWG-6 v2). BeadChips were then incubated for 16 – 20 h in hybridisation chambers to allow sample hybridisation. The following day, BeadChips were washed, blocked, treated with streptavidin Cy-3 to 'stain', washed, allowed to dry, and stored away from the light until scanned. BeadChips were scanned by an Illumina iSCAN array scanner. Intensity values were generated and background signal subtracted using BeadStudio software (Illumina). Microarray processing was done with the assistance of Dr. Christine Graham (Anne O'Garra laboratory) and Dr. Harsha Jani (Division of Systems Biology, NIMR, London).

2.9.2 Microarray data analysis

Further analysis of microarray data was done using GeneSpring GX version 12.6.1 or 14.5 (Agilent Technologies). All data shown was subjected to the following data processing and normalisation steps: lower threshold of signal intensity of 10. The expression values were log transformed (base 2) and scaled to the 75th percentile of all samples. Following this, the expression value of each gene probe was normalised to the median expression of that gene probe across all samples. After normalisation, all gene probes were quality filtered for those present ($p < 0.01$) in at least one sample, with 19,191 gene probes having remained. Prior to further analysis, a quality control evaluation was carried out to ensure the integrity of the data. All samples from the experiment were hierarchically clustered according to condition using GeneSpring software. Replicates within experimental groups clustered together demonstrating their similarity. A comparable observation was made using principal component analysis.

If additional statistical analysis has been done, it is defined in the relevant figure legends. Using the Ingenuity Pathway Analysis (IPA) software (QIAGEN Inc., https://www.qiagenbioinformatics.com/products/ingenuity-pathway-analysis), canonical pathway analysis was conducted. Expression data conform to the minimum information about a microarray experiment standards for microarray analysis. Microarray data have been deposited under accession number GSE79809 in the Gene Expression Omnibus database (http://www.ncbi.nlm.nih.gov/geo/). Parts of the dataset used in Figure 5.2 has not been published and is therefore not deposited.

2.10 Assay for transposase accessible chromatin (ATAC) - library preparation and computational analysis of sequencing data

2.10.1 ATAC library preparation

BMDMs were plated in a 48-well plate at 500,000 cells/well, rested for 20 h and then stimulated as indicated in figure legend. ATAC-library preparation was performed as described in Buenrostro *et al.* (332, 333) with slight adaptations. At indicated times cells were washed twice with PBS and lysis buffer containing 10 mM Tris-HCl (pH 7.4), 10 mM NaCl, 3 mM $MgCl_2$ and 0.1% IGEPAL CA-630 (Fluka) was added to the plate. 50,000 cells were pelleted and nuclei re-suspended in transposition reaction mix (25 µL 2x TD Buffer, 2.5 µL Tn5 Transposes (Illumina), 22.5 µL nuclease-free H_2O) for 2 h at 37°C. This transposition time was chosen after a time course analysis from 30 min to 2 h and evaluation of the fragment size (Figure 7.2). DNA was purified using the Qiagen PCR purification MinElute Kit and eluted in 10 µL elution buffer included in the kit. Transposed DNA fragments were then amplified via PCR (Table 2.4) using the following cycles: (1) 72°C, 5 min; (2) 98°C, 30 sec; (3) 98°C, 10 sec; (4) 63°C, 30 sec; (5) 72°C, 1 min; (6) repeat steps 3-5, 11x; (7) hold at 4°C. Primers used are summarised in Table 2.5.

Table 2.4 PCR mix

Reagent	Volume [µl]
Nuclease free H_2O	10
25 µM PCR Primer 1 (universal = Ad1_noMx)	2.5
25 µM PCR Primer 2 (any from Ad2)	2.5
NEBNext High-Fidelity 2x PCR Master Mix (New England Labs)	25
Transposed DNA	10

After amplification of transposed DNA fragments, the library was purified using the Qiagen PCR purification MiniElut kit followed by an additional clean up step with AMPure beads (Beckman Coulter). Beads were incubated with the library preparation for 5 min at room temperature, followed by two washing steps with 80% ethanol. DNA was eluted with 0.1x Tris-EDTA (Sigma) and stored at -20°C. The sizes of the library fragments were evaluated using the Bioanalyzer (Agilent Technologies). Libraries were then quantified using the Qubit and checked for adapters by ECO real qPCR before being run on the HiSeq2500 (PE50, 1 sample per lane, ~ 400 million reads per sample). Quality control and sequencing of the library were performed by the High Throughput Sequencing facility at the Francis Crick Institute.

Table 2.5 Primer sequences used for ATAC libraries

Primer name	Primer sequence
Ad1_noMX:	AATGATACGGCGACCACCGAGATCTACACTCGTCGGCAGCGTCAGATGTG
Ad2.1_TAAGGCGA	CAAGCAGAAGACGGCATACGAGATTCGCCTTAGTCTCGTGGGCTCGGAGATGT
Ad2.2_CGTACTAG	CAAGCAGAAGACGGCATACGAGATCTAGTACGGTCTCGTGGGCTCGGAGATGT
Ad2.3_AGGCAGAA	CAAGCAGAAGACGGCATACGAGATTTCTGCCTGTCTCGTGGGCTCGGAGATGT
Ad2.4_TCCTGAGC	CAAGCAGAAGACGGCATACGAGATGCTCAGGAGTCTCGTGGGCTCGGAGATGT
Ad2.5_GGACTCCT	CAAGCAGAAGACGGCATACGAGATAGGAGTCCGTCTCGTGGGCTCGGAGATGT
Ad2.6_TAGGCATG	CAAGCAGAAGACGGCATACGAGATCATGCCTAGTCTCGTGGGCTCGGAGATGT
Ad2.7_CTCTCTAC	CAAGCAGAAGACGGCATACGAGATGTAGAGAGGTCTCGTGGGCTCGGAGATGT
Ad2.8_CAGAGAGG	CAAGCAGAAGACGGCATACGAGATCCTCTCTGGTCTCGTGGGCTCGGAGATGT
Ad2.9_GCTACGCT	CAAGCAGAAGACGGCATACGAGATAGCGTAGCGTCTCGTGGGCTCGGAGATGT
Ad2.10_CGAGGCTG	CAAGCAGAAGACGGCATACGAGATCAGCCTCGGTCTCGTGGGCTCGGAGATGT
Ad2.11_AAGAGGCA	CAAGCAGAAGACGGCATACGAGATTGCCTCTTGTCTCGTGGGCTCGGAGATGT
Ad2.12_GTAGAGGA	CAAGCAGAAGACGGCATACGAGATTCCTCTACGTCTCGTGGGCTCGGAGATGT
Ad2.13_GTCGTGAT	CAAGCAGAAGACGGCATACGAGATATCACGACGTCTCGTGGGCTCGGAGATGT
Ad2.14_ACCACTGT	CAAGCAGAAGACGGCATACGAGATACAGTGGTGTCTCGTGGGCTCGGAGATGT
Ad2.15_TGGATCTG	CAAGCAGAAGACGGCATACGAGATCAGATCCAGTCTCGTGGGCTCGGAGATGT
Ad2.16_CCGTTTGT	CAAGCAGAAGACGGCATACGAGATACAAACGGGTCTCGTGGGCTCGGAGATGT
Ad2.17_TGCTGGGT	CAAGCAGAAGACGGCATACGAGATACCCAGCAGTCTCGTGGGCTCGGAGATGT
Ad2.18_GAGGGGTT	CAAGCAGAAGACGGCATACGAGATAACCCCTCGTCTCGTGGGCTCGGAGATGT
Ad2.19_AGGTTGGG	CAAGCAGAAGACGGCATACGAGATCCCAACCTGTCTCGTGGGCTCGGAGATGT
Ad2.20_GTGTGGTG	CAAGCAGAAGACGGCATACGAGATCACCACACGTCTCGTGGGCTCGGAGATGT
Ad2.21_TGGGTTTC	CAAGCAGAAGACGGCATACGAGATGAAACCCAGTCTCGTGGGCTCGGAGATGT
Ad2.22_TGGTCACA	CAAGCAGAAGACGGCATACGAGATTGTGACCAGTCTCGTGGGCTCGGAGATGT
Ad2.23_TTGACCCT	CAAGCAGAAGACGGCATACGAGATAGGGTCAAGTCTCGTGGGCTCGGAGATGT
Ad2.24_CCACTCCT	CAAGCAGAAGACGGCATACGAGATAGGAGTGGGTCTCGTGGGCTCGGAGATGT

2.10.2 Analysis of ATAC-sequencing data

All data shown were subjected to the following data processing and normalisation steps. Quality and integrity of the sequenced library was determined using FastQC v0.11.5, a quality control tool for high throughput sequence data developed by the Bioinformatics Group at the Babraham Institute, UK. Subsequent, reads were quality trimmed (Trimmomatic 0.36) using the following parameters: ILLUMINACLIP:NexteraPE-PE.fa:2:30:10, SLIDINGWINDOW:3:20 and MINLEN:35, and quality was checked again using FastQC. Reads were mapped to the GRCm38.83 (mm10) genome from UCSC using Bowtie2 (2.2.9-foss-2016b) with --sensitive-local parameters (-D 15 -R 2 -N 0 -L 20 -i S,1,0.75) as well as -X 2000 to increase the default of maximum fragment length for valid paired-end alignments from 500 to 2000. Duplications were removed using SAMtools (1.3.1-intel-2016b; rmdup) and artefact regions that tend to show artificially high signal were filtered out using the DAC blacklist for mm10, a comprehensive empirical blacklist identified by the ENCODE and modENCODE consortia (334). Before calling peaks with MACS2 (2.1.1.20160309-foss-2016b-Python-2.7.12) (https://github.com/taoliu/MACS; (335)), the read start sites were adjusted to represent the centre of the transposon binding event as Tn5 transposase was shown to bind as a dimer and inserts two adapters separated by 9 bp (336). Hence, reads aligning to the + strand were off-set by +4 bp, and reads aligning to the – strand were off-set −5 bp. To assess the similarity of biological repeats, DeepTools(337) and the R Bioconductor package DiffBind (338, 339) were used. DiffBind was also used to identify significantly different peaks between groups. For motif finding, significant peaks determined with DiffBind, were input for HOMER package motif finder algorithm findMotifGenome.pl(340).

2.11 Chromosome immune-precipitation – polymerase chain reaction (ChIP-PCR)

BMDMs were stimulated with LPS and at indicated time points supernatant was removed and cells washed with PBS. Cells were crosslinked in 1% paraformaldehyde for 8 min at room temperature. Glycine was added to a final concentration of 0.125 M and incubated at room temperature for 8 min. After three PBS wash steps cells were scraped off and the pellet snap frozen at -80°C. This step aids the lysis and therefore improves sonication. The defrosted pellet was lysed in 100 µl/10^6 cells of lysis buffer containing 1% SDS (Affymetrix Inc.), 10 mM EDTA (Sigma), 50 mM Tris-HCl pH 8.0 (Sigma) and 1 mM protease inhibitor cocktail (Roche). The lysate was incubated for 10 min on ice in a tube rotator before being sonicated for 40 min (30 sec on, 30 sec off on high setting; Diagenode Bioruptor). Sonication time was established by a previous sonication time course (Figure 7.3). After sonication 30 – 100 µl of the samples were frozen at -20°C as input. 5x10^6 cells were used per immunoprecipitation and diluted 1:10 in dilution buffer (0.01% SDS (Sigma), 1.1% Triton-X 100 (Sigma), 1.2 mM EDTA (Sigma), 16.7 mM Tris-HCl pH 8.0 (Sigma),167 mM NaCl (Sigma), 1 mM protease inhibitor cocktail (Roche)). 5 µg of antibody (anti-Atf3 Ab, polyclonal, Atlas Antibodies; Rabbit IgG, polyclonal, Isotype Control, Abcam) or a dilution of 1:150 for anti-Junb Ab (monoclonal (C37F9), Cell signalling) was incubated at 4°C in a tube rotator overnight. 50 µl of beads, pre-treated with 2 mg/ml BSA for at least 2 h, were added per sample and incubated on a rotator at 4°C for 4 h. Beads were washed once with low salt buffer (0.1% SDS (Affymetrix Inc.), 1% Triton-X 100 (Sigma), 2 mM EDTA (Sigma), 150 mM NaCl (Sigma), 20 mM Tris-HCl pH 8.0 (Sigma)), once with high salt buffer (0.1% SDS

(Affymetrix Inc.), 1% Triton-X 100 (Sigma), 2 mM EDTA (Sigma), 500 mM NaCl (Sigma), 20 mM Tris-HCl pH 8.0 (Sigma)), once with Lithium Chloride Immune wash (0.25 M LiCl (Sigma), 1% IGEPAL CA-630 (Fluka), 1% Sodium deoxycholate (Sigma), 1 mM EDTA (Sigma), 10 mM Tris-HCl pH 8.0 (Sigma)) and twice with Tris-EDTA (Sigma). Samples were eluted into 200 μl elution buffer (1% SDS (Affymetrix Inc.), 100 mM NaHCO3 (Sigma)) and incubated at room temperature for 15 min, followed by 15 min at 65 °C. The supernatant was collected, 8 μl of a 5 M NaCl solution added and incubated overnight at 65 °C to reverse the crosslinking. Inputs were defrosted, volume made up to 200 μl with Tris-EDTA, 8 μl of a 5 M NaCl solution added and samples were incubated at 65 °C overnight. To digest leftover RNA and proteins within the sample, Rnase A was added to a final concentration of 100 μg/ml (Invitrogen) and incubated for 1 h at 37 °C followed by 1 h incubation at 55 °C with Proteinase K (Thermo Scientific) (8 μl Tris-HCl (pH 6.5 1 M, Sigma), 4 μl EDTA (0.5 M, Sigma), 0.8 μl Proteinase K (20 mg/ml)). The Zymo Chip Clean and concentrate kit (Zymo Research) was used according to manufacturer's instructions to concentrate and clean the sample. qRT-PCR was performed using SYBRE Green and primers as listed in Table 2.6.

Table 2.6 Primers to detect Junb and Atf3 binding sites within the IL-10 TAD

No.	TF	Gene, Start site	Forward primer	Reverse primer
6	Junb	IL-10 intron 3	GTGGGAGTGACTTTGAGGCA	TGGAGAGAGAGGGGAGTAGC
7	Junb	IL10 TAD, intergenic, start 130997835	TCCTGTCCAGCCAGTCTCTA	AGAGTGTTCCCTCAGTGCTC
10	Junb	IL10 TAD, intergenic, start 131026049	GTGGGTGGGAGCTGACAAG	GCTTCCCACTTCCTTCCGAT

12	Junb	IL10 TAD, intergenic, start 131038102	TGGCCGCATTTCCATTATGT	AGTGACCAGAAACTCAATTAGCAG
14	Junb	IL10 TAD, intergenic, start 131038246	GCTTCCCCTCTTTGGTTCCT	CTCCATGCCTCCTGAACTCC
16	Junb	IL10 TAD, intergenic, start 131094756	CTGGAAGTGTGTGCGTGACT	TCTGGTAGATGCTGTCACCCT
17	Atf3	IL10 TAD, intergenic, start 130997603	CATGCGTCCTGTGTGAGAGA	TCTCAGGCAAAAGGAGTAGCC
18	Atf3	IL10 TAD, intergenic, start 130999023	GAGAGACCAAGGTTGGATTGG	GTCACAAGAGCCTGACCTACT
19	Atf3	IL10 TAD, intergenic, start 131001090	CTGAAGGAAAACCCTGTGTTGC	GCTCTGACCCAAACCCTAGA
22	Atf3	IL10 TAD, intergenic, start 131025876	ACTGACTTCTGCCTGGGGTA	CCCCTTATCCTCAAAGTCACGA
23	Atf3	IL10 TAD, intergenic, start 131029822	GACTCCACTCTCTAAGGGCAAA	TGTGTTGTCACCAAGAAAAGAACAA
24	Atf3	IL10 TAD, intergenic, start 131029850	CCCCTGGGCATATATATAGGTTTC	CAGACTGGGCTAAGTAAGTCTCC
25	Atf3	IL10 TAD, intergenic, start 131030006	TGGGGCCATGGATAGAGGTAT	AGCTGCTGGTGTTGTCAAGT
26	Atf3	IL10 TAD, intergenic, start 131038047	CGGGATGTTATGACTTTGTTGAA	CACATAATGGAAATGCGGCCA
28	Atf3	IL10 TAD, intergenic, start 131105759	TGTCAGAGCCCACGATGCTA	TTCCCTCCCTTGAGTCACCG
29	Atf3	IL10 TAD, intergenic, start 131005847	AGCTGGCAACTCCATGGTC	TTTTGGTTCCTCATGGGCCT
31	Atf3	IL-10 intron 3	GTGTCGGGTCTCTTGCTCAT	ATCTTCACGTGTGAGTGCCT
33	Atf3	IL10 TAD, intergenic, start 131094759	GAAGTGTGTGCGTGACTCAG	TGCTCTGGTAGATGCTGTCAC

ChIP-qPCR results were normalised using the Percent Input Method as this includes normalisation for both background levels and input chromatin going into the ChIP. First the dilution factor x of the input was calculated and log transformed (logx,2). This factor was subtracted from the input Ct value and forms the adjusted input Ct value, which gets averaged between the 3 technical replicates (average adjusted input Ct). The percentage of the input for a particular antibody or mock (IgG) was calculated as follows: $100 \times 2^{(\text{average adjusted input Ct} - \text{Ct IP})}$.

2.12 Statistics

All data analysis was performed using GraphPad Prism software 7 (GraphPad Software, San Diego, CA). Statistical test and significance values for each experiment are indicated in the figure legends.

Chapter 3.
Type I IFN as one major difference between C57BL/6 and BALB/c macrophages: How is type I IFN differentially regulated?

3.1 Background

During an infection PRRs detect microbial products and prompt signals that induce cytokine production, which then shapes the immunological response (52, 60). IL-12, TNF-α, and IL-1β are pro-inflammatory cytokines, which are crucial for resistance against infection. However, when produced at high levels they may contribute to immunopathology (341). In contrast, IL-10 is an immunosuppressive cytokine, which dampens pro-inflammatory responses, yet, it can also lead to defective pathogen clearance (160, 342). Therefore, the regulation of these cytokines is fundamental in order to allow the generation of an effective but balanced immune response.

C57BL/6 and BALB/c mice show significant differences in their immune responses, which leads to distinct outcomes of infection. Therefore, they are often used for studying susceptibility or resistance to various pathogens (320, 321, 323). We recently showed that C57BL/6 macrophages stimulated with LPS (TLR4), Pam3CSK4 (TLR2) and *B. pseudomallei* (TLR2 and 4) produce low levels of IL-12, TNF-α, and IL-1β, but high levels of IL-10 (268). In contrast, BALB/c macrophages show a reciprocal pattern in the production of these cytokines (268).

PRRs such as TLR2 and 4 are localised on the cell surface recognising bacterial motifs such as peptidoglycan (TLR2) or LPS (TLR4) (31, 52, 53). Upon TLR ligation adaptor molecules containing a TIR domain such as myeloid differentiation primary-response protein 88 (MyD88) and Toll/IL-1 receptor domain- containing adaptor (TRIF) are recruited (31, 32, 53). MyD88 is recruited to TLR2 and 4, while the TRIF-dependent pathway is used by TLR4 but not TLR2, and is critical for IFN-β production downstream of this receptor (31, 82). In macrophages, IL-10 production is induced

by TLRs via the MyD88-dependent and TRIF- dependent pathways (167). Stimulation of TLR4 leads to activation of both signalling pathways and, importantly, maximal IL-10 production requires the activation of MyD88 and TRIF (167). Although TLR4 is essential for the signalling of LPS, the response to LPS requires several additional molecules, one of them being CD14. CD14 is a glycosylphosphatidylinositol–anchored molecule preferentially expressed on monocytes/macrophages and neutrophils and is critically involved in the recognition of LPS together with TLR4. CD14 chaperones LPS molecules to the TLR4-MD-2 signalling complex and hence controls the trafficking and signalling functions of TLR4 (101, 104). Nevertheless, the signalling via MyD88 is CD14- dependent only at low LPS concentrations, whereas signalling through the TRIF pathway requires CD14 at low and high LPS concentrations (110).

3.2 Aims

Data from our laboratory showed that C57BL/6 macrophages produce higher levels of IL-10 compared to BALB/c macrophages upon stimulation of TLR2 and 4. The opposite trend for pro-inflammatory cytokines was observed. Therefore, we hypothesise that pathways leading to IL-10 and pro-inflammatory cytokine production downstream of TLR2 and 4 have to be differentially regulated in C57BL/6 and BALB/c macrophages.

In order to test this hypothesis, we aimed to:

- Investigate molecular pathways that are associated with the differential expression of IL-10 and pro-inflammatory cytokines in C57BL/6 and BALB/c macrophages using microarray analysis.

- Explore identified pathways.

3.3 Results

3.3.1 Type I IFN signalling as one major difference between C57BL/6 and BALB/c macrophages

To investigate the mechanism underlying the difference in cytokine production by C57BL/6 and BALB/c macrophages we took advantage of an existing model – the gram negative bacterium *B.pseudomallei*. C57BL/6 and BALB/c mice show differing resistance and susceptibility to *B.pseudomallei* infections (Table 1.2). Additionally, infections with *B.pseudomallei* serve as an important clinical and experimental example of gram negative sepsis. Hence, we stimulated macrophages with heat-killed *B. pseudomallei* for 3 and 6 h and undertook an unbiased microarray analysis. At 3 h post *B. pseudomallei* stimulation, 790 genes were found to be differentially regulated in C57BL/6 and BALB/c macrophages (Figure 3.1 A). Of these genes, most of them were upregulated by *B. pseudomallei* stimulation in macrophages of both strains of mice. The expression of the majority of these up-regulated genes was more strongly up-regulated in C57BL/6 compared to BALB/c macrophages. Downregulated genes in *B. pseudomallei* stimulated C57BL/6 macrophages were also downregulated in BALB/c macrophages. These down-regulated genes were either more highly or more weakly down-regulated in BALB/c macrophages in comparison to C57BL/6 macrophages. At 6 h post *B. pseudomallei* stimulation, 2246 genes were differentially regulated in C57BL/6 and BALB/c macrophages (Figure 3.1 A), suggesting a reinforcement of differential gene expression over time. Additionally, the difference in expression of these 2246 genes between C57BL/6 and BALB/c macrophages was increased compared to the 3 h time point (Figure 3.1 A).

To better understand the biological relationship between the differentially regulated genes in C57BL/6 and BALB/c macrophages upon *B. pseudomallei* stimulation, transcripts that were identified at 3 and 6 h post stimulation were subjected to canonical pathway analysis (IPA). The top 10 identified pathways at each time point were found to mainly relate to type I IFN- mediated processes (Figure 3.1 B). These included, at the 3 h time point, IFN signalling, JAK/STAT signalling, activation of IRF by cytosolic PRRs, and role of JAK1, JAK2, TYK2 in IFN signalling. Pathways that are related to type I IFN signalling at the 6 h time point are: the activation of IRF by cytosolic PRRs, role of PKR in IFN induction and antiviral response, and IFN signalling (Figure 3.1 B). Genes related to these pathways together with their fold change expression are listed in Table 7.1.

The induction of most of the differentially regulated genes within these type I IFN–related pathways was higher in C57BL/6 compared to BALB/c macrophages (Table 7.1). To validate genes of these pathways which had low log FC values (Table 7.1) including *Oas1g, Stat1, Stat3, Irf7*, and *Isgf3g* (*Irf9*), macrophages were stimulated with *B. pseudomallei* for 3 and 6 h and expression of these genes was evaluated by qRT-PCR (Figure 3.2). *Stat3* and *Irf9* expression was significantly increased in C57BL/6 macrophages 3 h post *B. pseudomallei* stimulation compared to BALB/c macrophages (Figure 3.2 A). *Oas1g, Stat1* and *Irf7* expression was not significantly different between C57BL/6 and BALB/c macrophages 3 h post *B. pseudomallei* stimulation (Figure 3.2 A). Nevertheless, there was a trend of increased transcription in stimulated C57BL/6 macrophages. Six hours post *B. pseudomallei* stimulation this trend was enhanced and *Oas1g, Stat1* and *Irf7* expression was significantly

increased in stimulated C57BL/6 compared to BALB/c macrophages as was the expression of *Stat3* and *Irf9* (Figure 3.2 B).

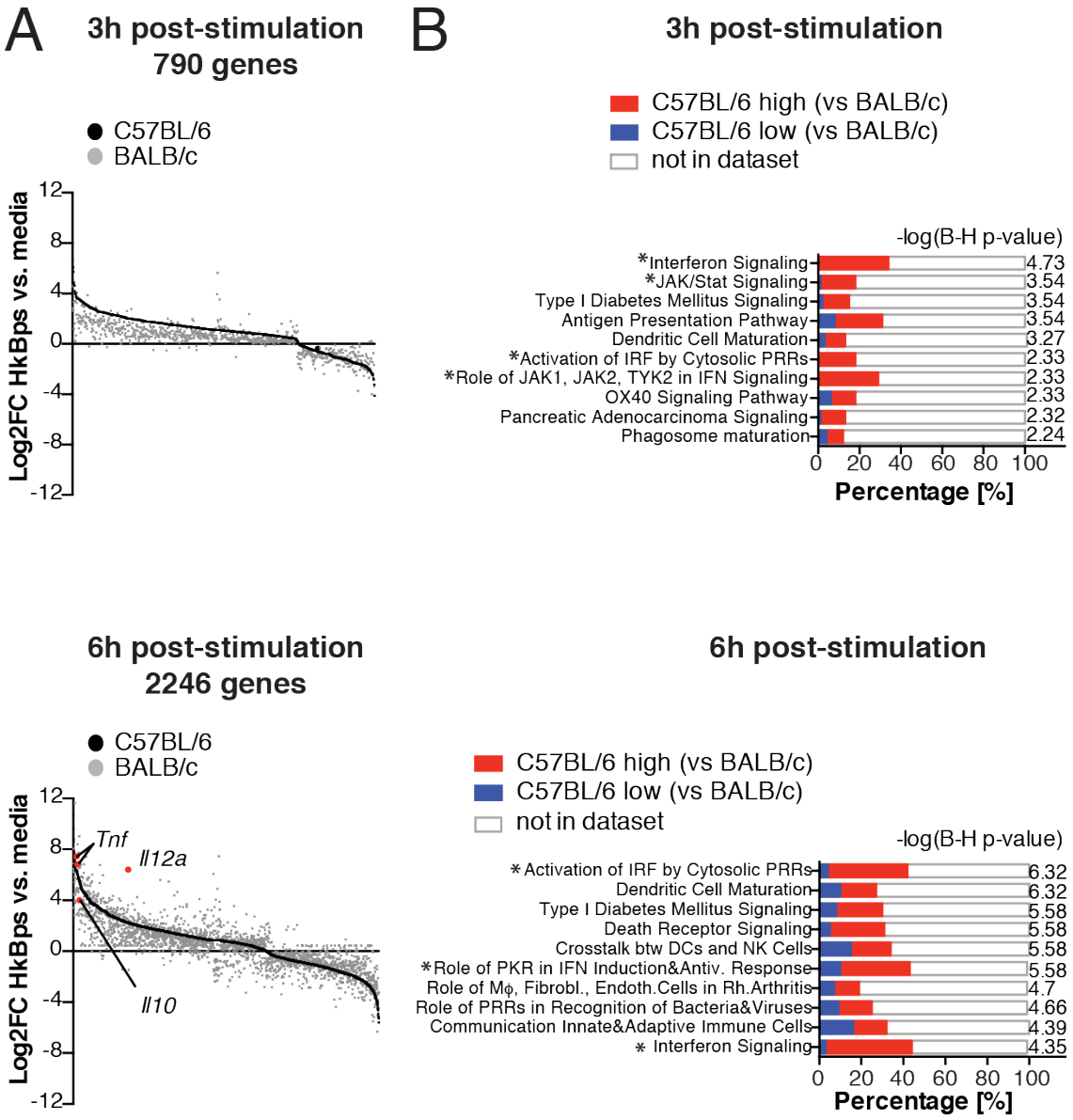

Figure 3.1 Type I IFN related pathways are more up-regulated in C57BL/6 versus BALB/c macrophages upon stimulation with *Burkholderia pseudomallei*.

C57BL/6 and BALB/c macrophages were stimulated with heat-killed *B. pseudomallei* (HkBps) for 3 or 6 h in triplicate cultures. Total RNA was isolated and processed for microarray analysis as described in 2.9.1 (A) Genes significantly differentially regulated by *B. pseudomallei* stimulation in C57BL/6 and BALB/c macrophages were identified by two-way ANOVA analysis ($p < 0.01$, Benjamini–Hochberg false discovery rate) and genes selected that were significantly different due to both stimulation and strain. Genes significantly changed due to stimulus alone or strain

alone were excluded from the analysis. Expression level of individual genes (black dots, C57BL/6; grey dots, BALB/c) are shown as log2 fold change over corresponding media control samples and ordered according to their C57BL/6 expression level. (B) Top 10 IPA pathways significantly associated with the genes differentially regulated by *B. pseudomallei* stimulation in C57BL/6 and BALB/c macrophages at each time point are shown. The x-axis represents the percentage of overlap between input genes and annotated genes within the pathway. Colours within bars denote genes that are more highly expressed in C57BL/6 (red) or BALB/c (blue) macrophages. Benjamini–Hochberg (B-H) corrected –log (p value) represents pathway association. *Type I IFN–related pathway. Data curated in collaboration with Ashleigh Howes.

Our results show that type I IFN signalling pathways as well as type I IFN inducible genes are significantly increased in *B. pseudomallei* stimulated macrophages from C57BL/6 compared to BALB/c mice. In line with these data, we have shown that mRNA levels of type I IFN are also increased upon *B. pseudomallei* and LPS stimulation in C57BL/6 macrophages compared to BALB/c macrophages 1 h after stimulation (data not shown here, Howes, Taubert *et al.*, Figure 3 A in published manuscript) (268). In concordance, type I IFN protein levels are increased in C57BL/6 macrophages compared to BALB/c macrophages, with its peak 3 h post stimulation (data not shown here, Howes, Taubert *et al.*, Figure 3 B in published manuscript) (268).

These data suggest that type I IFN production and consequently type I IFN signalling are a major difference in the responses of C57BL/6 and BALB/c macrophages to *B. pseudomallei* and LPS. These data in part explain the differential expression profile of IL-10 and pro-inflammatory cytokines in C57BL/6 and BALB/c macrophages, as we demonstrated in Howes, Taubert *et al.* (268).

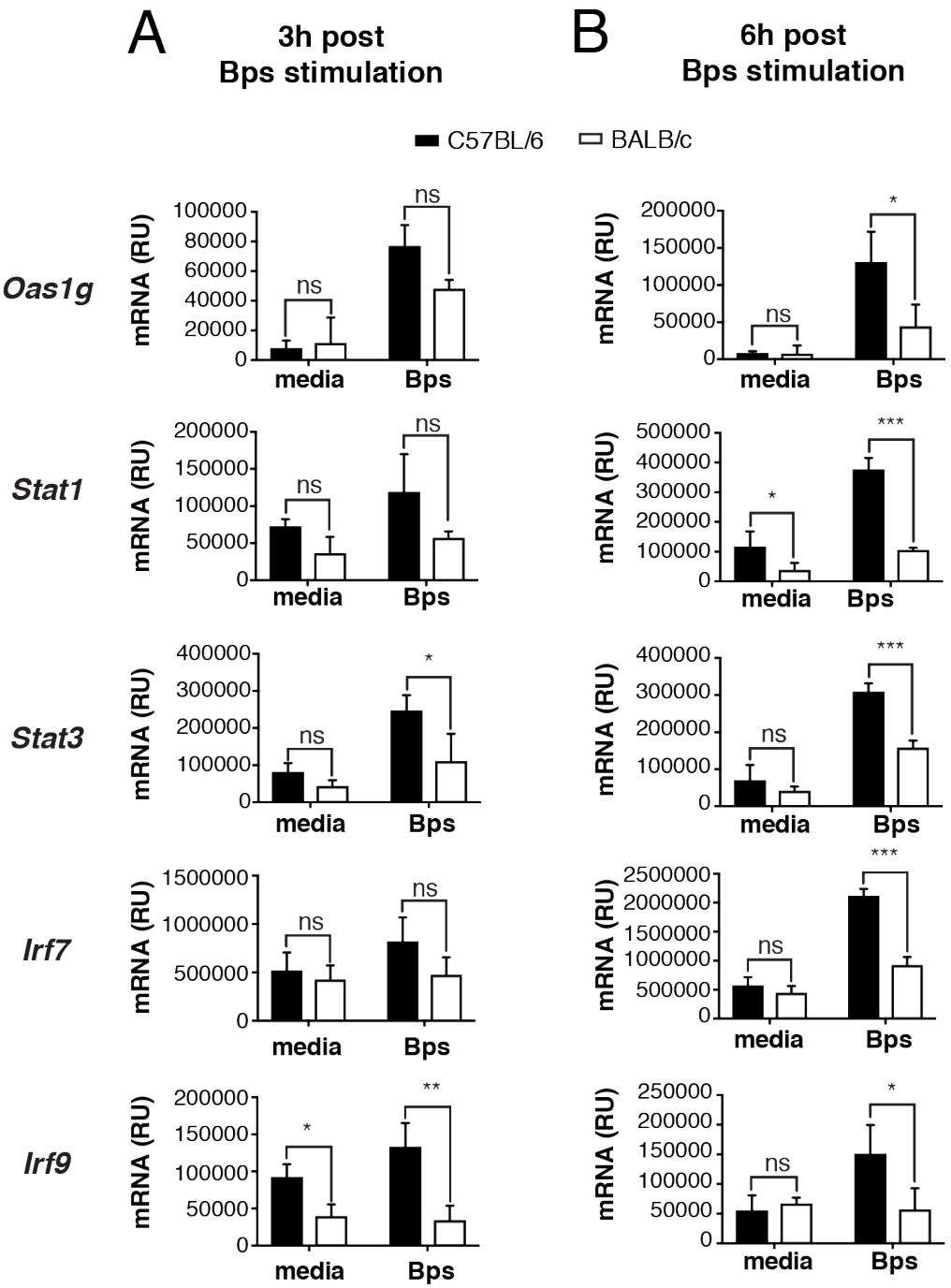

Figure 3.2 Type I IFN inducible genes are increased in C57BL/6 versus BALB/c macrophages following *Burkholderia pseudomallei* stimulation.

C57BL/6 and BALB/c macrophages were stimulated with *B. pseudomallei* (Bps) for (A) 3 h or (B) 6h. Gene expression was determined by qRT-PCR and expression values were normalised to *Hprt1* mRNA expression. All graphs show means ± SD of triplicate cultures. *p < 0.05, **p < 0.01, ***p < 0.001, ns – not significant as determined by two-way ANOVA (Bonferroni multiple comparison test). Representative of three independent experiments.

3.3.2 Expression and endocytosis of TLR4 and CD14 are similar in C57BL/6 and BALB/c macrophages

The mechanism of why type I IFN expression and signalling is different between these two mouse strains is not understood. Zanoni *et al.* (104) and Rajaiah *et al.* (110) reported that CD14 is required for LPS-/*Escherichia coli*-induced TLR4 internalisation into endosomes and that the activation of the TRIF pathway required CD14 at different LPS concentrations. CD14 leads to internalisation of the TLR4 complex into endosomes whereupon TRIF-mediated signalling in macrophages is activated, resulting in type I IFN production (104). To determine if CD14 expression on C57BL/6 and BALB/c macrophages is different and might therefore lead to an increased type I IFN expression and signalling in C57BL/6 macrophages, cells were stained with an anti-CD14 antibody and analysed by flow cytometry. The expression of CD14 was higher on C57BL/6 compared to BALB/c macrophages at steady state (Figure 3.3 A) and 90 min post LPS stimulation (Figure 3.3 B). CD14 expression over a time course of 90 min followed similar kinetics in C57BL/6 and BALB/c macrophages, although CD14 expression was always lower in BALB/c macrophages (Figure 3.3 C).

As CD14 is important in TLR4 endocytosis leading to the activation of the TRIF pathway and the production of type I IFN, we aimed to investigate TLR4 expression and endocytosis on these macrophages upon LPS stimulation. Therefore, we stimulated macrophages with LPS and undertook cell surface staining to evaluate the expression of TLR4 presentation at steady state and during LPS stimulation on the surface of C57BL/6 and BALB/c macrophages. At steady state TLR4 surface expression was similar on C57BL/6 and BALB/c macrophages (Figure 3.3 D). Also,

at 10, 30 and 90 min post LPS stimulation TLR4 expression was similar between C57BL/6 and BALB/c macrophages (Figure 3.3 E, F). The expression of TLR4 decreased over the time course of stimulation on both, C57BL/6 and BALB/c macrophages, indicating the endocytosis of the receptor upon stimulation (Figure 3.3 F). Hence, the rate of TLR4 endocytosis was not significantly different between C57BL/6 and BALB/c macrophages even though CD14 levels varied. Additionally, in support of these data, in Howes, Taubert *et al.* (268) we demonstrated that there is no difference in *Tlr4* mRNA expression between C57BL/6 and BALB/c macrophages at steady state.

In all experiments LPS was added at a final concentration of 10 ng/ml as at this dose IL-10 production was induced in both C57BL/6 and BALB/c macrophages. Additionally, upon stimulation with 10 ng/ml LPS differences in cytokine levels were distinct in C57BL/6 and BALB/c macrophages (titration previously carried out in the O'Garra laboratory). As Zanoni *et al.* (104) as well as Rajaiah *et al.* (110) used higher doses of LPS in their experiments, we repeated our experiments with 1 μg/ml of LPS (Figure 3.4). An increased CD14 expression on C57BL/6 compared to BALB/c macrophages at steady state as well as 90 min post LPS stimulation was confirmed (Figure 3.4 A). However, CD14 endocytosis over a time course of 90 min followed similar kinetics in C57BL/6 and BALB/c macrophages. Nevertheless, TLR4 expression and its endocytosis were not significantly different between C57BL/6 and BALB/c macrophages upon stimulation with 1 μg/ml LPS (Figure 3.4 B) confirming our previous finding using LPS at a concentration of 10 ng/ml (Figure 3.3). Thus, this mechanism could not account for differential cytokine production in C57BL/6 and BALB/c macrophages.

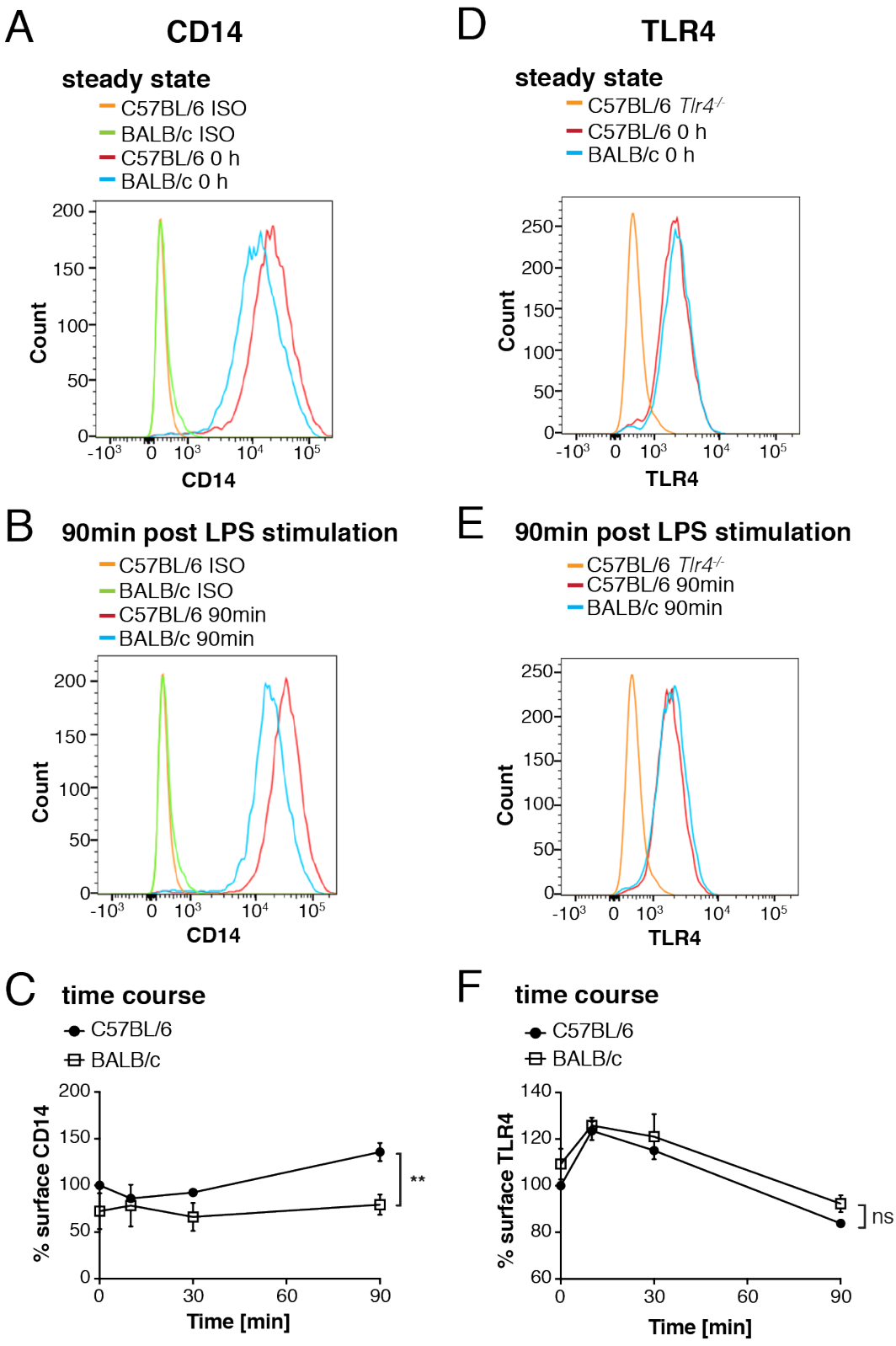

Figure 3.3 TLR4 expression and TLR4 endocytosis are similar upon LPS stimulation in C57BL/6 and BALB/c macrophages.

C57BL/6 and BALB/c macrophages were stimulated with LPS for the indicated times and CD14 (A-C) and TLR4 (D-F) expression was analysed by flow cytometry. Histogram (A, B, D, E) are representative of three independent experiments. (C, F) Graphs show percentage ± SEM of three independent experiments. **p < 0.01, ns – not significant as determined by two-way ANOVA (Bonferroni multiple comparison test). Representative of three independent experiments.

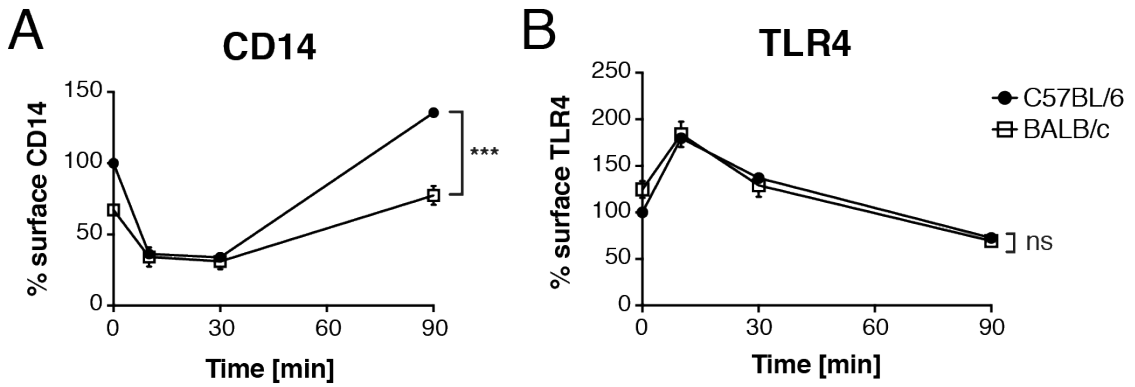

Figure 3.4 Increased dose of LPS does not reveal a difference in TLR4 expression on C57BL/6 and BALB/c macrophages.

C57BL/6 and BALB/c macrophages were stimulated with a high dose of LPS (1 μg/ml) for the indicated times and (A) CD14 and (B) TLR4 expression was analysed by flow cytometry as in Figure 3.3. Graphs show percentage ± SEM of two independent experiments. ***p < 0.001, ns – not significant as determined by two-way ANOVA (Bonferroni multiple comparison test). Representative of two independent experiments.

Altogether, these data suggest that there are no major differences in CD14 and TLR4 expression and endocytosis upon LPS stimulation in C57BL/6 and BALB/c macrophages that could explain the difference in type I IFN production by these cells.

3.3.3 TRIF signalling: TBK1 and IRF3 are more activated in stimulated C57BL/6 macrophages compared to BALB/c macrophages

LPS stimulates TLR4 resulting in the activation of two different downstream adapter molecules, MyD88 and TRIF (52). TRIF activates IRF3, a master transcription controller of antiviral responses that leads to the production of type I IFNs (52). Therefore, we investigated if any downstream targets of TRIF are differentially activated in C57BL/6 and BALB/c macrophages upon LPS stimulation.

The activation of TRIF leads to the recruitment and phosphorylation of TBK1 on Ser172 (343, 344) via TRAF3, which then phosphorylates the cognate upstream adaptor protein. IRF3 binds to the phosphorylated TRIF, and becomes phosphorylated by TBK1. Phosphorylated IRF3 (S396) subsequently dissociates from the adaptor protein and dimerizes before translocating into the nucleus to induce type I IFNs (345).

To investigate if the activation of TBK1 is different in LPS stimulated C57BL/6 and BALB/c macrophages, we blotted for TBK1 (pS172) in this system. Phosphorylation of TBK1 (S172) was reduced in BALB/c macrophages upon LPS stimulation compared to C57BL/6 macrophages (Figure 3.5 A). As this experiment has only been done once, this is a preliminary observation. Nevertheless, in accordance with a decrease in TBK1 (S172) phosphorylation we showed a significant difference in IRF3 activity/(S396) phosphorylation using two different methods (ELISA - Figure 3.5 B; western blotting - Figure 3.5 C) in C57BL/6 and BALB/c macrophages upon *B. pseudomallei* and LPS stimulation.

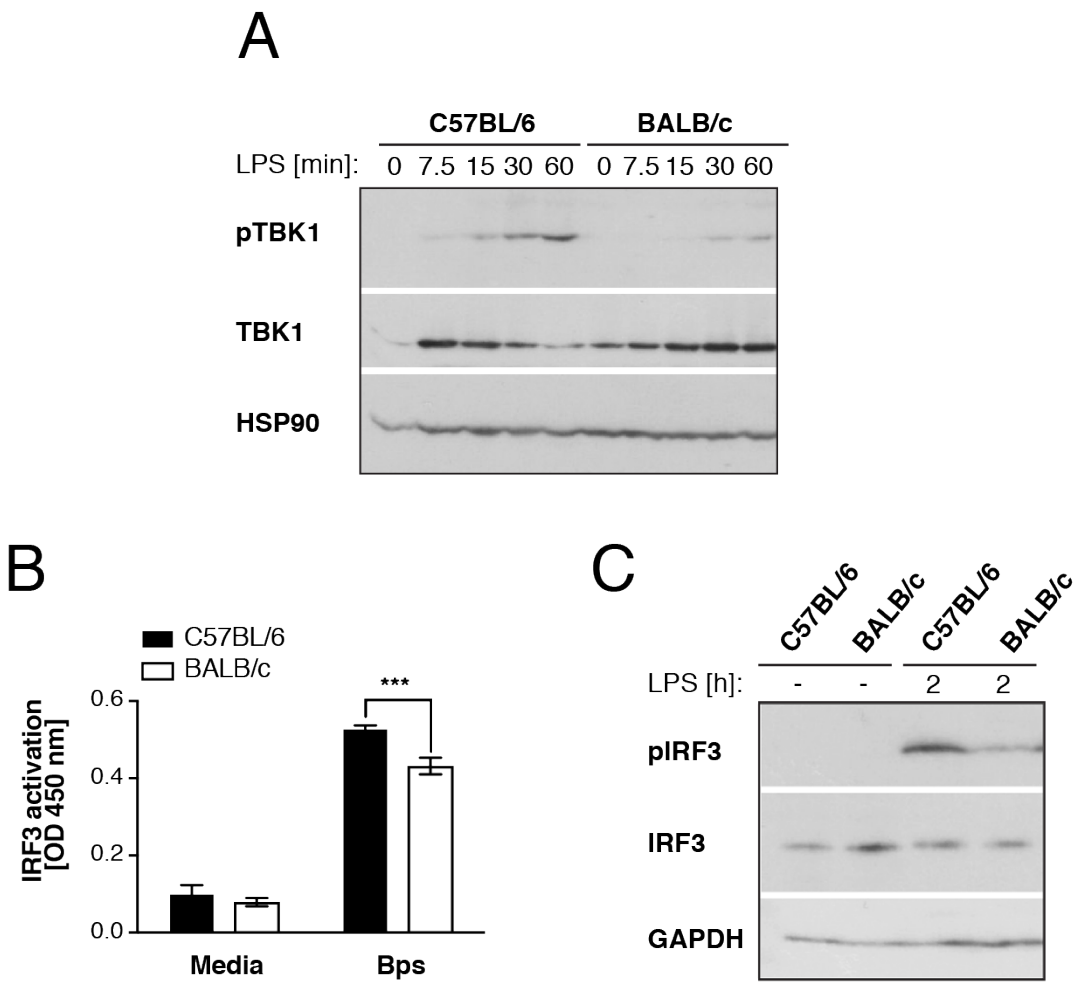

Figure 3.5 TBK1 and IRF3 phosphorylation is increased in C57BL/6 compared to BALB/c macrophages stimulated with *Burkholderia pseudomallei* or LPS.

(A) C57BL/6 and BALB/c macrophages were stimulated with LPS for the indicated time points. Whole-protein extracts were generated and analysed by Western blot for total and phosphorylated TBK1, and HSP90 as loading control. (B) C57BL/6 and BALB/c macrophages were stimulated with *B. pseudomallei* (Bps) for 2 h, and nuclear extracts were analysed for active IRF3 by ELISA. Graph shows means ± SD of triplicate cultures. ***$p < 0.001$ as determined by two-way ANOVA (Bonferroni multiple comparison test). (C) C57BL/6 and BALB/c macrophages were stimulated with LPS for 2 h. Whole-protein extracts were generated and analysed by Western blot for total and phosphorylated IRF3 and GAPDH as loading control. Representative of one (A), two (B) or three independent experiments (C).

In agreement with increased TBK1 and IRF3 activation and higher production of type I IFN in C57BL/6 macrophages, we additionally demonstrated an increased

phosphorylation of STAT1 (Y701) in LPS stimulated C57BL/6, BALB/c, and C57BL/6 *Ifnar1*$^{-/-}$ macrophages (data not shown here, Howes, Taubert *et al.,* Figure 3 C, D in published manuscript) (268). The phosphorylation of STAT1 (Y701) 2 h post stimulation was reduced in BALB/c macrophages compared to C57BL/6. Therefore, the amount of type I IFN produced by BALB/c macrophages is lower compared to C57BL/6 macrophages but is sufficient to activate STAT1. The activation of STAT1 is due to type I IFN signalling as the phosphorylation of STAT1 (Y701) in LPS stimulated C57BL/6 *Ifnar1*$^{-/-}$ macrophages is absent (Howes, Taubert *et al.*, Figure 3 C, D) (268).

3.3.4 MyD88 signalling does not account for differences in type I IFN production of C57BL/6 and BALB/c macrophages stimulated with LPS or *B. pseudomallei*

Our data demonstrate that TBK1 and IRF3 are more activated in C57BL/6 compared to BALB/c macrophages as well as downstream type I IFN signalling even though TLR4 expression and endocytosis are similar. As shown in many co-stimulation studies, MyD88- and TRIF-activating TLR ligands lead to synergistic cytokine production in innate immune cells (346, 347), indicating cross-talk between the MyD88 and TRIF pathways. Moreover, Liu *et al.* showed that TRIF-induced IRF1 can be suppressed by the MyD88 pathway, controlling the magnitude and timing of cytokine expression (348) adding to the complexity of the outcome of these signalling pathways.

We investigated if signalling through the cytosolic adapter protein MyD88 plays a role in the difference in IFN-β production in C57BL/6 and BALB/c macrophages. C57BL/6 and BALB/c WT and *MyD88*$^{-/-}$ macrophages were stimulated with LPS and *B. pseudomallei* and the production of IFN-β quantified by ELISA (Figure 3.6). The production of IFN-β increased significantly in C57BL/6 *MyD88*$^{-/-}$ compared to WT macrophages with both stimuli (Figure 3.6). Although, the deletion of *MyD88* in BALB/c macrophages did not lead to an increase in IFN-β production when stimulated with LPS, the production of IFN-β increased significantly upon *B. pseudomallei* stimulation (Figure 3.6). Nevertheless, IFN-β levels were not elevated in BALB/c *MyD88*$^{-/-}$ macrophages to the levels of WT C57BL/6 macrophages.

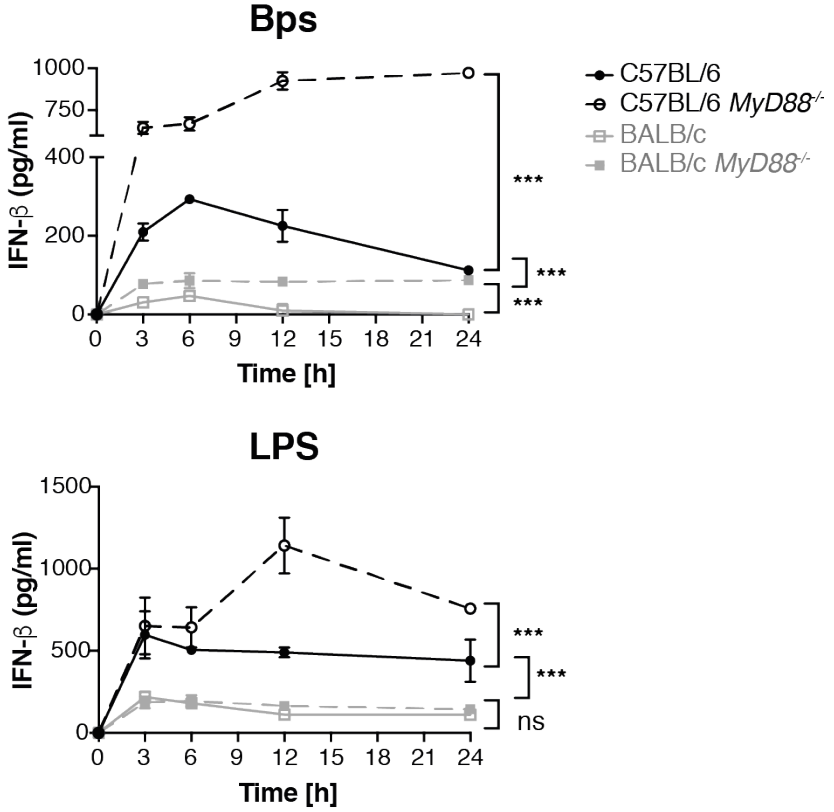

Figure 3.6 Differential production of IFN-β by stimulated C57BL/6 and BALB/c macrophages is independent of MyD88 signalling.

C57BL/6 and BALB/c WT and *MyD88*$^{-/-}$ macrophages were stimulated with LPS and *B. pseudomallei* (Bps) for the indicated times. IFN-β protein levels in supernatants were determined by ELISA. Graphs show means ± SD of triplicate cultures. ***p < 0.001, ns – not significant as determined by two-way ANOVA (Bonferroni multiple comparison test). Representative of two independent experiments.

Although MyD88 signalling inhibits IFN-β production in C57BL/6 macrophages, our data suggest that the differential cytokine production in C57BL/6 versus BALB/c macrophages was not due to inhibition of the TRIF pathway by MyD88-dependent signalling.

3.4 Discussion

Balancing pro- and anti-inflammatory immune responses is necessary to guarantee effective but safe pathogen clearance. C57BL/6 and BALB/c mice show significant differences in their immune responses leading to distinct outcomes of infection (320, 323) such as in *B. pseudomallei* infection, where C57BL/6 mice show enhanced resistance compared to BALB/c mice (349, 350). The higher production of pro-inflammatory cytokines in BALB/c mice has been associated with exacerbated pathology (349, 351, 352). However, it is unclear whether this exacerbated pathology is due to the cytokine storm or decreased control of the bacteria. Nevertheless, *in vivo* infection models show a high degree of complexity. Therefore, it is difficult to completely dissect the mechanisms that underlie the differential production of cytokines in these two strains of mice. Therefore, in Howes, Taubert *et al.* (268), we showed in an *in vitro* setting that C57BL/6 macrophages produce low levels of IL-12, TNF-α and IL-1β, but high levels of IL-10 in response to TLR4 and TLR2 ligands while BALB/c macrophages show a reciprocal cytokine production (268).

To study the underlying mechanisms of the differential cytokine production by stimulated C57BL/6 and BALB/c macrophages, we undertook a comparative microarray analysis of temporal gene expression in *B. pseudomallei* stimulated C57BL/6 and BALB/c macrophages. This analysis revealed major differences of type I IFN–responsive genes and type I IFN pathway genes, including *Oas1g, Stat1, Stat3, Irf7,* and *Irf9* in C57BL/6 compared with BALB/c macrophages. These differences are in accordance with a higher IFN-β production in *B. pseudomallei* stimulated C57BL/6 macrophages compared with BALB/c macrophages (268). These findings demonstrate that fundamental differences in type I IFN induction and signalling in

C57BL/6 and BALB/c macrophage responses may contribute to their differential cytokine production. These findings go in hand with findings by Oliveira *et al.* showing that defective TLR4 signalling for IFN-β expression is responsible for the decreased production of nitric oxide in BALB/c compared to C57BL/6 macrophages in response to LPS (327).

Type I IFNs play a critical role in innate and adaptive immunity during infection with viruses, bacteria, parasites and fungi (285). As well as for other cytokines, the tight regulation of type I IFN is necessary to keep the right balance between an IFN response that is sufficient while limiting tissue damage (285, 287). In most cell types, type I IFN is induced in response to activation of PRRs (285). In macrophages type I IFN is produced amongst others in response to TLR3 and 4 activation. Type I IFN production via TLR4 ligation is dependent on the TRIF pathway (31, 82) and requires CD14 at different LPS concentrations, leading to internalisation of the TLR4 complex into endosomes whereupon TRIF is recruited (110). CD14 expression was increased on C57BL/6 macrophages compared to BALB/c macrophages at steady state and 90 min post LPS stimulation. However, this variance did not lead to a difference in TLR4 endocytosis. Hence, the differential production of IFN-β by C57BL/6 and BALB/c macrophages observed in our study was not due to differential TLR4 expression or differences in the endocytosis rate.

Nevertheless, further downstream of the TLR4-TRIF axis TBK1 activation seems to be increased in LPS stimulated C57BL/6 compared to BALB/c macrophages. These data are supported by increased IRF3 activation/(S396) phosphorylation post LPS or *B. pseudomallei* stimulation in C57BL/6 compared to BALB/c macrophages.

These data suggest that signalling events affecting the TBK1-IRF3 axis, which are critical for the induction of type I IFN downstream of TLR4 (313), may be responsible for the enhanced production of type I IFN in C57BL/6 macrophages compared to BALB/c macrophages.

To exclude the possibility of cross-talk between the MyD88 and TRIF pathway and a possible inhibition of IRF3 activation in BALB/c macrophages as shown by Liu *et al.* (348) for IRF1, we evaluated IFN-β levels in C57BL/6 and BALB/c *MyD88*$^{-/-}$ macrophages. MyD88 signalling significantly inhibited IFN-β production in LPS- and *B. pseudomallei* stimulated C57BL/6 macrophages as well as in *B. pseudomallei* stimulated BALB/c macrophages. However, we found the differential production of IFN-β by stimulated C57BL/6 and BALB/c macrophages to be independent of MyD88 signalling. Sugiyama *et al.* showed that the stimulation of TLR3 and TLR4 pathways in *SMAD2/3*$^{-/-}$ macrophages lead to enhanced IFN-β production and STAT1 phosphorylation compared with WT macrophages. SMAD2 and SMAD3 were found to directly inhibit IRF3, resulting in reduced IFN-β production (353). It needs to be investigated if SMAD2/3 levels and activation are significantly different in C57BL/6 and BALB/c macrophages upon LPS stimulation and whether these might explain the difference in IRF3 activation and the type I IFN induction in these mouse strains. Furthermore, Zanoni *et al.* reported in DCs that TLR4 internalisation and IRF3 activation is mediated by PLC-γ2 and Syk (104). Further studies are required to investigate whether this pathway is existent in macrophages and differentially activated in C57BL/6 and BALB/c macrophages.

Recently, Wang *et al.* reported a new phosphorylation site of STAT2 on T387 that is constitutively phosphorylated in different untreated cancer cell lines and negatively regulates the signal transduction from the type I IFN receptor *(281).* We hypothesised that BALB/c macrophages might show a higher phosphorylation of STAT2 on T387 resulting in reduced type I IFN signalling and a lower production of ISGs. The antibody described and used in the publication by Wang *et al.* was kindly given to us to test this hypothesis. However, preliminary results were not clear as the antibody used was raised against human STAT2 and cross-reactivity was not tested by Wang *et al.*. Hence, further studies are required.

In summary, type I IFN production and type I IFN signalling are a major difference in *B. pseudomallei-* and LPS stimulated macrophages from C57BL/6 and BALB/c mice. This difference is associated with an increased TBK1 (S172) and IRF3 (S396) phosphorylation in stimulated C57BL/6 macrophages compared to BALB/c macrophages which suggests differential signalling downstream of TLR4 may play an important role and may in part explain the different susceptibilities of these two mouse strains in infection.

Chapter 4.
Effects of type I IFN on IL-10 and IL-12p40 upon stimulation with different TLR agonists

4.1 Background

Leading on from our results that type I IFN production and consequently type I IFN signalling are a major difference in the responses of C57BL/6 and BALB/c macrophage to *B. pseudomallei* and LPS and the fact that macrophages produce IL-10 in a type I IFN dependent manner in response to TLR4 stimulation but not upon TLR2 ligation (268), we wanted to investigate the role of type I IFN in the production of IL-10 as well as IL-12p40 in the context of different TLR ligations.

TLR2 and 4 are localised on the cell surface and recognise bacterial motifs such as LPS (TLR4) or peptidoglycan (TLR2). TLR3 and 9 are expressed in the endosomal membrane. TLR3 detects viral double-stranded RNA, small interfering RNAs and self-RNAs from damaged cells, while TLR9 recognises bacterial and viral DNA that is rich in un-methylated CpG-DNA motifs (31, 33, 53). Upon TLR ligation all TLRs with the exception of TLR3 recruit MyD88. TLR2 and 4 additionally need TIRAP, a sorting adaptor, for the recruitment of MyD88. Furthermore, TRAM is only recruited to TLR4 and acts as a linker between TRIF and TLR4 (33). The TRIF-dependent pathway is unique to TLR3 and 4 signalling and is critical for IFN-β production downstream of these receptors (31, 33, 82).

The effects of type I IFN on cytokine production are diverse. Mechanisms whereby type I IFN regulates distinct pro-inflammatory cytokines are as yet unclear (269, 274, 354-356). In the context of IL-10, type I IFN has been shown to promote the IL-10 production from murine macrophages (271, 357), human B cells (276) and human dendritic cells (275). Although much is known about how IL-10 is regulated downstream of TLRs, there is an incomplete understanding of how type I IFN

regulates IL-10 production in macrophages. Some reports suggest roles for STAT1 (274), the PI3K pathway (275) or IL-27 (266) in the regulation of IL-10 by type I IFN. However, a systematic analysis of the pathways and TFs required for type I IFN to regulate IL-10 has not yet been conducted. Therefore, we addressed the signalling pathways induced by type I IFN that are involved in the regulation of IL-10 in TLR activated macrophages.

4.2 Aims

We hypothesised that the regulation of IL-10 and IL-12p40 production through type I IFN in macrophages is context specific. The understanding of how type I IFN regulates IL-10 and pro-inflammatory cytokines in the setting of different TLR signalling pathways is important in the background of various bacterial and viral infections as these activate different TLRs and often type I IFN.

In order to address this hypothesis, we aimed to:

- Investigate the effect of type I IFN on IL-10 and IL-12p40 production in response to various TLR stimuli in macrophages.

4.3 Results

4.3.1 Type I IFN is produced by TLR3 and 4 stimulated macrophages

To address the role of type I IFN on IL-10 and IL-12p40 production, we first aimed to determine TLR signalling pathways that lead to the production of type I IFN in macrophages. We chose to work with four different TLR agonists, Pam3CSK4, Poly I:C, LPS and CpG, each of them stimulating different TLRs with a specific combination of adapter molecules. In the following, macrophages were stimulated with Pam3CSK4 (TLR2 – MyD88/TIRAP), Poly I:C (TLR3 -TRIF), LPS (TLR4 – MyD88/TIRAP, TRIF/TRAM) and CpG (TLR9 – MyD88) and IFN-β protein as well as *Ifnb1* RNA were analysed at different time points (Figure 4.1). TLR2 and 9 signalling did not lead to detectable production of IFN-β protein (Figure 4.1 A), but small amounts of *Ifnb1* mRNA were transcribed in macrophages over the evaluated time course of stimulation (Figure 4.1 B). However, the stimulation with LPS (TLR4) and Poly I:C (TLR3) resulted in IFN-β protein production (Figure 4.1 A) and *Ifnb1* mRNA expression with a weaker response in LPS stimulated macrophages (Figure 4.1 B). The mRNA expression peaked 1 h post LPS stimulation (Figure 4.1 B), and in accordance, protein levels were the highest 3 – 6 h post stimulation (Figure 4.1 A). In Poly I:C stimulated macrophages, *Ifnb1* mRNA expression peaked at 2 h post stimulation and was induced again after 3 h of stimulation with its expression increasing constantly (Figure 4.1 B). This was accompanied by a continuous increase in IFN-β protein levels (Figure 4.1 A).

Our results demonstrate the production of type I IFN upon TLR3 and 4 signalling, but not TLR2 and 9 activation in macrophages. This is in line with what has been previously published (52).

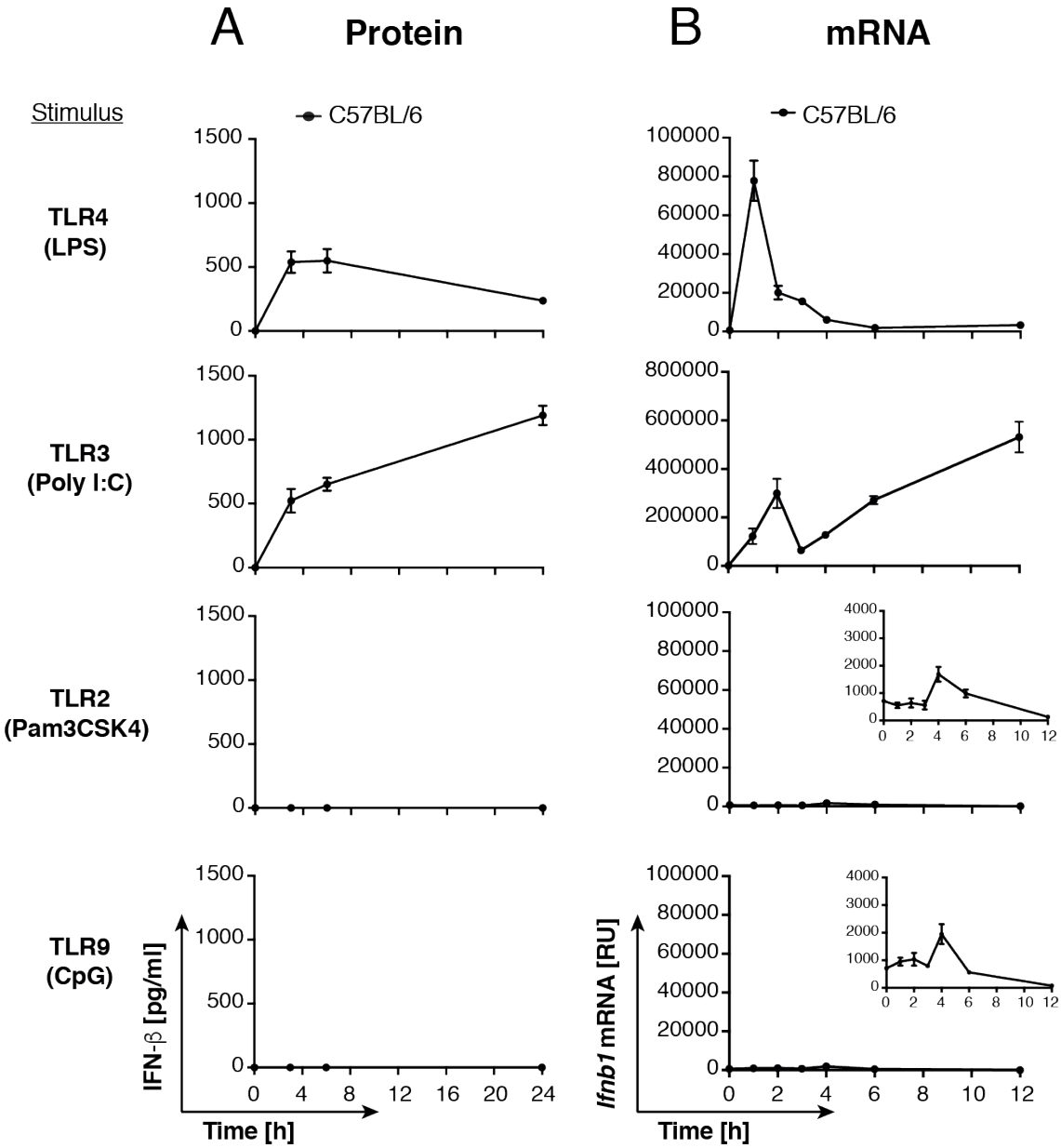

Figure 4.1 TLR3 and TLR4 but not TLR2 and 9 stimulation lead to type I IFN production in macrophages.

Macrophages were generated from C57BL/6 WT mice. (A) Cells were stimulated with LPS, Poly I:C, Pam3CSK4 or CpG for 3, 6 and 24 h and IFN-β protein was measured in supernatant by ELISA. (B) Cells were stimulated with LPS, Poly I:C, Pam3CSK4 or CpG for 1, 2, 3, 4, 6 and 12 h and *Ifnb1* mRNA was measured by

qRT-PCR and normalised to *Hprt1* mRNA. Graphs show means ± SD of triplicate cultures. Representative of two (B) or three (A) independent experiments.

4.3.2 Regulation of IL-10 and IL-12 production by autocrine type I IFN

4.3.2.1 Autocrine type I IFN increases IL-10 protein levels upon TLR3 and 4 stimulation

Positive regulation of IL-10 by type I IFN has been shown in macrophages stimulated with LPS (357) or infected with *Listeria monocytogenes* or *Mycobacterium tuberculosis* (72, 269, 271, 272, 357). To address the potential role of type I IFN on IL-10 production upon stimulation of various TLRs in macrophages, we compared IL-10 protein production in C57BL/6 WT and *Ifnar1*$^{-/-}$ macrophages after a 3, 6 and 24 h stimulation with Pam3CSK4 (TLR2), Poly I:C (TLR3), LPS (TLR4) and CpG (TLR9). *Il10* mRNA expression was also measured 1, 2, 3, 4, 6 and 12 h post stimulation. As shown in Howes, Taubert *et al.* (268), autocrine type I IFN led to an increase of IL-10 protein production upon stimulation with LPS (TLR4) (Figure 4.2 A). The initial induction of *Il10* mRNA transcription led to similar amounts of *Il10* mRNA after LPS in WT and *Ifnar1*$^{-/-}$ macrophages, and was only slightly affected in the absence of type I IFN signalling (Figure 4.2 B). After 3 h of stimulation of macrophages with LPS, however, a second peak of induction of *Il10* mRNA transcription was initiated, which was completely dependent on type I IFN, as this second peak was absent in macrophages lacking the IFN$\alpha\beta$R (Figure 4.2 B), in keeping with data from Howes, Taubert *et al.* (268). In Poly I:C stimulated macrophages, significantly lower levels of IL-10 protein were detected in supernatants from *Ifnar1*$^{-/-}$ macrophages compared to WT macrophages 24 h post

stimulation (Figure 4.2 A). Accordingly, TLR3 stimulation led only to a small increase of *Il10* mRNA at 1 h, which was abrogated by the lack of type I IFN signalling and a second peak of induction of high levels of *Il10* mRNA transcription was seen after 3 h of TLR3 stimulation, which again was completely dependent on type I IFN as it was absent in the *Ifnar1*$^{-/-}$ macrophages (Figure 4.2 B). After TLR2 and 9 ligation, no significant effects of autocrine type I IFN on IL-10 protein levels were observed (Figure 4.2 A). Upon TLR2 stimulation, the initial production of IL-10 protein was slightly lower in *Ifnar1*$^{-/-}$ compared to WT macrophages. However, after 6 h of stimulation IL-10 production was slightly increased upon TLR2 ligation in the absence of type I IFN (Figure 4.2 A). The kinetics of *Il10* mRNA transcription was similar in WT and *Ifnar1*$^{-/-}$ macrophages stimulated with either Pam3CSK4 or CpG (Figure 4.2 B). However, *Il10* mRNA levels were continuously lower in stimulated *Ifnar1*$^{-/-}$ macrophages in response to these ligands. The induction of a second peak of *Il10* mRNA detected in LPS and Poly I:C stimulated macrophages, was however missing in TLR2 and 9 stimulated cells (Figure 4.2 B).

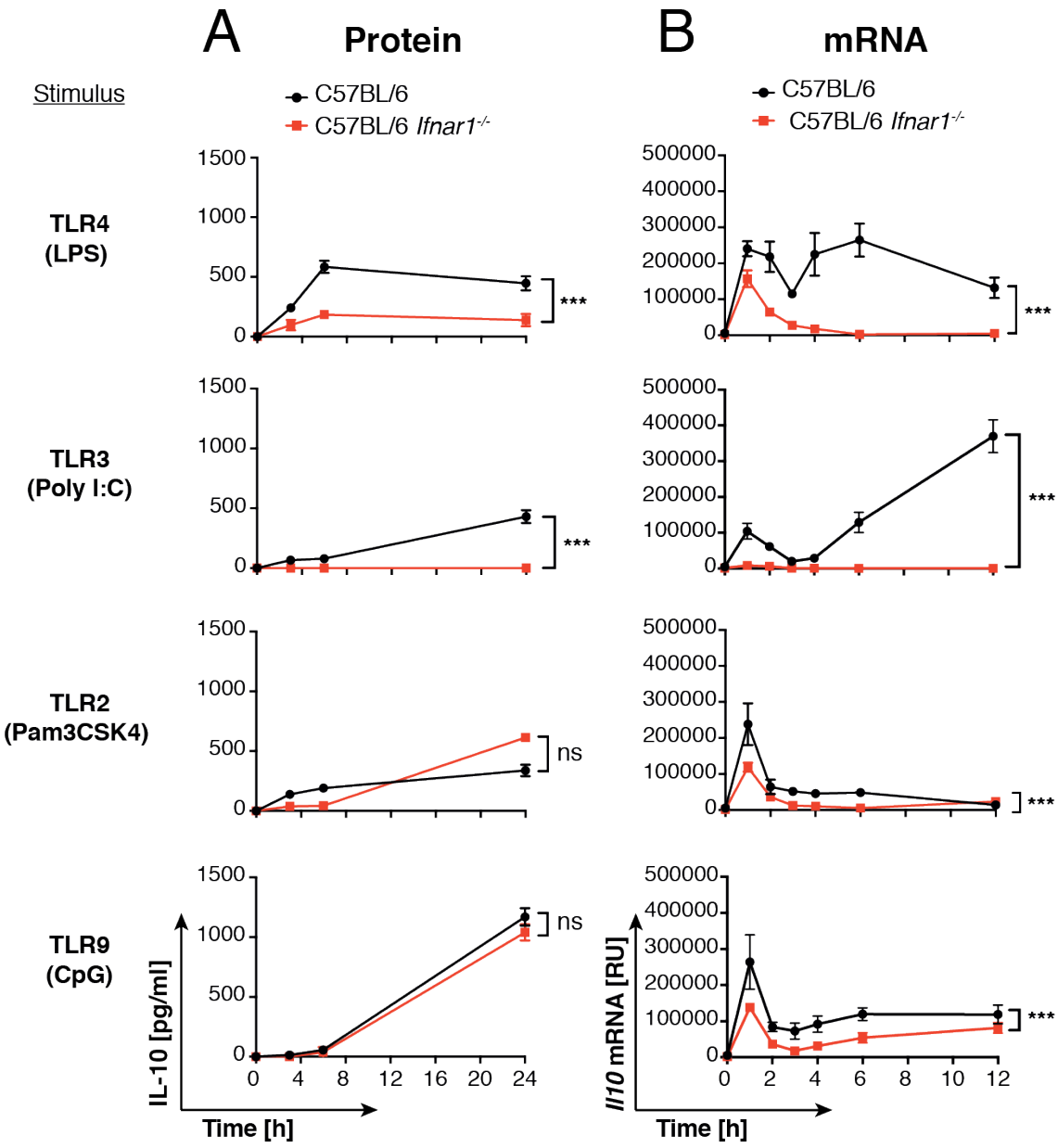

Figure 4.2 Autocrine type I IFN increases IL-10 expression in TLR stimulated macrophages.

Macrophages were generated from C57BL/6 WT and *Ifnar1*$^{-/-}$ mice. (A) Cells were stimulated with LPS, Poly I:C, Pam3CSK4 or CpG for 3, 6 and 24 h and IL-10 protein was measured in supernatant by ELISA. (B) Cells were stimulated with LPS, Poly I:C, Pam3CSK4 or CpG for 1, 2, 3, 4, 6 and 12 h and total RNA was harvested and isolated. *Il10* transcript levels were determined by qRT-PCR and normalised to *Hprt1* mRNA. Graphs show means ± SD of triplicate cultures. Data are representative of three to four (A) or two (B) independent experiments. ***$p < 0.001$, ns – not significant as determined by two-way ANOVA (Bonferroni multiple comparison test).

4.3.2.2 IL-12 production is dependent on type I IFN upon TLR ligation

Type I IFN has also been reported to modulate the levels of IL-12 production in various contexts (72, 269, 354-356). Hence, to determine the role of type I IFN on IL-12 production in macrophages in the context of various TLR ligations, we stimulated C57BL/6 WT and *Ifnar1*$^{-/-}$ macrophages with Pam3CSK4 (TLR2), Poly I:C (TLR3), LPS (TLR4) and CpG (TLR9) and measured IL-12p40 protein in the supernatant after 3, 6 and 24 h stimulation and *Il12b* mRNA expression 1, 2, 3, 4, 6 and 12 h post stimulation (Figure 4.3). IL-12p40 protein production was most highly induced in CpG stimulated WT macrophages (Figure 4.3 A), correlating with the highest *Il12b* mRNA expression levels in these cells (Figure 4.3 B). CpG stimulated WT macrophages produced significantly more IL-12p40 protein compared to *Ifnar1*$^{-/-}$ macrophages. Correspondingly, CpG stimulated WT macrophages also expressed significantly higher levels of *Il12b* mRNA compared to *Ifnar1*$^{-/-}$ macrophages, with the peak of expression at 6 h post stimulation (Figure 4.3 B). In Pam3CSK4, Poly I:C and LPS stimulated macrophages, IL-12p40 protein as well as *Il12b* mRNA levels were significantly higher in WT macrophages as compared to *Ifnar1*$^{-/-}$ macrophages (Figure 4.3). *Il12b* transcription peaked at 3 – 4 h for LPS and Poly I:C stimulated WT macrophages (Figure 4.3 B) resulting in a peak of protein levels at 6 h post stimulation (Figure 4.3 A). Cells stimulated with Pam3CSK4 showed highest *Il12b* mRNA levels 6 h post stimulation (Figure 4.3 B) with a peak in protein production at 24 h (within the time frame of investigation) (Figure 4.3 B).

In summary, autocrine type I IFN affects IL-10 production in macrophages only upon TLR3 and 4 stimulation (Figure 4.2) which is in accordance with type I IFN being produced only upon these stimulations (Figure 4.1). However, in regard to the IL-12

production in TLR stimulated macrophages, type I IFN signalling is important, as IL-12 production is impaired in *Ifnar1*$^{-/-}$ macrophages upon all stimulations tested even though macrophages do not produce type I IFN detectable by ELISA upon TLR2 and 9 activation (Figure 4.3). This might suggest that tonic type I IFN is important for maximal IL-12 production by TLR activated macrophages.

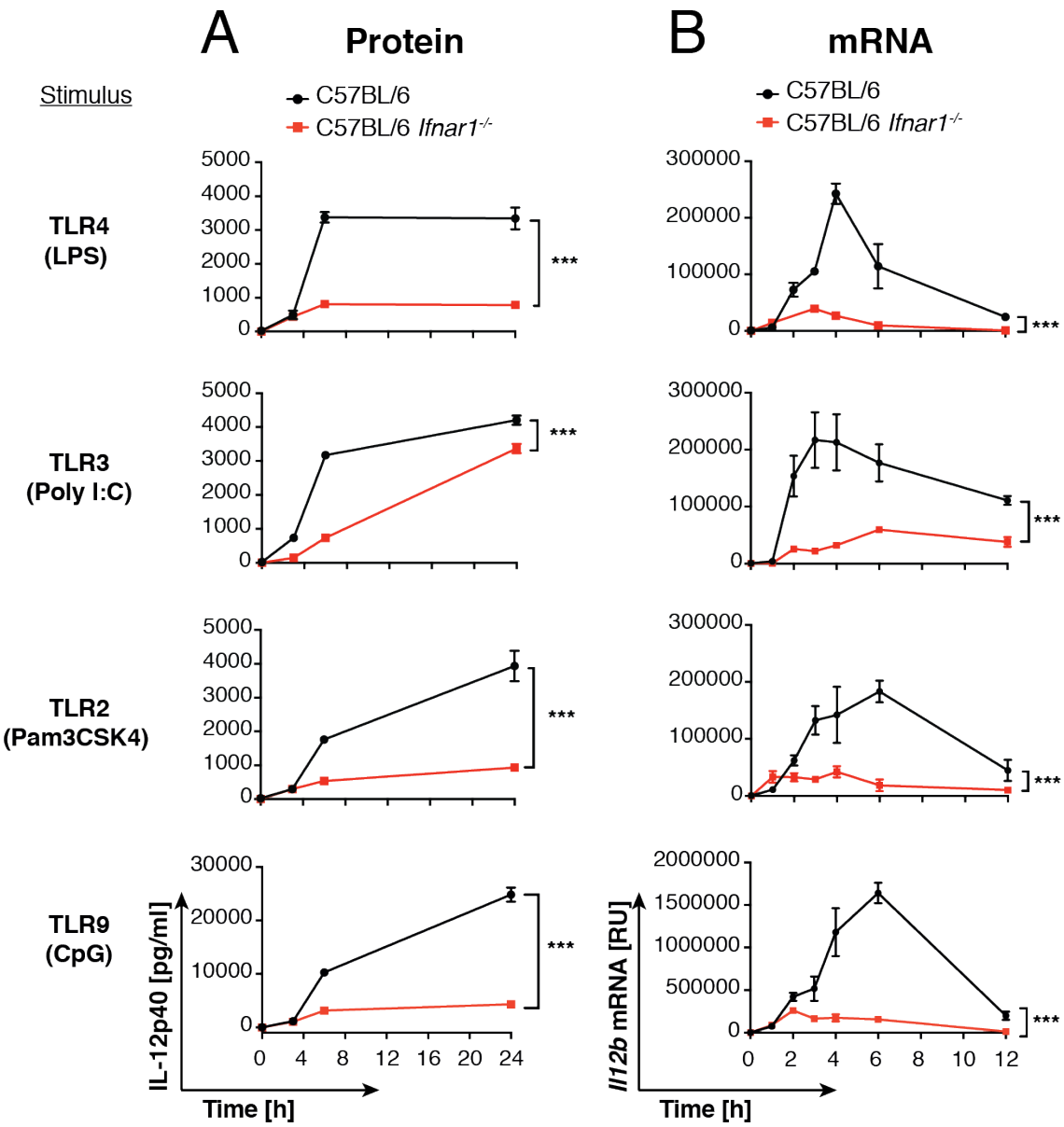

Figure 4.3 IL-12p40 production is dependent on type I IFN signalling upon TLR2, 3, 4 and 9 stimulation.

Macrophages were generated from C57BL/6 WT and *Ifnar1*$^{-/-}$ mice. (A) Cells were stimulated with LPS, Poly I:C, Pam3CSK4 or CpG for 3, 6 and 24 h and IL-12p40 protein was measured in supernatant by ELISA. (B) Cells were stimulated with LPS, Poly I:C, Pam3CSK4 or CpG for 1, 2, 3, 4, 6 and 12 h and total RNA was harvested and isolated. *Il12b* transcript levels were determined by qRT-PCR and normalised to *Hprt1* mRNA. Graphs show means ± SD of triplicate cultures. Data are representative of three to four (A) or two (B) independent experiments. ***$p < 0.001$ as determined by two-way ANOVA (Bonferroni multiple comparison test).

4.3.3 The role of exogenous type I IFN in IL-10 and IL-12 production upon TLR ligations

4.3.3.1 Exogenous type I IFN increases IL-10 production upon TLR2, 3 and 4 stimulation, but decreases its production upon TLR9 ligation

Since in an *in vivo* situation, a diverse range of cells produce type I IFN which could act in concert with TLR ligation on macrophages in a paracrine fashion, we wanted to evaluate the effect of exogenous type I IFN on IL-10 and IL-12 production in concert with stimulation of the different TLRs. To evaluate whether the addition of type I IFN could augment the production of IL-10 upon all TLR ligations, we treated C57BL/6 WT macrophages with exogenous IFN-β or IFN-α in the presence of Pam3CSK4, Poly I:C, LPS and CpG and measured IL-10 protein in the supernatant 24 h post stimulation (Figure 4.4). Treatment with IFN-β in the absence of PRR stimulation only induced minimal amounts of IL-10 production by macrophages even when high IFN-β concentrations were used (Figure 4.4 A). Similar results were obtained with addition of IFN-α alone (Figure 4.4 B). In Pam3CSK4 stimulated cells, the addition of IFN-β or IFN-α greatly enhanced IL-10 production in macrophages. In comparison, only a small increase of IL-10 was observed when IFN-α or IFN-β was added to LPS- and Poly I:C stimulated macrophages (Figure 4.4), as expected, since

these cells already produced type I IFN themselves upon LPS and Poly I:C stimulation (Figure 4.1). Surprisingly, no increase in IL-10 protein production was seen upon TLR9 ligation in the presence of IFN-α or IFN-β (Figure 4.4), despite the fact that we could detect no IFN-β production from these macrophages (Figure 4.1). In fact, a decrease in IL-10 production was observed upon type I IFN addition. Therefore, macrophages are able to produce increased levels of IL-10 in response to IFN-α/β in addition to most TLR ligations, while the addition of IFN-α/β to TLR9 stimulated cells decreased IL-10 production by macrophages.

Our data indicate that type I IFN increases IL-10 production via the induction of a second peak of *Il10* mRNA transcription in response to TLR4. We wanted to investigate if this induction is dependent on the specific TLR signalling pathway or if the presence of type I IFN irrespective of the type of TLR pathway activated is sufficient to induce this second wave of *Il10* mRNA transcription. Therefore, we stimulated cells with Pam3CSK4 together with IFN-β at the same time and evaluated IL-10 protein levels as well as *Il10* mRNA over a time course (Figure 4.5). The simultaneous stimulation of macrophages with Pam3CSK4 and IFN-β significantly increased IL-10 protein production by these cells over time (Figure 4.5 A). This increase was due to an induction of a second wave of *Il10* mRNA transcription by IFN-β (Figure 4.5 B) as seen upon TLR4 stimulation (Figure 4.2). Comparing IL-10 protein levels of LPS and Pam3CSK4 + IFN-β stimulated cells, similar levels could be observed (Figure 4.5 C). In accordance with these data, kinetics of *Il10* mRNA are also alike (Figure 4.5 D). Hence, a second wave of *Il10* transcription can be induced by type I IFN independent of the TLR signalling pathway activated.

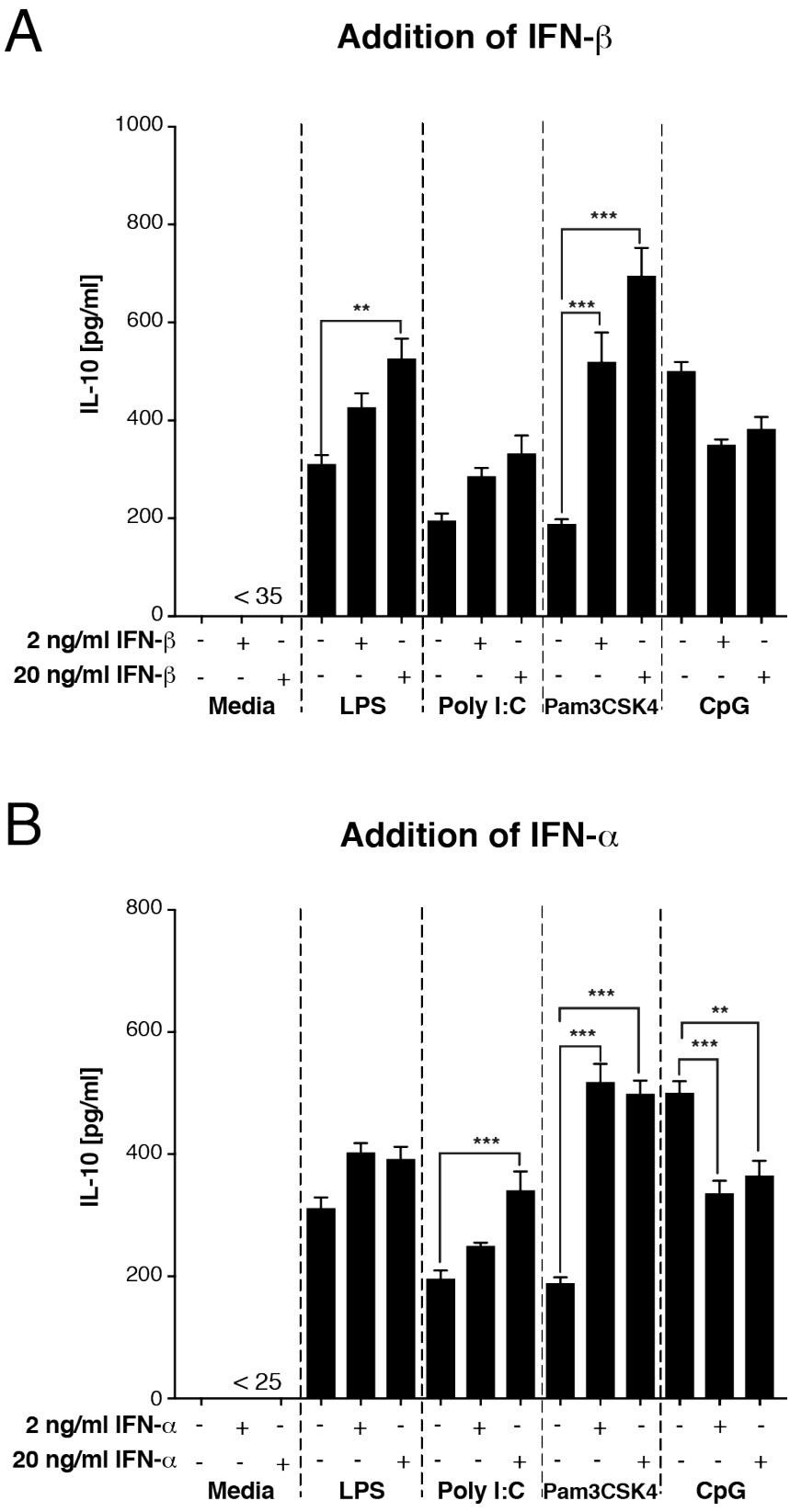

Figure 4.4 Exogenous type I IFN increases IL-10 production by macrophages following TLR2, 3 and 4 stimulation.

Macrophages were generated from C57BL/6 WT mice. Cells were stimulated with LPS, Poly I:C, Pam3CSK4 or CpG for 24 h and either IFN-β (A) or IFN-α (B) added at time of stimulation. IL-10 protein in supernatant was measured by ELISA. Graphs show means ± SD of triplicate cultures. Representative of 3 independent experiments. **p<0.01, ***p<0.001 as determined by One-Way ANOVA (Tukey's multiple comparisons test).

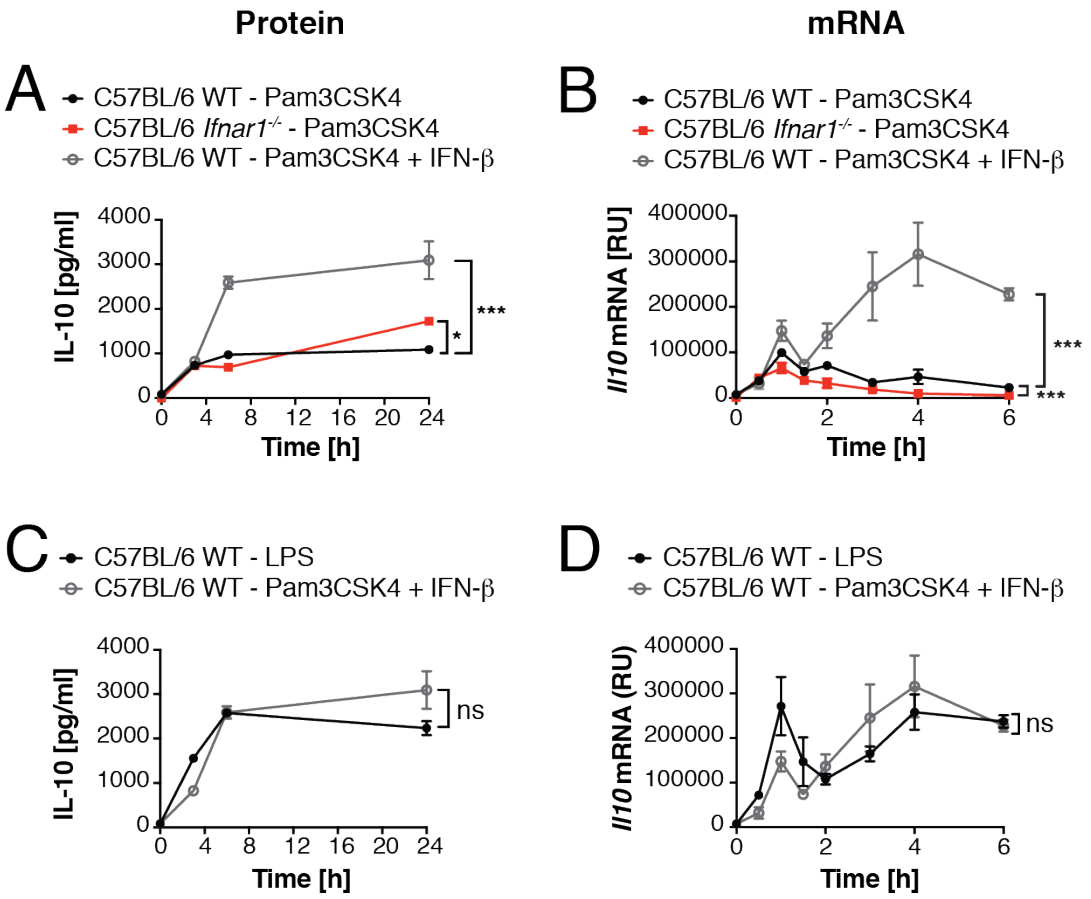

Figure 4.5 Addition of IFN-β induces a second wave of *Il10* mRNA transcription, leading to increased IL-10 in Pam3CSK4 stimulated macrophages.

Macrophages were generated from C57BL/6 WT and *Ifnar1*$^{-/-}$ mice. (A, C) Cells were stimulated with Pam3CSK4 + IFN+β or LPS as control for 3, 6 and 24 h and IL-10 protein was measured in supernatant by ELISA. (B, D) Cells were stimulated with Pam3CSK4 + IFN+β or LPS as control for 0.5, 1, 1.5, 2, 3, 4 and 6 h and total RNA was harvested and isolated. *Il10* transcript levels were determined by qRT-PCR and normalised to *Hprt1* mRNA. Graphs show means ± SD of triplicate cultures. Data are representative of three independent experiments. *p < 0.05, ***p < 0.001, ns – not significant as determined by two-way ANOVA (Bonferroni multiple comparison test).

4.3.3.2 Exogenous type I IFN decreases IL-12 production in TLR stimulated macrophages

Our previous findings demonstrated that IL-12p40 protein and *Il12b* mRNA are dependent on autocrine type I IFN signalling following all investigated TLR ligations. We wanted to extend these observations by investigating the effect of the addition of exogenous IFN-α/β on IL-12 production. To test this, we treated WT macrophages with exogenous IFN-β (Figure 4.6 A) or IFN-α (Figure 4.6 B) in the presence of PRR ligation by LPS, Poly I:C, Pam3CSK4 and CpG. Treatment with neither IFN-β nor IFN-α in the absence of PRR stimulation induced IL-12p40 production by macrophages (Figure 4.6). However, the addition of IFN-β or IFN-α significantly reduced IL-12p40 levels following stimulation via TLR2 and 9. IL-12p40 production was decreased to a lesser extent in TLR4- and Poly I:C stimulated macrophages (Figure 4.6), possibly because type I IFN was already present in these cultures as produced by macrophages themselves (Figure 4.1).

As described before by the O'Garra laboratory by McNab *et al.* (269) and ourselves, Howes, Taubert *et al.* (268) the inhibitory effects of type I IFN on IL-12 production in macrophages are largely dependent on IL-10. Therefore, in the remaining part of this thesis, only the mechanism of how type I IFN is regulating IL-10 will be evaluated further. Furthermore, we will focus on macrophages stimulated with LPS to investigate this interaction. TLR4 and TLR3 ligation are the only signalling pathways leading to detectable type I IFN production *in vitro*. Hence, addition of exogenous type I IFN was not needed. Furthermore, since TLR4 signalling gives higher IL-10 protein levels compared to Poly I:C stimulated macrophages the in-depth mechanism was subsequently investigated using TLR4 ligation.

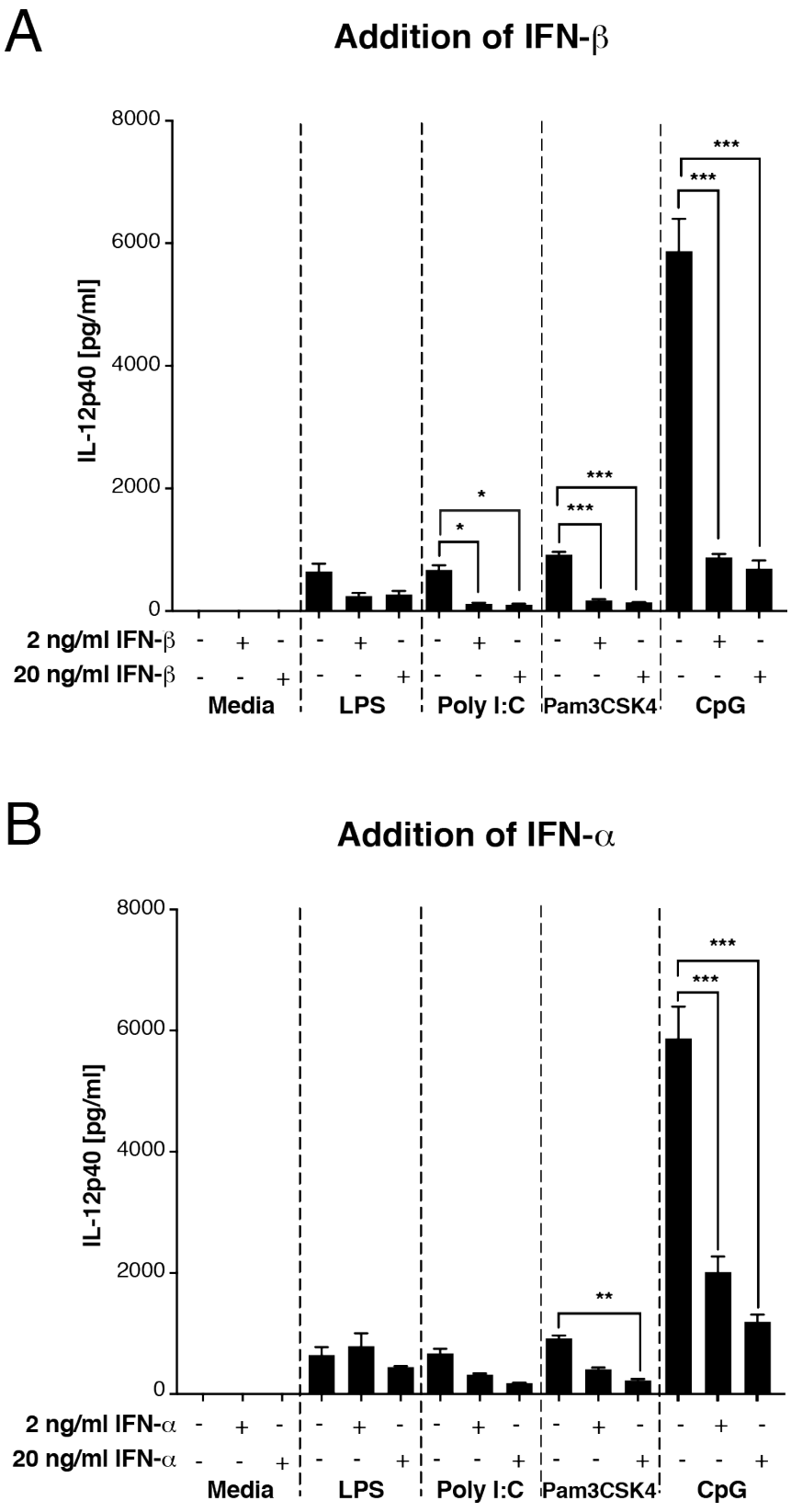

Figure 4.6 Exogenous type I IFN decreases IL-12p40 production in macrophages stimulated with TLR2, 3, 4 and 9 agonists.

Macrophages were generated from C57BL/6 WT mice. Cells were stimulated with LPS, Poly I:C, Pam3CSK4 or CpG for 24 h and either IFN-β (A) or IFN-α (B) added at time of stimulation. IL-12p40 protein in supernatant was measured by ELISA. Graphs show means ± SD of triplicate cultures. Representative of 3 independent experiments. *p<0.05, **p<0.01, ***p<0.001 as determined by One-Way ANOVA (Tukey's multiple comparisons test).

4.3.4 Autocrine type I IFN acts as a transcriptional regulator and stabilises *Il10* mRNA upon TLR4 stimulation

In Howes, Taubert *et al.*, we showed that LPS stimulated C57BL/6 WT macrophages expressed an initial *Il10* mRNA peak at 30 min followed by a second peak at 4 h (data not shown here, Howes, Taubert *et al.*, Fig. 5A in published manuscript (268), also repeated in Figure 4.2 of this chapter). C57BL/6 *Ifnar1*$^{-/-}$ macrophages expressed the initial peak of *Il10* mRNA, which was mostly unaffected by the absence of type I IFN signalling. However, *Ifnar1*$^{-/-}$ macrophages completely lacked the second peak of *Il10* mRNA (Howes, Taubert *et al.*, Fig. 5A; also repeated in Figure 4.2 B of this chapter), suggesting that a late transcriptional wave of *Il10* mRNA expression is activated by autocrine type I IFN. This observation was supported by the presence of a second peak of un-spliced *Il10* mRNA, indicative of active transcription, in LPS stimulated C57BL/6 WT but not *Ifnar1*$^{-/-}$ macrophages, as we reported in Howes, Taubert *et al.* (Figure 5 B in published manuscript, (268), (also repeated in Figure 4.7 of this chapter). Therefore, we postulated that the regulation of IL-10 by type I IFN is at the level of transcription.

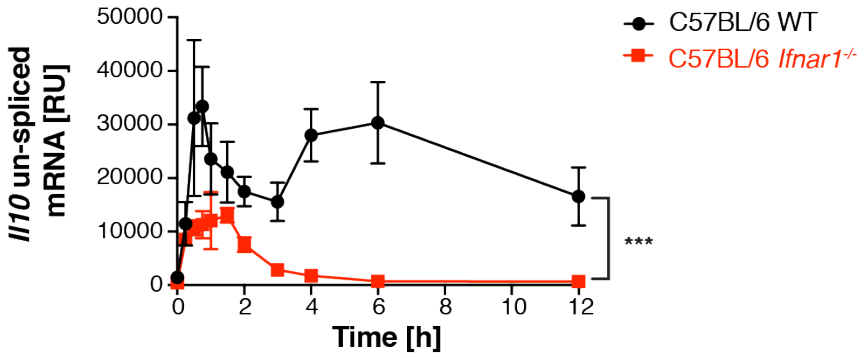

Figure 4.7 Autocrine type I IFN as transcriptional regulator of *Il10* mRNA in macrophages upon TLR4 stimulation.

Macrophages were generated from C57BL/6 WT and *Ifnar1*$^{-/-}$ mice. Cells were stimulated with LPS for 15, 30, 45min, 1, 1.5, 2, 3, 4, 6 and 12 h and total RNA was harvested and isolated. *Il10* un-spliced mRNA transcript levels were determined by qRT-PCR and normalised to *Hprt1* mRNA. Graph shows means ± SD of triplicate cultures. Data are from 1 experiment. Data curated as repeat of Ashleigh Howes experiment (268). ***p < 0.001 as determined by two-way ANOVA (Bonferroni multiple comparison test).

By adding Actinomycin D, a RNA synthesis inhibiting agent, to WT and *Ifnar1*$^{-/-}$ macrophages stimulated for 1 h with LPS or LPS + IFN-β, we investigated whether type I IFN has an additional effect on *Il10* mRNA stability. We showed that upon TLR4 stimulation *Il10* mRNA levels decay faster over time in macrophages lacking the IFNαβ receptor compared to WT macrophages (Figure 4.8). The addition of IFN-β to WT macrophages led to similar *Il10* transcription levels compared to the control (Figure 4.8), possibly due to production of type I IFN by macrophages upon LPS stimulation, to a level required for *Il10* mRNA stabilisation and already saturating the culture media. This suggests that autocrine type I IFN, in addition to inducing a second peak of transcription, can also stabilise *Il10* mRNA expression.

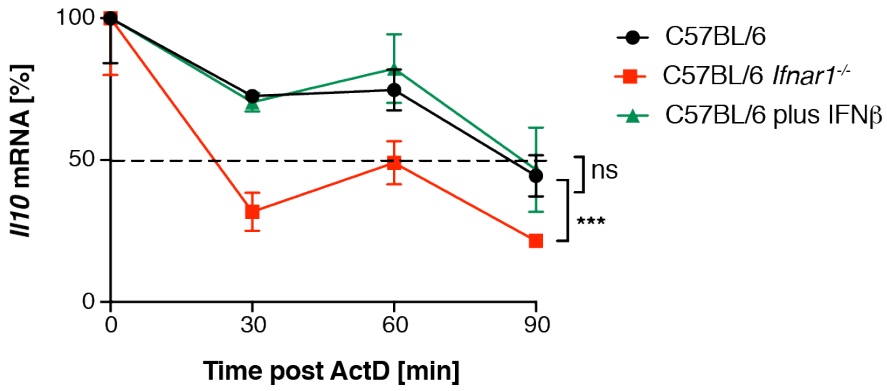

Figure 4.8 Autocrine type I IFN stabilises *Il10* mRNA in TLR4 stimulated macrophages.

C57BL/6 and C57BL/6 *Ifnar1*$^{-/-}$ macrophages were stimulated with LPS for 1 h +/- IFN-β and treated with actinomycin D (ActD). *Il10* mRNA was harvested and quantified by qRT-PCR, normalised to *Hprt1* mRNA levels. Graph shows means ± SD of triplicate cultures. Data are representative of three independent experiments. ***p < 0.001, ns – not significant as determined by two-way ANOVA (Bonferroni multiple comparison test).

4.3.5 The role of MAPKs in the type I IFN dependent regulation of IL-10 in LPS stimulated macrophages

Several studies investigating the molecular mechanisms of IL-10 regulation in macrophages have shown important roles for the TPL-2/ERK (70, 71, 225, 226), p38 (358), PI3K/AKT (92, 94) and NF-κB (227, 229, 359) pathways in the positive regulation of IL-10 production. We therefore wanted to determine whether any of these kinases are involved in the induction of the second, type I IFN dependent peak of *Il10* mRNA transcription.

Firstly, we aimed to validate these finding in our *in vitro* system. We made use of the Kinase Profiling Inhibitor Database (http://www.kinase-screen.mrc.ac.uk/kinase-

inhibitors) as well as publications (330, 331) to define the specific inhibitor and the correct concentration for maximal efficiency with minimal off-target effects. Initially we titrated different inhibitors for p38 (BIRB0796), MEK1/2 (PD0325901), PI3K (PI-103), mTOR (rapamycin) and GSK-3 (CT99021) to determine the optimal concentration for their use. The inhibitor or DMSO (used as vehicle control) was added 1 h before the 24 h-stimulation of WT macrophages with LPS as previously performed in the laboratory during optimisation of these assays. IL-10 protein production was measured in the supernatant by ELISA and an appropriate concentration for each inhibitor was chosen (Figure 4.9, red squares). Concentrations selected were then used for subsequent experiments. As published, inhibitors of p38, MEK1/2 (234) and mTOR (93) resulted in decreased IL-10 production in response to LPS. In contrast, inhibition of GSK-3 resulted in an increase in IL-10. The effect on IL-10 production by the PI3K inhibitor PI-103 is not clear, as only the addition of specific concentrations inhibits IL-10 production.

Comparing IL-10 production in macrophages treated with different kinase inhibitors at optimal concentrations 24 h post LPS stimulation, we showed a strong decrease in IL-10 levels upon MEK1/2, p38 and mTOR inhibition. The effect was less pronounced in PI3K inhibited LPS stimulated macrophages. Upon inhibition of GSK-3, IL-10 production increased greatly. All in all, these results are in keeping with previous literature (Figure 4.9, Figure 4.10) (93, 94, 230, 232).

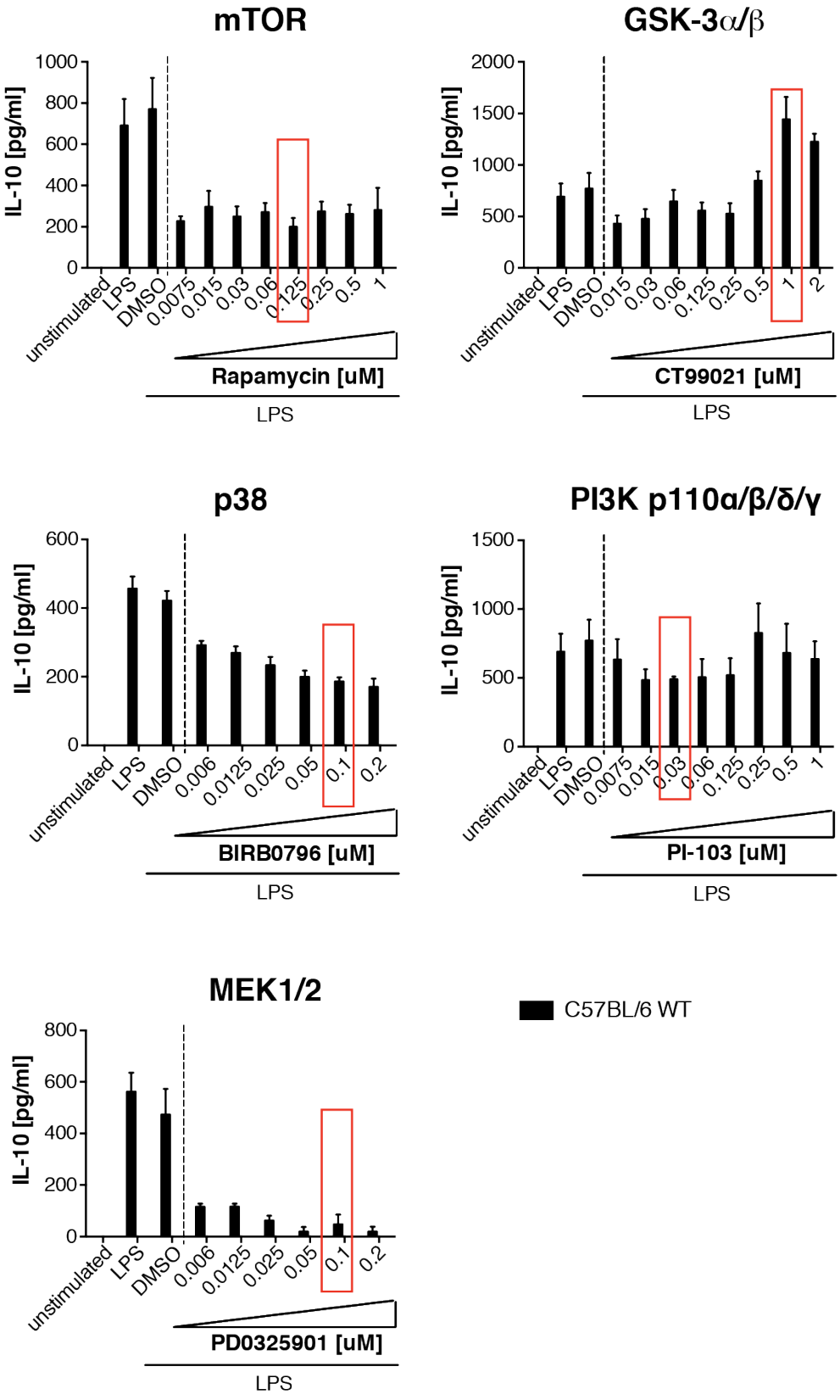

Figure 4.9 Optimal inhibitor concentration of MAPK inhibitors.

Macrophages were generated from C57BL/6 WT mice. Cells were pre-incubated with the inhibitor for 1 h and then stimulated with LPS for 24 h. IL-10 protein in supernatant was measured by ELISA. Red squares indicate chosen concentration. Graphs show means ± SD of triplicate cultures. Data are representative of one - two independent experiments. PD0325901 and BIRB0796 titration done by Ashleigh Howes.

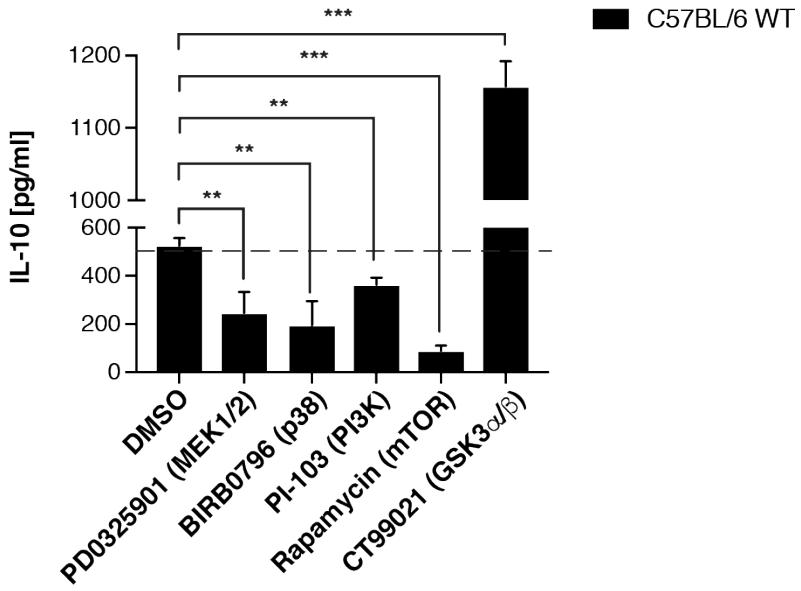

Figure 4.10 MEK1/2, p38, PI3K and mTOR inhibition decreases IL-10 production, while GSK-3 inhibition increases IL-10 levels.

Macrophages were generated from C57BL/6 WT mice. Cells were pre-incubated with the inhibitor for 1 h and then stimulated with LPS for 24 h. IL-10 protein in supernatant was measured by ELISA. Graphs show means ± SD of triplicate cultures. **p < 0.01, ***p < 0.001 as determined by two-tailed Student's t-test. Data are representative of three to four independent experiments.

To assess whether these kinases play a role during the induction of the second, type I IFN-dependent, peak of *Il10* mRNA transcription observed 3 h after LPS stimulation in macrophages, kinase inhibitors were added to cultures either 1 h prior to, or 2 h post stimulation. Thereby, it was possible to distinguish, whether these kinases play a role in the induction of the first or second peak of *Il10* mRNA transcription, or in both (Figure 4.11 A).

Upon p38 inhibition *Il10* mRNA expression levels were significantly lower when the inhibitor was added 1 h prior to as well as 2 h post stimulation (Figure 4.11 B, C). However, kinetics of *Il10* mRNA expression were similar between DMSO and p38 inhibited cells. The addition of the MEK1/2 inhibitor PD0325901 at either time point, did not interfere with the transcription of the first peak of *Il10* mRNA but the second peak of *Il10* mRNA transcription was absent compared with the DMSO control (Figure 4.11 B, C). Blocking mTOR and PI3K 1 h prior to stimulation with LPS led to significantly lower levels of *Il10* mRNA at the time points analysed (Figure 4.11 B). Nevertheless, the kinetics of *Il10* mRNA transcription were similar in control and inhibitor treated cells. Inhibition of mTOR and PI3K 2 h post stimulation did not alter *Il10* mRNA transcription (Figure 4.11 C). Independently of the time point of addition of the GSK-3 inhibitor to the cultures, a significant increase in *Il10* mRNA transcription was detected from 3 h after stimulation (Figure 4.11 B, C).

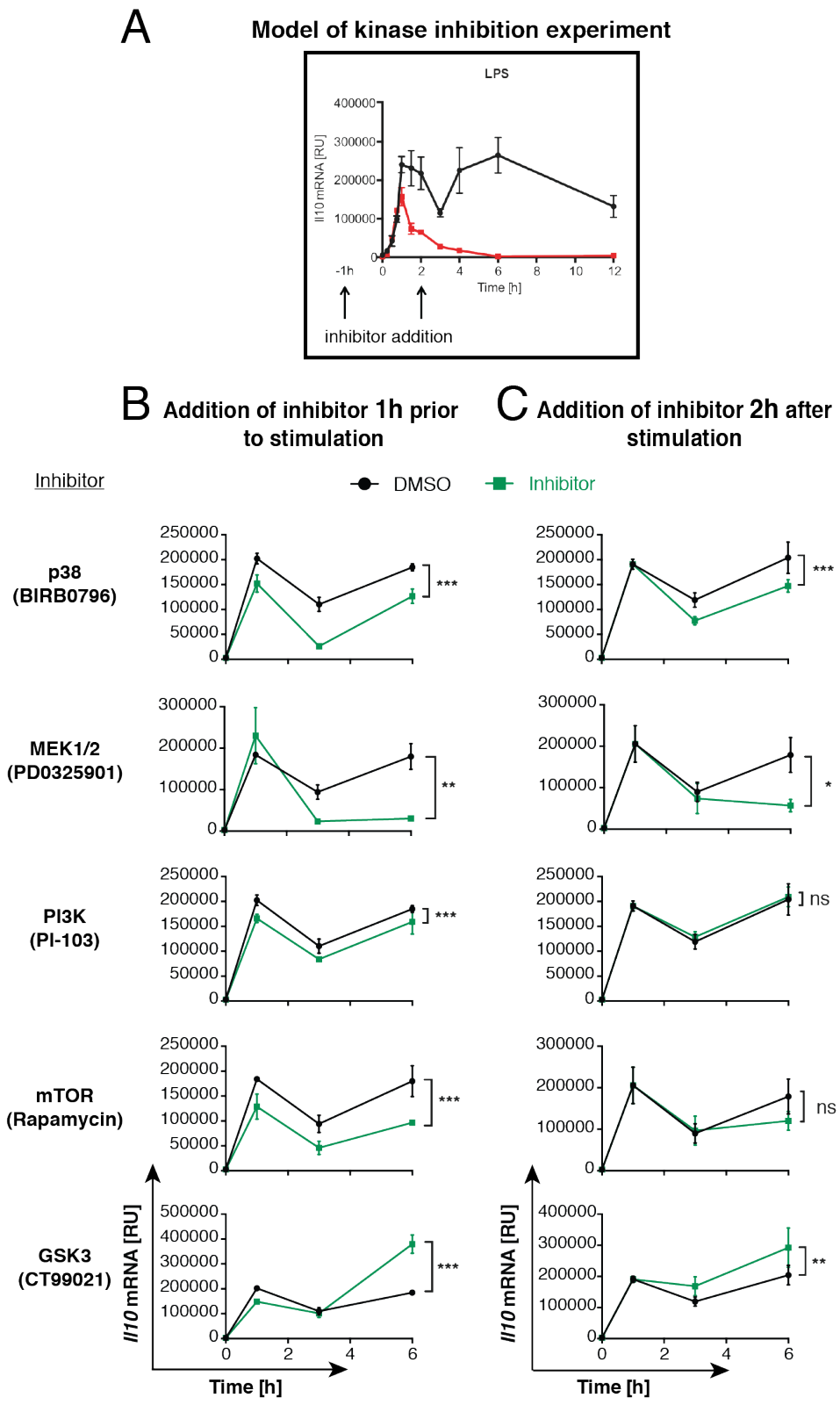

Figure 4.11 IFNβ-mediated increase in *Il10* transcript levels appears to be dependent on p38 and ERK1/2 signalling and is negatively regulated by GSK-3 upon LPS stimulation.

(A) Model of the experiment. (B, C) Macrophages were generated from C57BL/6 WT mice. Cells were stimulated with LPS and either pre-incubated with the inhibitor for 1 h (B) or the inhibitor was added 2 h (C) post stimulation. Total RNA was harvested 1, 3 and 6 h post stimulation and isolated. *Il10* transcript levels were determined by qRT-PCR and normalised to *Hprt1* mRNA. Graphs show means ± SD of triplicate cultures. *p < 0.05, **p < 0.01, ***p < 0.001, ns – not significant as determined by two-way ANOVA (Bonferroni multiple comparison test). Data are representative of three to four independent experiments.

Since p38, MEK1/2 and GSK-3 inhibition led to a significant change in *Il10* mRNA transcription if added 2 h post stimulation, these data suggested that these pathways might play a role in the type I IFN dependent regulation of IL-10 (Figure 4.11 C). To evaluate if the activity of these kinases is changed by type I IFN, macrophages from WT and *Ifnar1*$^{-/-}$ macrophages were stimulated with LPS for 1, 3 and 6 h and phosphorylation of these kinases determined (Figure 4.12). Phosphorylation of p38 at T180/Y182 was similar in WT and *Ifnar1*$^{-/-}$ macrophages at the evaluated time points (Figure 4.12 A). Phosphorylation of GSK-3α/β (S21/9) was likewise not different between WT and *Ifnar1*$^{-/-}$ macrophages (Figure 4.12 B). However, *Ifnar1*$^{-/-}$ macrophages showed reduced ERK1/2 (T185/Y187) phosphorylation at 1, 3 and 6 h post LPS stimulation compared to their WT counterparts (Figure 4.12 C).

In accordance with these data, we showed that IFN-β itself is able to phosphorylate ERK1/2 (T185/Y187) in WT but not in *Ifnar1*$^{-/-}$ macrophages, demonstrating the specificity of the IFN-β activation of ERK1/2 through the type I IFN receptor (Figure 4.13).

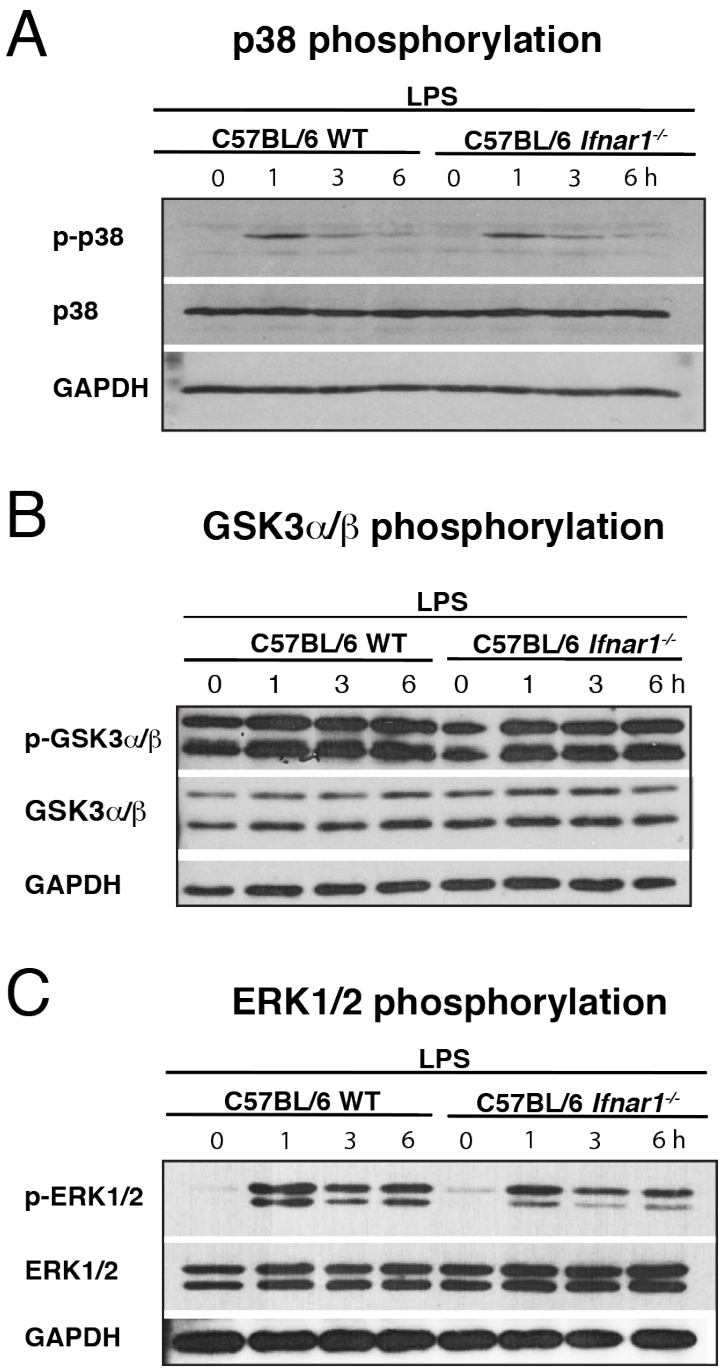

Figure 4.12 Type I IFN signalling increases the phosphorylation of ERK1/2 in LPS stimulated macrophages.

C57BL/6 WT and *Ifnar1*$^{-/-}$ macrophages were stimulated with LPS for the indicated time points. Whole-protein extracts were generated and analysed by Western blot for total and phosphorylated p38 (A), GSK-3α/β (B) and ERK1/2 (C) and GAPDH as loading control. Data are representative of two (A, B) or four (C) independent experiments.

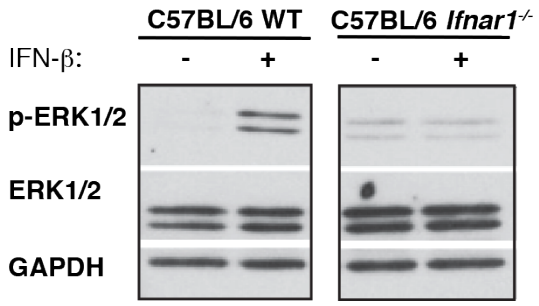

Figure 4.13 IFN-β alone leads to phosphorylation of ERK1/2.

C57BL/6 WT and *Ifnar1*$^{-/-}$ macrophages were stimulated with 20 ng/ml IFN-β for 30 min. Whole-protein extracts were generated and analysed by Western blot for total and phosphorylated ERK1/2 and GAPDH as loading control. The two blots are from the same gel, with same exposure time. Data are representative of three independent experiments.

To demonstrate that the regulation of IL-10 via type I IFN was mediated by ERK1/2 activation, WT and *Ifnar1*$^{-/-}$ macrophages were pre-treated for 1 h with either DMSO as vehicle control or the MEK1/2 inhibitor PD0325901 before being stimulated with LPS for 24 h. As shown before (Figure 4.10), the inhibition of MEK1/2 led to a significant decrease in IL-10 production in LPS stimulated WT macrophages. The level of IL-10 produced in MEK1/2 inhibited LPS stimulated WT cells was similar to the level of IL-10 produced by LPS stimulated *Ifnar1*$^{-/-}$ macrophages. Upon inhibition of MEK1/2 in LPS stimulated *Ifnar1*$^{-/-}$ macrophages, no further reduction in IL-10 levels were achieved (Figure 4.14), confirming that type I IFN signalling through ERK1/2 activation accounted for the increased type I IFN dependent IL-10 production observed. This result was validated using two different MEK1/2 inhibitors (Figure 7.4).

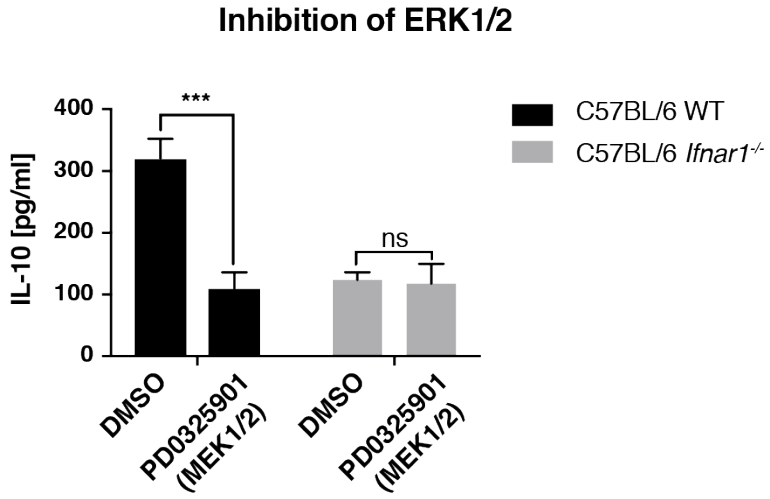

Figure 4.14 ERK1/2 signalling is required for type I IFN mediated IL-10 production in LPS stimulated C57BL/6 macrophages.

C57BL/6 WT and *Ifnar1*$^{-/-}$ macrophages were treated with PD0325901 or DMSO as vehicle control 1 h prior to stimulation with LPS for 24h. IL-10 production was quantified by ELISA. Graphs show means ± SD of triplicate cultures. ***$p < 0.001$, ns – not significant as determined by two-way ANOVA (Bonferroni multiple comparison test). Data are representative of three independent experiments.

To control for non-specific effects of the inhibitors, particularly inhibition of kinases downstream of the type I IFN receptor, IFN-β production was evaluated after inhibitor addition. Macrophages were pre-incubated with the inhibitor for 1 h and then stimulated with LPS. IFN-β protein (Figure 4.15 A) and *Ifnb1* mRNA (Figure 4.15 B) were measured. The inhibitors PI-103 (PI3K) and Rapamycin (mTOR) show no effects on IFN-β production, while PD0325901 (MEK1/2), BIRB0796 (p38) and CT99021 (GSK-3) led to an increase in IFN-β production (Figure 4.15 A). None of the inhibitors led to a significant change of *Ifnb1* mRNA transcription at 1 h post stimulation (Figure 4.15 B).

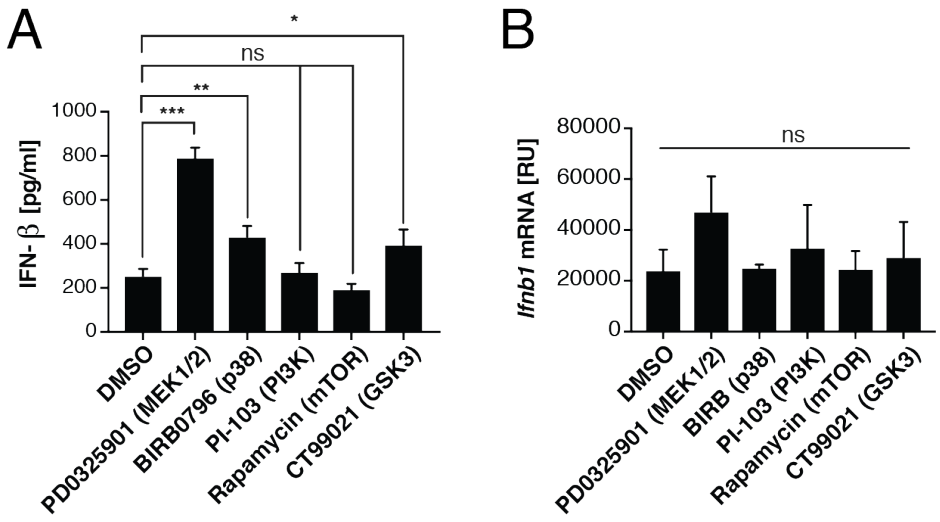

Figure 4.15 Kinase inhibition does not decrease IFN-β production by LPS stimulated macrophages.

C57BL/6 WT macrophages were pre-incubated with the inhibitor for 1 h and then stimulated with LPS. (A) IFN-β protein in supernatant was measured 6 h post stimulation by ELISA. (B) *Ifnb1* mRNA was harvested 1 h post stimulation and quantified by qRT-PCR and normalised to *Hprt1* mRNA levels. Graphs show means ± SD of triplicate cultures. *$p < 0.05$, **$p < 0.01$, ***$p < 0.001$, ns – not significant as determined by two-tailed Student's t-test. Data are representative of two independent experiments.

Additionally, we checked if STAT1 activation as well as transcription of various ISGs downstream of the type I IFN receptor were affected after addition of the inhibitors. We stimulated WT macrophages with LPS and added the inhibitors 1 h prior to stimulation. STAT1 phosphorylation (Y701) was determined 1 h post LPS stimulation and showed no difference in DMSO compared to inhibitor treated macrophages (Figure 4.16 A). To evaluate possible changes in the expression of *Irf7* and *Mx1,* WT macrophages were treated with DMSO as vehicle control or the respective inhibitor for 1 h, before stimulated with LPS. mRNA was harvested at 1, 3 and 6 h post stimulation. There was no significant difference in *Irf7* and *Mx1* expression upon kinase inhibition with the stated inhibitors (Figure 4.16 B, C). However, upon inhibition of mTOR I*rf7* was slightly decreased 6 h post LPS stimulation (Figure 4.16 B).

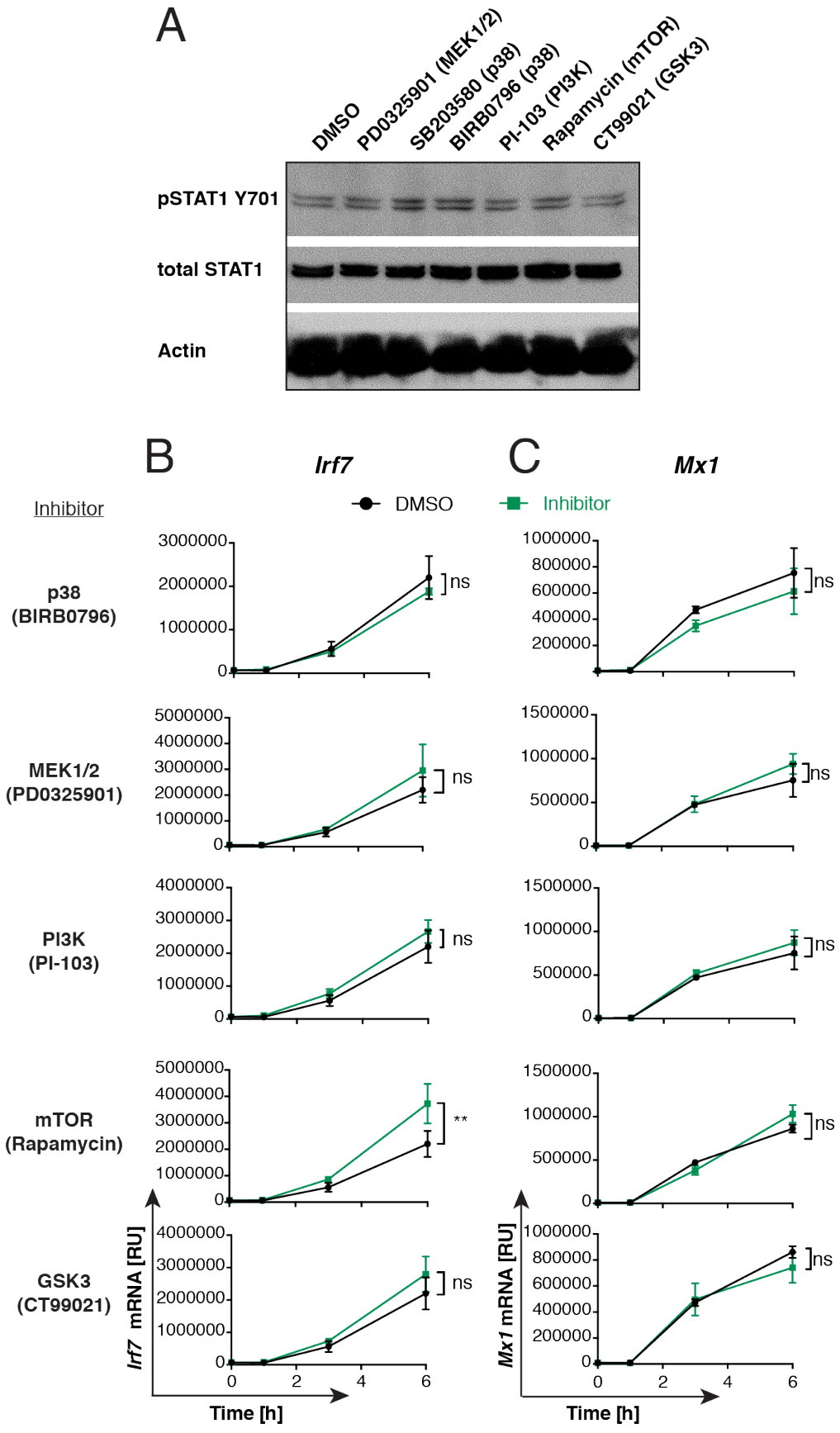

Figure 4.16 MAPK inhibition does not alter type I IFN signalling.

(A) C57BL/6 WT macrophages were pre-incubated with the inhibitor for 1 h and then stimulated with LPS for 1 h. Whole-protein extracts were generated and analysed by Western blot for total and phosphorylated STAT1 (Y701) and actin as loading control. (B, C) C57BL/6 WT macrophages were pre-incubated with the inhibitor for 1 h and then stimulated with LPS for the indicated time points. Total RNA was harvested and isolated. *Irf7* (B) and *Mx1* (C) transcript levels were determined by qRT-PCR and normalised to *Hprt1* mRNA. Graphs show means ± SD of triplicate cultures. **p < 0.01, ns – not significant as determined by two-way ANOVA (Bonferroni multiple comparison test). Data are representative of two independent experiments.

4.4 Discussion

4.4.1 Regulation of IL-10 by type I IFN

In our study, Howes, Taubert *et al.* (268), we showed that C57BL/6 macrophages produce higher levels of IL-10 compared to BALB/c macrophages in response to bacterial products and that type I IFN plays an important role in mediating this phenotype. Other studies have shown complex immunoregulatory roles for these cytokines. Type I IFN has been shown to increase IL-10 production from murine macrophages in a TRIF dependent manner (271), from human B cells (276), and from human dendritic cells (275). How type I IFN regulates IL-10 and in which context it is important for IL- 10 production is not fully understood. Thus, our initial studies examined the role of type I IFN signalling in the production of IL-10 following various TLR-stimulations of C57BL/6 macrophages.

Analysis of IL-10 protein levels produced by macrophages following stimulation with various TLR ligands such as Pam3CSK4 (TLR2), Poly I:C (TLR3), LPS (TLR4) and CpG (TLR9), showed that IL-10 is produced in different amounts following these stimulations. Autocrine type I IFN increased the expression of IL-10 upon LPS and Poly I:C stimulation, but not post Pam3CSK4 and CpG stimulation, as no type I IFN was detected upon these 2 stimulations.

A detailed kinetics of *Il10* mRNA expression demonstrated two peaks of *Il10* mRNA transcription upon stimulation with LPS (as described already in Howes, Taubert *et al.* (268)) and Poly I:C. The presence of two peaks of *Il10* mRNA upon TLR4 ligation and the late, highest expression of *Il10* mRNA upon Poly I:C stimulation is suggestive

of an autocrine loop to maintain IL-10 production. As previously shown in our study by Howes, Taubert *et al.* (268), the second peak of *Il10* mRNA expression upon stimulation with LPS (TLR4) is dependent on type I IFN signalling as the second induction of *Il10* mRNA was absent in macrophages deleted for the IFNαβR. The abrogation of the second *Il10* mRNA peak resulted in significantly reduced IL-10 protein levels. In keeping with these findings, we showed that IL-10 production is also abrogated in *Ifnar1*$^{-/-}$ macrophages upon TLR3 ligation at the protein and mRNA level. Pam3CSK4 or CpG stimulated WT and *Ifnar1*$^{-/-}$ macrophages only expressed the first peak of *Il10* mRNA. In general, *Il10* mRNA levels seem to be lower in *Ifnar1*$^{-/-}$ macrophages upon TLR2 and 9 activation, however, kinetics were similar over time. Teixeira-Coelho *et al.* (234) demonstrated that both TLR2 and TLR9 lack the activation of the TRIF-signalling cascade and subsequently failed to sustain the stability of *Il10* mRNA. They proposed type I IFN as a possible candidate for an indirect role of TRIF in this process. This hypothesis is supported by the fact that we were able to demonstrate a stabilising effect of autocrine type I IFN on *Il10* mRNA expression following LPS stimulation. This effect was not observed when IFN-β was added to the culture after LPS stimulation, suggesting that maximal effects are obtained by the autocrine levels of type I IFN. These experiments would need to be repeated with Pam3CSK4 and CpG stimulated macrophages to prove the hypothesis. However, McNab *et al*. also demonstrated a stabilising effect of IFN-β on *Il10* mRNA in *M. tuberculosis* infected macrophages (269).

The observation that the first *Il10* mRNA peak upon LPS stimulation is unaffected by the absence of type I IFN signalling, and that the second *Il10* mRNA peak occurs at the relatively late time point of 3 – 4 h post stimulation, suggest that type I IFN

produced during the response is important for the induction of the second *Il10* mRNA peak but not for the first one. This is in agreement with the findings of Pattison *et al.* where the absence of type I IFN only affected *Il10* mRNA expression at later time points (357). Supporting this hypothesis, we were able to show that type I IFN added to Pam3CSK4 stimulated macrophages, which themselves do not produce detectable levels of type I IFN, led to the induction of a second peak of *Il10* mRNA transcription and to increased amounts of IL-10 protein, comparable to LPS stimulated macrophages.

These findings are supported by previous reports showing that type I IFN is important for the production of IL-10 in LPS stimulated macrophages (271) and that the TRIF pathway, which induces type I IFN downstream of TLR4 (60) and 3 (33), contributes to IL-10 production (167, 271). In accordance with the literature, we only observed type I IFN production in LPS and Poly I:C stimulated macrophages, which was reported to be dependent on the TRIF pathway (60). Pam3CSK4 and CpG stimulated macrophages do not produce IFN-β protein detectable by ELISA; nevertheless, small amounts of *Ifnb1* mRNA could be measured. IFN-β and other type I IFNs are constitutively secreted at low amounts to maintain homeostasis and to prime cells to a rapid and robust innate and adaptive immune response to subsequent challenge (360). We postulated that the lack of detectable type I IFN protein in Pam3CSK4 and CpG stimulated macrophages was responsible for similar IL-10 production in WT and *Ifnar1*$^{-/-}$ macrophages.

As in an *in vivo* setting, type I IFN are produced by many other cells in addition to macrophages, we wanted to test the responsiveness to type I IFN following ligation

of different TLRs. IL-10 protein levels increased upon IFN-α and IFN-β addition when macrophages where stimulated with Pam3CSK4, Poly I:C and LPS. However, a largely significant increase in IL-10 levels was only detected upon TLR2 stimulation, possibly because macrophages do not produce type I IFN themselves following TLR2 ligation. The addition of either IFN-α or IFN-β to TLR9 stimulated macrophages did not lead to an increase of IL-10 protein levels, rather to a decrease under some conditions, despite their inability to themselves produce type I IFN. It needs to be investigated if the addition of type I IFN to CpG stimulated macrophages, leads to the induction of a second peak of *Il10* mRNA transcription, similar to what we showed in Pam3CSK4 stimulated macrophages. However, IL-10 production upon TLR9 stimulation seems to be independent of type I IFN. Yet, it would need to be tested if type I IFN addition to TLR9 stimulated macrophages leads to STAT1 (Y701) phosphorylation and ISGs induction. Although macrophages have the ability to produce more IL-10 following type I IFN addition after TLR3 and 4 stimulation, it was to a much lower extent, likely due to the already high levels of type I IFN produced in response to these TLR ligands. Thus, since macrophages produce IFN-β themselves following TLR3 and 4 ligation, type I IFN signalling may therefore already have reached saturation through endogenous levels of type I IFN.

To assess how type I IFN affects IL-10 production upon TLR3 and 4 ligation we first compared spliced and un-spliced *Il10* mRNA kinetics. We were able to demonstrate that the expression profiles closely correlate to those observed in LPS stimulated macrophages. Both showed two peaks of *Il10* mRNA transcription while the expression of the spliced RNA was shifted by roughly 15 min. However, the experimental procedure would need to be refined, as un-spliced *Il10* RNA was

measured from RNA extracted from the whole cell and not specifically from the nucleus. Nevertheless, the general assumption can be made that un-spliced RNA is located mostly in the nucleus and therefore no contamination of cytosolic RNA should occur (361). Furthermore, the primers were designed to detect only un-spliced RNA (reverse primer located in intron 4). Despite that, our data led us to the conclusion that type I IFN promotes IL-10 production by a transcriptional mechanism, supported by the fact that addition of IFN-β to Pam3CSK4 stimulated macrophages was able to induce a second peak of *Il10* mRNA transcription. Nevertheless, type I IFN also shows a stabilising effect on *Il10* mRNA as discussed above.

Overall, our data indicate that type I IFN positively regulates IL-10 production in macrophages following TLR2, 3 and 4 stimulation, although while enhanced IL-10 levels observed after TLR3 and 4 stimulation depend on autocrine type I IFN, in the case of TLR2 stimulation an external source of type I IFN is required. Type I IFN acts as transcriptional regulator as well as stabiliser of *Il10* mRNA. In contrast, type I IFNs have no effect on IL-10 production upon TLR9 signalling.

4.4.2 Regulation of IL-12 by type I IFN

In the context of pro-inflammatory cytokine production, type I IFN has various effects. Mechanisms whereby type I IFN regulates distinct pro-inflammatory cytokines are as yet unclear (269, 274, 354). In some settings, IFN-α/β-mediated signalling has been shown to be necessary for IL-12 production by DCs following PRR stimulation (355). However, high but physiological levels of IFN-α/β strongly inhibit IL-12 production during murine cytomegalovirus (MCMV) and LCMV infections (356, 362) as well as in *M. tuberculosis*-infected macrophages (269).

Our data showed that macrophages produce high amounts of IL-12p40 upon TLR9 stimulation compared to LPS-, Poly I:C- and Pam3CSK4 stimulated macrophages, which goes along with high mRNA transcription upon stimulation of these pathways. IL-12p40 protein and mRNA production was significantly lower in *Ifnar1*$^{-/-}$ compared to WT macrophages demonstrating a requirement for type I IFN signalling for IL-12 production in TLR2, 3, 4 and 9 stimulated macrophages. McNab *et al.* (269) previously described that low levels of basal type I IFN, which lead to tonic type I IFN signalling, are required for optimal IL-12p40 production by macrophages. Hence, we postulated that this may contribute to poor IL-12p40 production in *Ifnar1*$^{-/-}$ macrophages, as tonic type I IFN signalling is absent from C57BL/6 *Ifnar1*$^{-/-}$ macrophages. These results are in agreement with a study by Gautier *et al.,* where they show that type I IFN signalling was required for IL-12 production following TLR activation (355). Together these data suggest that maximal IL-12 production by macrophages upon TLR2, 3, 4 and 9 activation requires tonic type I IFN signalling.

In contrast to these findings, however, the addition of IFN-α or IFN-β significantly inhibited IL-12p40 production upon Pam3CSK4 and CpG stimulation. In the case of LPS- or Poly I:C, production of IL-12p40 did decrease, but levels were relatively low already in the control cells, potentially because of autocrine IFN-β production upon TLR3 and 4 signalling. These data suggest that type I IFN does have the capacity to inhibit IL-12p40 production in these systems. These results are in agreement with a number of studies showing suppression of IL-12 by type I IFN in viral and bacterial models (354, 356, 363, 364). Furthermore, as described in McNab *et al.* (269), IL-10-deficient C57BL/6 macrophages showed increased IL-12 production in *M. tuberculosis* stimulated macrophages compared to WT macrophages. These levels were reduced by the addition of IFN-β. However, IL-12 levels did not decrease to the same extent as if IFN-β was added to *M. tuberculosis*-infected WT macrophages. Hence, IL-12 production is regulated by exogenous type I IFN through IL-10 independent but often IL-10 dependent mechanisms (269).

Our investigation into different TLR ligations revealed type I IFN to be a central mediator of IL-12p40 production in C57BL/6 macrophages. While tonic type I IFN signalling is necessary for IL-12p40 expression upon all stimulations tested, exogenous type I IFN accounted for the reduced levels of IL-12 observed in C57BL/6 WT macrophages.

During this study, only IL-12p40 protein and *Il12b* mRNA were measured. As p40 is also a component of IL-23 when bound to p19 (133) and is often more abundant in the cells it would be important to repeat the experiment evaluating IL-12p70 and *Il12a*.

4.4.3 MAPKs and their role in type I IFN dependent IL-10 regulation

As shown in the literature, many different kinases such as p38 (226, 230, 255), ERK1/2 (70, 71, 225), PI3K/Akt, mTOR (92, 94) and GSK-3 (231, 232) are activated upon TLR ligation and have been suggested to regulate the induction of IL-10. By treating macrophages with selective inhibitors for these kinases, we have also observed that p38, MEK1/2 (ERK1/2), PI3K and mTOR activation are required for optimal IL-10 production in LPS stimulated macrophages while GSK-3 activation leads to a decrease in IL-10 levels, as reported in the literature.

Additionally, type I IFN has been reported to activate MAPKs downstream of the type I IFN receptor including ERK2 in a multiple myeloma cell line (283) and the protein kinase p38 in lymphoblastic cell lines (284). Type I IFNs have also been shown to activate PI3K signalling downstream of JAKs in an IRS-dependent manner leading to activation of mTOR in T lymphoblasts (280). We could not detect any significant differences in *Il10* mRNA levels in macrophages upon inhibition of PI3K and mTOR pathways 2 h after LPS stimulation. Pre-treatment with the inhibitor led to a general reduction in mRNA levels but not in a loss of the second peak of *Il10* mRNA transcription. Effects of mTOR and PI3K on IL-10 production was mostly reported in monocytes and DCs and mainly established at the protein level (93, 94), hence our results are in keeping with published reports.

Inhibition of p38 activation preceding LPS stimulation resulted in decreased *Il10* mRNA expression at all time points. This is in accordance with Teixeira-Coelho *et al.* (234), which reported that TLR4 signals protected *Il10* mRNA from rapid degradation, due to the activation of TRIF and enhanced p38 signalling. Additionally, Tudor *et al.*

described a mechanism whereby p38 signalling inhibits tristetraprolin (TTP)-directed decay of *Il10* mRNA (233). Hence, the inhibition of p38 leads to decreased inhibition of TTP and therefore a decrease in *Il10* mRNA stability upon LPS stimulation in macrophages (233). However, in our study the type I IFN–dependent second peak of *Il10* mRNA remained present in the absence of p38 signalling. Also, the inhibition of p38 at 2 h post-stimulation had no significant effect on *Il10* mRNA levels. Additionally, we showed by western blot that the activation of p38 (T180/Y182) was not different in WT and *Ifnar1*$^{-/-}$ macrophages upon LPS stimulation at later time points. This suggests that p38 does not increase IL-10 levels in a type I IFN dependent manner.

When we blocked GSK-3 1 h prior or 2 h post stimulation we detected an increase in *Il10* mRNA expression after 3 h of LPS stimulation, suggesting inhibition of the second peak of induction of *Il10* mRNA by GSK-3. Studies from Wang *et al.* (275) already showed that GSK-3α/β plays a role in regulating IFN-β mediated IL-10 production in human DCs via CREB. However, activation of GSK-3α/β (S21/9) was not affected in *Ifnar1*$^{-/-}$ macrophages upon LPS stimulation at later time points. Hence, GSK-3 might not play a role in type I IFN dependent IL-10 regulation.

Interestingly, inhibition of ERK1/2 signalling had no effect on the first peak of *Il10* mRNA independently of the time point of inhibitor addition, whereas it completely abrogated the second peak of *Il10* mRNA transcription independently of the time point when the inhibitor was added. This result was confirmed using two additional specific MEK1/2 inhibitors, indicating that type I IFN is acting via ERK1/2 activation to induce a second peak of *Il10* mRNA transcription. In support of these findings,

ERK1/2 (T185/Y187) phosphorylation was induced in C57BL/6 macrophages upon treatment with recombinant IFN-β and this was not observed in C57BL/6 *Ifnar1*$^{-/-}$ macrophages, demonstrating the specificity of the IFN-β activation of ERK1/2 and that this was not through activation of any PRR. Furthermore, ERK1/2 activity was reduced in *Ifnar1*$^{-/-}$ macrophages compared to WT macrophages upon LPS stimulation at later time points. Additionally, in LPS stimulated C57BL/6 *Ifnar1*$^{-/-}$ macrophages, ERK1/2 inhibition had no further effect on the reduction of IL-10 protein levels (268). These data show a requirement for ERK1/2 in the induction of type I IFN-dependent *Il10* mRNA expression in C57BL/6 macrophages stimulated with LPS. This hypothesis is underpinned by the fact that Liu *et al.* showed that type I IFN modulates TLR-mediated IL-10 production in B cells via ERK1/2 (365).

It has to be stated that JAK/STAT signalling is also involved in type I IFN dependent IL-10 regulation. It was demonstrated by Guarda *et al.* that the activation of STAT1 downstream of the type I IFN receptor in LPS stimulated macrophages leads to an increase in IL-10 (274). Additionally, the binding of IRF1 and STAT3 to the *Il10* promoter was reported in human B cells (276). However, we aimed to explore new pathways and therefore only used p38, MEK1/2, mTOR, PI3K and GSK3 inhibitors and no JA/STAT inhibitors.

In summary, TLR4 ligation of macrophages leads to IL-10 and type I IFN production, which is initiated via the adapter molecules MyD88/TIRAP/TRAM and TRIF. Type I IFN produced upon TLR ligation then positively feeds back via the type I IFN receptor, which leads to an increase in type I IFN production itself. Based on our results we hypothesise that type I IFN then reinforces IL-10 production via ERK1/2 activation.

Chapter 5.
Type I IFN changes chromatin accessibility and leads to increased binding of ATF3 and JUNB within the *Il10* topological associating domain

5.1 Background

We showed that type I IFN leads to the induction of a second wave of *Il10* mRNA transcription via the activation of ERK1/2 in LPS stimulated macrophages (chapter 4.3 and (268)). However, the underlying mechanism in macrophages is not well understood. Type I IFN promotes IL-10 production transcriptionally (Figure 4.7 and (268)), perhaps through the recruitment of IRF1 and STAT3 to the *Il10* promoter as it has been reported in the human B lymphocyte cell line RPMI 8226 (276) or by activating STAT1 in murine macrophages (274). A number of transcription family members, including SP1 (249, 255), STATs, IRFs (276), AP-1 (74), CREB (230, 251), C/EBP (258, 366), c-MAF (252), and NF-κB (229), have been reported as essential for IL-10 regulation. However, the mechanisms involved in the transcriptional regulation of IL-10 by type I IFN have not been investigated. Using microarray analysis and an assay for transposase-accessible chromatin with high throughput sequencing (ATAC-seq) we aimed to further unravel how type I IFN regulates *Il10* gene regulation by investigating chromatin accessibility and TF recruitment to the *Il10* regulatory region in macrophages upon LPS stimulation.

5.2 Aims

In chapter 4.3.4, we demonstrated that type I IFN transcriptionally regulates IL-10 production by activated macrophages. Additionally, we showed that in LPS stimulated macrophages, type I IFN leads to a second induction of *Il10* mRNA transcription via ERK1/2 activation (chapter 4.3.5). We hypothesised that type I IFN leads to a change in chromatin accessibility and/or differential TF recruitment at the *Il10* locus in LPS stimulated macrophages.

In order to address this hypothesis, we aimed to:

- Identify candidate transcription factors correlating with *Il10* mRNA expression in response to type I IFN post LPS stimulation in macrophages using microarray analysis.

- Investigate if type I IFN changes chromatin accessibility at the *Il10* regulatory region in macrophages upon LPS stimulation using ATAC-sequencing.

- Determine whether different transcription factors bind *Il10* regulatory regions in C57BL/6 WT and *Ifnar1*$^{-/-}$ macrophages 4 h post LPS stimulation using ATAC-sequencing and ChIP-PCR.

5.3 Results

5.3.1 Investigation of transcription factors positively correlating with *Il10* mRNA in response to type I IFN

To evaluate which TFs might play a role in type I IFN dependent *Il10* gene regulation, we performed microarray analysis comparing RNA from macrophages from WT and *Ifnar1*$^{-/-}$ mice stimulated with LPS or media for 0, 0.5, 1, 3, 4 and 6h. To ensure that the *Il10* mRNA expression by microarray analysis showed the same kinetic profile as in our previous experiments by qRT-PCR, *Il10* mRNA expression levels in WT and *Ifnar1*$^{-/-}$ macrophages at steady state and after LPS stimulation were extracted from the data set and plotted over time (Figure 5.1). In keeping with our previous results, we were able to demonstrate a second peak of induction of *Il10* mRNA transcription, initiated after 3 h post stimulation in macrophages from WT mice in the microarray dataset. Moreover, the second peak of induction of *Il10* mRNA was abrogated in macrophages from *Ifnar1*$^{-/-}$ mice (Figure 5.1).

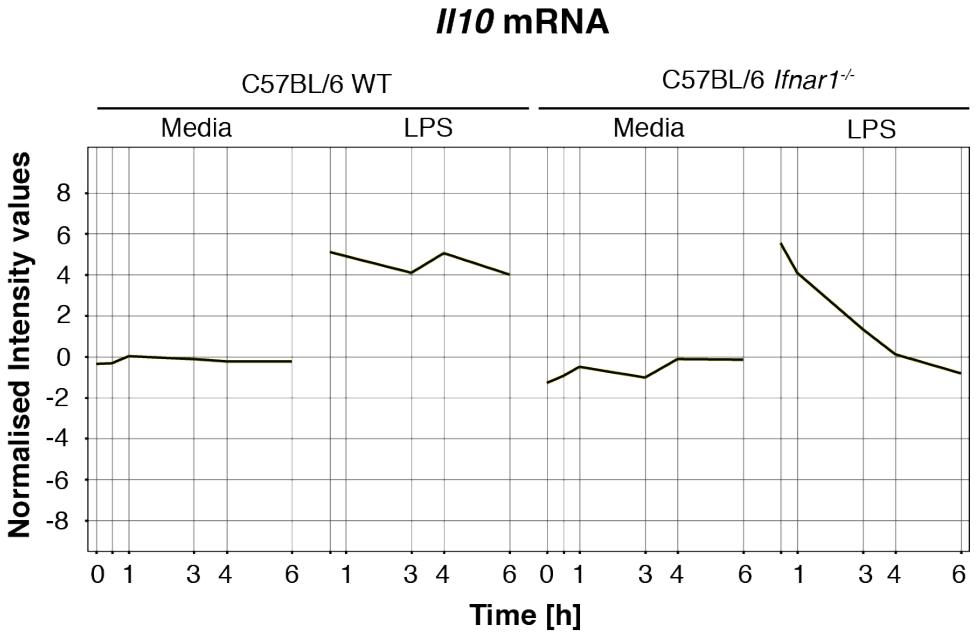

Figure 5.1 *Il10* mRNA expression in WT and *Ifnar1*$^{-/-}$ macrophages after LPS stimulation (microarray analysis).

Macrophages were generated from C57BL/6 WT and *Ifnar1*$^{-/-}$ mice. Cells were stimulated with LPS in triplicate cultures and total RNA harvested at 0, 0.5, 1, 3, 4 and 6 h and extracted for microarray analysis. Kinetic of *Il10* mRNA in WT and *Ifnar1*$^{-/-}$ macrophages upon LPS stimulation analysed by microarray. Data at each time point represent average of triplicate cultures.

Assuming that TFs that are regulating *Il10* show similar kinetics during LPS stimulation in WT and *Ifnar1*$^{-/-}$ macrophages as *Il10* mRNA itself, we identified genes positively correlating with *Il10* mRNA expression (1,867 entities, 1,063 genes) and overlapped them with a TF list (previously curated by Leona Gabrysova[1]) (Figure 5.2

[1] overlap of all TFs present in different databases: Affymetrix, GX GO annotations (nucleic acid (NA) binding TF activity) (1,248 entities, 694 genes); Illumina, GX GO annotations (NA binding TF activity (591 entities, 393 genes); Illumina, GX updated GO annotations (NA binding TF activity) (671 entities, 438 genes); Affymetrix, GCOS GO annotations (367. Wei G, Wei L, Zhu J, Zang C, Hu-Li J, Yao Z, Cui K, Kanno Y, Roh TY, Watford WT, Schones DE, Peng W, Sun HW, Paul WE, O'Shea JJ, Zhao K. 2009. Global mapping of H3K4me3 and H3K27me3 reveals specificity and plasticity in lineage fate determination of differentiating CD4+ T cells. *Immunity* 30: 155-67 (1,403 entities, 773 genes); Illumina, GX GO annotations (protein binding TF activity) (297 entities, 188 genes).

A). TFs with the highest Pearson correlation were *Atf3, Tgif, Axud1, Cited2, Irf1, Junb* and *Nfil3*. With the exception of *Aft3*, all these TFs were also validated in other microarray data sets analysing gene expression in macrophages of C57BL/6 and BALB/c mice either following LPS or HkBps stimulation (data not shown). mRNA expression profiles of the TFs with a high Pearson correlation showed a similar transcriptional profile as *Il10* mRNA. Figure 5.2 B and C depicts examples of *Atf3, Tgif, Junb* and *Nfil3* mRNA expression over time. *Atf3* (but also *Cited2* and *Irf1,* not shown*)* showed high mRNA expression at 3 – 4 h in WT macrophages following LPS stimulation, which is the time point of the initiation of the second peak of *Il10* mRNA transcription. In *Ifnar1*$^{-/-}$ macrophages levels of *Atf3* transcripts decreased after 0.5 h of LPS stimulation, similarly to *Il10* mRNA (Figure 5.2 B). *Tgif* mRNA expression followed exact *Il10* mRNA kinetics, as expression peaked 1 h post LPS stimulation and a second wave of transcription was initiated 3 h post stimulation in WT macrophages. However, in *Ifnar1*$^{-/-}$ macrophages *Tgif* mRNA expression was decreased already as early as 0.5h post stimulation (Figure 5.2 B). In contrast, *Junb* mRNA expression seemed similar in WT and *Ifnar1*$^{-/-}$ macrophages and decreased slightly 0.5 h post LPS stimulation (Figure 5.2 C). *Nfil3* showed high correlation with the transcription pattern of *Il10* mRNA in WT and *Ifnar1*$^{-/-}$ macrophages following LPS stimulation as its expression was greatly decreased in *Ifnar1*$^{-/-}$ macrophages 1 h post LPS stimulation. In WT macrophages *Nfil3* mRNA levels increased after 1 h of LPS stimulation (Figure 5.2 C).

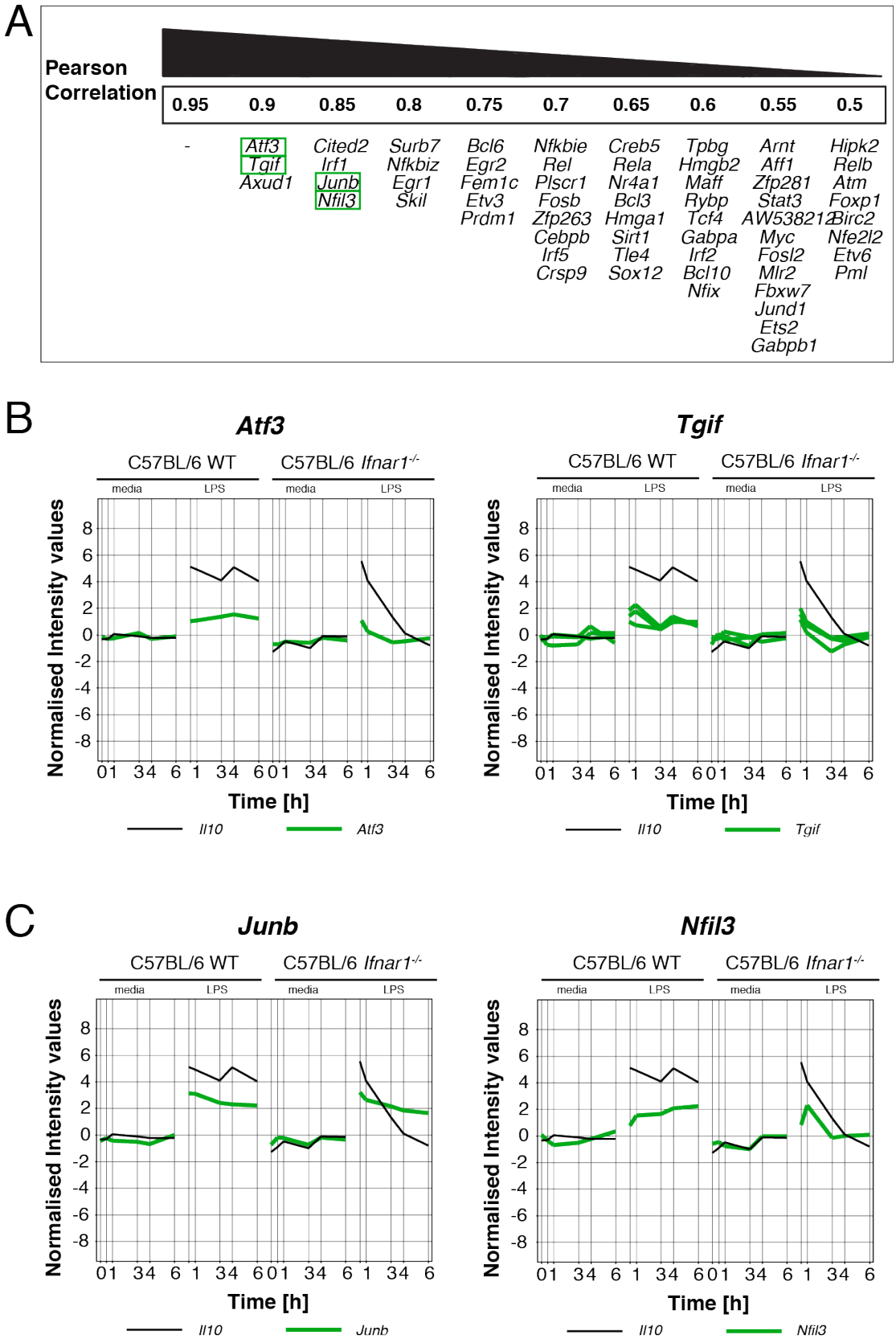

Figure 5.2 Transcription factors positively correlating with *Il10* mRNA transcription in LPS stimulated C57BL/6 WT and *Ifnar1*$^{-/-}$ macrophages.

Macrophages were generated from C57BL/6 WT and *Ifnar1*$^{-/-}$ mice. Cells were stimulated with LPS in triplicate cultures and total RNA harvested at 0, 0.5, 1, 3, 4 and 6 h and extracted for microarray analysis. (A) Transcripts were identified by normalising expression values to the median of all samples and filtered on flags present (19802 entities). Obtained transcripts were overlapped with a TF list curated by Leona Gabrysova (880 entities). Those, which correlated with *Il10* mRNA (Pearson Correlation) were identified and listed above. TFs in green box further analysed in B and C of this figure. B, C) mRNA kinetics of TFs with high Pearson correlation (green, different probes for TF) compared to *Il10* mRNA expression pattern (black). Data at each time point represent average of triplicate cultures.

Nfil3 (368, 369) had been described to play an important role in *Il10* regulation in T cells, but has not been reported in myeloid cells. As its mRNA expression correlated highly with *Il10* mRNA kinetics in WT and *Ifnar1*$^{-/-}$ macrophages (Figure 5.2), we postulate that type I IFN might induce a second wave of *Il10* mRNA transcription via the induction of NFIL3. To address this hypothesis, we compared IL-10 production in C57BL/6 WT, *Ifnar1*$^{-/-}$ and *Nfil3*$^{-/-}$ macrophages after a 3, 6 and 24 h stimulation with LPS (Figure 5.3). Surprisingly, levels of IL-10 protein were very similar in WT and *Nfil3*$^{-/-}$ macrophages. The lack of *Nfil3* did not alter levels of IL-10 production significantly compared to that of WT macrophages. Levels of IL-10 were unaffected in *Nfil3*$^{-/-}$ macrophages in response to LPS in contrast to IL-10 levels in *Ifnar1*$^{-/-}$ macrophages that were largely reduced (Figure 5.3).

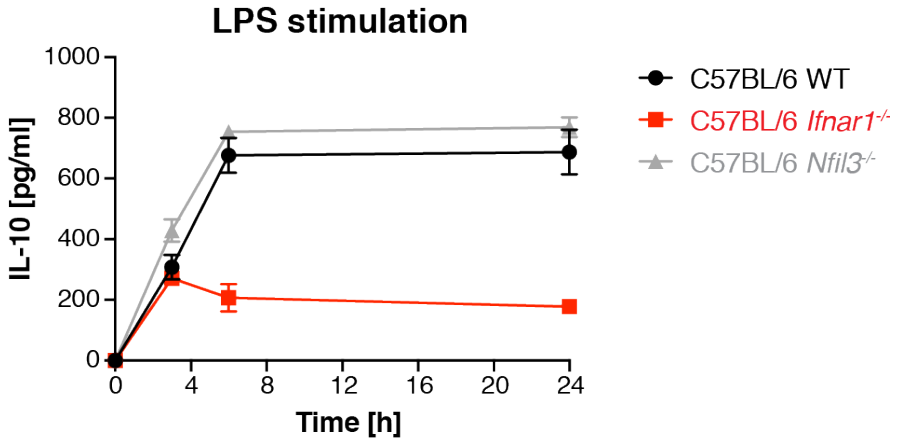

Figure 5.3 Type I IFN-induced IL-10 production is independent of NFIL3.
Macrophages were generated from C57BL/6 WT, *Ifnar1*$^{-/-}$ and *Nfil3*$^{-/-}$ mice. Cells were stimulated with LPS for 3, 6 and 24 h and IL-10 protein was measured in supernatant by ELISA. Graph shows means ± SD of triplicate cultures. Representative of 2 independent experiments.

5.3.2 Evaluation of ATAC-sequencing results

The identification of TF candidates via microarray analysis using Pearson correlation is based on the assumption that genes that regulate *Il10* mRNA are transcribed at the same time with the same kinetics as *Il10* mRNA and that these genes are regulated transcriptionally. However, as we have observed for NFIL3, even if the transcription of TF genes correlates with the type I IFN dependent induction of *Il10* mRNA, it does not necessarily imply that these TFs are involved in the regulation of IL-10 production. Therefore, we sought to establish a new method that allows us to predict TF binding at specific genes and also to evaluate whether type I IFN signalling changes chromosome accessibility – an assay for transposase-accessible chromatin using sequencing (ATAC-sequencing) (332). ATAC-seq uses a hyperactive Tn5 transposase (336) to simultaneously cut and ligate adapters for high-throughput

sequencing at regions of increased accessibility. Insertion ends can then be mapped genome-wide and open chromatin regions can be identified (Figure 5.4).

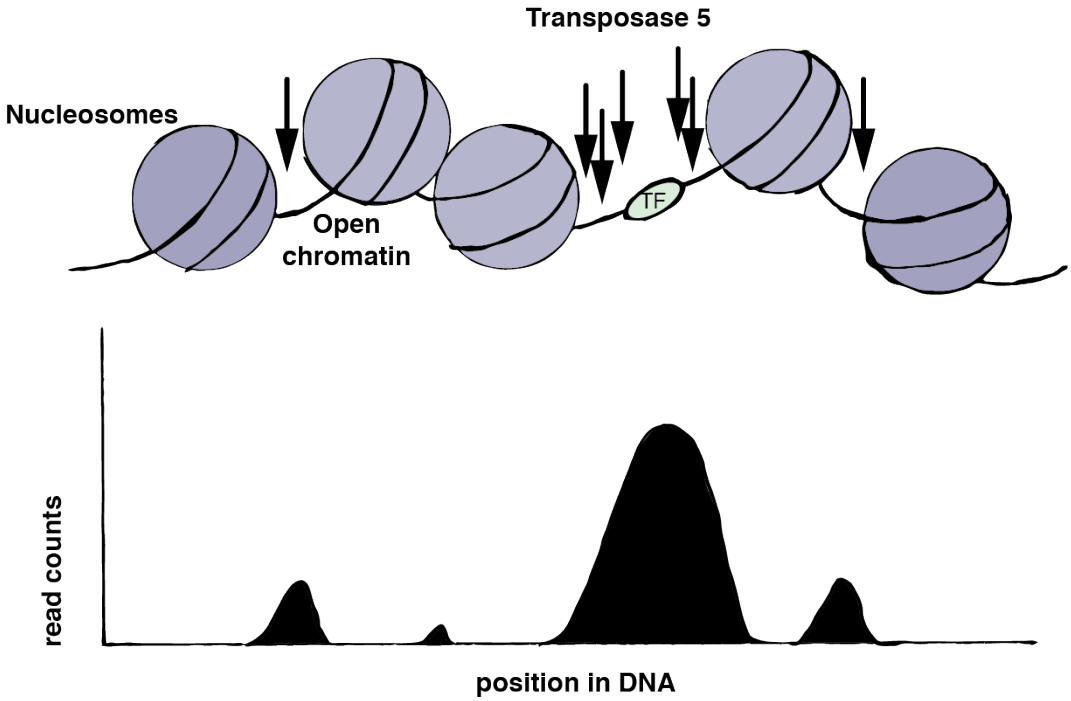

Figure 5.4 Principle of ATAC-sequencing.

Hyperactive Transposase 5 inserts only in regions of open chromatin (between nucleosomes) and generates fragments that can be PCR-amplified, sequenced and visualised as peaks using various bioinformatics tools (332). TF – transcription factor

As the protocol for ATAC-sequencing was developed using T cells (332), we firstly had to optimise it for macrophages and evaluate the accuracy of our results. As described in 2.10.1, the transposition time had to be adapted from 30 min to 2 h to allow for sufficient tagmentation (fragmentation and insertion of adapters) (Figure 7.2).

To evaluate the reproducibility of the data (three biological replicates per condition), we made use of the R Bioconductor package DiffBind. It is designed to work with

multiple peak sets simultaneously and identifies statistically significant differentially bound sites between two sample groups based on evidence of binding affinity (measured by differences in read densities) (338). Firstly, peak sets obtained by MACS2 (335) were read in for each sample separately. The resulting matrix showed how many peaks are in each peak set, as well as the total number of unique peaks after merging overlapping ones. Using this data, a correlation heat map was generated. Different samples were clustered in an unbiased approach using the cross-correlations of each row of the binding matrix. The correlation heat map showed that while the replicates for each LPS stimulated sample clustered together appropriately, the unstimulated replicate samples do not cluster into groups corresponding to WT or *Ifnar1*$^{-/-}$ macrophages (Figure 5.5 A).

Next, using the differential analysis edgeR a binding matrix was calculated with scores based on read counts for each sample (affinity scores). As a final step, we retrieved the differentially bound sites. Using only the differentially bound sites and a plot based on principal component analysis, a deeper insight into how the samples are associated was achieved. Figure 5.5 B shows all the stimulated samples cluster away from the unstimulated ones. Additionally, component 3 separates WT from *Ifnar1*$^{-/-}$ macrophages in stimulated samples; however, unstimulated samples do not separate into WT and *Ifnar1*$^{-/-}$ macrophages. This indicates that the stimulation of WT and *Ifnar1*$^{-/-}$ macrophages reveals their genetic differences, while at steady state the chromosome accessibility is fairly similar in WT and *Ifnar1*$^{-/-}$ macrophages.

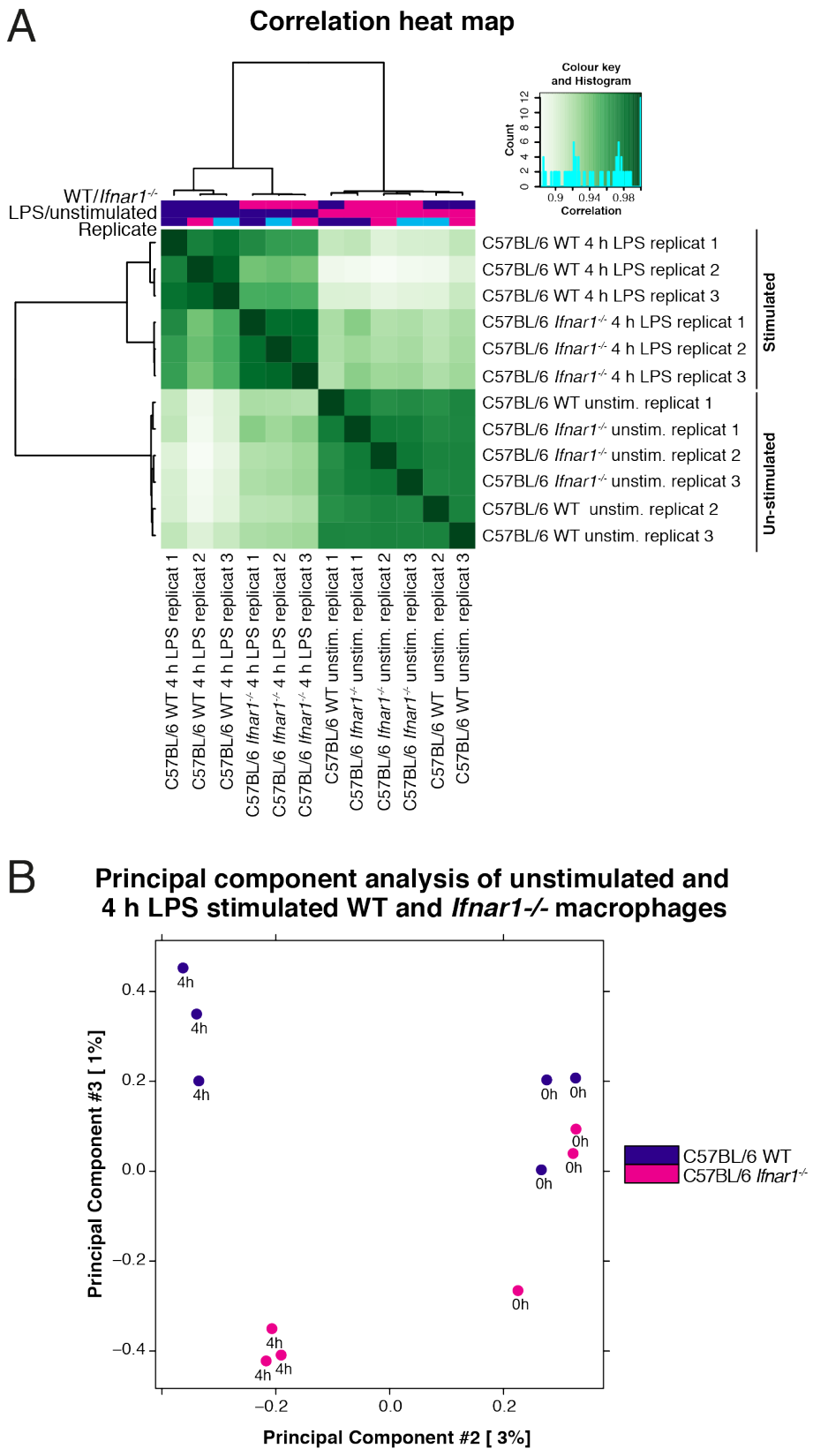

Figure 5.5 Quality control of replicate samples of LPS stimulated and unstimulated WT and *Ifnar1*$^{-/-}$ macrophages (ATAC-seq).

Macrophages were generated from C57BL/6 WT and *Ifnar1*$^{-/-}$ mice. Cells were stimulated with LPS for 0 or 4h, lysed and DNA transposed, amplified and library quantitated. Reads were aligned using Bowtie2 (mm10). MACS2 2.1.1 identified peak sets from C57BL/6 WT and *Ifnar1*$^{-/-}$ macrophages unstimulated and 4 h stimulated with LPS were uploaded together with correlating bam-files for use in Bioconductor package DiffBind (338), for all three biological triplicates per condition. (A) Correlation heat map, using occupancy (confidence scores for only those peaks called in a specific sample), before differential analysis. Initial clustering of the samples using the cross-correlations of each row of the binding matrix. (B) Principal component analysis plot based on normalised read counts for differentially bound sites determined via edgeR. Plots shown were generated using Bioconductor package DiffBind (338) taking into account triplicate samples of each experimental group.

To determine the biological accuracy of our data, we compared the peak profile of unstimulated macrophages obtained by ATAC-seq with ChIP-seq datasets for H3K27a, H3K4m3 and H3K4m1 of unstimulated macrophages (ChIP-sequencing data sets were taken from the ENCODE project, Dr. Genhong Cheng Lab at UCLA). Surprisingly, the ATAC-seq profile of unstimulated WT macrophages showed peaks at the *Il10* locus, resembling open chromatin already at the steady state (Figure 5.6 A). However, these peaks always correlated with peaks of either H3K4me3, H3K4me1 or H3K27ac and were not randomly distributed. Hence, peaks could be detected in the promoter region, marked by H3K4m3 which defines an active state of gene expression (370) and which predominantly locates to active promoters (371, 372). Other peaks corresponded with H3K27ac modifications which are found on active enhancers, or with H3K4me1, which is a mark associated with both inactive or potentially “poised” and active enhancers (373) (Figure 5.6 A). However, the *Il12a* locus was closed in unstimulated macrophages correlating with non-existing histone marks (Figure 5.6 B). Hence, the open chromatin regions at the *Il10* locus seem to be specific and not an artefact of the ATAC-seq protocol.

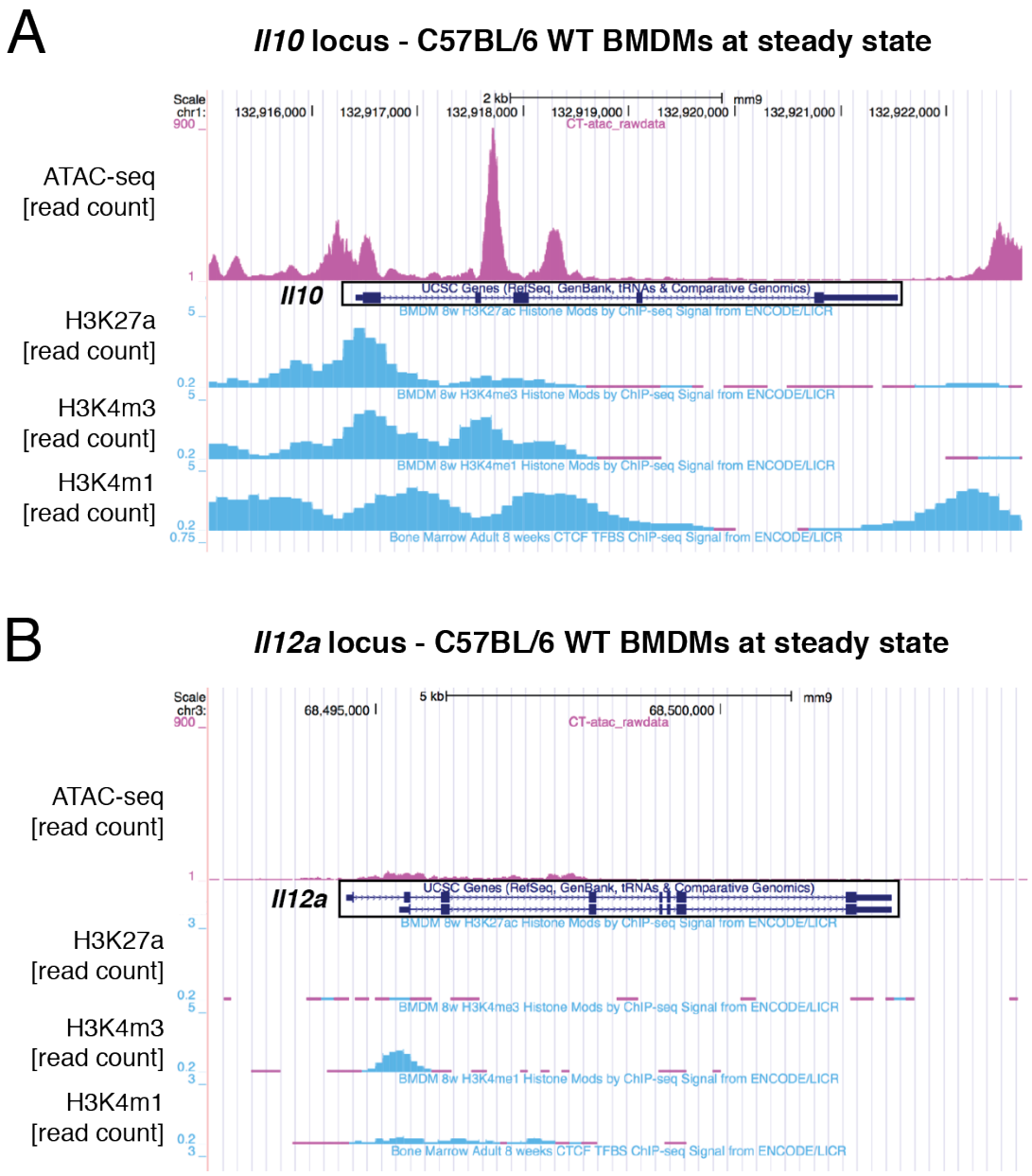

Figure 5.6 Histone activation marks coincide with open chromatin regions at *Il10* and *Il12a* locus.

Macrophages were generated from C57BL/6 WT mice. Cells were lysed directly and DNA transposed, amplified and library quantitated. Reads were aligned using Bowtie2 (mm9). ATAC-sequencing track from C57BL/6 WT macrophages at steady state was compared to ChIP-sequencing data for H3K27a, H3K4m3 and H3K4m1 at (A) the *Il10* locus and (B) the *Il12a* locus. ATAC-sequencing track is representative of three independent experiments. ChIP-sequencing data sets were taken from the ENCODE project, Dr. Genhong Cheng Lab at UCLA. UCSC genome browser was used to compare the tracks, mouse July 2007, NCBI37/mm9.

To evaluate further why the *Il10* locus is already open at steady state and whether this might be due to culture conditions and differentiation of the bone marrow cultures to BMDMs, we set out to compare different steady state *ex vivo* myeloid cell populations from published datasets with BMDMs. Raw sequencing data from Lavin *et al.* were obtained from the GEO database (GSE63341, GSE633384 (24)); raw data were analysed as described in 2.10.2 and visually compared with our unstimulated macrophages using IGV (Figure 5.7). No open chromatin regions at the *Il10* locus could be detected in small intestine macrophages, neutrophils and lung macrophages. Nevertheless, the highest detectable peak which is within the second intron of the *Il10* gene in our BMDMs was also found to be in microglia, spleen red pulp macrophages, peritoneal macrophages, monocytes, Kupffer cells and large intestinal macrophages. Furthermore, *ex vivo* monocytes, Kupffer cells and large intestine macrophages showed additional open chromatin regions within and around the *Il10* locus, resembling more the appearance of BMDMs.

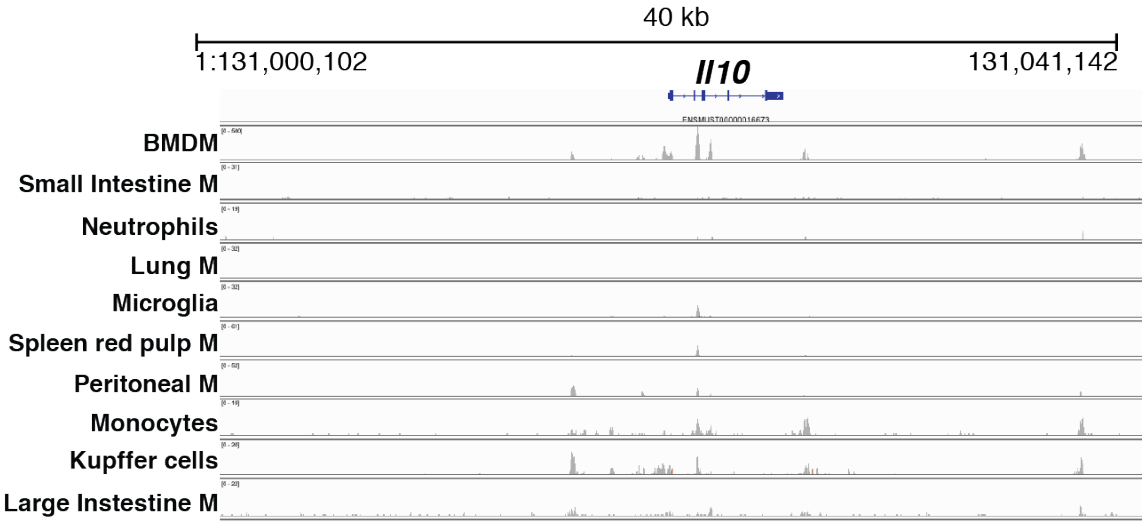

Figure 5.7 Chromosome accessibility at the *Il10* locus of BMDMs is comparable with *ex vivo* monocytes, Kupffer cells and large intestine macrophages.

Macrophages were generated from C57BL/6 WT mice. Cells were lysed and DNA transposed, amplified and library quantitated. Reads were aligned using Bowtie2

(mm9). Normalised ATAC-sequencing track of the *Il10* region from C57BL/6 WT macrophages at steady state was compared to various normalised ATAC-sequencing profiles of unstimulated *ex vivo* myeloid populations (raw sequencing data obtained from GSE63341, GSE633384 (24)). All dataset reads were aligned using Bowtie2 (mm9) and IGV_2.3.68 used for visualisation of ATAC-sequencing. ATAC-sequencing track for BMDMs is representative of three independent experiments. M – macrophages.

5.3.3 Type I IFN changes DNA accessibility and leads to increased binding of ATF3 and JUNB within the *Il10* topologically associating domain

After evaluating the biological accuracy of our results and demonstrating very good correlation between triplicate samples, we aimed to identify peaks that are differentially expressed between WT and *Ifnar1*$^{-/-}$ macrophages 4 h post LPS stimulation. This time point was chosen, as the second wave of *Il10* mRNA transcription at this point would be already initiated and the expression of *Il10* mRNA differentially in WT and *Ifnar1*$^{-/-}$ macrophages. Using Diffbind (edgeR, FDR < 0.01) (338), genome-wide differentially bound sites between LPS stimulated WT and *Ifnar1*$^{-/-}$ macrophages were identified taking into account triplicates of each group. In the MA plot (Figure 5.8), each point represents an open chromatin region, with points in pink representing sites identified with differential chromatin accessibility. Genome-wide, we identified 95,561 differentially accessible sites (Diffbind, edgeR, FDR < 0.01), indicating that type I IFN signalling induces a very high number of changes in chromosome accessibility. From the differential sites, 52,398 sites were significantly higher in WT macrophages genome-wide (Figure 5.8 A), whereas 43,163 sites were significantly lower (Figure 5.8 B). These data suggest that WT macrophages gain more differentially open chromatin sites 4 h post LPS stimulation (Figure 5.8, group A) than they lose (Figure 5.8, group B) compared to *Ifnar1*$^{-/-}$ macrophages.

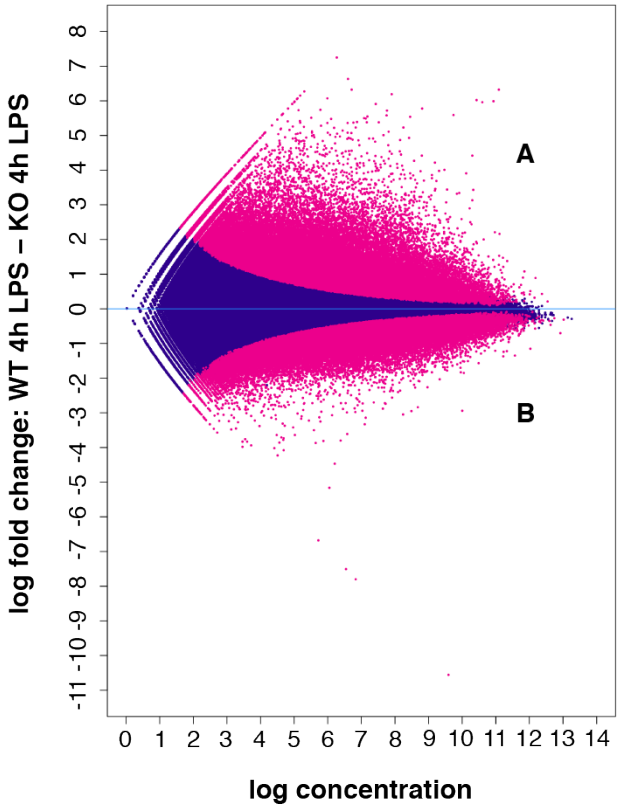

Figure 5.8 Differential genome wide DNA accessibility in C57BL/6 WT and *Ifnar1*$^{-/-}$ macrophages upon 4 h LPS stimulation.

Macrophages were generated from C57BL/6 WT and *Ifnar1*$^{-/-}$ mice. Cells were stimulated with LPS for 0 or 4 h, lysed and DNA transposed, amplified and library quantitated. Reads were aligned using Bowtie2 (mm10). MACS2 2.1.1 identified peak sets from C57BL/6 WT and *Ifnar1*$^{-/-}$ macrophages unstimulated and 4 h stimulated with LPS were uploaded together with correlating bam-files for use in Bioconductor package DiffBind (338), for all three biological triplicates per condition. In MA plot, each point represents a peak; peaks identified as significantly different are shown in pink. (A) Dots with log fold change > 0, represent peaks gained in C57BL/6 WT macrophages, while dots with (B) log fold change < 0 are peaks lost in WT macrophages compared to *Ifnar1*$^{-/-}$ macrophages. FDR < 0.01.

However, to investigate the effect of type I IFN signalling specifically on *Il10* gene regulation, a chromosome area containing possible *Il10* regulatory regions had to be identified. As regulatory elements can operate tens of thousands of base pairs away from the target gene (374), analysis of the *Il10* promoter alone would not be sufficient. Dixon *et al.* described a substructure within chromatin compartments, which form

large, megabase-sized local chromatin interaction domains; the so called 'topological associating domains' (TAD) (375), whose boundaries are enriched for the insulator binding protein CTCF. These domains are stable across different cell types and their positions are highly conserved across species. It was described that the frequency of intra-domain interactions is higher than inter-domain interactions (375). Hence, with a tool generated by the Lieberman-Aiden lab called "Juicebox" (376), we explored contact maps generated using Hi-C and other 3D genome-sequencing technologies and identified the TAD around *Il10* using a dataset generated from CH12-LX B-lymphoblasts (mouse). The topologically associating domain of *Il10* was found to be Chr1:130,448,908-131,272,748 (mm10) (Figure 5.9).

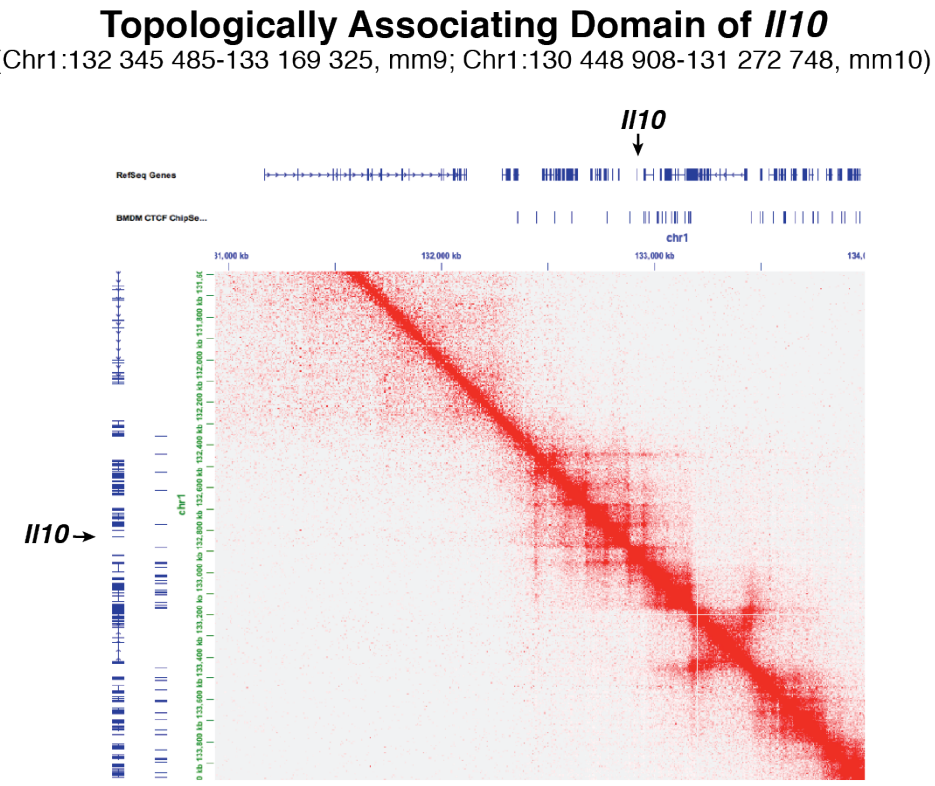

Figure 5.9 Topologically associating domain of *Il10*.

Topologically associating domain of *Il10* (mm9: Chr1:132,345,485-133,169,325; mm10: Chr1:130,448,908-131,272,748) was defined using Juicebox Version 1.0.(1) – 200616, a visualisation tool for high-resolution chromosome conformation capture data (376). The following data set was analysed: CH12-LX B-lymphoblasts (mouse) in situ combined (mm9) (376). Red area indicating are of high interactions.

Evaluating the *Il10* TAD region, an accumulation of peaks with increased height in WT versus *Ifnar1*$^{-/-}$ macrophages was observed around the *Il10* locus (Figure 5.10 A). This was visually seen by comparing the C57BL/6 WT versus the *Ifnar1*$^{-/-}$ track and was underpinned by the trace "peaks significantly increased in WT", which points out peaks that are significantly different between these two groups taking into account triplicate samples (Diffbind, edgeR, FDR <0.01) (Figure 5.10 A). Within the *Il10* TAD were also peaks that were significantly decreased in WT versus *Ifnar1*$^{-/-}$ macrophages (red trace, "peaks significantly decreased in WT", Diffbind, edgeR, FDR <0.01) (Figure 5.10 A). Nevertheless, a close-up of the *Il10* locus emphasised that chromosome accessibility proximal to and within the *Il10* gene was mostly increased in WT compared to *Ifnar1*$^{-/-}$ macrophages as peaks were lacking in the *Ifnar1*$^{-/-}$ macrophages or their size was in general diminished (Figure 5.10 B) indicating reduced DNA accessibility.

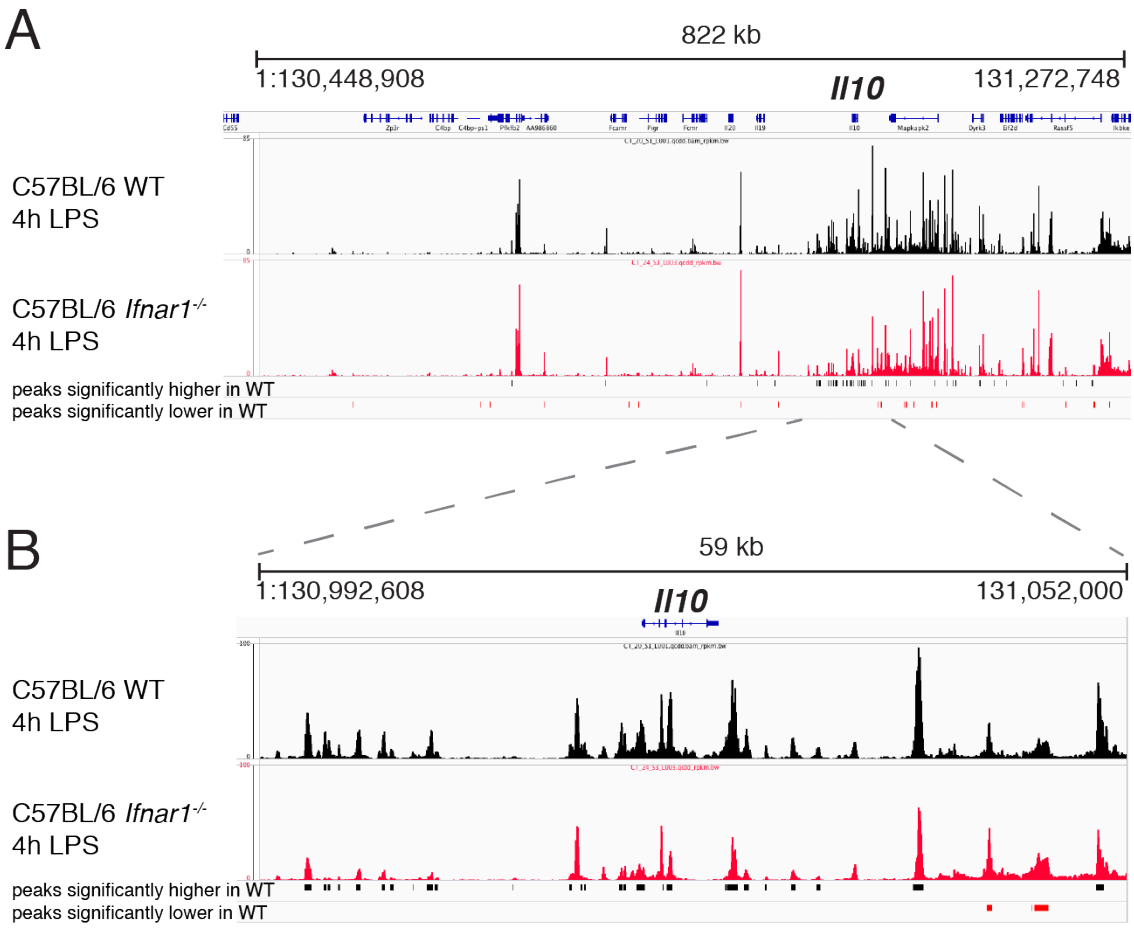

Figure 5.10 Type I IFN signalling changes accessibility of DNA within the *Il10* TAD in C57BL/6 macrophages after 4 h LPS stimulation.

Macrophages were generated from C57BL/6 WT and *Ifnar1*$^{-/-}$ mice. Cells were stimulated with LPS for 4 h and DNA transposed, amplified and library quantitated. Reads were aligned using Bowtie2 (mm10) and IGV_2.3.68 used for visualisation. Peaks were called by MACS2 2.1.1. Differentially expressed peaks were determined using DiffBind (edgeR, FDR < 0.01) taking into account triplicate samples of each experimental group. Black bars indicate peaks that are significantly higher expressed in WT macrophages, while red bars indicate peaks significantly lower in WT compared to *Ifnar1*$^{-/-}$ macrophages. ATAC-sequencing tracks shown are representative of 3 independent experiments. (A) Tracks shown, cover the whole region of the *Il10* TAD. (B) Tracks show chromatin accessibility around the *Il10* locus only.

To prove the principle and the accuracy of our data, we show in Figure 5.11 A that the accessibility of the *Mx1* locus, a type I IFN-induced gene, is highly increased in WT compared to *Ifnar1*$^{-/-}$ macrophages. In contrast, the *Il12b* locus was less

accessible in WT macrophages as it is in *Ifnar1*$^{-/-}$ macrophages (Figure 5.11 B), confirming the inhibitory effect of type I IFN on IL-12p40 production as shown in Figure 4.6.

In Figure 5.8, we showed that type I IFN signalling changes DNA accessibility genome wide and that 52,398 sites are significantly more accessible in LPS stimulated WT as compared to *Ifnar1*$^{-/-}$ macrophages (Figure 5.8 A). Using HOMER (Hypergeometric Optimization of Motif EnRichment) (340), a suite of tools for motif discovery and next-generation sequencing analysis, we analysed these sites with regard to TF motifs that are enriched within these peaks. The top 2 of 10 highly significant ($p < 1x10^{-50}$) TF motifs and their distribution around the peak summits are shown in Figure 5.12 A. Motif 1 could be a possible binding site for *Irf1, Irf2, Irf7, Irf8, Stat1, Stat2* and *Prdm1,* while motif 2 is a typical binding motif for AP-1 family members *Atf3, Batf, Fos, Junb, Fosl1, Fosl2, cJun* and *Jund* (Figure 5.12 B). Relating these findings back to the region of the *Il10* TAD, only 4 differentially expressed peaks comprised binding motif 1 (blue box) but 13 peaks contained motif 2 (green box) (Figure 5.12 C). Motifs 1 and 2 are mostly scattered within the *Il10* gene itself or just upstream of the promoter.

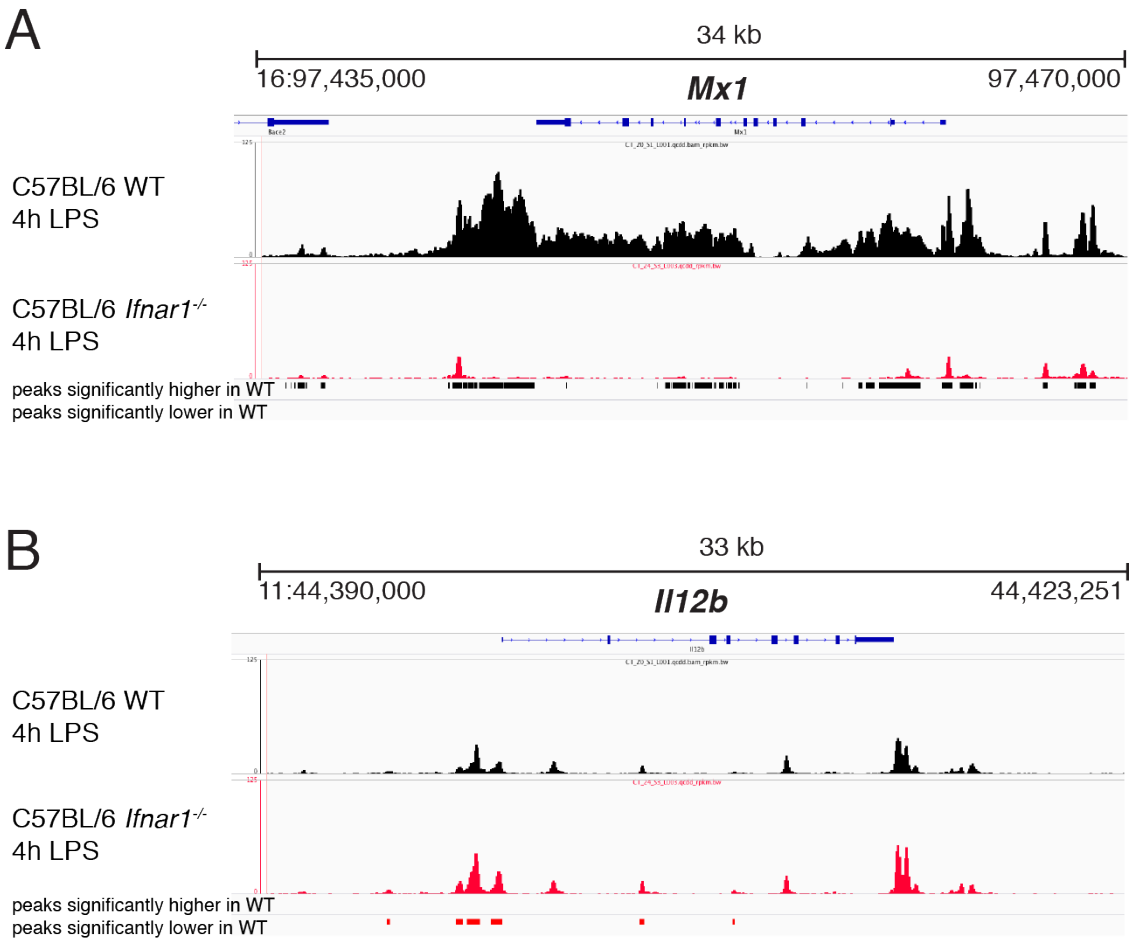

Figure 5.11 Type I IFN signalling increases accessibility of DNA significantly at the *Mx1* but decreases it at the *Il12b* locus in C57BL/6 macrophages 4 h after LPS stimulation.

Macrophages were generated from C57BL/6 WT and *Ifnar1*$^{-/-}$ mice. Cells were stimulated with LPS for 4 h and DNA transposed, amplified and library quantitated. Reads were aligned using Bowtie2 (mm10) and IGV_2.3.68 used for visualisation. Peaks were called by MACS2 2.1.1. Differentially expressed peaks were determined using DiffBind (edgeR, FDR < 0.01) taking into account triplicate samples of each experimental group. Black bars indicate peaks that are significantly higher expressed in WT macrophages, while red bars indicate peaks significantly lower in WT compared to *Ifnar1*$^{-/-}$ macrophages. ATAC-sequencing tracks shown are representative of 3 independent experiments. (A) Tracks shown for the *Mx1* locus. (B) Tracks shown for the *Il12b* locus.

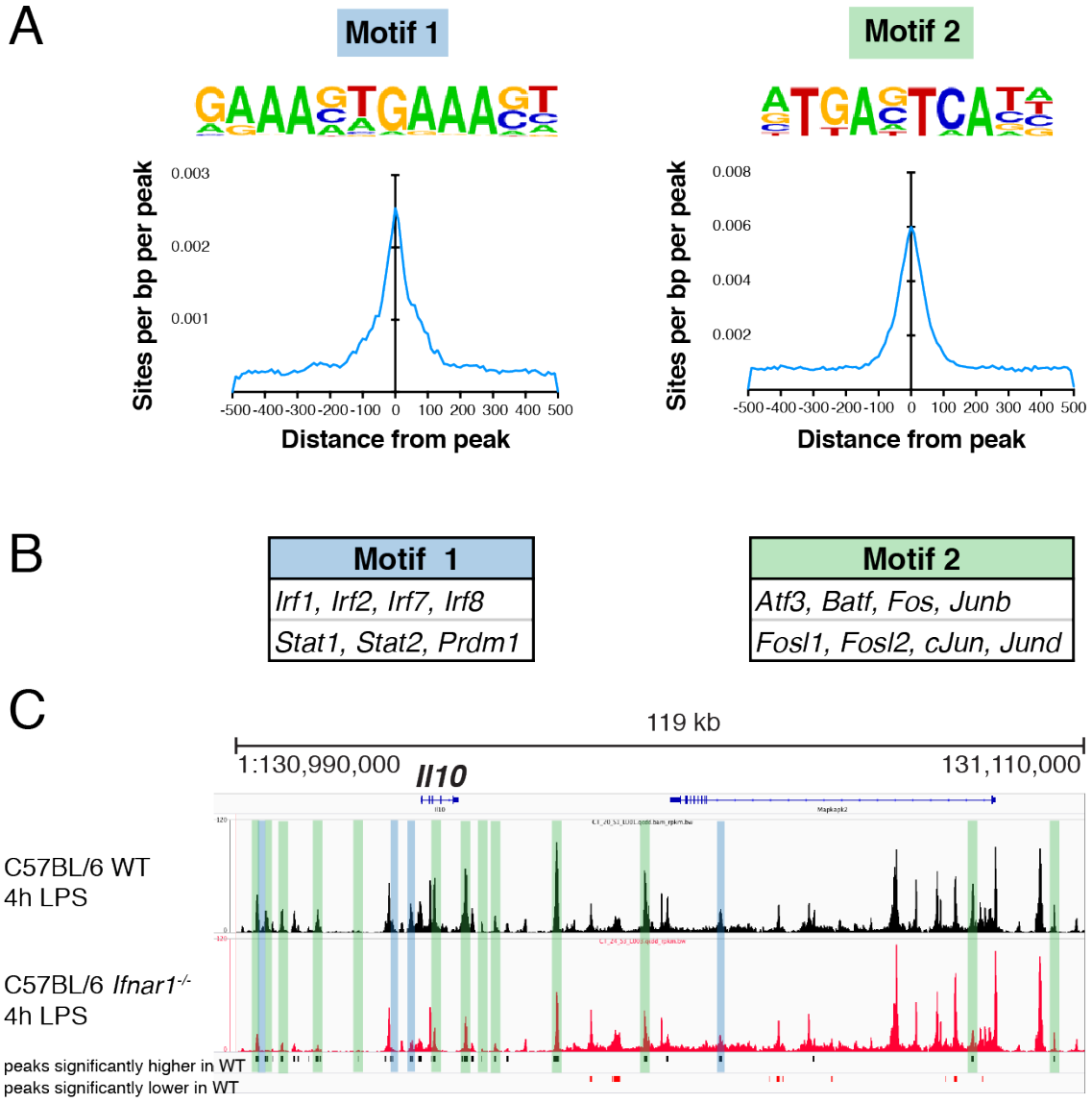

Figure 5.12 IRF and AP-1 transcription factor motifs are enriched within peaks significantly different in C57BL/6 WT compared to *Ifnar1*$^{-/-}$ macrophages 4 h post LPS stimulation.

Cells were prepared as described in Figure 5.8. Peak sets identified as "gained" in C57BL/6 WT macrophages compared to *Ifnar1*$^{-/-}$ macrophages 4 h post LPS stimulation (Figure 5.8 A) were subject to HOMER TF enrichment analysis. (A) Shown are the top 2 significantly enriched motifs with their peak distribution. (B) TFs that could possibly bind to the identified motifs. (C) Location of motif 1 (blue) and motif 2 (green) within peaks significantly increased in WT compared to *Ifnar1*$^{-/-}$ macrophages in vicinity of the *Il10* locus. Peaks were called by MACS2 2.1.1. Differentially expressed peaks were determined using DiffBind (edgeR, FDR < 0.01) taking into account triplicate samples of each experimental group. Black bars indicate peaks that are significantly higher expressed in WT macrophages, while red bars indicate peaks significantly lower in WT compared to *Ifnar1*$^{-/-}$ macrophages.

IGV_2.3.68 was used for visualisation of ATAC-sequencing track, which is representative of three independent experiments.

As shown in Chapter 4.3.5, the second wave of *Il10* mRNA expression is mediated by type I IFN via ERK1/2 activation. Hence, we investigated whether the inhibition of MEK1/2 upstream of ERK1/2 would lead to a similar reduction in chromosome accessibility within the *Il10* TAD as does the absence of the type I IFN signalling 4 h post LPS stimulation. Additionally, we investigated which TF motifs are enriched within peaks significantly higher in DMSO versus PD0325901 (MEK1/2 inhibitor) treated cells. Macrophages were pre-treated for 1 h with the inhibitor or DMSO as vehicle control, then stimulated for 4 h with LPS and samples processed as described in 2.10.1. As we only had one replicate per group, calculation of differentially accessible sites using Diffbind was not possible. Hence, the dataset of PD03259 treated macrophages was used as control file during peak calling with MACS2. This resulted in subtraction of the height of peaks present in PD03259 treated macrophages from those present in DMSO treated macrophages. Therefore, the final peak set consisted only of peaks higher or only present in DMSO treated macrophages. This peak set was then subjected to HOMER (340) TF motif discovery. Out of 11 significant ($p < 1x10^{-50}$) motifs enriched within these peaks genome-wide, the top motif was the AP-1 motif (Figure 5.13 A, B). This motif could be a possible binding site for *Atf3, Batf, Fos, Junb, Fosl1, Fosl2* and *cJun* (Figure 5.13 B). Relating these findings back to the region of the *Il10* TAD, 6 peaks that cover the binding motif were found (Figure 5.13 C). This motif was similar to the one identified by analysing WT versus *Ifnar1*$^{-/-}$ macrophages datasets (Figure 5.12 A, B). Peaks marked with *

in Figure 5.13 C are also significantly different and contained a binding site for AP-1 factors in the analysis comparing WT versus *Ifnar1*$^{-/-}$ macrophages (Figure 5.12 C).

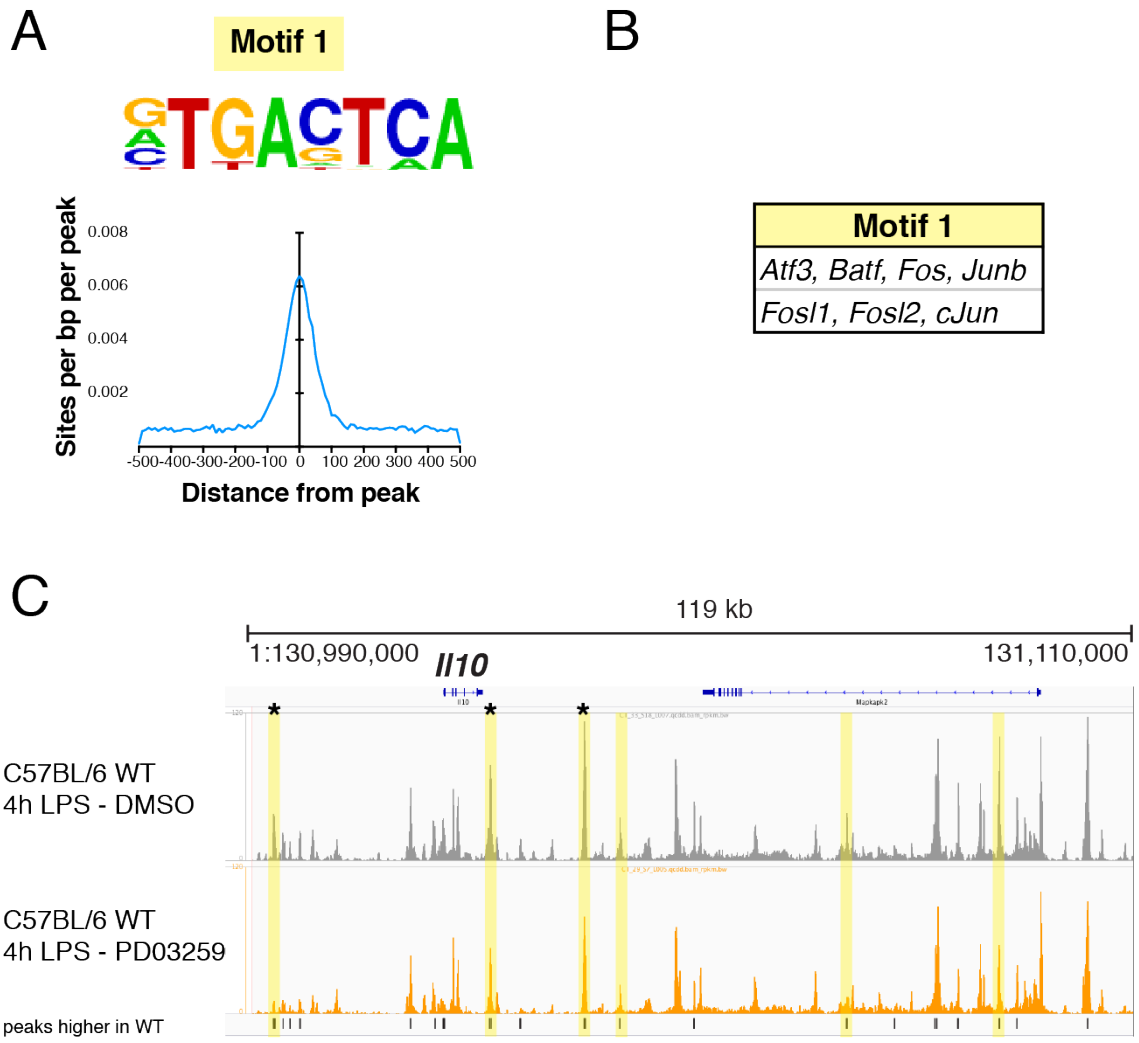

Figure 5.13 AP-1 transcription factor motif is highly enriched within peaks significantly different in macrophages treated with DMSO versus a MEK inhibitor 4 h post LPS stimulation.

Peak sets identified to be different in DMSO versus PD03259 treated macrophages 4 h post LPS stimulation were subject to HOMER TF enrichment analysis. (A) Shown is the top significantly enriched motif with its peak distribution. (B) TFs that could possibly bind to the identified motif. (C) Location of motif 1 (yellow) within peaks significantly increased in WT compared to *Ifnar1*$^{-/-}$ macrophages (black barres) in vicinity of the *Il10* locus. * these peaks are also significantly enriched in WT compared to *Ifnar1*$^{-/-}$ macrophages and contain the AP-1 motif (Figure 5.12). IGV_2.3.68 was used for visualisation of ATAC-sequencing tracks, which are representative of one experiment.

5.3.4 Validation of ATAC-sequencing analysis results *in vitro*

By comparing the chromosome accessibility within the *Il10* TAD in WT versus *Ifnar1*$^{-/-}$ macrophages and DMSO versus MEK1/2 (ERK1/2) inhibited macrophages and evaluating which TF motifs are enriched within differential peaks, we identified AP-1 family members as possible TF candidates involved in the second wave of *Il10* mRNA transcription induced in a type I IFN – ERK1/2 dependent manner (Figure 5.12 and Figure 5.13). To validate this hypothesis, firstly we aimed to determine whether TFs of the AP-1 family were constitutively expressed or induced post LPS stimulation in macrophages. Therefore, WT macrophages were stimulated for 1, 1.5, 2, 2.5, 3, 3.5, 4 and 4.5 h and mRNA of possible TF candidates was analysed (Figure 5.14 A). All TFs were induced at the mRNA level over the evaluated time points. *Fos, Fosl1* and *cJun* mRNA expression peaked at 1 h post LPS stimulation and dropped right after. *Fosl2* mRNA expression was slightly delayed and peaked at 1.5 h; however, its expression decreased right after. While *Fos*, *Fosl1* and *Fosl2* seemed to be expressed very early in response to LPS stimulation, *Atf3* was expressed already early but its expression stayed up over time. The expression of *Batf* mRNA was delayed but was constantly increasing over the time measured. *Junb* mRNA was highly expressed with an expression peak at 1 h followed by constant mRNA expression on high levels (Figure 5.14 A). Three to four hours after LPS stimulation, when the second wave of *Il10* mRNA transcription occurred, mostly *Atf3, Junb* but also *Batf* and *cJun* mRNA were expressed (Figure 5.14 and Figure 7.5). To assess, if these TFs are also expressed at the protein level, macrophages were stimulated with LPS for 4 h and protein levels determined (Figure 5.14 B). ATF3, BATF, JUNB and cJUN protein could be detected 4 h post LPS stimulation in WT macrophages, yet at various levels in keeping with the amount of mRNA present.

As shown above, ATF3, BATF, JUNB and cJUN are present in macrophages 4 h post LPS stimulation. To evaluate whether these TFs are able to carry out transcriptional activity in the nucleus 4 h post LPS stimulation, their location within the cells at this time point was determined. Macrophages were stimulated with LPS for 1 and 4h, nuclear and cellular fraction separated and protein of TFs analysed by western blot. cJUN and BATF were expressed mostly in the cytoplasm and protein expression was similar over time. However, JUNB was only expressed in the nucleus with the highest protein levels at 4 h post LPS stimulation. Similar results were found for ATF3 protein, which was expressed in the nucleus and its expression was also higher at 4 h post LPS stimulation.

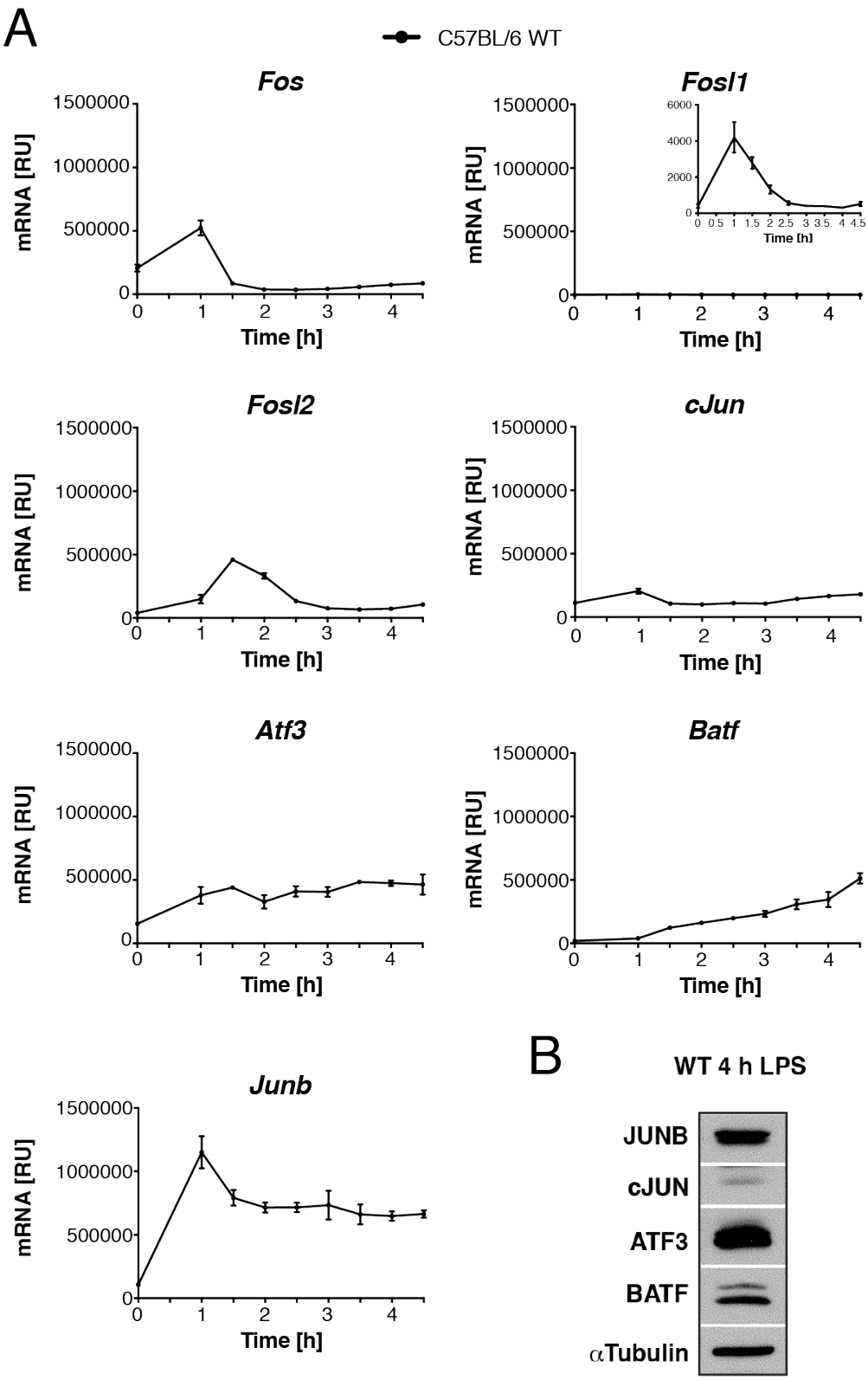

Figure 5.14 *Atf3*, *Batf*, *Junb* and *cJun* mRNA and protein are expressed in WT macrophages 4 h post LPS stimulation.

(A) Macrophages were generated from C57BL/6 WT mice and stimulated with LPS for 1, 1.5, 2, 2.5, 3, 3.5, 4 and 4.5h and total RNA was harvested and isolated. *Atf3, Batf, Fos, Junb, Fosl1, Fosl2* and *cJun* transcript levels were determined by qRT-PCR and normalised to *Hprt1* mRNA. (B) WT macrophages were stimulated with LPS for 4h. Whole-protein extracts were generated and analysed by Western blot for JUNB, cJUN, ATF3, BATF and αTubulin as loading control. Data are representative of one (A) or four (B) independent experiments.

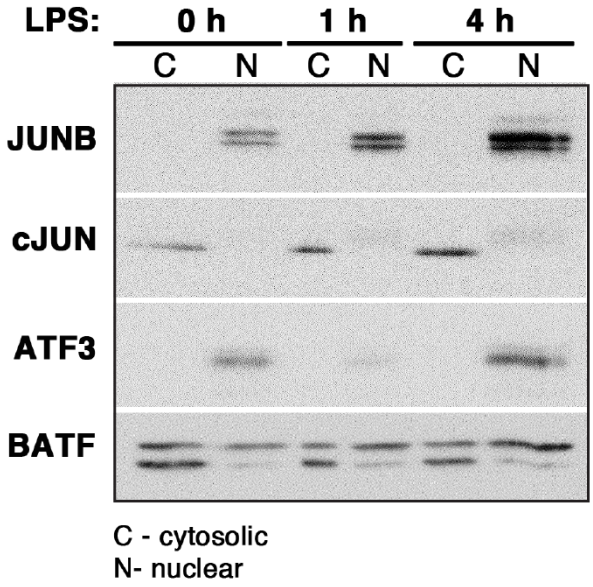

Figure 5.15 ATF3 and JUNB are localised in the nucleus 4 h post LPS stimulation.
Macrophages were generated from C57BL/6 WT mice and stimulated with LPS for 0, 1 and 4 h. Cellular and nuclear fractions were separated and extracts were analysed by western blot for JUNB, cJUN, ATF3 and BATF. Data are representative of three independent experiments.

Following on from these results, ATF3 and JUNB seem to be key candidates for TFs from the AP-1 family that might act within the *Il10* TAD to be responsible for the type I IFN-induced second wave of *Il10* mRNA transcription in LPS stimulated macrophages. We evaluated their ability to bind to open chromatin regions within the *Il10* TAD by ChIP-PCR. Differentially accessible chromatin regions within the *Il10* TAD were scanned for the ATF3 binding motif (TGACGTCA) and 10 primers

designed using NCBI Primer-Blast (Figure 5.16, grey dotted line). WT and *Ifnar1*$^{-/-}$ macrophages were stimulated for 0 or 4 h with LPS and processed as described in 2.11. In general, ATF3 bound more often in WT macrophages compared to *Ifnar1*$^{-/-}$ macrophages at regions analysed (Figure 5.16). In most cases, the size of the peak which accounts for the accessibility of the DNA, correlated with ATF3 binding. The higher the ATAC-seq peak (the higher the accessibility of the DNA), the more ATF3 binding. The biggest difference in binding of ATF3 between WT and *Ifnar1*$^{-/-}$ macrophages was in an accessible region downstream of the *Il10* gene (Figure 5.16). ATF3 ChIP-PCR results separate for each primer pair in C57BL/6 WT and *Ifnar1*$^{-/-}$ macrophages unstimulated or stimulated with LPS are represented in Figure 7.6.

Differentially accessible chromatin regions within the *Il10* TAD were scanned for the JUNB binding motif and 6 primers designed using NCBI Primer-Blast (Figure 5.17, grey dotted box). WT and *Ifnar1*$^{-/-}$ macrophages were stimulated for 0 or 4 h with LPS and processed as described in 2.11. JUNB did not bind differentially in WT and *Ifnar1*$^{-/-}$ macrophages upstream or within the *Il10* gene (Figure 5.17). However, a difference in JUNB binding was observed downstream of the *Il10* locus. JUNB ChIP-PCR results separate for each primer pair in C57BL/6 WT and *Ifnar1*$^{-/-}$ macrophages, either unstimulated or LPS stimulated are represented in Figure 7.7.

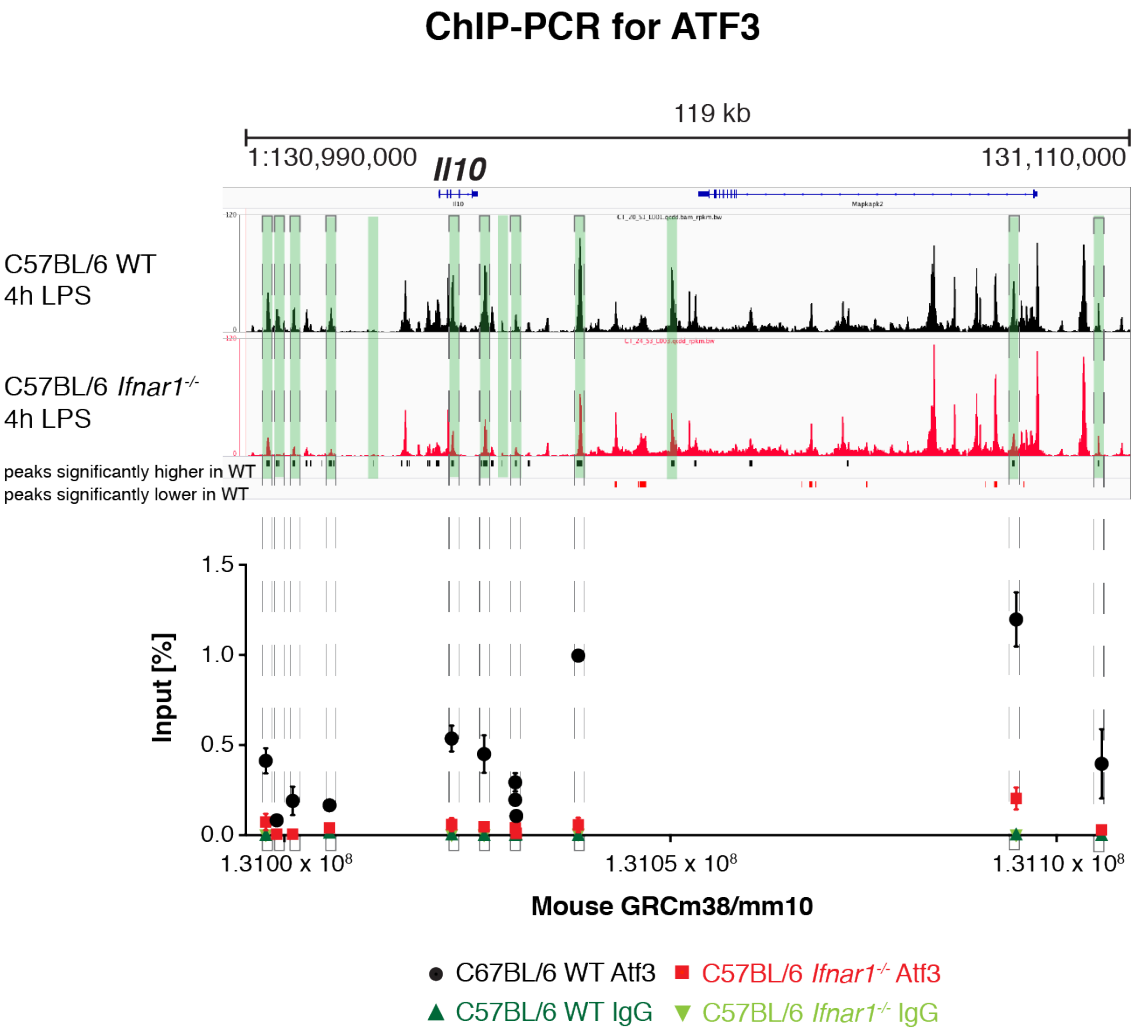

Figure 5.16 Increased direct binding of ATF3 at open chromatin regions within the *Il10* TAD in C57BL/6 WT compared to *Ifnar1*$^{-/-}$ macrophages 4 h post LPS stimulation.

Macrophages were generated from C57BL/6 WT and *Ifnar1*$^{-/-}$ mice. Cells were stimulated with LPS for 4 h and processed as described in 2.11. ChIP analysis of ATF3 interactions within the *Il10* TAD in comparison with ATAC-sequencing tracks for C57BL/6 WT and *Ifnar1*$^{-/-}$ macrophages are shown. ChIP-qPCR results were normalised using the Percent Input Method. Green boxes represent peaks that are significantly increased in WT macrophages 4 h post LPS stimulation and contain the AP-1 motif as identified by HOMER. The binding motif for ATF3 was only found in peaks surrounded by grey dotted lines. Data are representative of three independent experiments.

The positions within the *Il10* TAD that showed increased JUNB binding in WT compared to *Ifnar1*$^{-/-}$ macrophages also had increased ATF3 binding (Figure 5.16

and Figure 5.17). Furthermore, 2 out of 3 peaks that were differentially expressed in the WT versus *Ifnar1*$^{-/-}$ macrophages as well as in the DMSO versus MEK1/2 inhibitor treated cell dataset, showed increased JUNB as well as ATF3 binding (Figure 5.13, Figure 5.16 and Figure 5.17).

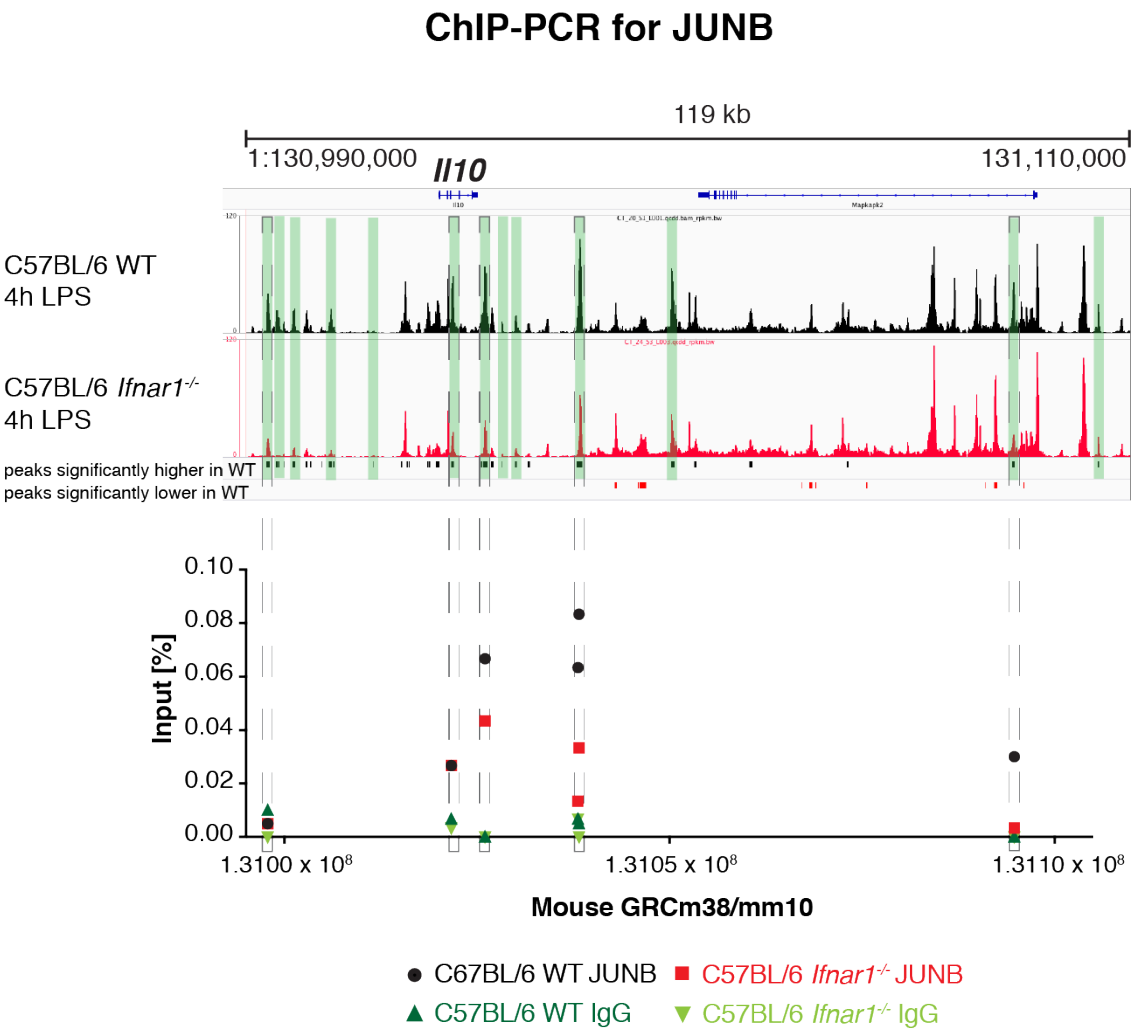

Figure 5.17 Increased direct binding of JUNB at open chromatin regions within *Il10* TAD in C57BL/6 WT compared to *Ifnar1*$^{-/-}$ macrophages 4 h post LPS stimulation.

Macrophages were generated from C57BL/6 WT and *Ifnar1*$^{-/-}$ mice. Cells were stimulated with LPS for 4 h and processed as described in 2.11. ChIP analysis of JUNB interactions within the *Il10* TAD in comparison with ATAC-sequencing tracks for C57BL/6 WT and *Ifnar1*$^{-/-}$ macrophages are shown. ChIP-qPCR results were normalised using the Percent Input Method. Green boxes represent peaks that are significantly increased in WT macrophages 4 h post LPS stimulation and contain the AP-1 motif as identified by HOMER. The binding motif for JUNB was only found in

peaks surrounded by grey dotted lines. Data are representative of two independent experiments.

To determine whether the differential binding of ATF3 and JUNB is only due to increased accessibility of DNA induced by type I IFN signalling or also to increased transcription of the TF itself, WT and *Ifnar1*$^{-/-}$ macrophages were stimulated with LPS for 3 h and *Atf3* and *Junb* mRNA analysed. mRNA expression of *Atf3* was significantly lower in *Ifnar1*$^{-/-}$ compared to WT macrophages 3 h post LPS stimulation. However, *Junb* mRNA levels were similar in WT and in *Ifnar1*$^{-/-}$ macrophages (Figure 5.18 A). These results were confirmed by analysing whole-cell extracts of WT and *Ifnar1*$^{-/-}$ macrophages stimulated for 4 h with LPS. ATF3 protein was lower in *Ifnar1*$^{-/-}$ compared to WT macrophages, while JUNB protein levels were similar (Figure 5.18 B).

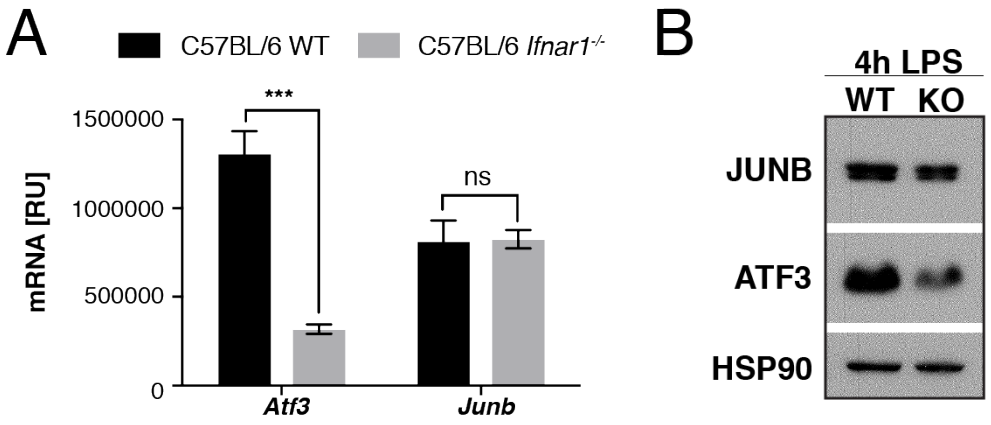

Figure 5.18 ATF3 but not JUNB is type I IFN inducible.

Macrophages were generated from C57BL/6 WT and *Ifnar1*$^{-/-}$ mice. (A) Cells were stimulated with LPS for 3 h and total RNA was harvested and isolated. *Atf3* and *Junb* mRNA transcript levels were determined by qRT-PCR and normalised to *Hprt1* mRNA. Graphs show means ± SD of triplicate cultures. (B) Macrophages were stimulated with LPS for 4 h. Whole-cell extracts were analysed by western blot for JUNB and ATF3 and HSP90 as loading control. Data are representative of two to

three independent experiments. ***p < 0.001, ns – not significant as determined by two-way ANOVA (Bonferroni multiple comparison test).

In summary, we showed that type I IFN signalling increases DNA accessibility genome-wide and within the *Il10* regulatory region. ATF3 and JUNB, both identified as TF candidates by microarray analysis as well as ATAC-sequencing, bind at open chromatin regions within the *Il10* TAD in a type I IFN dependent manner.

5.4 Discussion

Using ATAC-sequencing we showed that type I IFN signalling changes genome-wide DNA accessibility in macrophages. Type I IFN signalling mostly increased the number of accessible regions within the genome in LPS stimulated macrophages. However, *Ifnar1*$^{-/-}$ macrophages also showed regions of increased accessibility which were not present in the WT, suggesting that type I IFN signalling can decrease DNA accessibility at some loci. Furthermore, our data demonstrates that the *Il10* locus in macrophages is already accessible at steady state. Comparing the ATAC-sequencing tracks of the *Il10* locus with H3K4me1 marks, we postulate that the *Il10* gene is in a poised state as already suggested by Saraiva *et al.* (227), and that this likely permits rapid transcription from the *Il10* gene upon stimulation. This is in contrast to the *Il12a* gene, which is in a closed confirmation at steady state, in line with the absence of histone marks such as H3K4me1, H3K4me3 or H3K27ac in the vicinity of the *Il12a* gene. The comparison of chromatin accessibility of BMDMs with *ex vivo* myeloid cells demonstrated that the open state of the chromatin at the *Il10* locus does not have to be an artefact as *ex vivo* monocytes, Kupffer cells and large intestine macrophages also show accessibility at steady state. Further investigation of the *Il10* TAD in macrophages stimulated for 4 h with LPS revealed that type I IFN signalling mostly increased the DNA accessibility. Nevertheless, it also led to a more closed state in some regions of the *Il10* TAD. However, around the *Il10* promoter type I IFN only increased DNA accessibility. Many of the identified peaks coincide with HSS at the *Il10* gene locus as shown before by Saraiva *et al.* (227). In macrophages, five HSS sites have been identified upstream and downstream of the *Il10* transcription start site following stimulation with LPS, CpG and zymosan A (227). Regions that show increased accessibility in WT as compared to *Ifnar1*$^{-/-}$

macrophages, 4 h post LPS stimulation were enriched for the IRF/STAT motif as well as for the AP-1 motif. In the context of ERK-dependent *Il10* regulation, DNA regions that were more accessible in DMSO versus MEK1/2 inhibitor treated macrophages 4 h post LPS stimulation, also showed an enrichment for the AP-1 motif. Using qRT-PCR, western blotting and ChIP-PCR we identified ATF3 and JUNB as TF candidates that show increased binding in WT compared to *Ifnar1*$^{-/-}$ macrophages 4 h post LPS stimulation. ATF3 and JUNB also correlated highly with *Il10* mRNA expression in our time course microarray analysis of LPS stimulated WT and *Ifnar1*$^{-/-}$ macrophages. The increased binding of ATF3 could be due to a type I IFN-dependent increase of *Atf3* mRNA as well as protein expression 4 h post LPS stimulation; while increased binding of JUNB could be due to increased accessibility of the *Il10* locus as *Junb* mRNA and protein was not increased in a type I IFN-dependent manner.

We hypothesised that the type I IFN-dependent increase in DNA accessibility within the *Il10* TAD which we demonstrated could be responsible for the second initiation of *Il10* mRNA transcription in macrophages 3 h post LPS stimulation as shown in chapter 4.3.4. Factors that can change the accessibility of chromatin can include DNA methylation, nucleosome remodelling and covalent histone modifications such as acetylation or methylation (243). Histone modifying enzymes such as histone acetyl transferases (HATs) and histone deacetylases (HDACs) can alter histone 'tails', remodelling the chromatin from transcriptionally inactive heterochromatin to transcriptionally active euchromatin (243). It has been shown that the induction of ISGs by type I IFN requires chromatin remodelling, which occurs via STAT1-, STAT2- and IRF-mediated recruitment of nucleosome-remodelling enzymes and

HATs (377). ISG promoters associate with HATs and exhibit increased levels of histone acetylation; this acetylation is mediated in part by the recruitment of the HATs p300, CREB-binding protein (CBP) and GCN5 through interaction with the transcription activation domains of STAT1 and STAT2 (378). Although HATs have been implicated as positive regulators of type I IFN signalling, substantial evidence also documents positive roles for HDACs in type I IFN signalling pathways in innate immunity (379). The mechanism probably involves dependence on HDAC1, 2 and/or 3 in driving STAT1-dependent gene expression (380-382), although HDAC1 has been shown to also promote IFN-stimulated gene expression via interaction with the promyelocytic leukemia zinc finger (PLZF) TF (383). In total, these studies position class I HDACs as key regulators of IFN signalling (380, 384). Nusinzon and Horvath (380) showed a fundamental role for deacetylase activity and HDAC1 in transcriptional activation in response to IFN-α/β as HDAC1 augments the IFN-α response. Many studies also emphasised the importance of HDACs in the regulation of IL-10. Although HDAC11 acts as a transcriptional repressor of IL-10 (245), HDAC6 is required for *Il10* gene transcriptional activation in APCs as *Il10* mRNA expression is abrogated in the absence of HDAC6 (246). HDAC6 activity also leads to an increase in IFN-β (385). Hence, type I IFN might increase chromatin accessibility within the *Il10* TAD via the activation of HDACs or HTAs. However, this hypothesis remains to be tested. Besides HDACs and HATs, histone methyltransferases can modify chromatin and therefore regulate gene accessibility. Mixed-lineage leukemia 1 (MLL1), a histone methyltransferase, preferentially modifies lysine residue 4 on the histone H3 tail and has been shown to be initiated by signal transduction pathways activated by inflammatory stimuli (386). Carson *et al.* showed that type I IFNs, specifically IFN-α, were able to drive expression of *Mll1* mRNA in macrophages

(387). Hence, MLL1 could be leading to increased chromosome accessibility in WT compared to *Ifnar1*$^{-/-}$ macrophages stimulated with LPS. Again, this remains to be tested.

In order to define specific TFs that show type I IFN-dependent binding to the *Il10* gene, we first used microarray analysis correlating *Il10* gene expression with the expression of TFs over time in LPS stimulated WT and *Ifnar1*$^{-/-}$ macrophages. *Nfil3* mRNA kinetics highly correlated with that of *Il10* mRNA. However, we showed that IL-10 production was not affected in LPS stimulated *Nfil3*$^{-/-}$ macrophages which is in contrast to T cells where NFIL3 was shown to affect IL-10 production (368). Therefore, the correlation of the transcription of TF genes with *Il10* mRNA in LPS stimulated WT and *Ifnar1*$^{-/-}$ macrophages does not necessarily imply that these TFs are involved in the type I IFN- dependent regulation of *Il10*. Consequently, we reassessed our approach and set up ATAC-sequencing that allows us to predict TF binding at specific gene loci (332).

Using ATAC-sequencing, we demonstrated that the TF motifs of the IRF and AP-1 family were enriched within regions of higher chromatin accessibility in WT compared to *Ifnar1*$^{-/-}$ macrophages 4 h post LPS stimulation. As *Ifnar1*$^{-/-}$ macrophages do not allow type I IFN signalling, the most prominent enriched motif is the IRF/STAT motif as these genes are activated directly downstream of the IFN$\alpha\beta$R. However, the second most enriched motif, the AP-1 motif, was also enriched within areas of the DNA that were more accessible in DMSO versus MEK1/2 inhibited macrophages 4 h post LPS stimulation and therefore important in the type I IFN-ERK-dependent regulation of IL-10. The AP-1 complex has been shown to be activated downstream

of MAP kinase signalling (74), and specifically c-FOS, an AP-1 member, has been associated with the regulation of IL-10 in an ERK-dependent manner (71). Little is known about the regulation of *Il10* by the TFs FOSL1, which has been suggested to negatively regulate IL-10 in macrophages (388), or FOSL2. BATF plays a very important role in the regulation of *Il10* in T cells (389, 390) as does JUNB and cJUN (254). However, in macrophages stimulated with LPS for 4h, *Fos, Fosl1, Fosl2* and *cJun* mRNA were not highly expressed. The TF BATF was expressed, but not present in the nucleus 4 h post LPS stimulation, suggesting BATF is not actively binding to DNA at that time point. However, in our *in vitro* experiments we showed high expression of *Atf3* mRNA and protein in LPS stimulated macrophages and increased binding of ATF3 at the *Il10* locus in WT compared to *Ifnar1*$^{-/-}$ macrophages 4 h post activation. *Atf3* encodes for a member of the CREB/ATF protein family of TFs and was shown by Gilchrist *et al*. (391) to be induced by TLR4 stimulation and to act in a negative feedback loop, modulating the TLR4 stimulated inflammatory response of macrophages by altering chromatin structure. ATF3 binds to *Il6 and Il12b* promoters, and ATF3-associated HDAC1, a corepressor, deacetylates histones resulting in the closure of chromatin and the inhibition of transcription (391), possibly explaining the closed chromatin at the *Il12b* gene in WT macrophages 4 h post LPS stimulation and an increased opening in *Ifnar1*$^{-/-}$macrophages. In addition, ATF3 was described as having an important role in modulating IFN responses in macrophages by controlling basal and inducible levels of IFN-β, as well as the expression of genes downstream of IFN signalling (315). However, ATF3 has also been shown to directly bind Tat-interactive protein 60, a MYST histone acetyltransferase, at a region adjacent to the catalytic domain to promote the protein acetyltransferase activity in stress responses in epithelial-like HCT116 cells (392).

This demonstrates that dependent on the circumstances ATF3 can lead to closure or opening of chromatin. Hence, type I IFN-induced ATF3 might be the cause for increased chromosome accessibility at the *Il10* TAD. However, how ATF3 acts in the context of IL-10 is not known and needs further investigation. We were able to show that ATF3 binds DNA elements within and in the vicinity of the *Il10* gene in regions with increased accessibility in WT compared to *Ifnar1*$^{-/-}$ macrophages 4 h post LPS stimulation. However, some of the identified binding sites have been located within open chromatin close to other genes such as *Mapkapk2.* Hence, further experiments have to be done to validate the importance of ATF3 binding for *Il10* gene expression directly.

Additionally, we identified JUNB as another TF candidate that may lead to a second type I IFN-dependent induction of *Il10* mRNA transcription. In contrast to *Atf3* mRNA expression, *Junb* mRNA expression was not increased by type I IFN signalling. Hence, increased binding of JUNB within the *Il10* TAD in WT compared to *Ifnar1*$^{-/-}$ macrophages might occur due to increased accessibility of the DNA as opposed to increased expression. Furthermore, we only found differential binding of JUNB in WT and *Ifnar1*$^{-/-}$ macrophages in regions where ATF3 was also bound. This underlines the hypothesis that ATF3 may increase accessibility which may then facilitate JUNB binding. Gilchrist *et al.* showed, using Cytoscape, a potential interaction of ATF3 and JUNB (391). Nevertheless, co-immunoprecipitation experiments are required to formally establish the binding of both factors in our system. The role of JUNB in increasing IL-10 production was already described in T_H2 cells (242, 254). Wang *et al.* (254) identified a novel regulatory element that could specifically activate transcription of the *Il10* gene in T_H2 cells via JUNB and cJUN binding. Fontana *et al.,*

furthermore demonstrated a role for JUNB in myeloid inflammatory responses by showing that JUNB is required for the maximal expression of *Il1b* and additional genes involved in classical inflammation in macrophages treated with LPS and other immunostimulatory molecules (393). Their data suggested that JUNB is not absolutely required for activation of gene expression, but that it fine-tunes gene expression and, by inference, modulates the output of other TFs. Thus, JUNB regulates production of multiple cytokines and other immune-related genes in macrophages treated with LPS, affecting levels of both transcript and protein (393).

Our findings suggest that ATF3/JUNB association with the *Il10* locus may be important for the type I IFN-ERK mediated induction of *Il10* expression. However, the relationship between ERK1/2 signalling and ATF3/JUNB activity needs to be further evaluated. Lu *et al.* (394) showed that the ERK pathway is not necessary to induce ATF3, but the JNK pathway is involved in the activation of ATF3. However, these experiments were done in Hela Cells at early time points (394) and may not translate to events in primary macrophages. In TNFα-induced *Atf3* expression in vascular endothelial cells a requirement for the JNK pathway was also reported, while the ERK pathway was shown to inhibit the TNFα-mediated induction of *Atf3* mRNA (395). However, the effect of ERK1/2 on ATF3 in macrophages stimulated with LPS remains to be investigated. Furthermore, Lucas *et al.* reported that the activation of ERK leads to the phosphorylation of serine 10 on histone H3 at the *Il10* gene, causing remodelling of the chromatin at the *Il10* locus, thereby rendering it more accessible to TFs (247). Likewise, Zhang *et al.* (248) showed a rapid and dynamic phosphorylation of histone H3 by ERK1/2 at specific sites in the *Il10* promoter upon stimulation of macrophages. The timing of H3 phosphorylation closely correlates with

the timing of *Il10* gene transcription, proposing a link between the phosphorylation and transcriptional activation. Nevertheless, the precise role of this modification on gene expression remains unclear. It was hypothesised that phosphorylation of serine 10 on histone H3 is a predisposing mark for acetylation, which is itself a mark for active transcription (396). However, in contrast to histone phosphorylation, the peak of histone acetylation at the IL-10 promoter did not occur until after transcription had peaked and inhibition of histone deacetylase did not alter *Il10* gene expression. Hence, phosphorylation but not acetylation of the *Il10* promoter seems to be important for increased *Il10* mRNA transcription (248). However, acetylation and phosphorylation were only measured up to 2 h post LPS stimulation and not after 3 – 4 h when in our system the second wave of *Il10* transcription in response to type I IFN occurred. In tumour-associated macrophages, Banerjee *et al.* (397) also showed TRIF-dependent induction of high level of ERK1/2 activation leading to ERK1/2-dependent histone phosphorylation at the *Il10* promoter, resulting in increased IL-10 production.

In summary, we demonstrated that type I IFN signalling leads to increased DNA accessibility as well as to an increased binding of ATF3 and JUNB at the *Il10* locus which might lead to the induction of a second wave of *Il10* mRNA transcription. However, further experiments are needed to investigate the relationship between type I IFN, ERK1/2, ATF3/JUNB and the second wave of induction of *Il10* mRNA transcription.

Chapter 6.
Summary and future perspectives

6.1 Summary

Over the course of this investigation, we have analysed differential type I IFN production in C57BL/6 and BALB/c macrophages to further elucidate the molecular mechanisms underlying the reciprocal production of IL-10 and pro-inflammatory cytokines in these two strains. We then went on to investigate the mechanism underlying the type I IFN-dependent regulation of IL-10 production in macrophages. We began by analysing IL-10 and type I IFN production in response to several TLR-dependent PRR stimuli and subsequently narrowed our study to investigate IL-10 production in response to LPS.

Our data suggest that type I IFN production and consequently type I IFN signalling are a major difference in the responses of C57BL/6 and BALB/c macrophage to *B. pseudomallei* and LPS and in part explains their differential expression profile of IL-10 and pro-inflammatory cytokines, as we demonstrated in Howes, Taubert *et al.* (268) and in this thesis. These differences in type I IFN are neither due to differences in CD14 and TLR4 expression and/or endocytosis upon LPS stimulation in C57BL/6 and BALB/c macrophages nor to inhibition of the TRIF pathway by MyD88-dependent signalling. However, we showed increased TBK1 and IRF3 activation downstream of TLR4 signalling in LPS and Bps stimulated C57BL/6 macrophages compared to BALB/c macrophages.

The effect of type I IFN was further studied with focus on the anti-inflammatory cytokine IL-10 and the pro-inflammatory cytokine IL-12. Macrophages have the capacity to produce enhanced levels of IL-10 in response to IFN-α/β treatment in addition to most TLR ligations, with exception of TLR9 stimulated cells which

decreased IL-10 production upon IFN-α/β addition. With regard to the IL-12 production in TLR stimulated macrophages, low levels of type I IFN are important for the induction of IL-12 as reported before (269). However, increased amounts of either IFN-β or IFN-α significantly reduced IL-12 levels. As shown in McNab *et al.* (269), the effects of type I IFN on IL-12 are IL-10-dependent and –independent (also published in Howes, Taubert *et al.* (268)). Hence, we went to investigate the mechanism of type I IFN-dependent IL-10 regulation further using LPS stimulated macrophages. We showed that type I IFN, in addition to stabilising *Il10* mRNA expression, induced a second peak of *Il10* mRNA transcription in TLR4 but also TLR2 stimulated macrophages. This second induction was dependent on ERK1/2 activation in TLR4 activated macrophages (Figure 6.1).

Our investigation of chromosome accessibility and TF binding revealed a role for type I IFN in increasing chromosome accessibility genome wide as well as within the *Il10* TAD. Furthermore, we demonstrated that the *Il10* locus is already accessible at steady state. Comparing kinetics of *Il10* and *Il12b* mRNA showed that *Il10* mRNA is transcribed earlier upon stimulation as compared to *Il12b* mRNA. Hence, the *Il10* locus in macrophages is in a primed, poised state and macrophages are able to transcribe *Il10* mRNA quickly in response to TLR ligation. Areas of the chromosome that are more accessible in WT compared to *Ifnar1*$^{-/-}$ macrophages and additionally in DMSO versus MEK1/2 inhibitor treated macrophages 4 h post LPS stimulation, showed enrichment for the TF motif of the AP-1 family. However, the TFs BATF, FOS, cJUN, FOSL1 and FOSL2 are not highly expressed in 4 h LPS stimulated macrophages and NFIL3 does not alter levels of IL-10 in a type I IFN-dependent manner in LPS stimulated macrophages. Nevertheless, we showed increased

binding of ATF3 and JUNB within the *Il10* TAD in 4 h LPS stimulated macrophages (Figure 6.1). The increased binding of ATF3 may be due to the induction of ATF3 by type I IFN, since higher levels of *Atf3* mRNA were detected in LPS stimulated WT macrophages compared to *Ifnar1*$^{-/-}$ macrophages. However, levels of JUNB are not altered by type I IFN signalling. Hence, we suggest that the increased accessibility within the *Il10* TAD in response to type I IFN signalling results in increased binding of JUNB in 4 h LPS stimulated macrophages. Together, our findings suggest that type I IFN may regulate *Il10* expression by different mechanisms as by increasing chromosome accessibility but also by inducing the expression of TFs that regulate *Il10* expression.

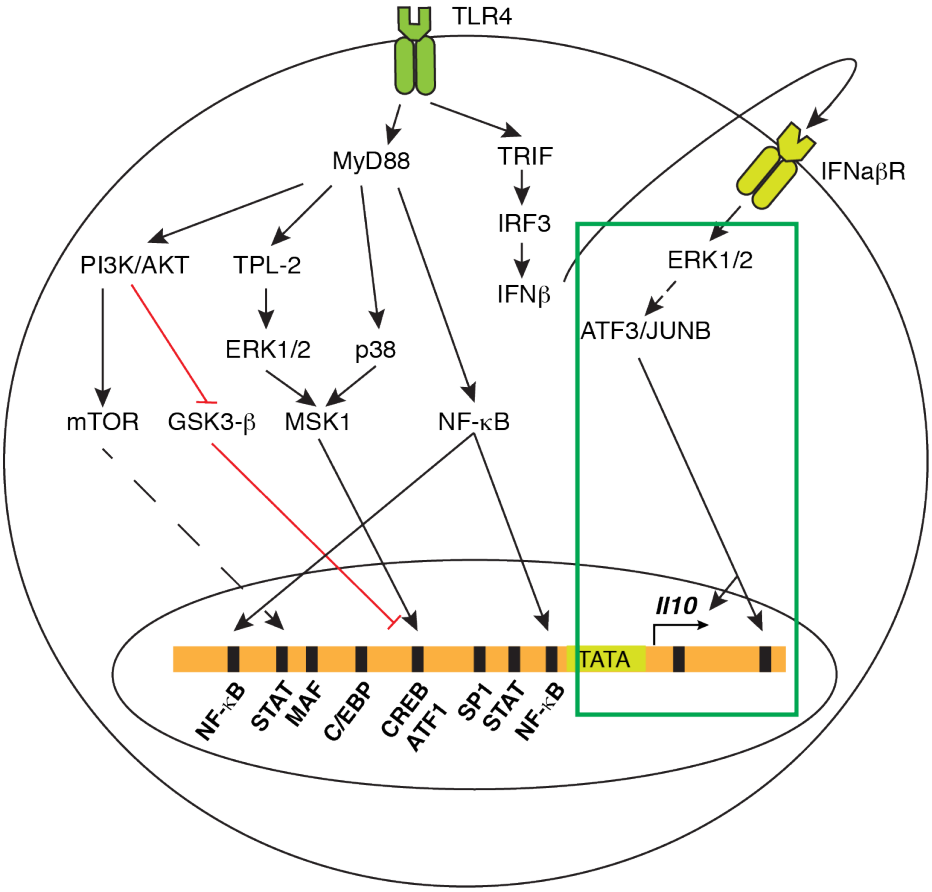

Figure 6.1 Summary of key findings: Type I IFN-dependent regulation of *Il10* expression in LPS stimulated macrophages.

Despite the induction of IL-10 by already described pathways such as PI3K/AKT, MAPK and NF-κB signalling upon TLR4 ligation, its transcription is reinforced by type I IFN. IFN-β which is produced upon TLR4 stimulation through the TRIF-dependent pathway activates ERK1/2 and leads to an increased binding of ATF3 and JUNB at the *Il10* locus as well as increased chromosome accessibility. Key findings in the type I IFN-dependent regulation of IL-10 are highlighted by green box.

6.2 Future perspectives

6.2.1 Investigate deeper the mechanism of how type I IFN regulates *Il10* mRNA expression in macrophages

6.2.1.1 Study the direct interactions between the molecules revealed to be important in type I IFN-dependent Il10 mRNA expression

We showed that type I IFN induces ERK1/2 (T185/Y187) phosphorylation. It was demonstrated before by David *et al.* (283) in a multiple myeloma cell line that MAPK, specifically ERK2, interacted with the α-subunit of the IFN-α/β receptor. However, it is not known in macrophages whether type I IFN induces ERK1/2 (T185/Y187) phosphorylation directly or indirectly, and needs to be investigated further. The use of cycloheximide, an antibiotic that inhibits translation, could allow us to establish whether type I IFN acts independently of *de novo* protein production. Additionally, using immunoprecipitation and mass spectrometry, we could identify whether ERK1/2 directly binds to the IFN-α/β receptor and further investigate other proteins that may interact with ERK1/2 in the presence or absence of type I IFN signalling.

Additionally, we demonstrate here that ATF3 and JUNB bind within the *Il10* TAD in a type I IFN-dependent manner. How much of this effect is due to a type I IFN –

ERK1/2 dependent pathway has to be further elucidated. We observed an enrichment for the AP-1 binding motif in the differential chromatin accessible regions in DMSO compared to MEK1/2 inhibitor treated macrophages 4 h post LPS stimulation. However, ChIP-PCR experiments using MEK1/2 inhibitors have to be performed to confirm whether the increased binding of ATF3 and JUNB is related to the type I IFN-dependent phosphorylation of ERK1/2 (T185/Y187). Additionally, ATF3 and JUNB often bound within similar accessible regions along the *Il10* TAD. We hypothesise that JUNB and ATF3 may form a complex, as members of the AP-1 family build homo- or heterodimers to execute their function (74). However, this would have to be investigated by co-precipitation. Furthermore, it has to be confirmed that JUNB and/or ATF3 indeed regulate *Il10* mRNA expression and IL-10 production and whether this is dependent on type I IFN signalling. This will be addressed by evaluating IL-10 levels in LPS stimulated *Atf3* and *Junb* KO macrophages in the presence or absence of anti-IFNAR neutralising antibodies.

6.2.1.2 Investigate the mechanism of how chromatin accessibility is regulated

Our data demonstrate that *Ifnar1*$^{-/-}$ macrophages show decreased chromosome accessibility compared to WT macrophages 4 h post LPS stimulation within the *Il10* TAD. Although, to a lower degree macrophages stimulated in the presence of MEK1/2 inhibitor also showed lower accessibility within the *Il10* TAD compared to their WT controls. ATF3 was shown do recruit HATs. Hence, one open question is: which factors lead to an increased opening of the *Il10* TAD and which HDACs, HATs or other mechanisms are involved? To investigate this question, one could do ChIP experiments for various histone modifications and evaluate changes in WT, *Ifnar1*$^{-/-}$,

Atf3$^{-/-}$ *and Junb*$^{-/-}$ macrophages as well as macrophages stimulated in the presence of MEK1/2 inhibitor. Additionally, the presence of various HDACS and HATs could be evaluated by western blotting.

6.2.2 Extend findings to an *in vivo* model

Hackstein *et al.* (398) recently described an experimental liver fibrosis model by bile duct ligation and subsequent *L. monocytogenes* infection where the signalling through the type I IFN receptor in myeloid cells triggers the expression of IL-10. This *Il10* expression by myeloid cells correlated with reduced phagocytic capacity and bactericidal functions of the myeloid cells (398). Using this model, Hackstein *et al.* (398) showed for the first time that type I IFN signalling regulates IL-10 production by myeloid cells *in vivo* during bacterial infection and that this IL-10 derived from myeloid cells may impair the control of the infection. Furthermore, they demonstrated that liver macrophages produced high levels of IL-10 two days post *L. monocytogenes* infection and increased levels of IFN-β were also detected in the liver. Taken together, in this model liver macrophages might show similar cytokine profiles and similar regulatory mechanism as we demonstrated in BMDMs. Moreover, as shown in Chapter 5.3.2, at steady state Kupffer cells (24) show increased chromosome accessibility at the *Il10* locus, similar to our BMDMs. Therefore, we are collaborating with Dr Zeinab Abdullah from the University of Bonn to establish further the mechanisms involved in the type I IFN- dependent IL-10 production in myeloid cells in this model. Using WT and *Ifnar1*$^{-/-}$ mice we aim to establish differences in the activity of MAPK signalling pathways by western blotting

and FACS as well as differences in TF binding and chromosome accessibility by ATAC-seq and ChIP-seq.

BMDMs are often used as a tool to study macrophage biology as they are easy to handle and lots of cells can be obtained for immunological and biochemical assays. However, an *in vivo* counterpart to *in vitro* derived BMDMs is still unknown (399) and makes the translation of the results to an *in vivo* setting challenging. Ultimately, however, it will be important to understand how the knowledge obtained using BMDMs relates to macrophage or monocyte populations found *in vivo*, and in the human system. We would like to address this question using *Il10*tm1.1Karp mice (IL-10 reporter mouse, reporting also in APCs) (400) that we have now crossed with the *Ifnar1*$^{-/-}$ mice. By comparing WT and *Ifnar1*$^{-/-}$ IL-10 reporter mice, we will be able to track *Il10* expressing myeloid cells and investigate their cytokine profiles, chromosome accessibility and regulatory mechanisms at steady state and upon infection, using the liver fibrosis model described above and other infection models established in the laboratory.

Chapter 7.
Appendix

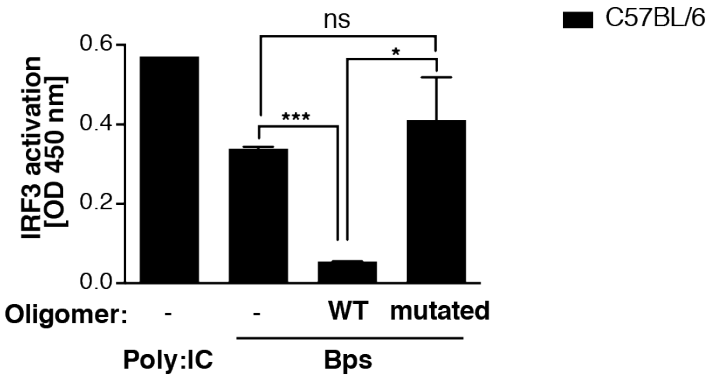

Figure 7.1 Specificity test for IRF3 activity assay.

C57BL/6 macrophages were stimulated for 2 h with *B. pseudomallei* (Bps) and the nuclear fraction of the cells was extracted. 2 min before addition of C57BL/6 (Bps 2 h) nuclear extract or Cos-7 (PolyI:C 2 h) nuclear extract as a positive control for IRF3 activation to the wells, wild type (WT) consensus oligonucleotides or mutated oligonucleotides were added. IRF3 activity was analysed by ELISA. Graph shows means ± SD of triplicate cultures. *$p < 0.05$, ***$p < 0.001$, ns – non significant as determined by two-tailed Student's t-test. Representative of two independent experiments.

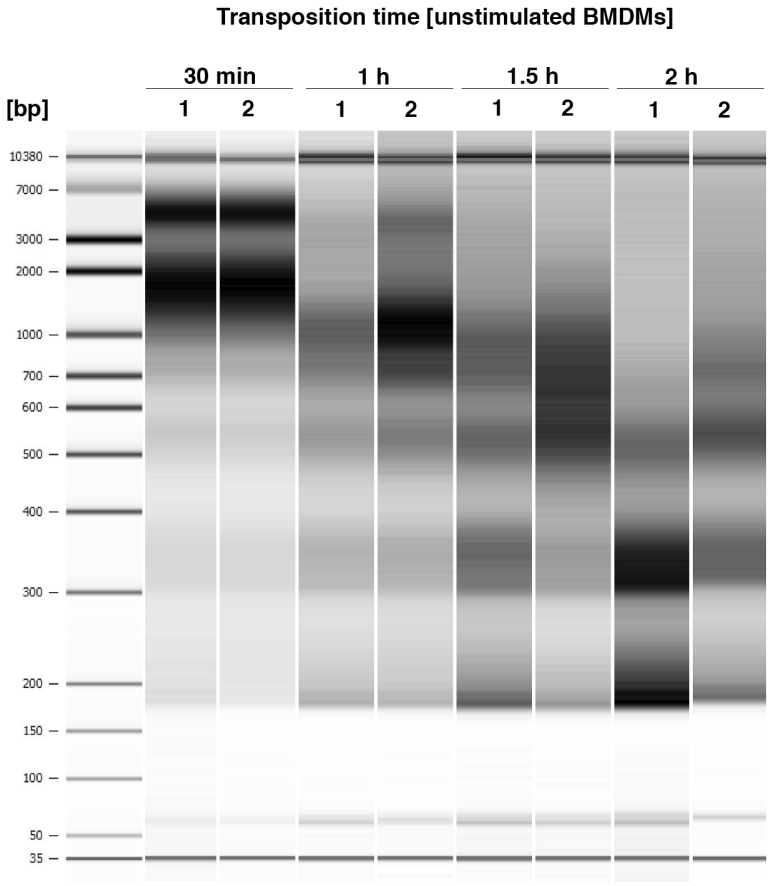

Figure 7.2 Evaluation of the transposition time for the preparation of the ATAC-sequencing library.

C57BL/6 macrophages were plated and after a 20 h rest lysed. 50,000 cells were pelleted, nuclei re-suspended in transposition reaction mix and incubated for 0.5, 1, 1.5 and 2 h at 37°C. Fragmentation size and pattern was evaluated using the Bioanalyzer (Agilent Technologies, High Sensitivity DNA Assay).

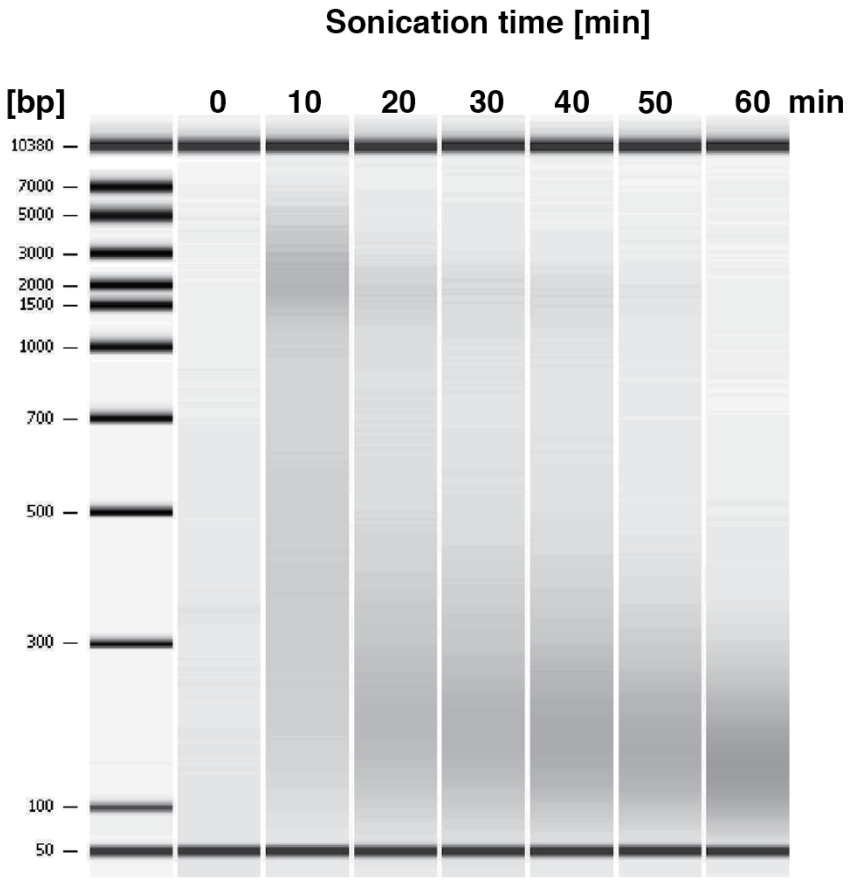

Figure 7.3 Evaluation of sonication time for ChIP-PCR.

Macrophages were stimulated for 4 h with LPS, lysed and then sonicate for 10, 20, 30, 40, 50 and 60 min. Samples were de-crosslinked before the fragment size was analysed using the Bioanalyzer (Agilent Technologies, DNA 7500).

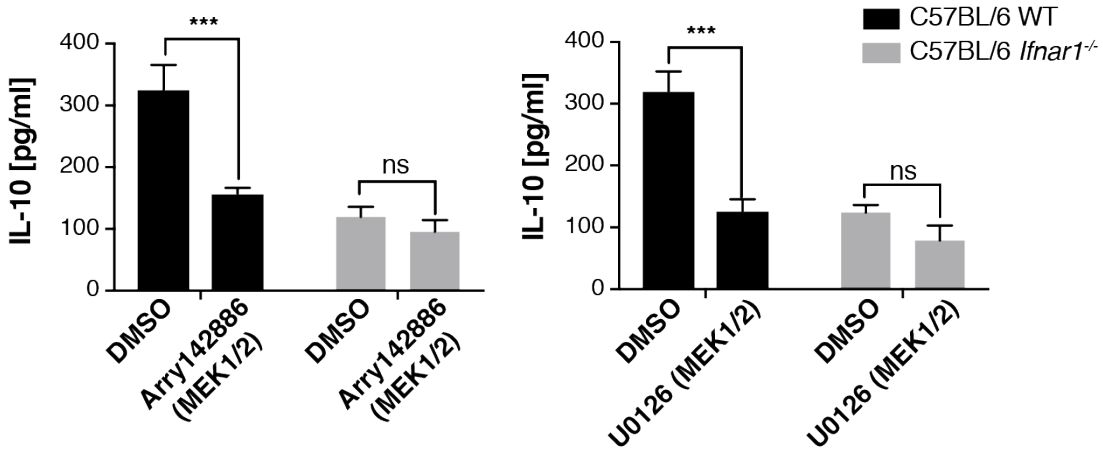

Figure 7.4 ERK1/2 signalling is required for type I IFN mediated IL-10 production in LPS stimulated C57BL/6 macrophages.

C57BL/6 WT and *Ifnar1*$^{-/-}$ macrophages were treated with the MEK1/2 inhibitors Arry142886, U0126 or DMSO as vehicle control 1 h prior to stimulation with LPS for 24 h. IL-10 production was quantified by ELISA. Graphs show means ± SD of triplicate cultures. ***p < 0.001, ns – non significant as determined by two-way ANOVA (Bonferroni multiple comparison test). Data are representative of three independent experiments.

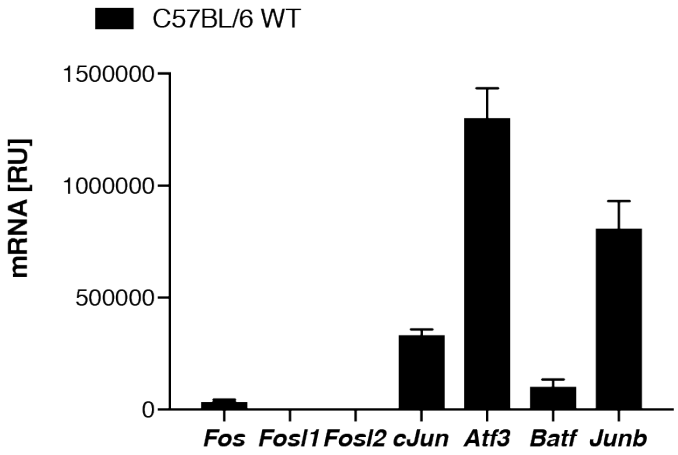

Figure 7.5 *Atf3*, *Junb*, *cJun* and *Batf* mRNA are expressed 3 h post LPS stimulation in macrophages.

Macrophages were generated from C57BL/6 WT mice and stimulated with LPS for 3 h. Total RNA was harvested and isolated. *Fos, Fosl1, Fosl2, cJun, Atf3, Batf* and *Junb* mRNA transcript levels were determined by qRT-PCR and normalised to *Hprt1* mRNA. Data are representative of three to four independent experiments.

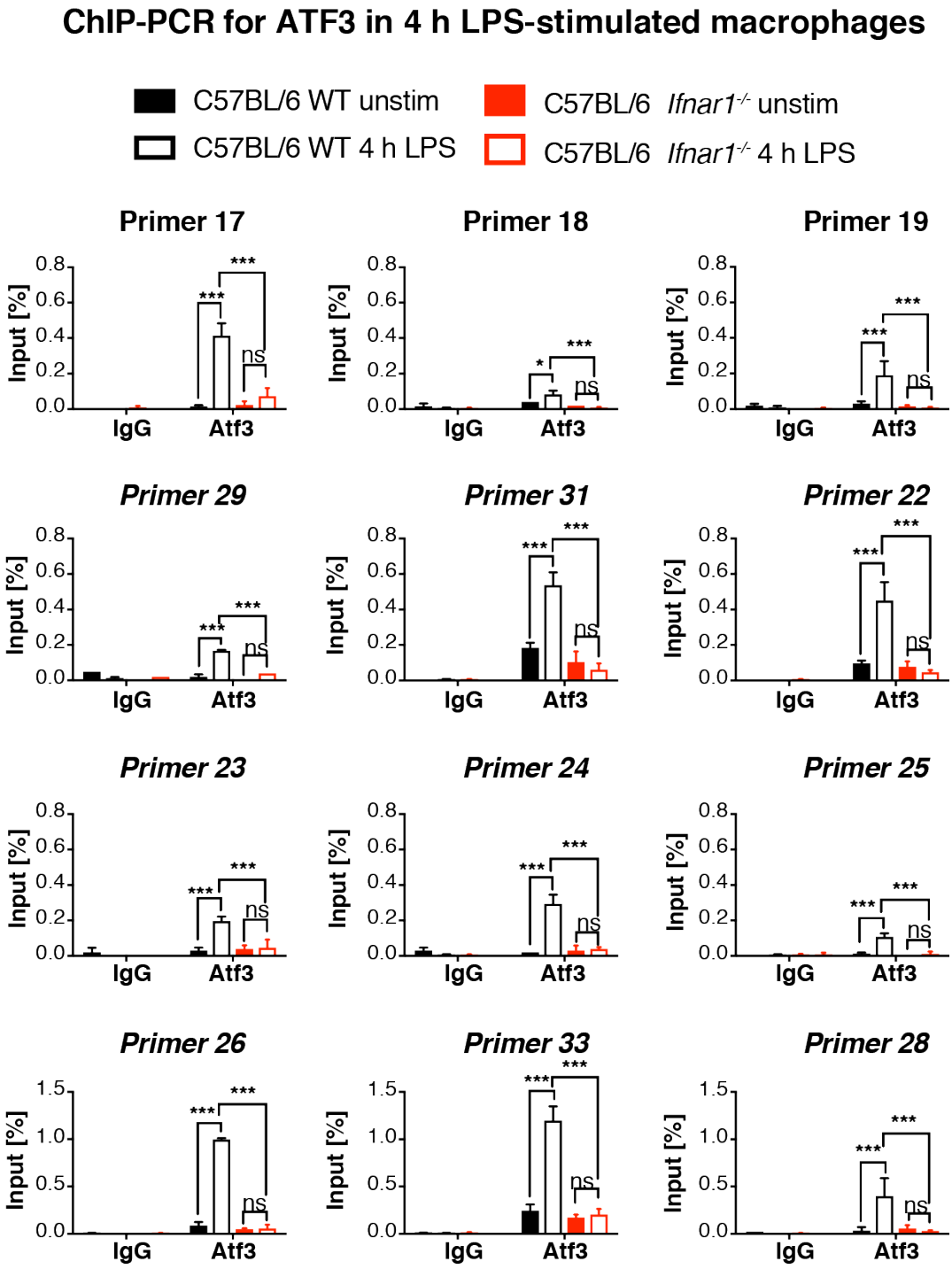

Figure 7.6 Increased direct binding of ATF3 at open chromatin regions within *Il10* TAD in C57BL/6 WT compared to *Ifnar1*$^{-/-}$ macrophages 4 h post LPS stimulation.

Macrophages were generated from C57BL/6 WT and *Ifnar1*$^{-/-}$ mice. Cells were stimulated with LPS for 0 or 4 h and processed as described in 2.11. ChIP-qPCR results were normalised using the Percent Input Method. Graphs show means ± SD of triplicate cultures. Data are representative of 3 independent experiments. *p < 0.05, ***p<0.001, ns – non significant as determined by two-way ANOVA (Sidak's multiple comparisons test). Primers are in order with peaks along *Il10* TAD.

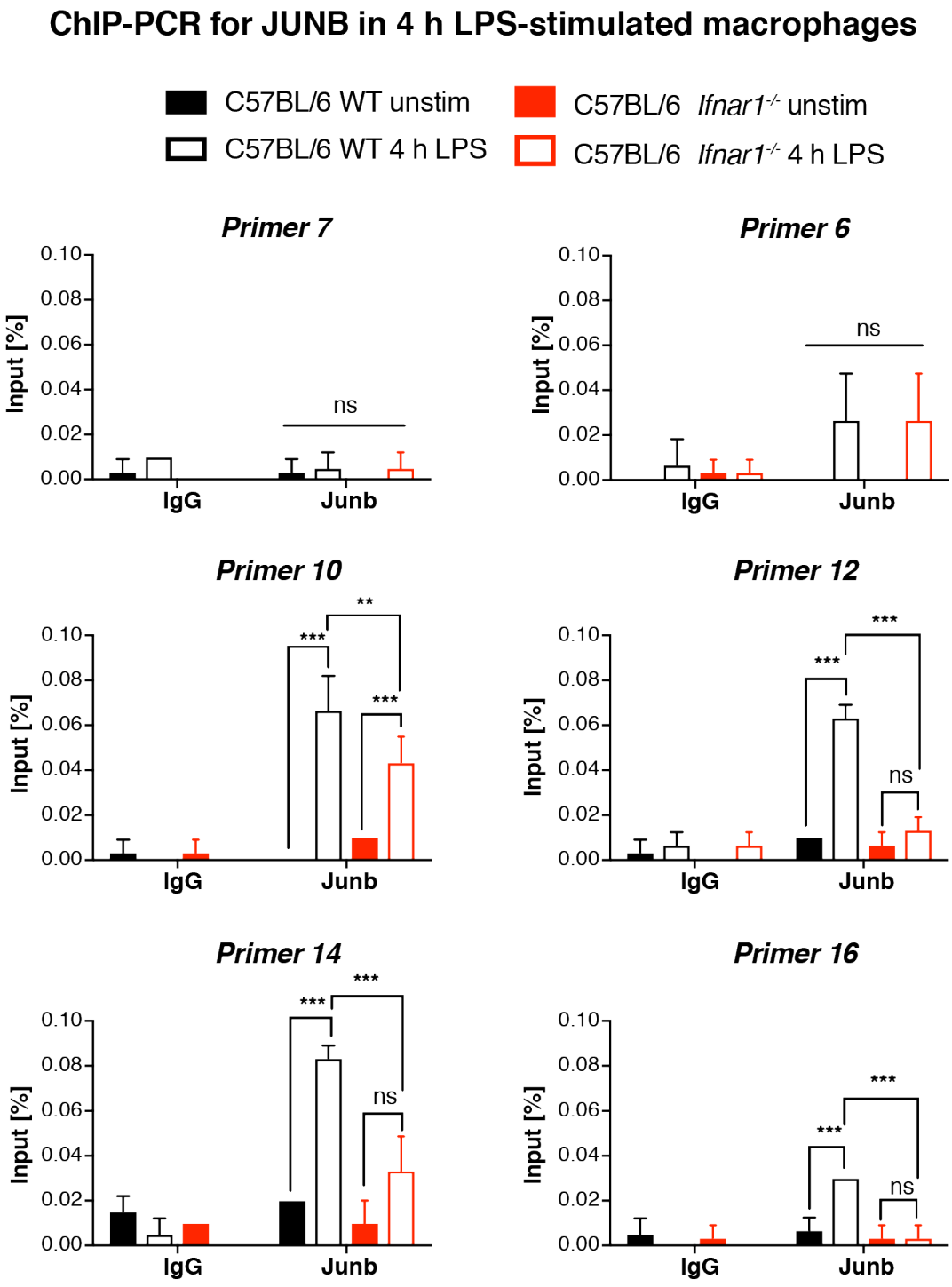

Figure 7.7 Increased direct binding of JUNB at open chromatin regions within *Il10* TAD in C57BL/6 WT compared to *Ifnar1*$^{-/-}$ macrophages 4 h post LPS stimulation.

Macrophages were generated from C57BL/6 WT and *Ifnar1*$^{-/-}$ mice. Cells were stimulated with LPS for 0 or 4 h and processed as described in 2.11. ChIP-qPCR results were normalised using the Percent Input Method. Graphs show means ± SD of triplicate cultures. Data are representative of 2 independent experiments. **p < 0.01, ***p<0.001, ns – non significant as determined by two-way ANOVA (Sidak's multiple comparisons test). Primers are in order with peaks along *Il10* TAD.

Table 7.1 Genes and related log FC associated with IPA canonical pathways.

Genes and related log FC related with the top 10 type I IFN–related IPA pathways significantly associated with the genes differentially regulated by *B. pseudomallei* stimulation in C57BL/6 and BALB/c macrophages at the 3 and 6 h time point are shown. Canonical pathway analysis was conducted using IPA software (QIAGEN Inc., https://www.qiagenbioinformatics.com/products/ingenuity-pathway-analysis).

Genes in the Interferon Signaling network

Symbol	Log FC C57BL/6-Bps vs. BALB/c-BPS (3h)	Log FC C57BL/6-Bps vs. BALB/c-BPS (6h)
G1P2	N/A	0.29
IFI35	1.33	0.61
IFIT1	2.53	2.77
IFIT3	N/A	1.33
IFITM2	0.58	N/A
IFNB1	N/A	-0.92
IFNGR2	0.62	0.92
IFNγRα	N/A	1.66
IRF9	N/A	0.41
NF-κBp65	N/A	0.33
OAS1	0.94	0.60
PIAS1	0.82	0.79
STAT1	1.01	0.55
STAT2	0.86	0.54
TAP1	1.22	0.72
TYK2	0.79	N/A

Genes in the JAK/Stat Signaling network

Symbol	Log FC C57BL/6-Bps vs. BALB/c-BPS (3h)	Log FC C57BL/6-Bps vs. BALB/c-BPS (6h)
c-FOS	N/A	1.99
c-JUN	2.03	N/A
CEBPβ	N/A	0.69
CIS	N/A	-1.22
GNAQ	0.78	N/A
KRAS	N/A	-1.60
MRAS	N/A	-1.70
NFKB2	2.97	3.51
PIAS1	0.82	0.79
PIAS3	-0.92	-0.56
PIK3CD	1.56	1.90
PIK3CG	1.10	N/A
RELA	N/A	0.33
RRAS2	N/A	-3.44
SOCS4	1.39	N/A
STAT1	1.01	0.55
STAT2	0.86	0.54
STAT3	1.76	1.39
STAT4	2.47	1.72
TYK2	0.79	N/A

Genes in the Activation of IRF by Cytosolic Pattern Recognition Receptors network

Symbol	Log FC C57BL/6-Bps vs. BALB/c-BPS (3h)	Log FC C57BL/6-Bps vs. BALB/c-BPS (6h)
ADAR1	1.21	0.55
c-Jun	2.03	N/A
CD-40	N/A	2.84
DAI	N/A	0.66
DDX58	1.24	N/A
DHX58	1.52	0.91
IFNB1	N/A	-0.92
IKBKB	N/A	0.93
IKBKE	N/A	0.85
IL-10	N/A	3.29
IRF-7	N/A	0.65
IRF9	N/A	0.41
ISG-15	N/A	0.29
ISG-54	1.10	1.13
MAP2K4	1.30	1.08
NFKB2	2.97	3.51
NFKBIA	N/A	0.21
p300/CBP	N/A	0.94
p65NFκB	N/A	0.33
STAT1	1.01	0.55
STAT2	0.86	0.54
TANK	N/A	0.56
TNFα	N/A	-0.14

Genes in the Role of JAK1, JAK2 and TYK2 in Interferon Signaling network

Symbol	Log FC C57BL/6-Bps vs. BALB/c-BPS (3h)	Log FC C57BL/6-Bps vs. BALB/c-BPS (6h)
IFNB1	N/A	-0.92
IFNGR1	N/A	1.66
IFNGR2	0.62	0.92
NFKB2	2.97	3.51
RELA	N/A	0.33
STAT1	1.01	0.55
STAT2	0.86	0.54
STAT3	1.76	1.39
TYK2	0.79	N/A

Genes in the Role of PKR in Interferon Induction and Antiviral Response network

Symbol	Log FC C57BL/6-Bps vs. BALB/c-BPS (3h)	Log FC C57BL/6-Bps vs. BALB/c-BPS (6h)
APAF-1	1.26	0.64
BID	0.47	0.77
CASP8	N/A	0.88
CASP9	N/A	-0.29
FcγRI	N/A	1.24
IFNβ	N/A	-0.92
IKBKB	N/A	0.93
IKBKE	N/A	0.85
MAP2K3	0.73	0.27
NFKB2	2.97	3.51
NFKBIA	N/A	0.21
p38MAPK	N/A	-0.77
RELA	N/A	0.33
STAT1	1.01	0.55
TNF-α	N/A	-0.14
TNFR1	1.44	1.23
TRAF2	N/A	0.42

Genes in the Type I Diabetes Mellitus Signaling network

Symbol	Log FC C57BL/6-Bps vs. BALB/c-BPS (3h)	Log FC C57BL/6-Bps vs. BALB/c-BPS (6h)
APAF1	1.26	0.64
BID	0.47	0.77
CASP8	N/A	0.88
CASP9	N/A	-0.29
CD86	1.97	1.40
CPE	N/A	-1.28
FAS	N/A	5.19
HLA-A	-3.94	-10.48
HLA-DMA	N/A	-0.87
HLA-DQB1	N/A	6.63
HLA-DRA	-5.16	-5.58
HLA-E	0.54	N/A
IFNγR1	N/A	1.66
IFNγR2	0.62	0.92
IKBKB	N/A	0.93
IKBKE	N/A	0.85
IL12A	N/A	-4.40
MAP2K3	0.73	0.27
MAP2K4	1.30	1.08
MAPK14	N/A	-0.77
MYD88	1.16	0.54
NFKB2	2.97	3.51
NFKBIA	N/A	0.21
PIAS1	0.82	0.79
RELA	N/A	0.33
SOCS4	1.39	N/A
STAT1	1.01	0.55
TNF-α	N/A	-0.14
TNFRSF1A	1.44	1.23
TNFRSF1B	N/A	0.62
TRAF2	N/A	0.42

Genes in the Antigen Presentation Pathway network

Symbol	Log FC C57BL/6-Bps vs. BALB/c-BPS (3h)	Log FC C57BL/6-Bps vs. BALB/c-BPS (6h)
CALR	N/A	-0.47
CLIP	1.28	0.45
HLA-A	-3.94	-10.48
HLA-DMA	N/A	-0.87
HLA-DRA	-5.16	-5.58
HLA-E	0.54	N/A
LMP2	N/A	5.03
LMPX	N/A	1.43
MHCI-β	0.76	N/A
NLRC5	1.56	1.06
TAP1	1.22	0.72
TAP2	N/A	0.39
TPN	1.66	1.53

Genes in the Dendritic Cell Maturation network

Symbol	Log FC C57BL/6-Bps vs. BALB/c-BPS (3h)	Log FC C57BL/6-Bps vs. BALB/c-BPS (6h)
ATF4	N/A	4.43
B2M	0.76	N/A
CD40	N/A	2.84
CD86	1.97	1.40
CREBBP	N/A	0.94
FCGR1A	N/A	1.24
FCGR2A	-0.24	-0.24
FCGR3A/FCGR3B	1.69	1.41
FSCN1	N/A	-0.99
GM-CSF	N/A	-3.41
HLA-A	-3.94	-10.48
HLA-DMA	N/A	-0.87
HLA-DQB1	N/A	6.63
HLA-DRA	-5.16	-5.58
IFNB1	N/A	-0.92
IKBKB	N/A	0.93
IKBKE	N/A	0.85
IL-10	N/A	3.29
IL-15	N/A	0.87
IL-23p19	N/A	-1.30
IL12A	N/A	-4.40
IL1A	N/A	-1.29
IL1RN	N/A	1.07
LTB	-2.19	-3.45
MAP2K4	1.30	1.08
MAPK14	N/A	-0.77
MYD88	1.16	0.54
NFKBIA	N/A	0.21
NFκBp52	2.97	3.51
PIK3CD	1.56	1.90
PIK3CG	1.10	N/A
PLCB2	2.63	1.69
PLCL2	1.03	N/A
RELA	N/A	0.33
STAT1	1.01	0.55
STAT2	0.86	0.54
STAT4	2.47	1.72
TLR2	N/A	-0.14
TLR4	N/A	1.61
TNF-α	N/A	-0.14
TNFRSF1A	1.44	1.23
TNFRSF1B	N/A	0.62

Genes in the OX40 Signaling Pathway network

Symbol	Log FC C57BL/6-Bps vs. BALB/c-BPS (3h)	Log FC C57BL/6-Bps vs. BALB/c-BPS (6h)
B2M	0.76	N/A
H2-K2/H2-Q9	N/A	1.88
H2-M2	N/A	0.56
H2-Q8	-1.35	-1.56
H2-T10	4.93	4.97
H2-T24	N/A	-0.32
HLA-A	-3.94	-10.48
HLA-DMA	N/A	-0.87
HLA-DQB1	N/A	6.63
HLA-DRA	-5.16	-5.58
HLA-E	0.54	N/A
JUN	2.03	N/A
MAP2K4	1.30	1.08
NFKB2	2.97	3.51
NFKBIA	N/A	0.21
RELA	N/A	0.33
TRAF2	N/A	0.42

Genes in the Pancreatic Adenocarcinoma Signaling network

Symbol	Log FC C57BL/6-Bps vs. BALB/c-BPS (3h)	Log FC C57BL/6-Bps vs. BALB/c-BPS (6h)
CASP9	N/A	-0.29
CDKN1B	1.87	N/A
CyclinD1	N/A	2.14
E2F2	N/A	0.18
E2F6	N/A	-1.40
HMOX1	N/A	1.05
K-Ras	N/A	-1.60
MAP2K4	1.30	1.08
MDM2	1.19	0.70
MMP9	-1.49	-2.80
NFKB2	2.97	3.51
PIK3CD	1.56	1.90
PIK3CG	1.10	N/A
PLD1	N/A	0.51
RELA	N/A	0.33
SMAD2	2.04	1.85
SMAD3	1.34	N/A
STAT1	1.01	0.55
STAT3	1.76	1.39
SURVIVIN	N/A	-0.83
TGFβR2	N/A	-1.56
TYK2	0.79	N/A
VEGFA	1.54	N/A

Genes in the phagosome maturation network

Symbol	Log FC C57BL/6-Bps vs. BALB/c-BPS (3h)	Log FC C57BL/6-Bps vs. BALB/c-BPS (6h)
ATP6V0A1	N/A	-0.32
ATP6V0B	1.05	0.59
ATP6V0E2	N/A	-2.46
B2M	0.76	N/A
CALR	N/A	-0.47
DCTN4	N/A	0.78
Dync1i2	N/A	0.97
DYNLRB1	0.83	0.44
HLA-A	-3.94	-10.48
HLA-DRA	-5.16	-5.58
LAMP2	0.55	0.81
NAPB	N/A	0.01
PRDX2	N/A	0.61
RAB7B	1.17	4.11
TAP1	1.22	0.72
TUBB2B	-0.55	-2.36
TUBG1	N/A	-1.09
VAMP3	0.90	N/A
VPS33A	-0.43	-0.74
VPS37B	1.24	N/A
VTI1A	N/A	1.34
VTI1B	N/A	2.89
YKT6	0.88	N/A

Genes in the Death Receptor Signaling network

Symbol	Log FC C57BL/6-Bps vs. BALB/c-BPS (3h)	Log FC C57BL/6-Bps vs. BALB/c-BPS (6h)
APAF1	1.26	0.64
BID	0.47	0.77
CASP9	N/A	-0.29
CASP8	N/A	0.88
DAXX	1.17	0.81
DR6	N/A	-0.47
FAS	N/A	5.19
HtrA2	N/A	-0.57
IKBKB	N/A	0.93
IKBKE	N/A	0.85
MAP2K4	1.30	1.08
NFKB2	2.97	3.51
NFKBIA	N/A	0.21
PARP12	N/A	0.68
PARP14	0.96	0.59
PARP2	N/A	0.18
PARP3	N/A	2.00
PARP4	N/A	0.71
PARP8	N/A	3.78
PARP9	N/A	0.72
RELA	N/A	0.33
TANK	N/A	0.56
TNF-R2	N/A	0.62
TNF-α	N/A	-0.14
TNFRSF1A	1.44	1.23
TRAF2	N/A	0.42
ZC3HAV1	N/A	0.35

Genes in the Crosstalk between Dendritic Cells and Natural Killer Cells network

Symbol	Log FC C57BL/6-Bps vs. BALB/c-BPS (3h)	Log FC C57BL/6-Bps vs. BALB/c-BPS (6h)
CD40	N/A	2.84
CD69	N/A	0.61
CD86	1.97	1.40
CSF2RB	N/A	0.65
Fas	N/A	5.19
FSCN1	N/A	-0.99
GM-CSF	N/A	-3.41
HLA-A	-3.94	-10.48
HLA-DRA	-5.16	-5.58
HLA-E	0.54	N/A
IFNB1	N/A	-0.92
IL-15	N/A	0.87
IL12A	N/A	-4.40
IL15RA	1.67	1.10
IL3RA	1.58	1.65
LFA-1	N/A	-1.00
LTB	-2.19	-3.45
MICB	1.07	N/A
Nectin2	N/A	-0.92
NFKB2	2.97	3.51
RELA	N/A	0.33
TLR4	N/A	1.61
TLR7	N/A	0.63
TNF-α	N/A	-0.14
TNFR2	N/A	0.62

Genes in the Role of Macrophages, Fibroblasts and Endothelial Cells in Rheumatoid Arthritis network

Symbol	Log FC C57BL/6-Bps vs. BALB/c-BPS (3h)	Log FC C57BL/6-Bps vs. BALB/c-BPS (6h)
ADAMTS4	N/A	-2.48
ATF4	N/A	4.43
c-Fos	N/A	1.99
c-Jun	2.03	N/A
C5AR	N/A	0.25
CEBPB	N/A	0.69
CREBBP	N/A	0.94
CyclinD1	N/A	2.14
DAMM1	1.66	N/A
DVL	N/A	-1.11
FcγRIIIa	1.69	1.41
FCγR1	N/A	1.24
FN1	N/A	-0.77
FZD7	N/A	1.02
GM-CSF	N/A	-3.41
GNAQ	0.78	N/A
IKBKB	N/A	0.93
IKBKE	N/A	0.85
IL-10	N/A	3.29
IL-15	N/A	0.87
IL-6R	N/A	1.00
IL1A	N/A	-1.29
IL1RN	N/A	1.07
IRAK3	N/A	0.23
KRAS	N/A	-1.60
LTB	-2.19	-3.45
MAP2K3	0.73	0.27
MAP2K4	1.30	1.08
MCP-1	N/A	0.61
MRAS	N/A	-1.70
MYD88	1.16	0.54
NFATC3	N/A	0.67
NFKBIA	N/A	0.21
NLK	N/A	-1.21
OSM	N/A	-0.64
p38 MAPKα	N/A	-0.77
PDGFB	N/A	0.78
PIK3CD	1.56	1.90
PIK3CG	1.10	N/A
PLCB2	2.63	1.69
PLCL2	1.03	N/A
PPP3R1	N/A	-0.37
PRKD3	N/A	-0.94
RANTES	N/A	0.22
RELA	N/A	0.33
RRAS2	N/A	-3.44
RYK	N/A	-3.28
Src	N/A	-0.80
STAT3	1.76	1.39
TCF4	0.85	1.00
TLR2	N/A	-0.14
TLR4	N/A	1.61
TLR6	N/A	-0.53
TLR7	N/A	0.63
TNF	N/A	-0.14
TNFRSF1A	1.44	1.23
TNFRSF1B	N/A	0.62
TRAF1	N/A	0.40
TRAF2	N/A	0.42
VCAM-1	N/A	-1.31
VEGFA	1.54	N/A

Genes in the Role of Pattern Recognition Receptors in Recognition of Bacteria and Viruses network

Symbol	Log FC C57BL/6-Bps vs. BALB/c-BPS (3h)	Log FC C57BL/6-Bps vs. BALB/c-BPS (6h)
C1QB	N/A	3.17
C3	N/A	0.35
C5aR	N/A	0.25
Casp1	N/A	0.48
CSF2	N/A	-3.41
DECTIN-1	N/A	-0.89
DECTIN-2	N/A	0.52
IFNB1	N/A	-0.92
IL-10	N/A	3.29
IL12A	N/A	-4.40
IL1A	N/A	-1.29
IRF-7	N/A	0.65
MAP2K4	1.30	1.08
MYD88	1.16	0.54
NFKB2	2.97	3.51
NOD1	N/A	1.42
NOD2	-1.50	-1.79
OAS1	0.94	0.60
OAS3	1.46	1.01
OSM	N/A	-0.64
PIK3CD	1.56	1.90
PIK3CG	1.10	N/A
PRKD3	N/A	-0.94
PTX3	N/A	4.34
RANTES	N/A	0.22
RELA	N/A	0.33
RIG-1	1.24	N/A
TLR2	N/A	-0.14
TLR4	N/A	1.61
TLR6	N/A	-0.53
TLR7	N/A	0.63
TNF-α	N/A	-0.14

Genes in the Communication between Innate and Adaptive Immune Cells network

Symbol	Log FC C57BL/6-Bps vs. BALB/c-BPS (3h)	Log FC C57BL/6-Bps vs. BALB/c-BPS (6h)
B2M	0.76	N/A
CCL3L3	N/A	0.25
CD40	N/A	2.84
CD86	1.97	1.40
CD8B	-0.76	-1.76
GM-CSF	N/A	-3.41
HLA-A	-3.94	-10.48
HLA-DRA	-5.16	-5.58
HLA-E	0.54	N/A
IFNB1	N/A	-0.92
IL-10	N/A	3.29
IL-15	N/A	0.87
IL12A	N/A	-4.40
IL1A	N/A	-1.29
IL1RN	N/A	1.07
IP-10	N/A	3.64
RANTES	N/A	0.22
TLR2	N/A	-0.14
TLR4	N/A	1.61
TLR6	N/A	-0.53
TLR7	N/A	0.63
TNF-α	N/A	-0.14

Reference List

1. Medzhitov R, Janeway C, Jr. 2000. Innate immunity. *N Engl J Med* 343: 338-44

2. Medzhitov R. 2007. Recognition of microorganisms and activation of the immune response. *Nature* 449: 819-26

3. Fujii S, Liu K, Smith C, Bonito AJ, Steinman RM. 2004. The linkage of innate to adaptive immunity via maturing dendritic cells in vivo requires CD40 ligation in addition to antigen presentation and CD80/86 costimulation. *J Exp Med* 199: 1607-18

4. Steinman RM. 2007. Dendritic cells: understanding immunogenicity. *Eur J Immunol* 37 Suppl 1: S53-60

5. Murphy KM, Ouyang W, Farrar JD, Yang J, Ranganath S, Asnagli H, Afkarian M, Murphy TL. 2000. Signaling and transcription in T helper development. *Annu Rev Immunol* 18: 451-94

6. Flynn JL, Chan J. 2001. Immunology of tuberculosis. *Annu Rev Immunol* 19: 93-129

7. Mosmann TR, Cherwinski H, Bond MW, Giedlin MA, Coffman RL. 1986. Two types of murine helper T cell clone. I. Definition according to profiles of lymphokine activities and secreted proteins. *J Immunol* 136: 2348-57

8. Sher A, Coffman RL. 1992. Regulation of immunity to parasites by T cells and T cell-derived cytokines. *Annu Rev Immunol* 10: 385-409

9. Szabo SJ, Kim ST, Costa GL, Zhang X, Fathman CG, Glimcher LH. 2000. A novel transcription factor, T-bet, directs Th1 lineage commitment. *Cell* 100: 655-69

10. Zheng W, Flavell RA. 1997. The transcription factor GATA-3 is necessary and sufficient for Th2 cytokine gene expression in CD4 T cells. *Cell* 89: 587-96

11. Maizels RM, Hewitson JP, Smith KA. 2012. Susceptibility and immunity to helminth parasites. *Curr Opin Immunol* 24: 459-66

12. Ivanov, II, McKenzie BS, Zhou L, Tadokoro CE, Lepelley A, Lafaille JJ, Cua DJ, Littman DR. 2006. The orphan nuclear receptor RORgammat directs the differentiation program of proinflammatory IL-17+ T helper cells. *Cell* 126: 1121-33

13. O'Quinn DB, Palmer MT, Lee YK, Weaver CT. 2008. Emergence of the Th17 pathway and its role in host defense. *Adv Immunol* 99: 115-63

14. Rudensky AY. 2011. Regulatory T cells and Foxp3. *Immunol Rev* 241: 260-8

15. Bacchetta R, Gambineri E, Roncarolo MG. 2007. Role of regulatory T cells and FOXP3 in human diseases. *J Allergy Clin Immunol* 120: 227-35; quiz 36-7

16. Harty JT, Tvinnereim AR, White DW. 2000. CD8+ T cell effector mechanisms in resistance to infection. *Annu Rev Immunol* 18: 275-308

17. Mauri C, Bosma A. 2012. Immune regulatory function of B cells. *Annu Rev Immunol* 30: 221-41

18. Perdiguero EG, Geissmann F. 2015. The development and maintenance of resident macrophages. *Nat Immunol* 17: 2-8

19. Varol C, Mildner A, Jung S. 2015. Macrophages: development and tissue specialization. *Annu Rev Immunol* 33: 643-75

20. Lavin Y, Merad M. 2013. Macrophages: gatekeepers of tissue integrity. *Cancer Immunol Res* 1: 201-9

21. Ginhoux F, Jung S. 2014. Monocytes and macrophages: developmental pathways and tissue homeostasis. *Nat Rev Immunol* 14: 392-404

22. Epelman S, Lavine Kory J, Randolph Gwendalyn J. 2014. Origin and Functions of Tissue Macrophages. *Immunity* 41: 21-35

23. Gordon S, Taylor PR. 2005. Monocyte and macrophage heterogeneity. *Nat Rev Immunol* 5: 953-64

24. Lavin Y, Winter D, Blecher-Gonen R, David E, Keren-Shaul H, Merad M, Jung S, Amit I. 2014. Tissue-resident macrophage enhancer landscapes are shaped by the local microenvironment. *Cell* 159: 1312-26

25. Mosser DM, Edwards JP. 2008. Exploring the full spectrum of macrophage activation. *Nat Rev Immunol* 8: 958-69

26. Rath M, Muller I, Kropf P, Closs EI, Munder M. 2014. Metabolism via Arginase or Nitric Oxide Synthase: Two Competing Arginine Pathways in Macrophages. *Front Immunol* 5: 532

27. Gordon S, Martinez FO. 2010. Alternative activation of macrophages: mechanism and functions. *Immunity* 32: 593-604

28. Anthony RM, Urban JF, Jr., Alem F, Hamed HA, Rozo CT, Boucher JL, Van Rooijen N, Gause WC. 2006. Memory T(H)2 cells induce alternatively activated macrophages to mediate protection against nematode parasites. *Nat Med* 12: 955-60

29. Wynn TA, Chawla A, Pollard JW. 2013. Macrophage biology in development, homeostasis and disease. *Nature* 496: 445-55

30. Okabe Y, Medzhitov R. 2015. Tissue biology perspective on macrophages. *Nat Immunol* 17: 9-17

31. Akira S, Takeda K. 2004. Toll-like receptor signalling. *Nat Rev Immunol* 4: 499-511

32. Akira S, Uematsu S, Takeuchi O. 2006. Pathogen recognition and innate immunity. *Cell* 124: 783-801

33. Kawasaki T, Kawai T. 2014. Toll-like receptor signaling pathways. *Front Immunol* 5: 461

34. Murray PJ, Wynn TA. 2011. Protective and pathogenic functions of macrophage subsets. *Nat Rev Immunol* 11: 723-37

35. Bogdan C, Vodovotz Y, Nathan C. 1991. Macrophage deactivation by interleukin 10. *J Exp Med* 174: 1549-55

36. McGreal EP, Miller JL, Gordon S. 2005. Ligand recognition by antigen-presenting cell C-type lectin receptors. *Curr Opin Immunol* 17: 18-24

37. Brown GD. 2006. Dectin-1: a signalling non-TLR pattern-recognition receptor. *Nat Rev Immunol* 6: 33-43

38. Rothfuchs AG, Bafica A, Feng CG, Egen JG, Williams DL, Brown GD, Sher A. 2007. Dectin-1 interaction with Mycobacterium tuberculosis leads to enhanced IL-12p40 production by splenic dendritic cells. *J Immunol* 179: 3463-71

39. Reid DM, Gow NA, Brown GD. 2009. Pattern recognition: recent insights from Dectin-1. *Curr Opin Immunol* 21: 30-7

40. LeibundGut-Landmann S, Gross O, Robinson MJ, Osorio F, Slack EC, Tsoni SV, Schweighoffer E, Tybulewicz V, Brown GD, Ruland J, Reis e Sousa C. 2007. Syk- and CARD9-dependent coupling of innate immunity to the induction of T helper cells that produce interleukin 17. *Nat Immunol* 8: 630-8

41. Franchi L, Warner N, Viani K, Nunez G. 2009. Function of Nod-like receptors in microbial recognition and host defense. *Immunol Rev* 227: 106-28

42. Inohara, Chamaillard, McDonald C, Nunez G. 2005. NOD-LRR proteins: role in host-microbial interactions and inflammatory disease. *Annu Rev Biochem* 74: 355-83

43. Chang Foreman HC, Van Scoy S, Cheng TF, Reich NC. 2012. Activation of interferon regulatory factor 5 by site specific phosphorylation. *PLoS One* 7: e33098

44. Sabbah A, Chang TH, Harnack R, Frohlich V, Tominaga K, Dube PH, Xiang Y, Bose S. 2009. Activation of innate immune antiviral responses by Nod2. *Nat Immunol* 10: 1073-80

45. Schroder K, Tschopp J. 2010. The inflammasomes. *Cell* 140: 821-32

46. Guo H, Callaway JB, Ting JP. 2015. Inflammasomes: mechanism of action, role in disease, and therapeutics. *Nat Med* 21: 677-87

47. Pichlmair A, Reis e Sousa C. 2007. Innate recognition of viruses. *Immunity* 27: 370-83

48. Loo YM, Gale M, Jr. 2011. Immune signaling by RIG-I-like receptors. *Immunity* 34: 680-92

49. Hornung V, Latz E. 2010. Intracellular DNA recognition. *Nat Rev Immunol* 10: 123-30

50. Hornung V, Hartmann R, Ablasser A, Hopfner KP. 2014. OAS proteins and cGAS: unifying concepts in sensing and responding to cytosolic nucleic acids. *Nat Rev Immunol* 14: 521-8

51. Thaiss CA, Levy M, Itav S, Elinav E. 2016. Integration of Innate Immune Signaling. *Trends in Immunology*

52. Takeda K, Akira S. 2015. Toll-like receptors. *Curr Protoc Immunol* 109: 14 2 1- 2 0

53. Kumar H, Kawai T, Akira S. 2009. Toll-like receptors and innate immunity. *Biochem Biophys Res Commun* 388: 621-5

54. Wyllie DH, Kiss-Toth E, Visintin A, Smith SC, Boussouf S, Segal DM, Duff GW, Dower SK. 2000. Evidence for an accessory protein function for Toll-like receptor 1 in anti-bacterial responses. *J Immunol* 165: 7125-32

55. Ozinsky A, Underhill DM, Fontenot JD, Hajjar AM, Smith KD, Wilson CB, Schroeder L, Aderem A. 2000. The repertoire for pattern recognition of pathogens by the innate immune system is defined by cooperation between toll-like receptors. *Proc Natl Acad Sci U S A* 97: 13766-71

56. Lord KA, Hoffman-Liebermann B, Liebermann DA. 1990. Nucleotide sequence and expression of a cDNA encoding MyD88, a novel myeloid differentiation primary response gene induced by IL6. *Oncogene* 5: 1095-7

57. Muzio M, Ni J, Feng P, Dixit VM. 1997. IRAK (Pelle) family member IRAK-2 and MyD88 as proximal mediators of IL-1 signaling. *Science* 278: 1612-5

58. Wesche H, Henzel WJ, Shillinglaw W, Li S, Cao Z. 1997. MyD88: an adapter that recruits IRAK to the IL-1 receptor complex. *Immunity* 7: 837-47

59. Kawai T, Adachi O, Ogawa T, Takeda K, Akira S. 1999. Unresponsiveness of MyD88-deficient mice to endotoxin. *Immunity* 11: 115-22

60. Kawai T, Akira S. 2010. The role of pattern-recognition receptors in innate immunity: update on Toll-like receptors. *Nat Immunol* 11: 373-84

61. Ikushima H, Negishi H, Taniguchi T. 2013. The IRF family transcription factors at the interface of innate and adaptive immune responses. *Cold Spring Harb Symp Quant Biol* 78: 105-16

62. Kawagoe T, Sato S, Matsushita K, Kato H, Matsui K, Kumagai Y, Saitoh T, Kawai T, Takeuchi O, Akira S. 2008. Sequential control of Toll-like receptor-dependent responses by IRAK1 and IRAK2. *Nat Immunol* 9: 684-91

63. Jimenez-Dalmaroni MJ, Gerswhin ME, Adamopoulos IE. 2016. The critical role of toll-like receptors--From microbial recognition to autoimmunity: A comprehensive review. *Autoimmun Rev* 15: 1-8

64. Sun J, Li N, Oh KS, Dutta B, Vayttaden SJ, Lin B, Ebert TS, De Nardo D, Davis J, Bagirzadeh R, Lounsbury NW, Pasare C, Latz E, Hornung V, Fraser ID. 2016.

Comprehensive RNAi-based screening of human and mouse TLR pathways identifies species-specific preferences in signaling protein use. *Sci Signal* 9: ra3

65. Arthur JSC, Ley SC. 2013. Mitogen-activated protein kinases in innate immunity. *Nat Rev Immunol* 13: 679-92

66. Bhoj VG, Chen ZJ. 2009. Ubiquitylation in innate and adaptive immunity. *Nature* 458: 430-7

67. Hayden MS, Ghosh S. 2008. Shared principles in NF-kappaB signaling. *Cell* 132: 344-62

68. Gantke T, Sriskantharajah S, Ley SC. 2011. Regulation and function of TPL-2, an IkappaB kinase-regulated MAP kinase kinase kinase. *Cell Res* 21: 131-45

69. Dumitru CD, Ceci JD, Tsatsanis C, Kontoyiannis D, Stamatakis K, Lin JH, Patriotis C, Jenkins NA, Copeland NG, Kollias G, Tsichlis PN. 2000. TNF-alpha induction by LPS is regulated posttranscriptionally via a Tpl2/ERK-dependent pathway. *Cell* 103: 1071-83

70. Banerjee A, Gugasyan R, McMahon M, Gerondakis S. 2006. Diverse Toll-like receptors utilize Tpl2 to activate extracellular signal-regulated kinase (ERK) in hemopoietic cells. *Proc Natl Acad Sci U S A* 103: 3274-9

71. Kaiser F, Cook D, Papoutsopoulou S, Rajsbaum R, Wu X, Yang HT, Grant S, Ricciardi-Castagnoli P, Tsichlis PN, Ley SC, O'Garra A. 2009. TPL-2 negatively regulates interferon-beta production in macrophages and myeloid dendritic cells. *J Exp Med* 206: 1863-71

72. McNab FW, Ewbank J, Rajsbaum R, Stavropoulos E, Martirosyan A, Redford PS, Wu X, Graham CM, Saraiva M, Tsichlis P, Chaussabel D, Ley SC, O'Garra A. 2013. TPL-2-ERK1/2 signaling promotes host resistance against intracellular bacterial infection by negative regulation of type I IFN production. *J Immunol* 191: 1732-43

73. Bouhamdan M, Bauerfeld C, Talreja J, Beuret L, Charron J, Samavati L. 2015. MEK1 dependent and independent ERK activation regulates IL-10 and IL-12 production in bone marrow derived macrophages. *Cell Signal*

74. Karin M, Liu Z, Zandi E. 1997. AP-1 function and regulation. *Curr Opin Cell Biol* 9: 240-6

75. Takaoka A, Yanai H, Kondo S, Duncan G, Negishi H, Mizutani T, Kano S, Honda K, Ohba Y, Mak TW, Taniguchi T. 2005. Integral role of IRF-5 in the gene induction programme activated by Toll-like receptors. *Nature* 434: 243-9

76. Negishi H, Ohba Y, Yanai H, Takaoka A, Honma K, Yui K, Matsuyama T, Taniguchi T, Honda K. 2005. Negative regulation of Toll-like-receptor signaling by IRF-4. *Proceedings of the National Academy of Sciences of the United States of America* 102: 15989-94

77. Honma K, Udono H, Kohno T, Yamamoto K, Ogawa A, Takemori T, Kumatori A, Suzuki S, Matsuyama T, Yui K. 2005. Interferon regulatory factor 4 negatively regulates the production of proinflammatory cytokines by macrophages in response to LPS. *Proceedings of the National Academy of Sciences of the United States of America* 102: 16001-6

78. Negishi H, Fujita Y, Yanai H, Sakaguchi S, Ouyang X, Shinohara M, Takayanagi H, Ohba Y, Taniguchi T, Honda K. 2006. Evidence for licensing of IFN-gamma-induced IFN regulatory factor 1 transcription factor by MyD88 in Toll-like receptor-dependent gene induction program. *Proc Natl Acad Sci U S A* 103: 15136-41

79. Liu J, Cao S, Herman LM, Ma X. 2003. Differential regulation of interleukin (IL)-12 p35 and p40 gene expression and interferon (IFN)-gamma-primed IL-12 production by IFN regulatory factor 1. *J Exp Med* 198: 1265-76

80. Zhao J, Kong HJ, Li H, Huang B, Yang M, Zhu C, Bogunovic M, Zheng F, Mayer L, Ozato K, Unkeless J, Xiong H. 2006. IRF-8/interferon (IFN) consensus sequence-binding protein is involved in Toll-like receptor (TLR) signaling and contributes to the cross-talk between TLR and IFN-gamma signaling pathways. *J Biol Chem* 281: 10073-80

81. Yamamoto M, Sato S, Hemmi H, Sanjo H, Uematsu S, Kaisho T, Hoshino K, Takeuchi O, Kobayashi M, Fujita T, Takeda K, Akira S. 2002. Essential role for TIRAP in activation of the signalling cascade shared by TLR2 and TLR4. *Nature* 420: 324-9

82. Yamamoto M, Sato S, Hemmi H, Hoshino K, Kaisho T, Sanjo H, Takeuchi O, Sugiyama M, Okabe M, Takeda K, Akira S. 2003. Role of adaptor TRIF in the MyD88-independent toll-like receptor signaling pathway. *Science* 301: 640-3

83. Fitzgerald KA, McWhirter SM, Faia KL, Rowe DC, Latz E, Golenbock DT, Coyle AJ, Liao SM, Maniatis T. 2003. IKKepsilon and TBK1 are essential components of the IRF3 signaling pathway. *Nat Immunol* 4: 491-6

84. Hacker H, Redecke V, Blagoev B, Kratchmarova I, Hsu LC, Wang GG, Kamps MP, Raz E, Wagner H, Hacker G, Mann M, Karin M. 2006. Specificity in Toll-like receptor signalling through distinct effector functions of TRAF3 and TRAF6. *Nature* 439: 204-7

85. Oganesyan G, Saha SK, Guo B, He JQ, Shahangian A, Zarnegar B, Perry A, Cheng G. 2006. Critical role of TRAF3 in the Toll-like receptor-dependent and -independent antiviral response. *Nature* 439: 208-11

86. Sharma S, tenOever BR, Grandvaux N, Zhou GP, Lin R, Hiscott J. 2003. Triggering the interferon antiviral response through an IKK-related pathway. *Science* 300: 1148-51

87. Doyle S, Vaidya S, O'Connell R, Dadgostar H, Dempsey P, Wu T, Rao G, Sun R, Haberland M, Modlin R, Cheng G. 2002. IRF3 mediates a TLR3/TLR4-specific antiviral gene program. *Immunity* 17: 251-63

88. Yamamoto M, Sato S, Hemmi H, Uematsu S, Hoshino K, Kaisho T, Takeuchi O, Takeda K, Akira S. 2003. TRAM is specifically involved in the Toll-like receptor 4-mediated MyD88-independent signaling pathway. *Nat Immunol* 4: 1144-50

89. Tseng PH, Matsuzawa A, Zhang W, Mino T, Vignali DA, Karin M. 2010. Different modes of ubiquitination of the adaptor TRAF3 selectively activate the expression of type I interferons and proinflammatory cytokines. *Nat Immunol* 11: 70-5

90. Sato S, Sugiyama M, Yamamoto M, Watanabe Y, Kawai T, Takeda K, Akira S. 2003. Toll/IL-1 receptor domain-containing adaptor inducing IFN-beta (TRIF) associates with TNF receptor-associated factor 6 and TANK-binding kinase 1, and activates two distinct transcription factors, NF-kappa B and IFN-regulatory factor-3, in the Toll-like receptor signaling. *J Immunol* 171: 4304-10

91. Schmitz F, Heit A, Dreher S, Eisenacher K, Mages J, Haas T, Krug A, Janssen KP, Kirschning CJ, Wagner H. 2008. Mammalian target of rapamycin (mTOR) orchestrates the defense program of innate immune cells. *Eur J Immunol* 38: 2981-92

92. Weichhart T, Saemann MD. 2009. The multiple facets of mTOR in immunity. *Trends Immunol* 30: 218-26

93. Weichhart T, Costantino G, Poglitsch M, Rosner M, Zeyda M, Stuhlmeier KM, Kolbe T, Stulnig TM, Horl WH, Hengstschlager M, Muller M, Saemann MD. 2008. The TSC-mTOR signaling pathway regulates the innate inflammatory response. *Immunity* 29: 565-77

94. Ohtani M, Nagai S, Kondo S, Mizuno S, Nakamura K, Tanabe M, Takeuchi T, Matsuda S, Koyasu S. 2008. Mammalian target of rapamycin and glycogen synthase kinase 3 differentially regulate lipopolysaccharide-induced interleukin-12 production in dendritic cells. *Blood* 112: 635-43

95. Wall AA, Luo L, Hung Y, Tong SJ, Condon ND, Blumenthal A, Sweet MJ, Stow JL. 2017. Small GTPase Rab8a-recruited Phosphatidylinositol 3-Kinase gamma Regulates Signaling and Cytokine Outputs from Endosomal Toll-like Receptors. *J Biol Chem* 292: 4411-22

96. Medzhitov R, Preston-Hurlburt P, Janeway CA, Jr. 1997. A human homologue of the Drosophila Toll protein signals activation of adaptive immunity. *Nature* 388: 394-7

97. Luo L, Bokil NJ, Wall AA, Kapetanovic R, Lansdaal NM, Marceline F, Burgess BJ, Tong SJ, Guo Z, Alexandrov K, Ross IL, Hibbs ML, Stow JL, Sweet MJ. 2017. SCIMP is a transmembrane non-TIR TLR adaptor that promotes proinflammatory cytokine production from macrophages. *Nat Commun* 8: 14133

98. Hoshino K, Takeuchi O, Kawai T, Sanjo H, Ogawa T, Takeda Y, Takeda K, Akira S. 1999. Cutting edge: Toll-like receptor 4 (TLR4)-deficient mice are hyporesponsive to lipopolysaccharide: evidence for TLR4 as the Lps gene product. *J Immunol* 162: 3749-52

99. Poltorak A, He X, Smirnova I, Liu MY, Van Huffel C, Du X, Birdwell D, Alejos E, Silva M, Galanos C, Freudenberg M, Ricciardi-Castagnoli P, Layton B, Beutler B. 1998. Defective LPS signaling in C3H/HeJ and C57BL/10ScCr mice: mutations in Tlr4 gene. *Science* 282: 2085-8

100. Nagai Y, Akashi S, Nagafuku M, Ogata M, Iwakura Y, Akira S, Kitamura T, Kosugi A, Kimoto M, Miyake K. 2002. Essential role of MD-2 in LPS responsiveness and TLR4 distribution. *Nat Immunol* 3: 667-72

101. da Silva Correia J, Soldau K, Christen U, Tobias PS, Ulevitch RJ. 2001. Lipopolysaccharide is in close proximity to each of the proteins in its membrane receptor complex. transfer from CD14 to TLR4 and MD-2. *J Biol Chem* 276: 21129-35

102. Jiang Q, Akashi S, Miyake K, Petty HR. 2000. Lipopolysaccharide induces physical proximity between CD14 and toll-like receptor 4 (TLR4) prior to nuclear translocation of NF-kappa B. *J Immunol* 165: 3541-4

103. Kagan JC, Su T, Horng T, Chow A, Akira S, Medzhitov R. 2008. TRAM couples endocytosis of Toll-like receptor 4 to the induction of interferon-beta. *Nat Immunol* 9: 361-8

104. Zanoni I, Ostuni R, Marek LR, Barresi S, Barbalat R, Barton GM, Granucci F, Kagan JC. 2011. CD14 controls the LPS-induced endocytosis of Toll-like receptor 4. *Cell* 147: 868-80

105. Lin YC, Huang DY, Chu CL, Lin YL, Lin WW. 2013. The tyrosine kinase Syk differentially regulates Toll-like receptor signaling downstream of the adaptor molecules TRAF6 and TRAF3. *Sci Signal* 6: ra71

106. Roy S, Karmakar M, Pearlman E. 2014. CD14 mediates Toll-like receptor 4 (TLR4) endocytosis and spleen tyrosine kinase (Syk) and interferon regulatory transcription factor 3 (IRF3) activation in epithelial cells and impairs neutrophil infiltration and Pseudomonas aeruginosa killing in vivo. *J Biol Chem* 289: 1174-82

107. Chiang CY, Veckman V, Limmer K, David M. 2012. Phospholipase Cgamma-2 and intracellular calcium are required for lipopolysaccharide-induced Toll-like receptor 4 (TLR4) endocytosis and interferon regulatory factor 3 (IRF3) activation. *J Biol Chem* 287: 3704-9

108. Husebye H, Aune MH, Stenvik J, Samstad E, Skjeldal F, Halaas O, Nilsen NJ, Stenmark H, Latz E, Lien E, Mollnes TE, Bakke O, Espevik T. 2010. The Rab11a GTPase controls Toll-like receptor 4-induced activation of interferon regulatory factor-3 on phagosomes. *Immunity* 33: 583-96

109. Van Acker T, Eyckerman S, Vande Walle L, Gerlo S, Goethals M, Lamkanfi M, Bovijn C, Tavernier J, Peelman F. 2014. The small GTPase Arf6 is essential for the Tram/Trif pathway in TLR4 signaling. *J Biol Chem* 289: 1364-76

110. Rajaiah R, Perkins DJ, Ireland DD, Vogel SN. 2015. CD14 dependence of TLR4 endocytosis and TRIF signaling displays ligand specificity and is dissociable in endotoxin tolerance. *Proc Natl Acad Sci U S A* 112: 8391-6

111. Voss OH, Murakami Y, Pena MY, Lee HN, Tian L, Margulies DH, Street JM, Yuen PS, Qi CF, Krzewski K, Coligan JE. 2016. Lipopolysaccharide-Induced CD300b Receptor Binding to Toll-like Receptor 4 Alters Signaling to Drive Cytokine Responses that Enhance Septic Shock. *Immunity* 44: 1365-78

112. Kobayashi M, Fitz L, Ryan M, Hewick RM, Clark SC, Chan S, Loudon R, Sherman F, Perussia B, Trinchieri G. 1989. Identification and purification of

natural killer cell stimulatory factor (NKSF), a cytokine with multiple biologic effects on human lymphocytes. *J Exp Med* 170: 827-45

113. Stern AS, Podlaski FJ, Hulmes JD, Pan YC, Quinn PM, Wolitzky AG, Familletti PC, Stremlo DL, Truitt T, Chizzonite R, et al. 1990. Purification to homogeneity and partial characterization of cytotoxic lymphocyte maturation factor from human B-lymphoblastoid cells. *Proc Natl Acad Sci U S A* 87: 6808-12

114. Gubler U, Chua AO, Schoenhaut DS, Dwyer CM, McComas W, Motyka R, Nabavi N, Wolitzky AG, Quinn PM, Familletti PC, et al. 1991. Coexpression of two distinct genes is required to generate secreted bioactive cytotoxic lymphocyte maturation factor. *Proc Natl Acad Sci U S A* 88: 4143-7

115. D'Andrea A, Rengaraju M, Valiante NM, Chehimi J, Kubin M, Aste M, Chan SH, Kobayashi M, Young D, Nickbarg E, et al. 1992. Production of natural killer cell stimulatory factor (interleukin 12) by peripheral blood mononuclear cells. *J Exp Med* 176: 1387-98

116. Macatonia SE, Hosken NA, Litton M, Vieira P, Hsieh CS, Culpepper JA, Wysocka M, Trinchieri G, Murphy KM, O'Garra A. 1995. Dendritic cells produce IL-12 and direct the development of Th1 cells from naive CD4+ T cells. *J Immunol* 154: 5071-9

117. Zundler S, Neurath MF. 2015. Interleukin-12: Functional activities and implications for disease. *Cytokine Growth Factor Rev* 26: 559-68

118. Babik JM, Adams E, Tone Y, Fairchild PJ, Tone M, Waldmann H. 1999. Expression of murine IL-12 is regulated by translational control of the p35 subunit. *J Immunol* 162: 4069-78

119. Goriely S, Molle C, Nguyen M, Albarani V, Haddou NO, Lin R, De Wit D, Flamand V, Willems F, Goldman M. 2006. Interferon regulatory factor 3 is involved in Toll-like receptor 4 (TLR4)- and TLR3-induced IL-12p35 gene activation. *Blood* 107: 1078-84

120. Liu J, Guan X, Tamura T, Ozato K, Ma X. 2004. Synergistic activation of interleukin-12 p35 gene transcription by interferon regulatory factor-1 and interferon consensus sequence-binding protein. *J Biol Chem* 279: 55609-17

121. Zhu C, Rao K, Xiong H, Gagnidze K, Li F, Horvath C, Plevy S. 2003. Activation of the murine interleukin-12 p40 promoter by functional interactions between NFAT and ICSBP. *J Biol Chem* 278: 39372-82

122. Murphy TL, Cleveland MG, Kulesza P, Magram J, Murphy KM. 1995. Regulation of interleukin 12 p40 expression through an NF-kappa B half-site. *Mol Cell Biol* 15: 5258-67

123. Ma X, Neurath M, Gri G, Trinchieri G. 1997. Identification and characterization of a novel Ets-2-related nuclear complex implicated in the activation of the human interleukin-12 p40 gene promoter. *J Biol Chem* 272: 10389-95

124. Becker C, Wirtz S, Ma X, Blessing M, Galle PR, Neurath MF. 2001. Regulation of IL-12 p40 promoter activity in primary human monocytes: roles of NF-kappaB, CCAAT/enhancer-binding protein beta, and PU.1 and identification of a novel repressor element (GA-12) that responds to IL-4 and prostaglandin E(2). *J Immunol* 167: 2608-18

125. Kobayashi T, Matsuoka K, Sheikh SZ, Elloumi HZ, Kamada N, Hisamatsu T, Hansen JJ, Doty KR, Pope SD, Smale ST, Hibi T, Rothman PB, Kashiwada M, Plevy SE. 2011. NFIL3 is a regulator of IL-12 p40 in macrophages and mucosal immunity. *J Immunol* 186: 4649-55

126. Re F, Strominger JL. 2001. Toll-like receptor 2 (TLR2) and TLR4 differentially activate human dendritic cells. *J Biol Chem* 276: 37692-9

127. Bekeredjian-Ding I, Roth SI, Gilles S, Giese T, Ablasser A, Hornung V, Endres S, Hartmann G. 2006. T cell-independent, TLR-induced IL-12p70 production in primary human monocytes. *J Immunol* 176: 7438-46

128. Ma X, Chow JM, Gri G, Carra G, Gerosa F, Wolf SF, Dzialo R, Trinchieri G. 1996. The interleukin 12 p40 gene promoter is primed by interferon gamma in monocytic cells. *J Exp Med* 183: 147-57

129. Stuber E, Strober W, Neurath M. 1996. Blocking the CD40L-CD40 interaction in vivo specifically prevents the priming of T helper 1 cells through the inhibition of interleukin 12 secretion. *J Exp Med* 183: 693-8

130. Cella M, Scheidegger D, Palmer-Lehmann K, Lane P, Lanzavecchia A, Alber G. 1996. Ligation of CD40 on dendritic cells triggers production of high levels of interleukin-12 and enhances T cell stimulatory capacity: T-T help via APC activation. *J Exp Med* 184: 747-52

131. Goriely S, Neurath MF, Goldman M. 2008. How microorganisms tip the balance between interleukin-12 family members. *Nat Rev Immunol* 8: 81-6

132. Vignali DA, Kuchroo VK. 2012. IL-12 family cytokines: immunological playmakers. *Nat Immunol* 13: 722-8

133. Oppmann B, Lesley R, Blom B, Timans JC, Xu Y, Hunte B, Vega F, Yu N, Wang J, Singh K, Zonin F, Vaisberg E, Churakova T, Liu M, Gorman D, Wagner J, Zurawski S, Liu Y, Abrams JS, Moore KW, Rennick D, de Waal-Malefyt R, Hannum C, Bazan JF, Kastelein RA. 2000. Novel p19 protein engages IL-12p40 to form a cytokine, IL-23, with biological activities similar as well as distinct from IL-12. *Immunity* 13: 715-25

134. Niedbala W, Wei XQ, Cai B, Hueber AJ, Leung BP, McInnes IB, Liew FY. 2007. IL-35 is a novel cytokine with therapeutic effects against collagen-induced arthritis through the expansion of regulatory T cells and suppression of Th17 cells. *Eur J Immunol* 37: 3021-9

135. Collison LW, Workman CJ, Kuo TT, Boyd K, Wang Y, Vignali KM, Cross R, Sehy D, Blumberg RS, Vignali DA. 2007. The inhibitory cytokine IL-35 contributes to regulatory T-cell function. *Nature* 450: 566-9

136. Pflanz S, Timans JC, Cheung J, Rosales R, Kanzler H, Gilbert J, Hibbert L, Churakova T, Travis M, Vaisberg E, Blumenschein WM, Mattson JD, Wagner JL, To W, Zurawski S, McClanahan TK, Gorman DM, Bazan JF, de Waal Malefyt R, Rennick D, Kastelein RA. 2002. IL-27, a heterodimeric cytokine composed of EBI3 and p28 protein, induces proliferation of naive CD4+ T cells. *Immunity* 16: 779-90

137. Desai BB, Quinn PM, Wolitzky AG, Mongini PK, Chizzonite R, Gately MK. 1992. IL-12 receptor. II. Distribution and regulation of receptor expression. *J Immunol* 148: 3125-32

138. Presky DH, Yang H, Minetti LJ, Chua AO, Nabavi N, Wu CY, Gately MK, Gubler U. 1996. A functional interleukin 12 receptor complex is composed of two beta-type cytokine receptor subunits. *Proc Natl Acad Sci U S A* 93: 14002-7

139. Bacon CM, McVicar DW, Ortaldo JR, Rees RC, O'Shea JJ, Johnston JA. 1995. Interleukin 12 (IL-12) induces tyrosine phosphorylation of JAK2 and TYK2: differential use of Janus family tyrosine kinases by IL-2 and IL-12. *J Exp Med* 181: 399-404

140. Bacon CM, Petricoin EF, 3rd, Ortaldo JR, Rees RC, Larner AC, Johnston JA, O'Shea JJ. 1995. Interleukin 12 induces tyrosine phosphorylation and activation of STAT4 in human lymphocytes. *Proc Natl Acad Sci U S A* 92: 7307-11

141. Jacobson NG, Szabo SJ, Weber-Nordt RM, Zhong Z, Schreiber RD, Darnell JE, Jr., Murphy KM. 1995. Interleukin 12 signaling in T helper type 1 (Th1) cells involves tyrosine phosphorylation of signal transducer and activator of transcription (Stat)3 and Stat4. *J Exp Med* 181: 1755-62

142. Xu X, Sun YL, Hoey T. 1996. Cooperative DNA binding and sequence-selective recognition conferred by the STAT amino-terminal domain. *Science* 273: 794-7

143. Thierfelder WE, van Deursen JM, Yamamoto K, Tripp RA, Sarawar SR, Carson RT, Sangster MY, Vignali DA, Doherty PC, Grosveld GC, Ihle JN. 1996. Requirement for Stat4 in interleukin-12-mediated responses of natural killer and T cells. *Nature* 382: 171-4

144. Kaplan MH, Sun YL, Hoey T, Grusby MJ. 1996. Impaired IL-12 responses and enhanced development of Th2 cells in Stat4-deficient mice. *Nature* 382: 174-7

145. Hsieh CS, Macatonia SE, Tripp CS, Wolf SF, O'Garra A, Murphy KM. 1993. Development of TH1 CD4+ T cells through IL-12 produced by Listeria-induced macrophages. *Science* 260: 547-9

146. Manetti R, Parronchi P, Giudizi MG, Piccinni MP, Maggi E, Trinchieri G, Romagnani S. 1993. Natural killer cell stimulatory factor (interleukin 12 [IL-12]) induces T helper type 1 (Th1)-specific immune responses and inhibits the development of IL-4-producing Th cells. *J Exp Med* 177: 1199-204

147. Trinchieri G. 2003. Interleukin-12 and the regulation of innate resistance and adaptive immunity. *Nat Rev Immunol* 3: 133-46

148. Chan SH, Perussia B, Gupta JW, Kobayashi M, Pospisil M, Young HA, Wolf SF, Young D, Clark SC, Trinchieri G. 1991. Induction of interferon gamma production by natural killer cell stimulatory factor: characterization of the responder cells and synergy with other inducers. *J Exp Med* 173: 869-79

149. Varesio L, Blasi E, Thurman GB, Talmadge JE, Wiltrout RH, Herberman RB. 1984. Potent activation of mouse macrophages by recombinant interferon-gamma. *Cancer Res* 44: 4465-9

150. Becker C, Wirtz S, Neurath MF. 2005. Stepwise regulation of TH1 responses in autoimmunity: IL-12-related cytokines and their receptors. *Inflamm Bowel Dis* 11: 755-64

151. Yap G, Pesin M, Sher A. 2000. Cutting edge: IL-12 is required for the maintenance of IFN-gamma production in T cells mediating chronic resistance to the intracellular pathogen, Toxoplasma gondii. *J Immunol* 165: 628-31

152. Gazzinelli RT, Wysocka M, Hayashi S, Denkers EY, Hieny S, Caspar P, Trinchieri G, Sher A. 1994. Parasite-induced IL-12 stimulates early IFN-gamma synthesis and resistance during acute infection with Toxoplasma gondii. *J Immunol* 153: 2533-43

153. Tripp CS, Gately MK, Hakimi J, Ling P, Unanue ER. 1994. Neutralization of IL-12 decreases resistance to Listeria in SCID and C.B-17 mice. Reversal by IFN-gamma. *J Immunol* 152: 1883-7

154. Cooper AM, Magram J, Ferrante J, Orme IM. 1997. Interleukin 12 (IL-12) is crucial to the development of protective immunity in mice intravenously infected with mycobacterium tuberculosis. *J Exp Med* 186: 39-45

155. O'Garra A, Redford PS, McNab FW, Bloom CI, Wilkinson RJ, Berry MP. 2013. The immune response in tuberculosis. *Annu Rev Immunol* 31: 475-527

156. Monteiro JM, Harvey C, Trinchieri G. 1998. Role of interleukin-12 in primary influenza virus infection. *J Virol* 72: 4825-31

157. Cousens LP, Peterson R, Hsu S, Dorner A, Altman JD, Ahmed R, Biron CA. 1999. Two roads diverged: interferon alpha/beta- and interleukin 12-mediated pathways in promoting T cell interferon gamma responses during viral infection. *J Exp Med* 189: 1315-28

158. Davidson NJ, Hudak SA, Lesley RE, Menon S, Leach MW, Rennick DM. 1998. IL-12, but not IFN-gamma, plays a major role in sustaining the chronic phase of colitis in IL-10-deficient mice. *J Immunol* 161: 3143-9

159. Teng MW, Bowman EP, McElwee JJ, Smyth MJ, Casanova JL, Cooper AM, Cua DJ. 2015. IL-12 and IL-23 cytokines: from discovery to targeted therapies for immune-mediated inflammatory diseases. *Nat Med* 21: 719-29

160. Moore KW, de Waal Malefyt R, Coffman RL, O'Garra A. 2001. Interleukin-10 and the interleukin-10 receptor. *Annu Rev Immunol* 19: 683-765

161. Fiorentino DF, Bond MW, Mosmann TR. 1989. Two types of mouse T helper cell. IV. Th2 clones secrete a factor that inhibits cytokine production by Th1 clones. *J Exp Med* 170: 2081-95

162. Fiorentino DF, Zlotnik A, Mosmann TR, Howard M, O'Garra A. 1991. IL-10 inhibits cytokine production by activated macrophages. *J Immunol* 147: 3815-22

163. Fiorentino DF, Zlotnik A, Vieira P, Mosmann TR, Howard M, Moore KW, O'Garra A. 1991. IL-10 acts on the antigen-presenting cell to inhibit cytokine production by Th1 cells. *J Immunol* 146: 3444-51

164. Macatonia SE, Doherty TM, Knight SC, O'Garra A. 1993. Differential effect of IL-10 on dendritic cell-induced T cell proliferation and IFN-gamma production. *J Immunol* 150: 3755-65

165. Saraiva M, O'Garra A. 2010. The regulation of IL-10 production by immune cells. *Nat Rev Immunol* 10: 170-81

166. Ouyang W, Rutz S, Crellin NK, Valdez PA, Hymowitz SG. 2011. Regulation and functions of the IL-10 family of cytokines in inflammation and disease. *Annu Rev Immunol* 29: 71-109

167. Boonstra A, Rajsbaum R, Holman M, Marques R, Asselin-Paturel C, Pereira JP, Bates EE, Akira S, Vieira P, Liu YJ, Trinchieri G, O'Garra A. 2006. Macrophages and myeloid dendritic cells, but not plasmacytoid dendritic cells, produce IL-10 in response to MyD88- and TRIF-dependent TLR signals, and TLR-independent signals. *J Immunol* 177: 7551-8

168. Ito T, Kanzler H, Duramad O, Cao W, Liu YJ. 2006. Specialization, kinetics, and repertoire of type 1 interferon responses by human plasmacytoid predendritic cells. *Blood* 107: 2423-31

169. O'Garra A, Vieira P. 2007. T(H)1 cells control themselves by producing interleukin-10. *Nat Rev Immunol* 7: 425-8

170. Saxena A, Khosraviani S, Noel S, Mohan D, Donner T, Hamad AR. 2015. Interleukin-10 paradox: A potent immunoregulatory cytokine that has been difficult to harness for immunotherapy. *Cytokine* 74: 27-34

171. Mittal SK, Roche PA. 2015. Suppression of antigen presentation by IL-10. *Current Opinion in Immunology* 34: 22-7

172. Murray PJ. 2006. Understanding and exploiting the endogenous interleukin-10/STAT3-mediated anti-inflammatory response. *Curr Opin Pharmacol* 6: 379-86

173. Liu Y, Wei SH, Ho AS, de Waal Malefyt R, Moore KW. 1994. Expression cloning and characterization of a human IL-10 receptor. *J Immunol* 152: 1821-9

174. Kotenko SV, Krause CD, Izotova LS, Pollack BP, Wu W, Pestka S. 1997. Identification and functional characterization of a second chain of the interleukin-10 receptor complex. *EMBO J* 16: 5894-903

175. Tan JC, Braun S, Rong H, DiGiacomo R, Dolphin E, Baldwin S, Narula SK, Zavodny PJ, Chou CC. 1995. Characterization of recombinant extracellular domain of human interleukin-10 receptor. *J Biol Chem* 270: 12906-11

176. Yoon SI, Logsdon NJ, Sheikh F, Donnelly RP, Walter MR. 2006. Conformational changes mediate interleukin-10 receptor 2 (IL-10R2) binding to IL-10 and assembly of the signaling complex. *J Biol Chem* 281: 35088-96

177. Wang Y, Li T, Wu B, Liu H, Luo J, Feng D, Shi Y. 2014. STAT1 regulates MD-2 expression in monocytes of sepsis via miR-30a. *Inflammation* 37: 1903-11

178. Takeda K, Clausen BE, Kaisho T, Tsujimura T, Terada N, Forster I, Akira S. 1999. Enhanced Th1 activity and development of chronic enterocolitis in mice devoid of Stat3 in macrophages and neutrophils. *Immunity* 10: 39-49

179. Lang R, Patel D, Morris JJ, Rutschman RL, Murray PJ. 2002. Shaping gene expression in activated and resting primary macrophages by IL-10. *J Immunol* 169: 2253-63

180. Antoniv TT, Ivashkiv LB. 2011. Interleukin-10-induced gene expression and suppressive function are selectively modulated by the PI3K-Akt-GSK3 pathway. *Immunology* 132: 567-77

181. Murray PJ. 2005. The primary mechanism of the IL-10-regulated antiinflammatory response is to selectively inhibit transcription. *Proc Natl Acad Sci U S A* 102: 8686-91

182. Denys A, Udalova IA, Smith C, Williams LM, Ciesielski CJ, Campbell J, Andrews C, Kwaitkowski D, Foxwell BM. 2002. Evidence for a dual mechanism for IL-10 suppression of TNF-alpha production that does not involve inhibition of p38 mitogen-activated protein kinase or NF-kappa B in primary human macrophages. *J Immunol* 168: 4837-45

183. Smallie T, Ricchetti G, Horwood NJ, Feldmann M, Clark AR, Williams LM. 2010. IL-10 inhibits transcription elongation of the human TNF gene in primary macrophages. *J Exp Med* 207: 2081-8

184. Smith AM, Qualls JE, O'Brien K, Balouzian L, Johnson PF, Schultz-Cherry S, Smale ST, Murray PJ. 2011. A distal enhancer in Il12b is the target of transcriptional repression by the STAT3 pathway and requires the basic leucine zipper (B-ZIP) protein NFIL3. *J Biol Chem* 286: 23582-90

185. Aste-Amezaga M, Ma X, Sartori A, Trinchieri G. 1998. Molecular mechanisms of the induction of IL-12 and its inhibition by IL-10. *J Immunol* 160: 5936-44

186. Kobayashi T, Matsuoka K, Sheikh SZ, Russo SM, Mishima Y, Collins C, deZoeten EF, Karp CL, Ting JP, Sartor RB, Plevy SE. 2012. IL-10 regulates Il12b expression via histone deacetylation: implications for intestinal macrophage homeostasis. *J Immunol* 189: 1792-9

187. El Kasmi KC, Smith AM, Williams L, Neale G, Panopoulos AD, Watowich SS, Hacker H, Foxwell BM, Murray PJ. 2007. Cutting edge: A transcriptional repressor and corepressor induced by the STAT3-regulated anti-inflammatory signaling pathway. *J Immunol* 179: 7215-9

188. Hutchins AP, Poulain S, Miranda-Saavedra D. 2012. Genome-wide analysis of STAT3 binding in vivo predicts effectors of the anti-inflammatory response in macrophages. *Blood* 119: e110-9

189. Rossato M, Curtale G, Tamassia N, Castellucci M, Mori L, Gasperini S, Mariotti B, De Luca M, Mirolo M, Cassatella MA, Locati M, Bazzoni F. 2012. IL-10-induced microRNA-187 negatively regulates TNF-alpha, IL-6, and IL-12p40 production in TLR4-stimulated monocytes. *Proc Natl Acad Sci U S A* 109: E3101-10

190. Ip WKE, Hoshi N, Shouval DS, Snapper S, Medzhitov R. 2017. Anti-inflammatory effect of IL-10 mediated by metabolic reprogramming of macrophages. *Science* 356: 513-9

191. Huber S, Gagliani N, Esplugues E, O'Connor W, Jr., Huber FJ, Chaudhry A, Kamanaka M, Kobayashi Y, Booth CJ, Rudensky AY, Roncarolo MG, Battaglia M, Flavell RA. 2011. Th17 cells express interleukin-10 receptor and are controlled by Foxp3(-) and Foxp3+ regulatory CD4+ T cells in an interleukin-10-dependent manner. *Immunity* 34: 554-65

192. Murai M, Turovskaya O, Kim G, Madan R, Karp CL, Cheroutre H, Kronenberg M. 2009. Interleukin 10 acts on regulatory T cells to maintain expression of the transcription factor Foxp3 and suppressive function in mice with colitis. *Nat Immunol* 10: 1178-84

193. Chaudhry A, Samstein RM, Treuting P, Liang Y, Pils MC, Heinrich JM, Jack RS, Wunderlich FT, Bruning JC, Muller W, Rudensky AY. 2011. Interleukin-10 signaling in regulatory T cells is required for suppression of Th17 cell-mediated inflammation. *Immunity* 34: 566-78

194. De Kock I, Van Daele C, Poelaert J. 2010. Sepsis and septic shock: pathophysiological and cardiovascular background as basis for therapy. *Acta Clin Belg* 65: 323-9

195. Berg DJ, Kuhn R, Rajewsky K, Muller W, Menon S, Davidson N, Grunig G, Rennick D. 1995. Interleukin-10 is a central regulator of the response to LPS in murine models of endotoxic shock and the Shwartzman reaction but not endotoxin tolerance. *J Clin Invest* 96: 2339-47

196. Howard M, Muchamuel T, Andrade S, Menon S. 1993. Interleukin 10 protects mice from lethal endotoxemia. *J Exp Med* 177: 1205-8

197. Li C, Corraliza I, Langhorne J. 1999. A defect in interleukin-10 leads to enhanced malarial disease in Plasmodium chabaudi chabaudi infection in mice. *Infect Immun* 67: 4435-42

198. Gazzinelli RT, Wysocka M, Hieny S, Scharton-Kersten T, Cheever A, Kuhn R, Muller W, Trinchieri G, Sher A. 1996. In the absence of endogenous IL-10, mice acutely infected with Toxoplasma gondii succumb to a lethal immune response dependent on CD4+ T cells and accompanied by overproduction of IL-12, IFN-gamma and TNF-alpha. *J Immunol* 157: 798-805

199. Suzuki Y, Sher A, Yap G, Park D, Neyer LE, Liesenfeld O, Fort M, Kang H, Gufwoli E. 2000. IL-10 is required for prevention of necrosis in the small intestine and mortality in both genetically resistant BALB/c and susceptible C57BL/6 mice following peroral infection with Toxoplasma gondii. *J Immunol* 164: 5375-82

200. Jankovic D, Kullberg MC, Feng CG, Goldszmid RS, Collazo CM, Wilson M, Wynn TA, Kamanaka M, Flavell RA, Sher A. 2007. Conventional T-bet(+)Foxp3(-) Th1 cells are the major source of host-protective regulatory IL-10 during intracellular protozoan infection. *J Exp Med* 204: 273-83

201. Freitas do Rosario AP, Lamb T, Spence P, Stephens R, Lang A, Roers A, Muller W, O'Garra A, Langhorne J. 2012. IL-27 promotes IL-10 production by effector Th1 CD4+ T cells: a critical mechanism for protection from severe immunopathology during malaria infection. *J Immunol* 188: 1178-90

202. Hunter CA, Ellis-Neyes LA, Slifer T, Kanaly S, Grunig G, Fort M, Rennick D, Araujo FG. 1997. IL-10 is required to prevent immune hyperactivity during infection with Trypanosoma cruzi. *J Immunol* 158: 3311-6

203. Kullberg MC, Ward JM, Gorelick PL, Caspar P, Hieny S, Cheever A, Jankovic D, Sher A. 1998. Helicobacter hepaticus triggers colitis in specific-pathogen-free interleukin-10 (IL-10)-deficient mice through an IL-12- and gamma interferon-dependent mechanism. *Infect Immun* 66: 5157-66

204. Franke A, Balschun T, Karlsen TH, Sventoraityte J, Nikolaus S, Mayr G, Domingues FS, Albrecht M, Nothnagel M, Ellinghaus D, Sina C, Onnie CM,

Weersma RK, Stokkers PC, Wijmenga C, Gazouli M, Strachan D, McArdle WL, Vermeire S, Rutgeerts P, Rosenstiel P, Krawczak M, Vatn MH, Mathew CG, Schreiber S. 2008. Sequence variants in IL10, ARPC2 and multiple other loci contribute to ulcerative colitis susceptibility. *Nat Genet* 40: 1319-23

205. Franke A, McGovern DP, Barrett JC, Wang K, Radford-Smith GL, Ahmad T, Lees CW, Balschun T, Lee J, Roberts R, Anderson CA, Bis JC, Bumpstead S, Ellinghaus D, Festen EM, Georges M, Green T, Haritunians T, Jostins L, Latiano A, Mathew CG, Montgomery GW, Prescott NJ, Raychaudhuri S, Rotter JI, Schumm P, Sharma Y, Simms LA, Taylor KD, Whiteman D, Wijmenga C, Baldassano RN, Barclay M, Bayless TM, Brand S, Buning C, Cohen A, Colombel JF, Cottone M, Stronati L, Denson T, De Vos M, D'Inca R, Dubinsky M, Edwards C, Florin T, Franchimont D, Gearry R, Glas J, Van Gossum A, Guthery SL, Halfvarson J, Verspaget HW, Hugot JP, Karban A, Laukens D, Lawrance I, Lemann M, Levine A, Libioulle C, Louis E, Mowat C, Newman W, Panes J, Phillips A, Proctor DD, Regueiro M, Russell R, Rutgeerts P, Sanderson J, Sans M, Seibold F, Steinhart AH, Stokkers PC, Torkvist L, Kullak-Ublick G, Wilson D, Walters T, Targan SR, Brant SR, Rioux JD, D'Amato M, Weersma RK, Kugathasan S, Griffiths AM, Mansfield JC, Vermeire S, Duerr RH, Silverberg MS, Satsangi J, Schreiber S, Cho JH, Annese V, Hakonarson H, Daly MJ, Parkes M. 2010. Genome-wide meta-analysis increases to 71 the number of confirmed Crohn's disease susceptibility loci. *Nat Genet* 42: 1118-25

206. Glocker EO, Kotlarz D, Boztug K, Gertz EM, Schaffer AA, Noyan F, Perro M, Diestelhorst J, Allroth A, Murugan D, Hatscher N, Pfeifer D, Sykora KW, Sauer M, Kreipe H, Lacher M, Nustede R, Woellner C, Baumann U, Salzer U, Koletzko S, Shah N, Segal AW, Sauerbrey A, Buderus S, Snapper SB, Grimbacher B, Klein C. 2009. Inflammatory bowel disease and mutations affecting the interleukin-10 receptor. *N Engl J Med* 361: 2033-45

207. Kuhn R, Lohler J, Rennick D, Rajewsky K, Muller W. 1993. Interleukin-10-deficient mice develop chronic enterocolitis. *Cell* 75: 263-74

208. Berg DJ, Davidson N, Kuhn R, Muller W, Menon S, Holland G, Thompson-Snipes L, Leach MW, Rennick D. 1996. Enterocolitis and colon cancer in interleukin-10-

deficient mice are associated with aberrant cytokine production and CD4(+) TH1-like responses. *J Clin Invest* 98: 1010-20

209. Roers A, Siewe L, Strittmatter E, Deckert M, Schluter D, Stenzel W, Gruber AD, Krieg T, Rajewsky K, Muller W. 2004. T cell-specific inactivation of the interleukin 10 gene in mice results in enhanced T cell responses but normal innate responses to lipopolysaccharide or skin irritation. *J Exp Med* 200: 1289-97

210. Hawrylowicz CM, O'Garra A. 2005. Potential role of interleukin-10-secreting regulatory T cells in allergy and asthma. *Nat Rev Immunol* 5: 271-83

211. Dai WJ, Kohler G, Brombacher F. 1997. Both innate and acquired immunity to Listeria monocytogenes infection are increased in IL-10-deficient mice. *J Immunol* 158: 2259-67

212. Redford PS, Boonstra A, Read S, Pitt J, Graham C, Stavropoulos E, Bancroft GJ, O'Garra A. 2010. Enhanced protection to Mycobacterium tuberculosis infection in IL-10-deficient mice is accompanied by early and enhanced Th1 responses in the lung. *Eur J Immunol* 40: 2200-10

213. Moreira-Teixeira L, Redford PS, Stavropoulos E, Ghilardi N, Maynard CL, Weaver CT, Freitas do Rosario AP, Wu X, Langhorne J, O'Garra A. 2017. T Cell-Derived IL-10 Impairs Host Resistance to Mycobacterium tuberculosis Infection. *J Immunol* 199: 613-23

214. Belkaid Y, Hoffmann KF, Mendez S, Kamhawi S, Udey MC, Wynn TA, Sacks DL. 2001. The role of interleukin (IL)-10 in the persistence of Leishmania major in the skin after healing and the therapeutic potential of anti-IL-10 receptor antibody for sterile cure. *J Exp Med* 194: 1497-506

215. Belkaid Y, Piccirillo CA, Mendez S, Shevach EM, Sacks DL. 2002. CD4+CD25+ regulatory T cells control Leishmania major persistence and immunity. *Nature* 420: 502-7

216. O'Garra A, Barrat FJ, Castro AG, Vicari A, Hawrylowicz C. 2008. Strategies for use of IL-10 or its antagonists in human disease. *Immunol Rev* 223: 114-31

217. Pitt JM, Stavropoulos E, Redford PS, Beebe AM, Bancroft GJ, Young DB, O'Garra A. 2012. Blockade of IL-10 signaling during bacillus Calmette-Guerin vaccination enhances and sustains Th1, Th17, and innate lymphoid IFN-gamma and IL-17 responses and increases protection to Mycobacterium tuberculosis infection. *J Immunol* 189: 4079-87

218. Persson S, Mikulowska A, Narula S, O'Garra A, Holmdahl R. 1996. Interleukin-10 suppresses the development of collagen type II-induced arthritis and ameliorates sustained arthritis in rats. *Scand J Immunol* 44: 607-14

219. Asadullah K, Sterry W, Stephanek K, Jasulaitis D, Leupold M, Audring H, Volk HD, Docke WD. 1998. IL-10 is a key cytokine in psoriasis. Proof of principle by IL-10 therapy: a new therapeutic approach. *J Clin Invest* 101: 783-94

220. Bettelli E, Das MP, Howard ED, Weiner HL, Sobel RA, Kuchroo VK. 1998. IL-10 is critical in the regulation of autoimmune encephalomyelitis as demonstrated by studies of IL-10- and IL-4-deficient and transgenic mice. *J Immunol* 161: 3299-306

221. Samoilova EB, Horton JL, Chen Y. 1998. Acceleration of experimental autoimmune encephalomyelitis in interleukin-10-deficient mice: roles of interleukin-10 in disease progression and recovery. *Cell Immunol* 188: 118-24

222. Banchereau J, Pascual V. 2006. Type I interferon in systemic lupus erythematosus and other autoimmune diseases. *Immunity* 25: 383-92

223. Beebe AM, Cua DJ, de Waal Malefyt R. 2002. The role of interleukin-10 in autoimmune disease: systemic lupus erythematosus (SLE) and multiple sclerosis (MS). *Cytokine Growth Factor Rev* 13: 403-12

224. Kim JM, Brannan CI, Copeland NG, Jenkins NA, Khan TA, Moore KW. 1992. Structure of the mouse IL-10 gene and chromosomal localization of the mouse and human genes. *J Immunol* 148: 3618-23

225. Dillon S, Agrawal A, Van Dyke T, Landreth G, McCauley L, Koh A, Maliszewski C, Akira S, Pulendran B. 2004. A Toll-like receptor 2 ligand stimulates Th2

responses in vivo, via induction of extracellular signal-regulated kinase mitogen-activated protein kinase and c-Fos in dendritic cells. *J Immunol* 172: 4733-43

226. Yi AK, Yoon JG, Yeo SJ, Hong SC, English BK, Krieg AM. 2002. Role of mitogen-activated protein kinases in CpG DNA-mediated IL-10 and IL-12 production: central role of extracellular signal-regulated kinase in the negative feedback loop of the CpG DNA-mediated Th1 response. *J Immunol* 168: 4711-20

227. Saraiva M, Christensen JR, Tsytsykova AV, Goldfeld AE, Ley SC, Kioussis D, O'Garra A. 2005. Identification of a macrophage-specific chromatin signature in the IL-10 locus. *J Immunol* 175: 1041-6

228. Chakrabarti A, Sadler AJ, Kar N, Young HA, Silverman RH, Williams BR. 2008. Protein kinase R-dependent regulation of interleukin-10 in response to double-stranded RNA. *J Biol Chem* 283: 25132-9

229. Cao S, Zhang X, Edwards JP, Mosser DM. 2006. NF-kappaB1 (p50) homodimers differentially regulate pro- and anti-inflammatory cytokines in macrophages. *J Biol Chem* 281: 26041-50

230. Ananieva O, Darragh J, Johansen C, Carr JM, McIlrath J, Park JM, Wingate A, Monk CE, Toth R, Santos SG, Iversen L, Arthur JS. 2008. The kinases MSK1 and MSK2 act as negative regulators of Toll-like receptor signaling. *Nat Immunol* 9: 1028-36

231. Hu X, Paik PK, Chen J, Yarilina A, Kockeritz L, Lu TT, Woodgett JR, Ivashkiv LB. 2006. IFN-gamma suppresses IL-10 production and synergizes with TLR2 by regulating GSK3 and CREB/AP-1 proteins. *Immunity* 24: 563-74

232. Martin M, Rehani K, Jope RS, Michalek SM. 2005. Toll-like receptor-mediated cytokine production is differentially regulated by glycogen synthase kinase 3. *Nat Immunol* 6: 777-84

233. Tudor C, Marchese FP, Hitti E, Aubareda A, Rawlinson L, Gaestel M, Blackshear PJ, Clark AR, Saklatvala J, Dean JL. 2009. The p38 MAPK pathway inhibits

tristetraprolin-directed decay of interleukin-10 and pro-inflammatory mediator mRNAs in murine macrophages. *FEBS Lett* 583: 1933-8

234. Teixeira-Coelho M, Guedes J, Ferreirinha P, Howes A, Pedrosa J, Rodrigues F, Lai WS, Blackshear PJ, O'Garra A, Castro AG, Saraiva M. 2013. Differential post-transcriptional regulation of IL-10 by TLR2 and TLR4-activated macrophages. *Eur J Immunol*

235. Martin M, Schifferle RE, Cuesta N, Vogel SN, Katz J, Michalek SM. 2003. Role of the phosphatidylinositol 3 kinase-Akt pathway in the regulation of IL-10 and IL-12 by Porphyromonas gingivalis lipopolysaccharide. *J Immunol* 171: 717-25

236. Nandan D, Camargo de Oliveira C, Moeenrezakhanlou A, Lopez M, Silverman JM, Subek J, Reiner NE. 2012. Myeloid cell IL-10 production in response to leishmania involves inactivation of glycogen synthase kinase-3beta downstream of phosphatidylinositol-3 kinase. *J Immunol* 188: 367-78

237. Katholnig K, Kaltenecker CC, Hayakawa H, Rosner M, Lassnig C, Zlabinger GJ, Gaestel M, Muller M, Hengstschlager M, Horl WH, Park JM, Saemann MD, Weichhart T. 2013. p38alpha senses environmental stress to control innate immune responses via mechanistic target of rapamycin. *J Immunol* 190: 1519-27

238. Hayashi S, Hamada T, Zinsou DGA, Oshiro M, Itoi K, Yamamoto T, Kadowaki M. 2017. PI3K p85alpha Subunit-deficient Macrophages Protect Mice from Acute Colitis due to the Enhancement of IL-10 Production. *Sci Rep* 7: 6187

239. Hammer M, Mages J, Dietrich H, Schmitz F, Striebel F, Murray PJ, Wagner H, Lang R. 2005. Control of dual-specificity phosphatase-1 expression in activated macrophages by IL-10. *Eur J Immunol* 35: 2991-3001

240. Smallie T, Ross EA, Ammit AJ, Cunliffe HE, Tang T, Rosner DR, Ridley ML, Buckley CD, Saklatvala J, Dean JL, Clark AR. 2015. Dual-Specificity Phosphatase 1 and Tristetraprolin Cooperate To Regulate Macrophage Responses to Lipopolysaccharide. *J Immunol* 195: 277-88

241. Gabrysova L, Howes A, Saraiva M, O'Garra A. 2014. The regulation of IL-10 expression. *Curr Top Microbiol Immunol* 380: 157-90

242. Jones EA, Flavell RA. 2005. Distal enhancer elements transcribe intergenic RNA in the IL-10 family gene cluster. *J Immunol* 175: 7437-46

243. Jenuwein T, Allis CD. 2001. Translating the histone code. *Science* 293: 1074-80

244. Lenhard B, Sandelin A, Carninci P. 2012. Metazoan promoters: emerging characteristics and insights into transcriptional regulation. *Nat Rev Genet* 13: 233-45

245. Villagra A, Cheng F, Wang HW, Suarez I, Glozak M, Maurin M, Nguyen D, Wright KL, Atadja PW, Bhalla K, Pinilla-Ibarz J, Seto E, Sotomayor EM. 2009. The histone deacetylase HDAC11 regulates the expression of interleukin 10 and immune tolerance. *Nat Immunol* 10: 92-100

246. Cheng F, Lienlaf M, Perez-Villarroel P, Wang HW, Lee C, Woan K, Woods D, Knox T, Bergman J, Pinilla-Ibarz J, Kozikowski A, Seto E, Sotomayor EM, Villagra A. 2014. Divergent roles of histone deacetylase 6 (HDAC6) and histone deacetylase 11 (HDAC11) on the transcriptional regulation of IL10 in antigen presenting cells. *Mol Immunol* 60: 44-53

247. Lucas M, Zhang X, Prasanna V, Mosser DM. 2005. ERK activation following macrophage FcgammaR ligation leads to chromatin modifications at the IL-10 locus. *J Immunol* 175: 469-77

248. Zhang X, Edwards JP, Mosser DM. 2006. Dynamic and transient remodeling of the macrophage IL-10 promoter during transcription. *J Immunol* 177: 1282-8

249. Brightbill HD, Plevy SE, Modlin RL, Smale ST. 2000. A prominent role for Sp1 during lipopolysaccharide-mediated induction of the IL-10 promoter in macrophages. *J Immunol* 164: 1940-51

250. Tone M, Powell MJ, Tone Y, Thompson SA, Waldmann H. 2000. IL-10 gene expression is controlled by the transcription factors Sp1 and Sp3. *J Immunol* 165: 286-91

251. Platzer C, Fritsch E, Elsner T, Lehmann MH, Volk HD, Prosch S. 1999. Cyclic adenosine monophosphate-responsive elements are involved in the transcriptional activation of the human IL-10 gene in monocytic cells. *Eur J Immunol* 29: 3098-104

252. Cao S, Liu J, Song L, Ma X. 2005. The protooncogene c-Maf is an essential transcription factor for IL-10 gene expression in macrophages. *J Immunol* 174: 3484-92

253. Benkhart EM, Siedlar M, Wedel A, Werner T, Ziegler-Heitbrock HW. 2000. Role of Stat3 in lipopolysaccharide-induced IL-10 gene expression. *J Immunol* 165: 1612-7

254. Wang ZY, Sato H, Kusam S, Sehra S, Toney LM, Dent AL. 2005. Regulation of IL-10 gene expression in Th2 cells by Jun proteins. *J Immunol* 174: 2098-105

255. Ma W, Lim W, Gee K, Aucoin S, Nandan D, Kozlowski M, Diaz-Mitoma F, Kumar A. 2001. The p38 mitogen-activated kinase pathway regulates the human interleukin-10 promoter via the activation of Sp1 transcription factor in lipopolysaccharide-stimulated human macrophages. *J Biol Chem* 276: 13664-74

256. Chung EY, Liu J, Homma Y, Zhang Y, Brendolan A, Saggese M, Han J, Silverstein R, Selleri L, Ma X. 2007. Interleukin-10 expression in macrophages during phagocytosis of apoptotic cells is mediated by homeodomain proteins Pbx1 and Prep-1. *Immunity* 27: 952-64

257. Staples KJ, Smallie T, Williams LM, Foey A, Burke B, Foxwell BM, Ziegler-Heitbrock L. 2007. IL-10 induces IL-10 in primary human monocyte-derived macrophages via the transcription factor Stat3. *J Immunol* 178: 4779-85

258. Brenner S, Prösch S, Schenke-Layland K, Riese U, Gausmann U, Platzer C. 2003. cAMP-induced Interleukin-10 Promoter Activation Depends on

CCAAT/Enhancer-binding Protein Expression and Monocytic Differentiation. *Journal of Biological Chemistry* 278: 5597-604

259. Liu YW, Tseng HP, Chen LC, Chen BK, Chang WC. 2003. Functional cooperation of simian virus 40 promoter factor 1 and CCAAT/enhancer-binding protein beta and delta in lipopolysaccharide-induced gene activation of IL-10 in mouse macrophages. *J Immunol* 171: 821-8

260. Kimura A, Naka T, Nakahama T, Chinen I, Masuda K, Nohara K, Fujii-Kuriyama Y, Kishimoto T. 2009. Aryl hydrocarbon receptor in combination with Stat1 regulates LPS-induced inflammatory responses. *J Exp Med* 206: 2027-35

261. Yee CS, Yao Y, Xu Q, McCarthy B, Sun-Lin D, Tone M, Waldmann H, Chang CH. 2005. Enhanced production of IL-10 by dendritic cells deficient in CIITA. *J Immunol* 174: 1222-9

262. Krausgruber T, Blazek K, Smallie T, Alzabin S, Lockstone H, Sahgal N, Hussell T, Feldmann M, Udalova IA. 2011. IRF5 promotes inflammatory macrophage polarization and TH1-TH17 responses. *Nat Immunol* 12: 231-8

263. Stoecklin G, Tenenbaum SA, Mayo T, Chittur SV, George AD, Baroni TE, Blackshear PJ, Anderson P. 2008. Genome-wide analysis identifies interleukin-10 mRNA as target of tristetraprolin. *J Biol Chem* 283: 11689-99

264. Gaba A, Grivennikov SI, Do MV, Stumpo DJ, Blackshear PJ, Karin M. 2012. Cutting edge: IL-10-mediated tristetraprolin induction is part of a feedback loop that controls macrophage STAT3 activation and cytokine production. *J Immunol* 189: 2089-93

265. Lee BC, Lee SG, Choo MK, Kim JH, Lee HM, Kim S, Fomenko DE, Kim HY, Park JM, Gladyshev VN. 2017. Selenoprotein MsrB1 promotes anti-inflammatory cytokine gene expression in macrophages and controls immune response in vivo. *Sci Rep* 7: 5119

266. Iyer SS, Ghaffari AA, Cheng G. 2010. Lipopolysaccharide-mediated IL-10 transcriptional regulation requires sequential induction of type I IFNs and IL-27 in macrophages. *J Immunol* 185: 6599-607

267. Kalliolias GD, Ivashkiv LB. 2008. IL-27 activates human monocytes via STAT1 and suppresses IL-10 production but the inflammatory functions of IL-27 are abrogated by TLRs and p38. *J Immunol* 180: 6325-33

268. Howes A, Taubert C, Blankley S, Spink N, Wu X, Graham CM, Zhao J, Saraiva M, Ricciardi-Castagnoli P, Bancroft GJ, O'Garra A. 2016. Differential Production of Type I IFN Determines the Reciprocal Levels of IL-10 and Proinflammatory Cytokines Produced by C57BL/6 and BALB/c Macrophages. *J Immunol* 197: 2838-53

269. McNab FW, Ewbank J, Howes A, Moreira-Teixeira L, Martirosyan A, Ghilardi N, Saraiva M, O'Garra A. 2014. Type I IFN Induces IL-10 Production in an IL-27-Independent Manner and Blocks Responsiveness to IFN-gamma for Production of IL-12 and Bacterial Killing in Mycobacterium tuberculosis-Infected Macrophages. *J Immunol* 193: 3600-12

270. Aman MJ, Tretter T, Eisenbeis I, Bug G, Decker T, Aulitzky WE, Tilg H, Huber C, Peschel C. 1996. Interferon-alpha stimulates production of interleukin-10 in activated CD4+ T cells and monocytes. *Blood* 87: 4731-6

271. Chang EY, Guo B, Doyle SE, Cheng G. 2007. Cutting edge: involvement of the type I IFN production and signaling pathway in lipopolysaccharide-induced IL-10 production. *J Immunol* 178: 6705-9

272. Mayer-Barber KD, Andrade BB, Barber DL, Hieny S, Feng CG, Caspar P, Oland S, Gordon S, Sher A. 2011. Innate and adaptive interferons suppress IL-1alpha and IL-1beta production by distinct pulmonary myeloid subsets during Mycobacterium tuberculosis infection. *Immunity* 35: 1023-34

273. Lobo-Silva D, Carriche GM, Castro AG, Roque S, Saraiva M. 2017. Interferon-beta regulates the production of IL-10 by toll-like receptor-activated microglia. *Glia* 65: 1439-51

274. Guarda G, Braun M, Staehli F, Tardivel A, Mattmann C, Forster I, Farlik M, Decker T, Du Pasquier RA, Romero P, Tschopp J. 2011. Type I interferon inhibits interleukin-1 production and inflammasome activation. *Immunity* 34: 213-23

275. Wang H, Brown J, Garcia CA, Tang Y, Benakanakere MR, Greenway T, Alard P, Kinane DF, Martin M. 2011. The role of glycogen synthase kinase 3 in regulating IFN-beta-mediated IL-10 production. *J Immunol* 186: 675-84

276. Ziegler-Heitbrock L, Lotzerich M, Schaefer A, Werner T, Frankenberger M, Benkhart E. 2003. IFN-alpha induces the human IL-10 gene by recruiting both IFN regulatory factor 1 and Stat3. *J Immunol* 171: 285-90

277. Pestka S, Krause CD, Walter MR. 2004. Interferons, interferon-like cytokines, and their receptors. *Immunol Rev* 202: 8-32

278. O'Brien TR, Prokunina-Olsson L, Donnelly RP. 2014. IFN-lambda4: the paradoxical new member of the interferon lambda family. *J Interferon Cytokine Res* 34: 829-38

279. Trinchieri G. 2010. Type I interferon: friend or foe? *J Exp Med* 207: 2053-63

280. Platanias LC. 2005. Mechanisms of type-I- and type-II-interferon-mediated signalling. *Nat Rev Immunol* 5: 375-86

281. Wang Y, Nan J, Willard B, Wang X, Yang J, Stark GR. 2017. Negative regulation of type I IFN signaling by phosphorylation of STAT2 on T387. *The EMBO Journal* 36: 202-12

282. Decker T, Muller M, Stockinger S. 2005. The yin and yang of type I interferon activity in bacterial infection. *Nat Rev Immunol* 5: 675-87

283. David M, Petricoin E, 3rd, Benjamin C, Pine R, Weber MJ, Larner AC. 1995. Requirement for MAP kinase (ERK2) activity in interferon alpha- and interferon beta-stimulated gene expression through STAT proteins. *Science* 269: 1721-3

284. Uddin S, Majchrzak B, Woodson J, Arunkumar P, Alsayed Y, Pine R, Young PR, Fish EN, Platanias LC. 1999. Activation of the p38 mitogen-activated protein kinase by type I interferons. *J Biol Chem* 274: 30127-31

285. McNab F, Mayer-Barber K, Sher A, Wack A, O'Garra A. 2015. Type I interferons in infectious disease. *Nat Rev Immunol* 15: 87-103

286. Rauch I, Muller M, Decker T. 2013. The regulation of inflammation by interferons and their STATs. *JAKSTAT* 2: e23820

287. Porritt RA, Hertzog PJ. 2015. Dynamic control of type I IFN signalling by an integrated network of negative regulators. *Trends Immunol* 36: 150-60

288. Piganis RA, De Weerd NA, Gould JA, Schindler CW, Mansell A, Nicholson SE, Hertzog PJ. 2011. Suppressor of cytokine signaling (SOCS) 1 inhibits type I interferon (IFN) signaling via the interferon alpha receptor (IFNAR1)-associated tyrosine kinase Tyk2. *J Biol Chem* 286: 33811-8

289. Francois-Newton V, Magno de Freitas Almeida G, Payelle-Brogard B, Monneron D, Pichard-Garcia L, Piehler J, Pellegrini S, Uze G. 2011. USP18-based negative feedback control is induced by type I and type III interferons and specifically inactivates interferon alpha response. *PLoS One* 6: e22200

290. Malakhov MP, Malakhova OA, Kim KI, Ritchie KJ, Zhang DE. 2002. UBP43 (USP18) specifically removes ISG15 from conjugated proteins. *J Biol Chem* 277: 9976-81

291. Schoggins JW, Wilson SJ, Panis M, Murphy MY, Jones CT, Bieniasz P, Rice CM. 2011. A diverse range of gene products are effectors of the type I interferon antiviral response. *Nature* 472: 481-5

292. Durbin JE, Fernandez-Sesma A, Lee CK, Rao TD, Frey AB, Moran TM, Vukmanovic S, Garcia-Sastre A, Levy DE. 2000. Type I IFN modulates innate and specific antiviral immunity. *J Immunol* 164: 4220-8

293. Garcia-Sastre A, Durbin RK, Zheng H, Palese P, Gertner R, Levy DE, Durbin JE. 1998. The role of interferon in influenza virus tissue tropism. *J Virol* 72: 8550-8

294. Koerner I, Kochs G, Kalinke U, Weiss S, Staeheli P. 2007. Protective role of beta interferon in host defense against influenza A virus. *J Virol* 81: 2025-30

295. Mordstein M, Kochs G, Dumoutier L, Renauld JC, Paludan SR, Klucher K, Staeheli P. 2008. Interferon-lambda contributes to innate immunity of mice against influenza A virus but not against hepatotropic viruses. *PLoS Pathog* 4: e1000151

296. Auerbuch V, Brockstedt DG, Meyer-Morse N, O'Riordan M, Portnoy DA. 2004. Mice lacking the type I interferon receptor are resistant to Listeria monocytogenes. *J Exp Med* 200: 527-33

297. Manca C, Tsenova L, Freeman S, Barczak AK, Tovey M, Murray PJ, Barry C, Kaplan G. 2005. Hypervirulent M. tuberculosis W/Beijing strains upregulate type I IFNs and increase expression of negative regulators of the Jak-Stat pathway. *J Interferon Cytokine Res* 25: 694-701

298. Carrero JA, Calderon B, Unanue ER. 2006. Lymphocytes are detrimental during the early innate immune response against Listeria monocytogenes. *J Exp Med* 203: 933-40

299. Rayamajhi M, Humann J, Penheiter K, Andreasen K, Lenz LL. 2010. Induction of IFN-alphabeta enables Listeria monocytogenes to suppress macrophage activation by IFN-gamma. *J Exp Med* 207: 327-37

300. Berry MP, Graham CM, McNab FW, Xu Z, Bloch SA, Oni T, Wilkinson KA, Banchereau R, Skinner J, Wilkinson RJ, Quinn C, Blankenship D, Dhawan R, Cush JJ, Mejias A, Ramilo O, Kon OM, Pascual V, Banchereau J, Chaussabel D, O'Garra A. 2010. An interferon-inducible neutrophil-driven blood transcriptional signature in human tuberculosis. *Nature* 466: 973-7

301. Bennett L, Palucka AK, Arce E, Cantrell V, Borvak J, Banchereau J, Pascual V. 2003. Interferon and granulopoiesis signatures in systemic lupus erythematosus blood. *J Exp Med* 197: 711-23

302. Ronnblom L. 2011. The type I interferon system in the etiopathogenesis of autoimmune diseases. *Ups J Med Sci* 116: 227-37

303. Ann Marrie R, Rudick RA. 2006. Drug Insight: interferon treatment in multiple sclerosis. *Nat Clin Pract Neurol* 2: 34-44

304. Rudick RA, Ransohoff RM, Peppler R, VanderBrug Medendorp S, Lehmann P, Alam J. 1996. Interferon beta induces interleukin-10 expression: relevance to multiple sclerosis. *Ann Neurol* 40: 618-27

305. Friedman RM. 2008. Clinical uses of interferons. *Br J Clin Pharmacol* 65: 158-62

306. Marie I, Durbin JE, Levy DE. 1998. Differential viral induction of distinct interferon-alpha genes by positive feedback through interferon regulatory factor-7. *EMBO J* 17: 6660-9

307. Goubau D, Deddouche S, Reis e Sousa C. 2013. Cytosolic sensing of viruses. *Immunity* 38: 855-69

308. Watanabe T, Asano N, Fichtner-Feigl S, Gorelick PL, Tsuji Y, Matsumoto Y, Chiba T, Fuss IJ, Kitani A, Strober W. 2010. NOD1 contributes to mouse host defense against Helicobacter pylori via induction of type I IFN and activation of the ISGF3 signaling pathway. *J Clin Invest* 120: 1645-62

309. Pandey AK, Yang Y, Jiang Z, Fortune SM, Coulombe F, Behr MA, Fitzgerald KA, Sassetti CM, Kelliher MA. 2009. NOD2, RIP2 and IRF5 play a critical role in the type I interferon response to Mycobacterium tuberculosis. *PLoS Pathog* 5: e1000500

310. Watson RO, Bell SL, MacDuff DA, Kimmey JM, Diner EJ, Olivas J, Vance RE, Stallings CL, Virgin HW, Cox JS. 2015. The Cytosolic Sensor cGAS Detects

Mycobacterium tuberculosis DNA to Induce Type I Interferons and Activate Autophagy. *Cell Host Microbe* 17: 811-9

311. Manzanillo PS, Shiloh MU, Portnoy DA, Cox JS. 2012. Mycobacterium tuberculosis activates the DNA-dependent cytosolic surveillance pathway within macrophages. *Cell Host Microbe* 11: 469-80

312. Paludan SR, Bowie AG. 2013. Immune sensing of DNA. *Immunity* 38: 870-80

313. Honda K, Yanai H, Takaoka A, Taniguchi T. 2005. Regulation of the type I IFN induction: a current view. *Int Immunol* 17: 1367-78

314. Thanos D, Maniatis T. 1995. Virus induction of human IFN beta gene expression requires the assembly of an enhanceosome. *Cell* 83: 1091-100

315. Labzin LI, Schmidt SV, Masters SL, Beyer M, Krebs W, Klee K, Stahl R, Lutjohann D, Schultze JL, Latz E, De Nardo D. 2015. ATF3 Is a Key Regulator of Macrophage IFN Responses. *J Immunol* 195: 4446-55

316. Tamura T, Yanai H, Savitsky D, Taniguchi T. 2008. The IRF family transcription factors in immunity and oncogenesis. *Annu Rev Immunol* 26: 535-84

317. Moynagh PN. 2005. TLR signalling and activation of IRFs: revisiting old friends from the NF-kappaB pathway. *Trends Immunol* 26: 469-76

318. Yang HT, Wang Y, Zhao X, Demissie E, Papoutsopoulou S, Mambole A, O'Garra A, Tomczak MF, Erdman SE, Fox JG, Ley SC, Horwitz BH. 2011. NF-kappaB1 inhibits TLR-induced IFN-beta production in macrophages through TPL-2-dependent ERK activation. *J Immunol* 186: 1989-96

319. Leakey AK, Ulett GC, Hirst RG. 1998. BALB/c and C57Bl/6 mice infected with virulent Burkholderia pseudomallei provide contrasting animal models for the acute and chronic forms of human melioidosis. *Microb Pathog* 24: 269-75

320. Sacks D, Noben-Trauth N. 2002. The immunology of susceptibility and resistance to Leishmania major in mice. *Nat Rev Immunol* 2: 845-58

321. Mainou-Fowler T, MacGowan AP, Postlethwaite R. 1988. Virulence of Listeria spp.: course of infection in resistant and susceptible mice. *J Med Microbiol* 27: 131-40

322. Roque S, Nobrega C, Appelberg R, Correia-Neves M. 2007. IL-10 underlies distinct susceptibility of BALB/c and C57BL/6 mice to Mycobacterium avium infection and influences efficacy of antibiotic therapy. *J Immunol* 178: 8028-35

323. Schluter D, Deckert-Schluter M, Lorenz E, Meyer T, Rollinghoff M, Bogdan C. 1999. Inhibition of inducible nitric oxide synthase exacerbates chronic cerebral toxoplasmosis in Toxoplasma gondii-susceptible C57BL/6 mice but does not reactivate the latent disease in T. gondii-resistant BALB/c mice. *J Immunol* 162: 3512-8

324. Mohammadi M, Redline R, Nedrud J, Czinn S. 1996. Role of the host in pathogenesis of Helicobacter-associated gastritis: H. felis infection of inbred and congenic mouse strains. *Infect Immun* 64: 238-45

325. Sellon RK, Tonkonogy S, Schultz M, Dieleman LA, Grenther W, Balish E, Rennick DM, Sartor RB. 1998. Resident enteric bacteria are necessary for development of spontaneous colitis and immune system activation in interleukin-10-deficient mice. *Infect Immun* 66: 5224-31

326. Heinzel FP, Sadick MD, Holaday BJ, Coffman RL, Locksley RM. 1989. Reciprocal expression of interferon gamma or interleukin 4 during the resolution or progression of murine leishmaniasis. Evidence for expansion of distinct helper T cell subsets. *J Exp Med* 169: 59-72

327. Oliveira LS, de Queiroz NM, Veloso LV, Moreira TG, Oliveira FS, Carneiro MB, Faria AM, Vieira LQ, Oliveira SC, Horta MF. 2014. A defective TLR4 signaling for IFN-beta expression is responsible for the innately lower ability of BALB/c macrophages to produce NO in response to LPS as compared to C57BL/6. *PLoS One* 9: e98913

328. Depke M, Breitbach K, Dinh Hoang Dang K, Brinkmann L, Salazar MG, Dhople VM, Bast A, Steil L, Schmidt F, Steinmetz I, Volker U. 2014. Bone marrow-derived

macrophages from BALB/c and C57BL/6 mice fundamentally differ in their respiratory chain complex proteins, lysosomal enzymes and components of antioxidant stress systems. *J Proteomics* 103: 72-86

329. Tsukamoto H, Fukudome K, Takao S, Tsuneyoshi N, Ohta S, Nagai Y, Ihara H, Miyake K, Ikeda Y, Kimoto M. 2013. Reduced surface expression of TLR4 by a V254I point mutation accounts for the low lipopolysaccharide responder phenotype of BALB/c B cells. *J Immunol* 190: 195-204

330. Cohen P. 2009. Targeting protein kinases for the development of anti-inflammatory drugs. *Curr Opin Cell Biol* 21: 317-24

331. Bain J, Plater L, Elliott M, Shpiro N, Hastie CJ, McLauchlan H, Klevernic I, Arthur JS, Alessi DR, Cohen P. 2007. The selectivity of protein kinase inhibitors: a further update. *Biochem J* 408: 297-315

332. Buenrostro JD, Giresi PG, Zaba LC, Chang HY, Greenleaf WJ. 2013. Transposition of native chromatin for fast and sensitive epigenomic profiling of open chromatin, DNA-binding proteins and nucleosome position. *Nat Methods* 10: 1213-8

333. Buenrostro JD, Wu B, Chang HY, Greenleaf WJ. 2015. ATAC-seq: A Method for Assaying Chromatin Accessibility Genome-Wide. *Curr Protoc Mol Biol* 109: 21 9 1-9

334. Consortium EP. 2012. An integrated encyclopedia of DNA elements in the human genome. *Nature* 489: 57-74

335. Feng J, Liu T, Zhang Y. 2011. Using MACS to identify peaks from ChIP-Seq data. *Curr Protoc Bioinformatics* Chapter 2: Unit 2.14

336. Adey A, Morrison HG, Asan, Xun X, Kitzman JO, Turner EH, Stackhouse B, MacKenzie AP, Caruccio NC, Zhang X, Shendure J. 2010. Rapid, low-input, low-bias construction of shotgun fragment libraries by high-density in vitro transposition. *Genome Biol* 11: R119

337. Ramirez F, Dundar F, Diehl S, Gruning BA, Manke T. 2014. deepTools: a flexible platform for exploring deep-sequencing data. *Nucleic Acids Res* 42: W187-91

338. Ross-Innes CS, Stark R, Teschendorff AE, Holmes KA, Ali HR, Dunning MJ, Brown GD, Gojis O, Ellis IO, Green AR, Ali S, Chin SF, Palmieri C, Caldas C, Carroll JS. 2012. Differential oestrogen receptor binding is associated with clinical outcome in breast cancer. *Nature* 481: 389-93

339. Stark R, Brown G. 2011. DiffBind: differential binding analysis of ChIP-Seq peak data. http://bioconductor.org/packages/release/bioc/vignettes/DiffBind/inst/doc/DiffBind.pdf

340. Heinz S, Benner C, Spann N, Bertolino E, Lin YC, Laslo P, Cheng JX, Murre C, Singh H, Glass CK. 2010. Simple Combinations of Lineage-Determining Transcription Factors Prime cis-Regulatory Elements Required for Macrophage and B Cell Identities. *Molecular Cell* 38: 576-89

341. Nathan C, Ding A. 2010. Nonresolving inflammation. *Cell* 140: 871-82

342. Murray PJ, Smale ST. 2012. Restraint of inflammatory signaling by interdependent strata of negative regulatory pathways. *Nat Immunol* 13: 916-24

343. Tu D, Zhu Z, Zhou Alicia Y, Yun C-h, Lee K-E, Toms Angela V, Li Y, Dunn Gavin P, Chan E, Thai T, Yang S, Ficarro Scott B, Marto Jarrod A, Jeon H, Hahn William C, Barbie David A, Eck Michael J. 2013. Structure and Ubiquitination-Dependent Activation of TANK-Binding Kinase 1. *Cell Reports* 3: 747-58

344. Larabi A, Devos Juliette M, Ng S-L, Nanao Max H, Round A, Maniatis T, Panne D. 2013. Crystal Structure and Mechanism of Activation of TANK-Binding Kinase 1. *Cell Reports* 3: 734-46

345. Liu S, Cai X, Wu J, Cong Q, Chen X, Li T, Du F, Ren J, Wu Y-T, Grishin NV, Chen ZJ. 2015. Phosphorylation of innate immune adaptor proteins MAVS, STING, and TRIF induces IRF3 activation. *Science* 347

346. Ting Tan RS, Lin B, Liu Q, Tucker-Kellogg L, Ho B, Leung BPL, Ding JL. 2013. The synergy in cytokine production through MyD88-TRIF pathways is co-ordinated with ERK phosphorylation in macrophages. *Immunol Cell Biol* 91: 377-87

347. Whitmore MM, DeVeer MJ, Edling A, Oates RK, Simons B, Lindner D, Williams BR. 2004. Synergistic activation of innate immunity by double-stranded RNA and CpG DNA promotes enhanced antitumor activity. *Cancer Res* 64: 5850-60

348. Liu Q, Zhu Y, Yong WK, Sze NS, Tan NS, Ding JL. 2015. Cutting Edge: Synchronization of IRF1, JunB, and C/EBPbeta Activities during TLR3-TLR7 Cross-Talk Orchestrates Timely Cytokine Synergy in the Proinflammatory Response. *J Immunol* 195: 801-5

349. Tan GY, Liu Y, Sivalingam SP, Sim SH, Wang D, Paucod JC, Gauthier Y, Ooi EE. 2008. Burkholderia pseudomallei aerosol infection results in differential inflammatory responses in BALB/c and C57Bl/6 mice. *J Med Microbiol* 57: 508-15

350. Titball RW, Russell P, Cuccui J, Easton A, Haque A, Atkins T, Sarkar-Tyson M, Harley V, Wren B, Bancroft GJ. 2008. Burkholderia pseudomallei: animal models of infection. *Trans R Soc Trop Med Hyg* 102 Suppl 1: S111-6

351. Ulett GC, Ketheesan N, Hirst RG. 2000. Cytokine gene expression in innately susceptible BALB/c mice and relatively resistant C57BL/6 mice during infection with virulent Burkholderia pseudomallei. *Infect Immun* 68: 2034-42

352. Ulett GC, Ketheesan N, Hirst RG. 2000. Proinflammatory cytokine mRNA responses in experimental Burkholderia pseudomallei infection in mice. *Acta Trop* 74: 229-34

353. Sugiyama Y, Kakoi K, Kimura A, Takada I, Kashiwagi I, Wakabayashi Y, Morita R, Nomura M, Yoshimura A. 2012. Smad2 and Smad3 are redundantly essential for the suppression of iNOS synthesis in macrophages by regulating IRF3 and STAT1 pathways. *Int Immunol* 24: 253-65

354. Byrnes AA, Ma X, Cuomo P, Park K, Wahl L, Wolf SF, Zhou H, Trinchieri G, Karp CL. 2001. Type I interferons and IL-12: convergence and cross-regulation among mediators of cellular immunity. *Eur J Immunol* 31: 2026-34

355. Gautier G, Humbert M, Deauvieau F, Scuiller M, Hiscott J, Bates EE, Trinchieri G, Caux C, Garrone P. 2005. A type I interferon autocrine-paracrine loop is involved in Toll-like receptor-induced interleukin-12p70 secretion by dendritic cells. *J Exp Med* 201: 1435-46

356. Cousens LP, Orange JS, Su HC, Biron CA. 1997. Interferon-alpha/beta inhibition of interleukin 12 and interferon-gamma production in vitro and endogenously during viral infection. *Proc Natl Acad Sci U S A* 94: 634-9

357. Pattison MJ, Mackenzie KF, Arthur JS. 2012. Inhibition of JAKs in macrophages increases lipopolysaccharide-induced cytokine production by blocking IL-10-mediated feedback. *J Immunol* 189: 2784-92

358. Kim C, Sano Y, Todorova K, Carlson BA, Arpa L, Celada A, Lawrence T, Otsu K, Brissette JL, Arthur JS, Park JM. 2008. The kinase p38 alpha serves cell type-specific inflammatory functions in skin injury and coordinates pro- and anti-inflammatory gene expression. *Nat Immunol* 9: 1019-27

359. Kanters E, Pasparakis M, Gijbels MJ, Vergouwe MN, Partouns-Hendriks I, Fijneman RJ, Clausen BE, Forster I, Kockx MM, Rajewsky K, Kraal G, Hofker MH, de Winther MP. 2003. Inhibition of NF-kappaB activation in macrophages increases atherosclerosis in LDL receptor-deficient mice. *J Clin Invest* 112: 1176-85

360. Gough DJ, Messina NL, Clarke CJ, Johnstone RW, Levy DE. 2012. Constitutive type I interferon modulates homeostatic balance through tonic signaling. *Immunity* 36: 166-74

361. Zeisel A, Kostler WJ, Molotski N, Tsai JM, Krauthgamer R, Jacob-Hirsch J, Rechavi G, Soen Y, Jung S, Yarden Y, Domany E. 2011. Coupled pre-mRNA and mRNA dynamics unveil operational strategies underlying transcriptional responses to stimuli. *Mol Syst Biol* 7: 529

362. Dalod M, Salazar-Mather TP, Malmgaard L, Lewis C, Asselin-Paturel C, Briere F, Trinchieri G, Biron CA. 2002. Interferon alpha/beta and interleukin 12 responses to viral infections: pathways regulating dendritic cell cytokine expression in vivo. *J Exp Med* 195: 517-28

363. Stanley SA, Johndrow JE, Manzanillo P, Cox JS. 2007. The Type I IFN response to infection with Mycobacterium tuberculosis requires ESX-1-mediated secretion and contributes to pathogenesis. *J Immunol* 178: 3143-52

364. Dalod M, Hamilton T, Salomon R, Salazar-Mather TP, Henry SC, Hamilton JD, Biron CA. 2003. Dendritic cell responses to early murine cytomegalovirus infection: subset functional specialization and differential regulation by interferon alpha/beta. *J Exp Med* 197: 885-98

365. Liu BS, Cao Y, Huizinga TW, Hafler DA, Toes RE. 2014. TLR-mediated STAT3 and ERK activation controls IL-10 secretion by human B cells. *Eur J Immunol*

366. Csoka B, Nemeth ZH, Virag L, Gergely P, Leibovich SJ, Pacher P, Sun CX, Blackburn MR, Vizi ES, Deitch EA, Hasko G. 2007. A2A adenosine receptors and C/EBPbeta are crucially required for IL-10 production by macrophages exposed to Escherichia coli. *Blood* 110: 2685-95

367. Wei G, Wei L, Zhu J, Zang C, Hu-Li J, Yao Z, Cui K, Kanno Y, Roh TY, Watford WT, Schones DE, Peng W, Sun HW, Paul WE, O'Shea JJ, Zhao K. 2009. Global mapping of H3K4me3 and H3K27me3 reveals specificity and plasticity in lineage fate determination of differentiating CD4+ T cells. *Immunity* 30: 155-67

368. Zhu C, Sakuishi K, Xiao S, Sun Z, Zaghouani S, Gu G, Wang C, Tan DJ, Wu C, Rangachari M, Pertel T, Jin HT, Ahmed R, Anderson AC, Kuchroo VK. 2015. An IL-27/NFIL3 signalling axis drives Tim-3 and IL-10 expression and T-cell dysfunction. *Nat Commun* 6: 6072

369. Motomura Y, Kitamura H, Hijikata A, Matsunaga Y, Matsumoto K, Inoue H, Atarashi K, Hori S, Watarai H, Zhu J, Taniguchi M, Kubo M. 2011. The transcription factor E4BP4 regulates the production of IL-10 and IL-13 in CD4+ T cells. *Nat Immunol* 12: 450-9

370. Santos-Rosa H, Schneider R, Bannister AJ, Sherriff J, Bernstein BE, Emre NC, Schreiber SL, Mellor J, Kouzarides T. 2002. Active genes are tri-methylated at K4 of histone H3. *Nature* 419: 407-11

371. Zhou VW, Goren A, Bernstein BE. 2011. Charting histone modifications and the functional organization of mammalian genomes. *Nat Rev Genet* 12: 7-18

372. Heintzman ND, Stuart RK, Hon G, Fu Y, Ching CW, Hawkins RD, Barrera LO, Van Calcar S, Qu C, Ching KA, Wang W, Weng Z, Green RD, Crawford GE, Ren B. 2007. Distinct and predictive chromatin signatures of transcriptional promoters and enhancers in the human genome. *Nat Genet* 39: 311-8

373. Creyghton MP, Cheng AW, Welstead GG, Kooistra T, Carey BW, Steine EJ, Hanna J, Lodato MA, Frampton GM, Sharp PA, Boyer LA, Young RA, Jaenisch R. 2010. Histone H3K27ac separates active from poised enhancers and predicts developmental state. *Proc Natl Acad Sci U S A* 107: 21931-6

374. Khoury G, Gruss P. 1983. Enhancer elements. *Cell* 33: 313-4

375. Dixon JR, Selvaraj S, Yue F, Kim A, Li Y, Shen Y, Hu M, Liu JS, Ren B. 2012. Topological domains in mammalian genomes identified by analysis of chromatin interactions. *Nature* 485: 376-80

376. Durand NC, Robinson JT, Shamim MS, Machol I, Mesirov JP, Lander ES, Aiden EL. 2016. Juicebox Provides a Visualization System for Hi-C Contact Maps with Unlimited Zoom. *Cell Syst* 3: 99-101

377. Zentner GE, Henikoff S. 2013. Regulation of nucleosome dynamics by histone modifications. *Nat Struct Mol Biol* 20: 259-66

378. Stark GR, Darnell JE, Jr. 2012. The JAK-STAT pathway at twenty. *Immunity* 36: 503-14

379. Ivashkiv LB, Donlin LT. 2014. Regulation of type I interferon responses. *Nat Rev Immunol* 14: 36-49

380. Nusinzon I, Horvath CM. 2003. Interferon-stimulated transcription and innate antiviral immunity require deacetylase activity and histone deacetylase 1. *Proc Natl Acad Sci U S A* 100: 14742-7

381. Zupkovitz G, Tischler J, Posch M, Sadzak I, Ramsauer K, Egger G, Grausenburger R, Schweifer N, Chiocca S, Decker T, Seiser C. 2006. Negative and positive regulation of gene expression by mouse histone deacetylase 1. *Mol Cell Biol* 26: 7913-28

382. Klampfer L, Huang J, Swaby LA, Augenlicht L. 2004. Requirement of histone deacetylase activity for signaling by STAT1. *J Biol Chem* 279: 30358-68

383. Xu D, Holko M, Sadler AJ, Scott B, Higashiyama S, Berkofsky-Fessler W, McConnell MJ, Pandolfi PP, Licht JD, Williams BR. 2009. Promyelocytic leukemia zinc finger protein regulates interferon-mediated innate immunity. *Immunity* 30: 802-16

384. Chang HM, Paulson M, Holko M, Rice CM, Williams BR, Marie I, Levy DE. 2004. Induction of interferon-stimulated gene expression and antiviral responses require protein deacetylase activity. *Proc Natl Acad Sci U S A* 101: 9578-83

385. Nusinzon I, Horvath CM. 2006. Positive and negative regulation of the innate antiviral response and beta interferon gene expression by deacetylation. *Mol Cell Biol* 26: 3106-13

386. Wang X, Zhu K, Li S, Liao Y, Du R, Zhang X, Shu HB, Guo AY, Li L, Wu M. 2012. MLL1, a H3K4 methyltransferase, regulates the TNFalpha-stimulated activation of genes downstream of NF-kappaB. *J Cell Sci* 125: 4058-66

387. Carson WFt, Cavassani KA, Soares EM, Hirai S, Kittan NA, Schaller MA, Scola MM, Joshi A, Matsukawa A, Aronoff DM, Johnson CN, Dou Y, Gallagher KA, Kunkel SL. 2017. The STAT4/MLL1 Epigenetic Axis Regulates the Antimicrobial Functions of Murine Macrophages. *J Immunol*

388. Morishita H, Saito F, Kayama H, Atarashi K, Kuwata H, Yamamoto M, Takeda K. 2009. Fra-1 negatively regulates lipopolysaccharide-mediated inflammatory responses. *Int Immunol* 21: 457-65

389. Li P, Spolski R, Liao W, Wang L, Murphy TL, Murphy KM, Leonard WJ. 2012. BATF-JUN is critical for IRF4-mediated transcription in T cells. *Nature* 490: 543-6

390. Karwacz K, Miraldi ER, Pokrovskii M, Madi A, Yosef N, Wortman I, Chen X, Watters A, Carriero N, Awasthi A, Regev A, Bonneau R, Littman D, Kuchroo VK. 2017. Critical role of IRF1 and BATF in forming chromatin landscape during type 1 regulatory cell differentiation. *Nat Immunol*

391. Gilchrist M, Thorsson V, Li B, Rust AG, Korb M, Roach JC, Kennedy K, Hai T, Bolouri H, Aderem A. 2006. Systems biology approaches identify ATF3 as a negative regulator of Toll-like receptor 4. *Nature* 441: 173-8

392. Cui H, Guo M, Xu D, Ding ZC, Zhou G, Ding HF, Zhang J, Tang Y, Yan C. 2015. The stress-responsive gene ATF3 regulates the histone acetyltransferase Tip60. *Nat Commun* 6: 6752

393. Fontana MF, Baccarella A, Pancholi N, Pufall MA, Herbert DR, Kim CC. 2015. JUNB is a key transcriptional modulator of macrophage activation. *J Immunol* 194: 177-86

394. Lu D, Chen J, Hai T. 2007. The regulation of ATF3 gene expression by mitogen-activated protein kinases. *Biochem J* 401: 559-67

395. Inoue K, Zama T, Kamimoto T, Aoki R, Ikeda Y, Kimura H, Hagiwara M. 2004. TNFalpha-induced ATF3 expression is bidirectionally regulated by the JNK and ERK pathways in vascular endothelial cells. *Genes Cells* 9: 59-70

396. Cheung P, Allis CD, Sassone-Corsi P. 2000. Signaling to chromatin through histone modifications. *Cell* 103: 263-71

397. Banerjee S, Halder K, Bose A, Bhattacharya P, Gupta G, Karmahapatra S, Das S, Chaudhuri S, Bhattacharyya Majumdar S, Majumdar S. 2011. TLR signaling-mediated differential histone modification at IL-10 and IL-12 promoter region leads to functional impairments in tumor-associated macrophages. *Carcinogenesis* 32: 1789-97

398. Hackstein CP, Assmus LM, Welz M, Klein S, Schwandt T, Schultze J, Forster I, Gondorf F, Beyer M, Kroy D, Kurts C, Trebicka J, Kastenmuller W, Knolle PA, Abdullah Z. 2017. Gut microbial translocation corrupts myeloid cell function to control bacterial infection during liver cirrhosis. *Gut* 66: 507-18

399. Geissmann F, Gordon S, Hume DA, Mowat AM, Randolph GJ. 2010. Unravelling mononuclear phagocyte heterogeneity. *Nat Rev Immunol* 10: 453-60

400. Madan R, Demircik F, Surianarayanan S, Allen JL, Divanovic S, Trompette A, Yogev N, Gu Y, Khodoun M, Hildeman D, Boespflug N, Fogolin MB, Grobe L, Greweling M, Finkelman FD, Cardin R, Mohrs M, Muller W, Waisman A, Roers A, Karp CL. 2009. Nonredundant roles for B cell-derived IL-10 in immune counter-regulation. *J Immunol* 183: 2312-20